Investigating the Profile of miRNAs in the Mammalian Male Reproductive Tract

Jackson Nicholas Reilly, B. Biotech (Hons, CI) (*University of Newcastle*)

c3145027

M. Philosophy (Biological Sciences)

School of Environmental and Life Sciences

University of Newcastle

2017

Index

Figure List

F: Figure, T: Table, and A: Appendix

Acknowledgements

First and foremost I wish to thank my family – Mum, Dad and Tamara – without whom completion would not have been possible. To all three of you: I thank you for your continued support and encouragement throughout my time at the University of Newcastle, for keeping on top of me when requested, and providing me with a loving environment in which I have been able to complete my studies. I would also like to extend my thanks to my grandparents – Nanna and Papa – whose constant concern and positive attitudes helped me hold my chin high and push on when times were tough. I am eternally grateful for all of the love and support the five of you have given me over my 25 years – I love you all dearly.

I would also like to take the time to thank each of my friends – Aaron, Ethan, Georgia, Pete, Riley, Scott, and Tyler – that supported me throughout my post-graduate endeavour. I could always rely on each of you to lend an ear, give me impartial and valuable advice, as well as a format in which I could destress when I was well and truly run down. Whether our time was spent in the gym, jamming out on instruments, playing videogames, hitting the beach, learning to paint, or just sitting down and enjoying a nice cup of coffee and a chat, every single one of you have been there for me and for that I will always be there for you. You are the best friends anyone could ask for.

Finally, I would like to thank my supervisors – Brett and Andy – for giving me the opportunity to undertake post-graduate studies at the University of Newcastle. Working with the two of you has been an eye-opening experience that has truly broadened my horizons. Thanks to you taking me on, I have had some incredibly unique experiences, met some very interesting people, progressed further academically, and made significant strides forward as an individual. The advice, critique and direction you gave me during my time as your student helped me to develop my knowledge, improve my analytical skills, further understand the research community, and generate this thesis – the culmination of my efforts as a university student. Thank you.

Abstract

Approximately 20 % of the human population is affected by infertility, leading to an increasing concern regarding the reproductive health of our species. In around half these cases, a male factor is implicated and as a result, many research groups are actively exploring the causes of male infertility and the development of therapeutic interventions to alleviate this infertility. After leaving the testis, nascent sperm gain their potential for functional competence as they progressively transit the epididymis, a long and convoluted tubule that connects the testes to the vas deferens. This accessory organ of the male reproductive tract is characterised by segment specific microenvironments that result from differential protein secretion by the epithelium of the tubule. Recently, it has been shown that an additional tier of regulation involving non-protein-coding RNAs (ncRNAs), such as the microRNA (miRNA) small RNAs, is also highly influential in creating the dynamic intraluminal environment of the epididymis. There is also emerging interest in the contribution that these species of epididymal small RNA (sRNA) have in transgenerational inheritance owing to their potential to be transferred to maturing spermatozoa within the lumen of the duct. Thus, in recognition of the potential importance of epididymal sRNA, the aims of this project were to investigate the profile of miRNAs differentially expressed throughout the mouse epididymis, with a particular focus on identifying novel and miRNAs generated within this organ. The results of this study revealed that mouse epididymal epithelial cells are characterised by a cohort of 218 miRNAs. Interestingly, these populations were relatively stable, with only a small portion of these molecules (15 %) undergoing the significant changes expected of candidates involved in regulating differential gene expression along the length of the tubule. A number of these miRNAs were identified as playing regulatory roles in pathways well documented to influence epididymal physiology, including 12 and 10 miRNAs mapping to androgen regulation and endocytotic pathways, respectively. An impressive 295 miRNA species were identified within the spermatozoa sourced from differing epididymal segments. In marked contrast to epithelial cells, the miRNA population harboured by epididymal spermatozoa was found to be far more variable, with pronounced changed in both the number and abundance of

miRNAs in sperm being observed as these cells progress through the epididymis. Among the miRNAs enriched in caudal sperm are a cohort of 28 molecules that have been experimentally confirmed to target the genes encoding several members of the TGFβ signalling pathway, which has been documented in the modulation of the female reproductive tract prior to fertilization. Further studies revealed that epididymosomes, small exosome-like vesicles produced by the epididymal epithelium, are replete with 358 miRNAs, ~48 % of which were characterised by significant changes in accumulation between proximal and distal ends of the tract. Additionally, the first empirical evidence to suggest that epididymosomes may transfer their payload to sperm after co-incubation *in vitro* has been provided. Analysis of the presence of novel miRNAs (*Nov-miR*s) in the mouse epididymis resulted in the identification of 22 putative candidates, mapping to > 6,200 reads. Of these, five were selected for further validation and target identification, resulting in the documentation of 19 key biological processes potentially regulated by these molecules. Three of the five *Nov-miR*s chosen for validation were confirmed to be present in sperm via RT-qPCR. The ongoing characterisation of these *Nov-miR*s and the role they play in regulation of epididymal physiology will form the basis of future work in the Nixon laboratory.

Declaration

“I hereby certify that the work embodied in this thesis is the result of original research that has not been submitted for a higher degree to any other University or Institution”

Signed: _____

Jackson Reilly

Author Contributions

Publication Title

Next Generation Sequencing Analysis Reveals Segmental Patterns of microRNA Expression in Mouse Epididymal Epithelial Cells

Authors

Brett Nixon, Simone J. Stanger, Bettina P. Mihalas, Jackson N. Reilly, Amanda L. Anderson, Mathew D. Dun, Sonika Tyagi, Janet E. Holt, Eileen McLaughlin

Citation

Nixon, B., et al., Next Generation Sequencing Analysis Reveals Segmental Patterns of microRNA Expression in Mouse Epididymal Epithelial Cells. PLoS One, 2015. 10(8): p. e0135605.

Statement of Contribution

Conceived and designed the experiments: B.N, J.E.H and E.A.M. Performed the experiments: S.J.S, B.P.M, J.N.R, A.L.A, and M.D.D. Analyzed the data: B.N, E.A.M, J.E.H, S.J.S, B.P.M and S.T. Contributed reagents/materials/analysis tools: B.N and S.T. Wrote the paper: B.N, S.J.S, B.P.M, J.N.R, A.L.A, M.D.D, S.T, J.E.H and E.A.M.

Author	Signature	Date
Brett Nixon		5/06/17
Simone J. Stanger		05/06/17
Bettina P. Mihalas		17/05/17
Jackson N. Reilly		05/06/17
Amanda L. Anderson		17/05/17
Mathew D. Dun		17/05/17
Sonika Tyagi		16/05/17
Janet E. Holt		18/05/17
Eileen A. McLaughlin		15/07/17

Publication Title

The microRNA signature of mouse spermatozoa is substantially modified during epididymal maturation

Authors

Brett Nixon, Simone J. Stanger, Bettina P. Mihalas, Jackson N. Reilly, Amanda L. Anderson, Sonika Tyagi, Janet E. Holt, Eileen A. McLaughlin

Citation

Nixon, B., et al., The microRNA signature of mouse spermatozoa is substantially modified during epididymal maturation. Biol Reprod, 2015. 93(4): p. 91.

Statement of Contribution

Conceived and designed the experiments: B.N, J.E.H and E.A.M. Performed the experiments: S.J.S, B.P.M, J.N.R and A.L.A. Analyzed the data: B.N, E.A.M, J.E.H, S.J.S, B.P.M and S.T. Contributed reagents/materials/analysis tools: B.N and S.T. Wrote the paper: B.N, S.J.S, B.P.M, J.N.R, A.L.A, S.T, J.E.H and E.A.M.

Author	Signature	Date
Brett Nixon		5/06/17
Simone J. Stanger		05/06/17
Bettina P. Mihalas		17/05/17
Jackson N. Reilly		05/06/17
Amanda L. Anderson		17/05/17
Sonika Tyagi		16/05/17
Janet E. Holt		18/05/17
Eileen A. McLaughlin		15/07/17

Publication Title

Characterisation of mouse epididymosomes reveals a complex profile of microRNAs and a potential mechanism for modification of the sperm epigenome

Authors

Jackson N. Reilly, Eileen A. McLaughlin, Simone J. Stanger, Amanda L. Anderson, Kate Hutcheon, Kiralee Church, Bettina P. Mihalas, Sonika Tyagi, Janet E. Holt, Andrew L. Eamens, Brett Nixon

Citation

Reilly, J.N., et al., Characterisation of mouse epididymosomes reveals a complex profile of microRNAs and a potential mechanism for modification of the sperm epigenome. Sci Rep, 2016. 6: p. 31794.

Statement of Contribution

J.N.R., S.J.S., A.L.A., K.H., K.C. and B.P.M. carried out the laboratory work and participated in data analysis and drafting of the manuscript; S.T. performed next generation sequence analyses and bioinformatics. E.A.M., J.E.H. and A.L.E. participated in the design of the study, data analysis, and drafting of the manuscript; B.N. conceived of the study, designed the study, coordinated the study and helped draft the manuscript. All authors gave final approval for publication.

Author	Signature	Date
Jackson N. Reilly		05/06/17
Eileen A. McLaughlin		15/07/17
Simone J. Stanger		05/06/17
Amanda L. Anderson		17/05/17
Kate Hutcheon		26/05/17
Kiralee Church		17/05/17
Bettina P. Mihalas		17/05/17

Sonika Tyagi		16/05/17
Janet E. Holt		18/05/17
Andrew L. Eamens		7th June 2017
Brett Nixon		5/06/17

Abbreviations

AGO2	Argonaute 2
AGRF	Australian Genome Research Facility
BLVRA	Bilverdin Reductase A
Ces7	Carboxylesterase 7
CPM	Counts Per Million
DCR1	DICER1
DGCR8	DiGeorge Syndrome Critical Region 8
ESCRT	Endosomal Sorting Complex
Exportin 5	Exp5
ICSI	Intracytoplasmic Sperm Injection
lncRNA	Long-non-coding RNA
MDS	Multi-Dimensional Scaling
miRNA	microRNA
ncRNA	Non-protein-coding RNA
NFW	Nuclease Free Water
NGS	Next Generation Sequencing
PACT	Protein Kinase R-activating
PAZ	Piwi/Argonaute/Zwille
PBS	Phosphate Buffered Saline
PCR	Polymerase Chain Reaction
piRNA	Piwi-Interacting RNA
pre-miRNA	Precursor miRNA
pri-miRNA	Primary miRNA

qPCR	Quantitative PCR
RISC	RNA Induced Silencing Complex
RNAi	RNA Interference
ROS	Reactive Oxygen Species
RT-qPCR	Reverse Transcription qPCR
sRNA	Small ncRNA
sRNA WB	Small RNA Workbench
TGFβ	Transforming Growth Factor Beta
TRBP	*trans*-Activation Response RNA Binding Protein
tRF	Transfer RNA Fragment
UTR	Untranslated Region

Chapter 1: Literature Review and Project Rationale

1.1 Introduction

Approximately 20 % of the human population is affected by infertility, leading to an increasing concern regarding the reproductive health of our species [1]. Approximately 50 % of these cases can be attributed to male factor infertility, which is most commonly manifested in the idiopathic failure of spermatozoa-oocyte recognition [2, 3]. In a significant portion of these cases, sperm are produced in sufficient quantity to achieve conception. However, the quality of these gametes is so diminished that normal conception avenues are ineffective, thus increasingly leading to infertile couples having to take recourse to use assisted reproductive technologies [3]. Though individual sperm can be injected into an egg via ICSI (intracytoplasmic sperm injection), recent studies have suggested that children conceived using this assisted reproductive technology are placed at an elevated risk of deleterious conditions, including a variety of epigenetic-related syndromes arising from genomic imprinting of parental gene expression [4-8]. With the ultimate goal of circumventing such complications, many research groups are actively exploring the restoration of male fertility by dissecting the molecular mechanisms governing the generation of functionally competent spermatozoa. In this regard, non-protein-coding RNAs (ncRNAs) are emerging as a focus of reproductive research, with a number of recent studies highlighting the importance of such regulatory molecules in promoting both the development and functional maturation of the male gamete [9]. Indeed, with the development of new technologies, principally next generation sequencing, small RNA (sRNA) research has become increasingly prominent in the context of reproductive systems, leading to speculation that these small regulatory molecules, including the microRNA (miRNA) class of sRNA, play a crucial role in the cellular processes involved in producing functionally mature male gametes. Of equal interest is the role that these sperm-borne regulatory molecules may play in promoting fertilisation and normal embryonic

development.

1.2 MicroRNA production in animal cells

MicroRNAs are short, approximately 22 nucleotides (nt) in length, ncRNAs which possess central roles in the regulation of post-transcriptional gene expression in eukaryotes [10]. Specifically, miRNA-directed gene expression regulation is now recognised as a key contributor to virtually all aspects of eukaryote development [11-14]. This is highlighted by each mammalian miRNA regulating the expression of many, functionally diverse, target genes [15, 16]. Further, in developmentally important tissues, miRNAs can represent up to 10 % of the total sRNA pool, and in such tissues miRNA-directed expression regulation is thought to control the levels of an impressive 60 % of all protein-coding genes [17-19]. It follows that alterations in the miRNA profile of a cell are now well established as a major contributor to the pathogenesis of a myriad of diseases, including; reproductive dysfunction, cardiovascular disease, inflammatory disease, various cancers, auto-immune diseases, skeletal muscle disease, and a suite of neuro-developmental diseases [20-26]. During the past decade it has become apparent that heritable information can be transmitted alongside the DNA, and without a change to the DNA sequence itself. Such 'epigenetic inheritance' can occur via several mechanisms, e.g. generation of specific species of non-protein-coding RNAs (including sncRNAs) or chemical modification of DNA and/or histone proteins. However, the only universal feature of epigenetic inheritance in all studied organisms is sncRNA. Indeed, sncRNAs direct epigenetic-mediated alterations to gene expression in all animal germlines, regardless of whether the studied organism possesses the ability to methylate its DNA [21, 23].

1.3 MicroRNA production – the nucleus

In animals, miRNA production initiates in the nucleus. Here, miRNA production follows one of two paths, the; i) primary miRNA production pathway, or; ii) the alternative miRNA production pathway (Figure 1).

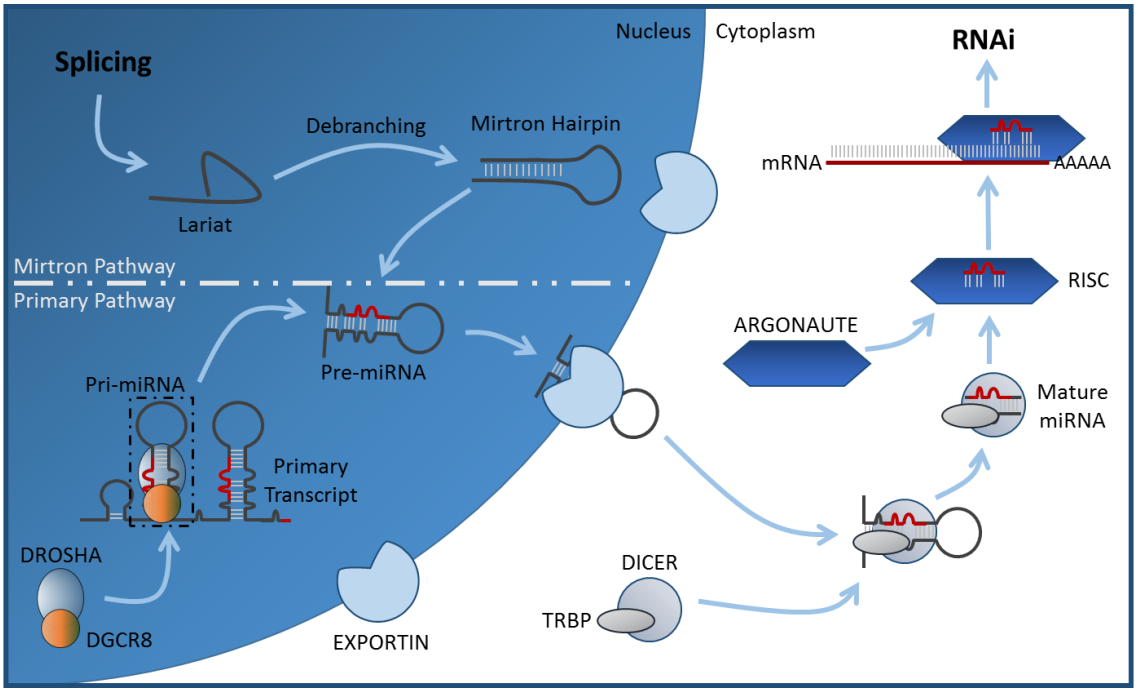

Figure 1.1: The miRNA production pathways of animal cells. In the primary miRNA production pathway, primary miRNA transcripts (pri-miRNA) are transcribed from miRNA encoding loci by RNA polymerase II. The pri-miRNA transcript, a long ncRNA that contains a region of partial complementarity that folds back on to itself to form the stem-loop structure of imperfectly dsRNA. The stem-looped structured pri-miRNA is recognised and processed by the nucleus localised Dicer (DROSHA)/double-stranded RNA binding protein (DGCR8) functional partnership to liberate the precursor-miRNA (pre-miRNA) from the pri-miRNA. In the alternative production pathway, processing of precursor-mRNAs (pre-mRNAs) during intron splicing of protein-coding genes releases lariats, also termed mirtrons, which are acted upon by a debranching enzyme to reshape the lariat into a hairpin structure closely resembling the structure of a pre-miRNA. Exportin5 (Exp-5), a pre-miRNA-specific exportin protein family member, next exports the pre-miRNA (including mirtron-derived pre-miRNAs) from the nucleus to the cytoplasm. In the cytoplasm, the pre-miRNA is recognised and processed by the DICER / TRBP (*trans*-Activation Response RNA Binding Protein; a dsRNA binding protein) functional partnership to produce the miRNA/miRNA* duplex. The liberated duplex is next loaded onto the RNA-induced silencing complex (RISC) where the two duplex strands are unwound; the miRNA* strand is degraded while the miRNA strand is retained by RISC. miRNA-loaded RISC (miRISC) contains Argonaute2 (Ago2) at its catalytic core and Ago2 uses the loaded miRNA as a guide to regulate the expression of genes that harbour miRNA target sequences in the mRNA 3′ UTR.

Primary-miRNA (pri-miRNAs) transcripts, are long ncRNAs transcribed by RNA polymerase II (Pol II). Pri-miRNAs harbour a region of partial self-complementarity which allows the pri-miRNA to fold back onto itself to form a stem-loop structure of imperfectly double stranded RNA (dsRNA). In the nucleus, the stem-loop structure is recognised by the Dicer

endonuclease, Drosha. With the assistance of its functional partner protein, a dsRNA binding protein termed DiGeorge Syndrome Critical Region 8 (DGCR8), Drosha cleaves the pri-miRNA transcript to liberate the stem-loop intermediate molecule, the precursor miRNA (pre-miRNA) [27, 28]. Interestingly, pri-miRNAs are identified as separate entities from other hairpin containing RNAs by DGCR8 binding protein in a process that is dependent on a number of important sequence and structural features. These include, an 11 base pair basal stem and downstream CNNC motifs/SRp20 binding sites, which distinguish pri-miRNAs from non-miRNA hairpin structures and enhance processing by the DGCR8/DROSHA microprocessor complex [29, 30]. Processing of pri-miRNAs is initiated once DGCR8 is activated by the binding of an Fe(III) heme cofactor [31]. Once activated, the dimeric heme-binding domain works to assemble two DGCR8 dimers that bind to the pri-miRNA hairpin at each end of the stem-loop structure and this is essential for maintaining the DGCR8-pri-miRNA complex [32]. After binding to the pri-miRNA, DGCR8 recruits, and positions DROSHA, 11 base pairs from the ssRNA-dsRNA junction. Once in position, the A and B RNase III domains of DROSHA form an intramolecular dimer that cleaves the 3′ and 5′ ends of the hairpin loop, liberating the pre-miRNA, an approximately 70 nucleotide transcript with 2-nt 3′ overhangs at its termini [33, 34].

An alternate, and DROSHA/DGCR8-independent pathway, exists within animal cells for miRNA production, termed the alternate or mirtron pathway [35-37]. During this process, spliced introns adopt a loop structure (lariat) comprising a 5′ splice site that is covalently linked to a 3′ branch point. Some of these structures have the potential to further fold to form a mirtron; a hairpin structure that closely resembles a pre-miRNA. Mirtron formation is catalysed by a lariat-debranching enzyme and these mirtron structures are subsequently primed for export from the nucleus [35, 36]. For further processing of pre-miRNAs and mirtrons, both molecules require export to the cytoplasm. This occurs via a common transport mechanism mediated by Exportin-5 (EXP5). EXP5 recognises the 2-nt 3′ overhang present on both the pre-miRNA and mirtron molecule and shuttles these RNAs across the nuclear envelope in a RanGTP-dependent process [38-40].

1.4 Cytoplasmic Processing of pre-miRNAs

RNA interference (RNAi) pathways are initiated in the cytoplasm, where nucleus processed mirtrons and pre-miRNAs are further acted upon by the cytoplasmic localised endonuclease, Dicer1 (DCR1). DCR1 harbours numerous functional domains with each mediating a key role in miRNA processing, including; i) an ATP-dependent helicase domain; ii) a PAZ (Piwi/Argonaute/Zwille) domain; iii) two dsRNA binding domains, and; iv) two RNase III domains [41-43]. Though it has been demonstrated that DCR1 alone can process pre-miRNAs and mirtrons, other research has shown that the efficiency of DCR1 processing is enhanced via interaction with the dsRNA binding protein, *trans*-activation response RNA binding protein (TRBP) [44, 45]. The PAZ domain of DCR1 is separated from the RNase III domain by a 65 angstrom long, positively-charged surface that recognises and binds the 2-nt 3′ overhang of the pre-miRNA [34]. Thereafter, the two RNase III domains form a pseudo-dimer around the dsRNA region of the pre-miRNA and cleave each strand at the loop end to liberate the miRNA/miRNA* duplex.

Argonaute2 (AGO2) forms the catalytic core of miRNA-loaded RISC (miRISC) and following a dynamic and ATP-dependent conformational change, AGO2 loads the miRNA/miRNA* duplex onto miRISC [46, 47]. Here, the duplex strands are unwound from one another and the miRNA guide strand is retained by miRISC while the corresponding duplex strand, the miRNA* passenger strand, is degraded. For those pre-miRNA molecules that exhibit strand accumulation bias in humans, guide strand selection appears to rely on specific sequence characteristics; (i) an abundance of Uracil in the 5′ region and a surplus of purines in the guide strand, (ii) an abundance of Cytosine in the 3′ region and a surplus of pyrimidines in the passenger strand [48]. However, it should be noted that strand selection can vary between differing tissues, developmental and disease states, suggesting that other mechanisms of selecting a miRNA guide strand may be at play [49-51].

Most miRNAs act to regulate gene expression at a post-transcriptional level via interactions with the 3′ UTR of mRNA transcripts. Typically, partial duplexes with mismatches

or nucleotide bulges are formed between miRNAs and the target site however, rare cases of near-perfect complementarity is achieved, such as the interaction documented between *miR-196* and the *Hoxb8* mRNA, and this enables cleavage of the mRNA [52]. The most common miRNA/target motif documented is perfect pairing between the 'seed' sequence of the miRNA, which spans from nucleotides 2 – 8, and the target site [53-56]. Though Watson-Crick pairing of this 5' region of the miRNA to the target is preferential, functional target sites with seed sequence G-U wobble pairs have been identified. Furthermore, mismatches between the seed sequence and a target site can be compensated for by standard Watson-Crick base pairing in the 3' region of the miRNA at nucleotides 13-16 of the miRNA in a position termed the 'centred site' [57]. Due to the seemingly flexible rules governing animal miRNA-target interactions, it is not surprising that multiple mRNAs are able to be targeted by a single miRNA, with recent studies suggested that any given miRNA has the potential to target upwards of 200 distinct mRNAs [53, 55].

The method of post-transcriptional regulation driven by miRNAs occurs according to the sequence of the miRNA loaded into RISC and involves either mRNA degradation or translational repression. As stated previously, in cases where the loaded miRNA has near-perfect complementarity to the mRNA 3' UTR, AGO2 mediates cleavage of the mRNA at the site of the nucleotides pairing to residues 10 and 11 of the miRNA [58-60]. However, despite being the more common mode of regulation in plants, mRNA cleavage in mammalian species is rare due to the lack of highly complementary transcriptome sites. Imperfect miRNA:mRNA complementarity results in bulges forming in the RNA duplex, which inhibit the slicer activity of AGO2 (the only mammalian AGO with this ability), and therefore prevents cleavage of mRNAs [61-63]. Instead, miRNAs in mammals most commonly perform their regulatory roles by way of translational repression. Initiation of translation can be inhibited by RISC in several ways: RISC can outcompete the eIF4E initiation factor by binding to the m7G 5' cap of an mRNA [64]; degradation of an mRNA polyA tail can be achieved by RISC via deadenlyation, which leaves insufficient space for PolyA-Binding Proteins (PABPs) to bind and function [65]; the generation

of a functional 80S ribosomal can be hindered through interference between 40S and 60S interactions via the binding of RISC to EIF6 [66].

Since their initial discovery over a decade ago, in excess of 2000 mature miRNA sRNAs have been identified and implicated in the regulation of an ever increasing spectrum of genes within most eukaryotic cells [16]. Indeed, recent evidence secured by a number of independent research groups points to miRNAs as playing key roles in regulating the various biological processes essential for optimal generation, and acquisition of functional competence, of the male germ line (refer to Section 1.5 and Table 1.1). Such evidence continues to provide an exciting avenue of research, with an increasing number of research groups converging on the identification of specific roles that miRNAs may play in this realm of cellular development.

1.5 Production of male gametes

The production of highly specialised sperm cells is an inordinately complex process predicated on finely controlled temporal and spatial patterns of gene expression [67]. Accordingly, sRNAs are increasingly being recognised as an important tier of gene expression regulation within the male reproductive system, with roles extending from the control of the gene products associated with the cytological differentiation of germ cells within the germinal epithelium of the testes, through to those that are expressed in a highly regionalised manner to drive the acquisition of sperm functional competence within the male reproductive tract (epididymis).

In mammalian species, the generation of fertilisation-competent male gametes begins during embryogenesis, whereupon primordial germ cells are incorporated into the sex cords of the male genital ridge. The germ cells reside in this position until maturity, coinciding with the development of the seminiferous tubules and Sertoli cells. The Sertoli cells form a structure known as the blood-testis barrier to separate the basal and adluminal compartments of the seminiferous tubules. Upon formation, the Sertoli cells bind spermatogenic germ cells and are responsible for both their protection and nourishment throughout differentiation [68, 69]. Primordial gem cells undergo division when reaching the gonad and form the A_1 spermatogonia,

which are characterised by an ovoid, chromatin-containing nucleus. The A_1 spermatogonia divide, producing one polar A_2 spermatogonium, as well as the A_1 spermatogonium. After another round of division, the A_2 spermatid produces an A_3 spermatid, which in turn divides to form the A_4 spermatogonia [70]. From here, A_4 spermatogonia have three options; i) self-replicate to produce another A_4 spermatogonia; ii) undergo apoptosis, or; iii) differentiate into a committed stem cell type. When the A_4 spermatogonia undergo route (iii), an intermediate spermatogonium, which divides once more to form a type B spermatogonia, is created and it is these cells that are committed to becoming spermatozoa cells. The type B spermatogonia undergo another round of mitosis resulting in the formation of the primary spermatocytes. Primary spermatocytes immediately undergo subsequent rounds of mitotic division, producing the secondary spermatocytes, followed by the haploid cells known as spermatids, thus completing spermatogenesis [68, 71-73].

The round, unflagellated spermatids undergo further maturation in the form of spermiogenesis, which comprises four stages. The first stage of spermiogenesis, termed the Golgi stage, is initiated when a perinuclear Golgi apparatus commences the gathering of proacrosomal vesicles, leading to the eventual formation of an acrosomal vesicle. The second stage, termed the capping phase, is denoted by the flattening of the acrosomal vesicle to form a cap-like structure that covers the nucleus, while the third acrosomal phase, is characterised by the migration of this cap to the underside of the nucleus. Importantly, the nucleus is rotated so that the cap faces the basal membrane of the seminiferous tubule while the centriole faces the lumen [71, 74-77]. Spermatids then undergo nuclear condensation, which is driven by the replacement of the majority of histones and nucleosomes with protamines within the chromatin. This process enhances the efficiency of DNA packaging and consequently leads to complete repression of active gene transcription within the nucleus of the elongating cells. As the flagellum begins to form, the nucleus continues to condense while excess cytoplasm is stripped from the cell and jettisoned in the form of the cytoplasmic droplet [71]. The degree of specialisation achieved during the spermatogenic process results in a complete silencing of both the transcriptional and translational

machinery in the testicular spermatozoa. Therefore, further maturation of these cells after they leave the testes is driven exclusively by the extrinsic factors they are exposed to upon transit through the subsequent male reproductive tract.

Utilising a suite of expression technologies, including microarray, RNA-seq and RT-qPCR, a number of independent research groups have shown that miRNAs abundantly accumulate within the testes and developing male germ cells [78-80]. Moreover, there is mounting evidence that miRNAs possess critical roles in regulating the successive waves of spermatogenesis [78-81]. Indeed, it has been shown that specific miRNAs, including *miR-34c*, *miR-122*, *miR-449* and *miR-469*, significantly accumulate as the testes develop, and these miRNAs have been implicated in: regulation of post-meiotic gene expression [82], meiotic initiation [83], TGFβ signalling [84], heat-shock protein regulation [85], and chromatin remodelling [86]. The importance of miRNAs in the testes is further exemplified by the selective ablation of testicular *Dicer1*. The elimination of miRNA production in the testes of *Dicer1* knockout animals has been demonstrated to result in severely reduced testes size and disrupted spermatogenesis [87]. Further, the resulting sperm are characterised by poor cellular morphology, possessing smaller or abnormally shaped heads, as well as thin tails with disorganised accessory structures [88]. Such defects manifest in a delayed progression of meiosis and an increase in apoptosis among the spermatocyte pool (and hence a decrease in the haploid cell population) and ultimately a concomitant reduction in fertility [87-91].

While a more thorough description of spermatogenesis and the role that miRNAs play in this process lies beyond the scope of this review, the suite of miRNAs identified as playing key roles in the process of germ cell production are summarised in Table 1. Furthermore, the reader is directed to a number of excellent recent reviews of this topic [72, 73, 76, 92].

Table 1.1: miRNA molecules involved in regulating the generation of male germ cells.

Cell Type	miRNA	References
PGC's	***let-7*** family (LIN28: mature gamete differentiation, tumour suppression), ***miR-17-92*** cluster (STAT3, E2F1, PTEN: differentiation, proliferation and apoptosis regulation), ***mir-290-295*** cluster (WEE1, FBXL5: control of cell cycle), ***miR-302–367*** cluster (NR2F2: transcription, cell growth and pluripotency maintenance), ***miR-383*** (FMRP)	[93-102]
Early	***miR-141*** (SIP1: cell migration inhibition), ***miR-200a*** (SIRT1, ZEB2: tumour suppression, cell migration inhibition), ***miR-200c*** (ZEB1, TRKB: tumour suppression, cell migration inhibition, apoptosis regulation), ***miR-323*** (PB1: H1N1 replication inhibition)	[90, 93, 103-107]
Late	***miR-9*** (LIN28: gamete differentiation regulation), ***miR-125a*** (LIN28: gamete differentiation regulation)	[93, 101, 103]
Spermatocytes	***miR-15b***, ***miR-18a***, ***miR-34b*** (NOTCH1, LGR4, VEZT, MAN2A2, FOXJ2: tumour suppression, apoptosis, cell cycle arrest), ***miR-34c*** (CCND3, CCNG1, CCNB1, CCNC, CCNE1, CDK4, CDK6, E2F5, FOS, CDC2, TGIF2, NOTCH2, STRBP, LGR4, KLF4, NOTCH1, PPP1CC, GALT, KITLG, SPAG4, CCNL, ZFP148, GMFB: regulation of cell cycle, germ cell phenotype enhancement), ***miR-296-5p***, ***miR-375***, ***miR-425***, ***miR-449a***, ***miR-3085-5p***, ***miR-3570a***, ***miR-466i-5p***	[80]
Spermatogonia	***miR-16-5p*** (CCND1: cell cycle regulation), ***miR-20*** (spermatogonia maintenance), ***miR-21*** (spermatogonia maintenance), ***miR-34a***, ***miR-34c***, ***miR-99a***, ***miR-106a*** (spermatogonia maintenance), ***miR-136*** (SOX11, PTEN), ***miR-146*** (cell differentiation regulation), ***miR-146a***, ***miR-149*** (PPIA, NDKB: TGFβ signalling regulation), ***miR-182***, ***miR-183***, ***miR-199a-3p*** (PPIA, NDKB: TGFβ signalling regulation), ***miR-201***, ***miR-204***, ***miR-221/222*** (spermatogonia maintenance), ***miR-290-5p*** (SOX2, SOX11, PTEN), ***miR-291a-5p*** (BMPR1A, SOX11, SMAD4, PTEN) ***miR-293***, ***miR-294****, ***miR-322***, ***miR-463****, ***miR-465a-3p***, ***miR-465b-3p***, ***miR-465c-3p***, ***miR-465c-5p***, ***miR-547***, ***miR-743a*** (BMPR1A, PTEN)	[80, 108-113]

Spermatids	***miR-18*** (HSF2: influences heat shock protein function), ***miR-34c*** (CCND3, CCNG1, CCNB1, CCNC, CCNE1, CDK4, CDK6, E2F5, FOS, CDC2, TGIF2, NOTCH2, STRBP LGR4 KLF4, NOTCH1 PPP1CC, GALT, KITLG, SPAG4, CCNL, ZFP148, GMFB: cell cycle regulation and germ cell phenotype enhancement), ***miR-17-92*** cluster (STAT3, E2F1, PTEN: regulation of differentiation, proliferation and apoptosis), ***miR-122a*** (TP2: Chromatin condensation), ***miR-124a*** (QKI, MYO10, SP3, MITF, FGGR2, CDK4, KLF4, SLUG, IQGAP1, ITGB1: Cell cycle migration and pluripotency regulation), ***miR-184*** (AKT2: tumour suppression), ***miR290-295*** cluster (WEE, FBXL5: cell cycle control), ***miR-302-367*** cluster (NR2F2: transcription, cell growth and metabolism, maintenance of pluripotency), ***miR-440***, ***miR-469*** (TP2, PRM2: chromatin condensation)	[85, 114-117]
Testis		
7 - 10 dpp	***miR-100*** (FRAP1/mTOR: tumour suppression, cancer)	[103, 118]
7 - 14 dpp	***miR-9*** (LIN28: Control of differentiation), ***miR-34a*** (CCND2, BLC2, GMFB, SIRT1: proliferation inhibition, apoptosis induction), ***miR-34c*** (CCND3, CCNG1, CCNB1, CCNC, CCNE1, CDK4, CDK6, E2F5, FOS, CDC2, TGIF2, NOTCH2, STRBP LGR4 KLF4, NOTCH1 PPP1CC, GALT, KITLG, SPAG4, CCNL, ZFP148, GMFB: regulation of cell cycle, germ cell phenotype enhancement), ***miR-34b*** (NOTCH1, LGR4, VEZT, MAN2A2, FOXJ2: tumour suppression, apoptosis induction, cell cycle arrest), ***miR-141*** (SIP1: cell migration inhibition), ***miR-375*** (IGR1R: tumour suppression, metastasis inhibition), ***miR-449*** (MECP2, ASB1, BCL2, NOTCH1, CASP2, KITLG, VCL, FOXJ2, INHBB, SOX11, CCNE2, GMFB, DLL1)	[84, 89, 93, 101, 103, 105, 109, 119-123]
Mature	***let-7*** family (LIN28: differentiation of gametes, tumour suppression), ***miR-34c*** (CCND3, CCNG1, CCNB1, CCNC, CCNE1, CDK4, CDK6, E2F5, FOS, CDC2, TGIF2, NOTCH2, STRBP, LGR4, KLF4, NOTCH1, PPP1CC, GALT, KITLG, SPAG4, CCNL, ZFP148, GMFB: regulation of cell cycle, germ cell phenotype enhancement), ***miR-98*** (TP53, CASP3, FASL: regulation of apoptosis), ***miR-143***, ***miR-210*** (IGF2: insulin regulation), ***miR-371*** cluster (Suv39-H1, LATS2: segregation of chromosome, mitotic progression), **miR-509-3p**, **miR-709** (BORIS: DNA methylation control)	[89, 94, 97, 98, 100, 101, 103, 117, 122, 124-126]
Down-regulated in mature testis	***let-7e*** (NR6A1, TAF5, FASL, EIF4G2, SUV39H2, DZIP1, DDX19B, MYCN: tumour suppression), ***miR-127*** (BRD2: lung development), ***miR-154*** (PPP1CC, PCNA, AQP9, HMGA2: lung development), ***miR-181b*** (TBP11, RSBN1, AMD, DAZAP2, PIK3R3, RNF6, BCL2: tumour suppression), ***miR-181c*** (KPNB1, NR6A1, SOX6, RAD21, CREB1, SOX5, RSBN1, AMD, TNPO1, DAZAP2, NOTCH4, KRAS: Tumour suppressor), ***miR-181d*** (TIMP3, RNF6, KPNB1, BCL2: Drug resistance, regulation of apoptosis), ***miR-214*** (HSPD1, TEX27, ADCYAP1R1, HBP1, AP1G1,	[89, 93, 100, 104, 122, 127-138]

	SSR1, PTEN, AP-2Ɣ, ITGA3: Cell survival, cell migration and invasion), ***miR-335*** (CCNT2, CCD2, RSBN1, RUNX2: Maintenance of pluripotency in mesenchymal stem cells), ***miR-337*** (TBX, AP1G1, TAF5, TAf12, CREB1 CCNL1), ***miR-361*** (KPNB1, ZFP148, BMPR2, CALM2), ***miR-376a*** (CDK2, AGO2: Maintenance of pluripotency, and cell cycle arrest), ***miR-379*** (EIF4G2, EDN1, RNF6, ABCC2: Membrane transport), ***miR-411*** (USP42), ***miR-434-5p***, ***miR-487b***	
Up-regulated in mature testis	***miR-29b*** (CREB5, BAK1, USP42, MLF1, HBP1, SNX24, PTEN: Oncogene, represses apoptosis promotes cell motility), ***miR-34a*** (CCND2, BLC2, GMFB, SIRT1: Repression of cell proliferation, Inducer of apoptiosis), ***miR-34b*** (NOTCH1, LGR4, VEZT, MAN2A2, FOXJ2: Tumour suppressor, promotes apoptosis, cell cycle arrest and senescence), ***miR-122a*** (TNP2: Later stage germ cell maturation), ***miR-124a*** (QKI, MYO10, SP3, MITF, FGGR2, CDK4, KLF4, SLUG, IQGAP1, ITGB1: Suppression of cell migration, pluripotency), ***miR-191****, ***miR-296*** (NCALD, SCRIB: Tumour suppressor, cell motility repressor), ***miR-449*** (MECP2, ASB1, BCL2, NOTCH1, CASP2, KITLG, VCL, FOXJ2, INHBB, SOX11, CCNE2, GMFB, DLL1: Differentiation of ciliated cell progenitors), ***miR-557*** (EIF4G2, STAG2, VCP), ***miR-702*** (SBF1, MMP14), ***miR-714***, ***miR-715*** (KPNB1), ***miR-1260b***, ***miR-4454***, ***miR-5100***	[89, 103, 116, 119, 120, 122, 123, 135, 136, 139-141]

1.6 Post-testicular epididymal sperm maturation

Fully differentiated spermatozoa released from the germinal epithelium of the testes are functionally immature as they lack both motility and the capacity to engage in the complex array of cellular interactions required for fertilising an egg [142]. In all mammalian species studied, these attributes are progressively acquired as the sperm descend through the successive segments of the epididymis. This highly specialised region of male reproductive tract comprises a long (6 meters in humans) convoluted tubule that serves to connect the testes to the vas deferens. As documented above, the maturation of spermatozoa within the lumen of the epididymis occurs in the complete absence of sperm nuclear gene transcription, and is therefore driven entirely by extrinsic factors [143]. Such factors are produced by the epithelial cells lining the epididymal tubule and display an extraordinary level of segment specificity [144]. While once thought to be predominated by inorganic ions and proteins, it is becoming increasingly apparent that epididymal secretions comprise a number of additional macromolecules, including various sRNAs (discussed

in Section 1.7).

Upon entering the caput segment of the epididymis (Figure 1.2), sperm encounter a unique intraluminal milieu created by the combined secretory and absorptive activity of the lining epithelia [145]. Through continuous interaction with this microenvironment, the sperm membrane composition and biochemical properties are successively modified such that by the time the sperm are conveyed into the corpus they begin to express signatures of functional competence in the form of progressive motility and the ability to recognise an ovum. These attributes continue to be optimised until fertilising potential is fully achieved as the cells reach the cauda and are stored in this segment in a quiescent state prior to ejaculation [146].

The marked division of labour that characterises epididymal function is, in turn, driven by tightly regulated and highly segment-specific patterns of gene expression [147]. However, the way in which these differential gene expression profiles are established and maintained remains to be resolved. Among the primary candidates are androgens, which have long been known to exert an overriding influence over epididymal physiology and have been widely implicated in the control of numerous genes, including; epidermal growth factor and insulin-like growth factor-1 as well as the diverse downstream targets of these growth factors [148, 149]. Indeed, proximal epididymis-specific knockout of the androgen receptor in mice results in dysregulation of the epithelium lining the initial segment of the epididymis, to the point where sperm passage through this segment is compromised, ultimately culminating in azoospermia [150]. Additional lumicrine factors of testicular origin have also been implicated in the suppression of apoptosis and thus maintenance of the epididymal epithelium, particularly in the initial segment [151]. However, androgens and lumicrine factors alone fail to account for the reported differential gene expression as the receptors required for induction of androgen responsive elements are uniformly expressed along the length of the epididymal tract [152, 153]. Rather, technological advances in the field of high throughput sequencing technologies, including sRNA profiling, have led to a new appreciation of additional tiers of gene expression regulation in this developmentally important tissue.

1.7 Role of miRNAs in regulating epididymal function

One recently identified central regulator of differential gene expression within the epididymal soma is that of the miRNAs. Indeed, it has demonstrated that a conditional block in global miRNA production via the elimination of the central miRNA pathway enzyme DCR1, can lead to rapid dedifferentiation of the epididymal epithelium [154]. Specifically, the complete, caput-specific ablation of DCL1 in *Dicer1* animals led to the regression of epididymal morphology such that the tract of an adult 45 day old *Dicer1* knockout mice closely resembled that of the juvenile 12 day old control mice. Such marked morphological changes were mirrored by significant perturbation in the gene expression profiles within the principal cells of the caput epididymal segment. This, in turn, resulted in an imbalance in sex-steroid receptors denoted by the overproduction of estrogen receptors and a concomitant decrease in the production of androgen receptors [154]. A subsequent study of the *Dicer1* proximal-caput epididymis knockout mice identified pronounced alterations in lipid homeostasis within the duct, resulting in the generation of spermatozoa with destabilised membranes marked by deficient polyunsaturated fatty acid content. Such defects were further manifest in the form of an infertility phenotype associated with an inability of sperm to interact with an oocyte [155]. Together, these findings provide evidence that miRNAs play a central, and crucial role, in mediating hormonal regulation and the establishment / maintenance of the epididymal microenvironments that drive sperm maturation. Further empirical support for this notion has been established by the demonstration that the manipulation (over-expression) of even a single epididymis-specific miRNA can precipitate a marked reduction in male fertility [156]. In this study, it was shown that the expression of the epididymis-specific gene coding for Carboxylesterase 7 (*Ces7*) was significantly suppressed upon microinjection of *mil-HongrES2*, a ‘miRNA-like sRNA’, into the epididymal epithelium. This, in turn, led to a marked reduction in the levels of the CES7 protein being secreted into the epididymal lumen and the production of spermatozoa exhibiting pronounced defects in both motility, and the ability to complete capacitation, culminating in a clear diminution of fertility [156]. These findings are potentially of great significance, as they

suggest that the perturbation of just a single miRNA sRNA is sufficient to compromise the efficacy of epididymal sperm maturation.

In light of these findings, and fuelled by rapid technological advancements in the detection of global nucleic acid profiles, contemporary research has increasingly focused on unravelling the complexity of the miRNA profiles of each epididymal segment and across several model species [157-163]. In one such study focused on the human epididymis, over 200 miRNAs were detected [157]. Further, a marked decrease in the total miRNA pool was recorded in the epididymis as males aged [164]. Such findings contrast that of the corresponding mRNA and transcription factor expression levels in the epididymis of these individuals, which were found to increase during the ageing process, suggesting that epididymal miRNAs affect age-specific gene expression by way of mRNA cleavage. These data reinforce the notion that miRNAs regulate epididymal gene expression in an androgen-dependent manner [164]. In addition, sequencing of over 250 sRNA libraries sampled from 26 different organs and/or cell types revealed that specific miRNA clusters, such as *miR-888*, are particularly enriched within epididymal tissue where they have been implicated in the homeostatic regulation of normal epididymal physiology via regulation of cellular processes including; cell-cell adhesion, metal-ion transport, anatomical structure development, system development, epithelium morphogenesis, tube development and cell motility [165]. Microarray-based studies focussing on the miRNA content of the human epididymal epithelium, identified 35 miRNAs that exhibited differential accumulation between the caput and caudal segments of the tubule [159]. Many of these miRNAs showed strict correlation with the pattern of target gene expression in the respective epididymal segments, an observation that mirrors those reported in studies of rat and bovine epididymal miRNA profiles [158, 166], suggesting that epididymal gene expression is universally controlled by miRNA-mediated translation inhibition.

Taken together, these findings suggest that a broad range of miRNAs are likely responsible for maintaining the structural and functional integrity of the epididymis [158, 159, 166]. A key limitation of these studies however, is that they have generally not been designed to

discriminate between the relative contributions of the epididymal epithelial cells versus that of the luminal contents in terms of defining the origin of each miRNA. In this context, it is known that both spermatozoa and other luminal content potentially represent a rich source of miRNA species. Thus, in seeking to address this limitation, studies conducted within our own research group have sought to systematically dissect the miRNA profile of epididymal epithelial cells from that of the spermatozoa and extracellular vesicles (epididymosomes) that reside in the epididymal lumen [161-163, 167]. Such an approach has confirmed a highly sophisticated network of miRNAs in each surveyed sample [161]. Indeed, using a next generation sequencing platform, over 200 miRNAs were identified within the epididymal epithelium, the majority of which (~75 %) were characterised by equivalent levels of expression between each epididymal segment. Such findings are consistent with those previously reported in studies of the bovine epididymis, suggesting that the majority of epididymal miRNAs are likely to fulfil housekeeping roles, with only a relatively small subset being devoted to regulation of segmental patterns of gene expression. Indeed, a portion of the miRNAs characterised by high fold changes between differing epididymal segments mapped to key components of androgen signalling, cell proliferation and oncogenic pathways to further emphasise that these small regulatory molecules potentially play a crucial role in establishing and maintaining the unique physiological compartments of the epididymis [161].

As an extension of this work, next generation sequencing has recently been employed to determine the miRNA profiles of enriched populations of spermatozoa sampled from differing segments of the mouse epididymis [162]. These studies afforded some of the first evidence that, despite their transcriptionally inert state, sperm miRNA profiles are highly dynamic. Indeed, among the profile of sperm miRNAs identified, almost half were found to undergo significant accumulation change, or be completely lost, between the proximal (caput) and distal (caudal) segments of the epididymis. Among those that preferentially accumulated in maturing spermatozoa, several were found to map to putative targets implicated in modulating the peri-conceptional environment of the female reproductive tract [162, 168]. Among other notable

findings, it was shown that mouse spermatozoa harbour several pre-miRNA species, as well as the core protein machinery of the miRNA pathway, including DCR1 and AGO2. Though this principle has yet to be directly explored, these findings raise the interesting possibility that spermatozoa may possess their own, partial or fully functional miRNA processing pathway [162]. Alternatively, miRNA precursor transcripts may be directly delivered to the female reproductive tract in an incompletely processed state as an additional tier in target gene expression regulation. However, such hypotheses remain to be experimentally validated. Irrespective of their role, this previously unappreciated plasticity in the epididymal sperm miRNA profile also raises the prospect that epididymal transit may present a key developmental window for the establishment of the sperm epigenome.

Such a model takes on considerable importance in view of the rapidly accumulating body of evidence that the sperm sRNA profile can be profoundly influenced by paternal exposure to a range of environment insults. Notably among these studies, Rogers and colleagues (2013) recently provided compelling evidence that exposure of male mice to chronic stress can lead to differential accumulation of nine sperm miRNAs [169]. Further, the embryos arising from stressed fathers exhibited global alterations in gene transcription, suggesting that the sperm miRNA profile influences the epigenetic (re)programming of progeny [169]. In a separate study also featuring a paternal stress insult, sperm sRNAs were injected directly into an oocyte that had been fertilised by control spermatozoa [170]. Remarkably, the resulting offspring exhibited the same behavioural and metabolic alterations as those documented in the unrelated, stress–exposed mice, thus affording additional support for the significance of sperm miRNAs in the context of epigenetically reprograming of an embryo [170]. In a similar context, a variety of alternative environmental insults such as exposure of males to cigarette smoke [171], or dietary perturbations [172, 173], have also been shown to exert influence over sperm miRNA signatures with implications for the progeny of treated animals. It is now apparent that the health of offspring is readily able to be affected by paternal factors, with nutritional intake of fathers having been documented to influence the metabolism of their progeny [174]. For example, restriction of protein consumption

in the diet of male mice prior to mating has resulted in altered cholesterol metabolism in offspring [175]. Similarly, over-nourished fathers have been documented to produce daughters with reduced ability to metabolize glucose [176]. These collective data highlight a previously unappreciated legacy of male exposure to environmental stressors and emphasise the importance of miRNAs in the transmission of such information to spermatozoa and consequently to subsequent generations. At present, the developmental timing of these changes and the precise mechanism(s) by which they are transmitted to spermatozoa remains uncertain. However, a very recent study by Sharma and colleagues (2016) has served to focused attention on exosome-like microvesicles secreted by the epididymis, termed epididymosomes [158, 177-183], as a key mediator of this novel form of intracellular communication [184].

1.8 Role of epididymosomes in epididymal intercellular communication

Epididymosomes are small, membrane-bound vesicles produced by the principal cells of the epididymal epithelium [185, 186]. These entities are released via an apocrine mechanism of secretion, whereby blebs comprising cytosolic contents form along the apical margin of epididymal principal cells and project into the lumen of the duct. Upon release from the parent cell, the blebs degenerate to release their contents into the luminal microenvironment [185, 186]. Among the entities that are released are epididymosomes, a heterogeneous pool of membrane bound vesicles that range in size from ~50 nm to 150 nm. Epididymosomes appear to be a common secretory product of all mammalian species, having now been identified in bulls, rats, mice, rams, hamsters, rabbits, and humans [187-194]. Interestingly, it has been shown that these extracellular vesicles have an affinity for the mid-piece and head of epididymal sperm [181], and have been implicated in the selective delivery of various macromolecules to these specific domains. The best characterised of this epididymosome-borne macromolecular cargo are proteins, and epididymosome protein cargo displays considerable variability depending on the site of epididymosomes biogenesis. Indeed, a defining characteristic of epididymosomes are the segment specific changes in their proteomic composition. For instance, among the 555 and 438 epididymosome proteins identified in the bovine caput and cauda epididymis, only 231 are

common to both segments [180].

Notwithstanding such variability, conserved classes of proteins have been used as biomarkers to differentiate between subpopulations of epididymosomes. In this regard, studies in the bovine model have identified two epididymosome proteomic subpopulations based on the presence or absence of the tetraspanin, CD9 [195]. Of note, CD9 positive epididymosomes are enriched with proteins that have been implicated in mediation of sperm-egg interactions (e.g. P25B and GLIPRIL1) as well as a cohort of proteins essential for sperm motility (e.g. MIF and AKR1B1) [195]. This finding takes on added significance in view of the demonstration that CD9 positive epididymosomes preferentially interact with live spermatozoa, thus suggesting they may mediate the bulk delivery of proteins that promote the acquisition of sperm motility and fertilising ability as the cells progress through the epididymis. In contrast, CD9 negative epididymosomes are enriched in a different repertoire of proteins and show preferential binding to dead spermatozoa. Accordingly, one of the dominant proteins recorded in this subpopulation is epididymal sperm binding protein 1 (ELSPBP1), a protein that acts in tandem with biliverdin reductase A (BLVRA) to protect live spermatozoa from reactive oxygen species generated by their dead counterparts [178, 196]. One of the fascinating implications to arise from such observations is that the epididymis may be able stratify its investment depending on the vitality of the spermatozoa within its lumen. At present, the selective mechanism(s) by which epididymosomes adhere, and deliver their cargo to, spermatozoa remains to be determined. The extent to which such mechanisms confer the ability to transfer other macromolecular cargo to spermatozoa also remains to be fully elucidated.

Nevertheless, recent studies have shown that, in addition to their protein cargo, epididymosomes also harbour an impressive repertoire of sRNA. Indeed, some 80, 246 and 358 miRNAs have recently been identified in the epididymosomes of the bovine, human and mouse, respectively [157, 158, 163]. Similar to their proteomic content, the profile of epididymosome miRNA cargo also varies considerably between the caput and caudal segments of the epididymis [158]. Indeed, among the ~350 miRNAs that our research recently identified in mouse

epididymosomes, some ~46 % are characterised by significant changes in accumulation between proximal and distal epididymal segments, thus enabling the differentiation of quite unique subpopulations of epididymosomes [163]. Increasing evidence now suggests that at least a portion of these epididymosome-borne miRNAs may be directly conveyed to maturing spermatozoa [158, 162] and/or epithelial cells lining downstream epididymal segments [158]. In a previous study, we adapted an *in vitro* co-incubation strategy originally pioneered by Frenette and colleagues [197] to provide direct evidence for significant accumulation of a subset of miRNAs (including, *miR-191*, *miR-375*, *miR-476a* and *miR-467e*) into mouse spermatozoa. We have yet to explore the full extent of such transfer and thus whether such a mechanism could account for the substantive changes in the miRNA profile we have documented in maturing epididymal mouse spermatozoa [163]. Nevertheless, the work of Sharma and colleagues (2016), now suggests that epididymosome-mediated transfer may be a common pathway that underpins the delivery to spermatozoa of other forms of regulatory sRNA, such as those belonging to the transfer RNA fragment (tRFs) subclass [184]. With regard to epididymosome-epithelial cell communication, the work of Belleannee and colleagues (2013) has provided the first demonstration that epididymosomes are able to participate in a paracrine form of control via the delivery of miRNA cargo to cultured epididymal epithelial cells [158]. Such data reinforce the notion that miRNAs form an integral part of the sophisticated signalling network that controls epididymal function and hence sperm maturation (Figure 1.2).

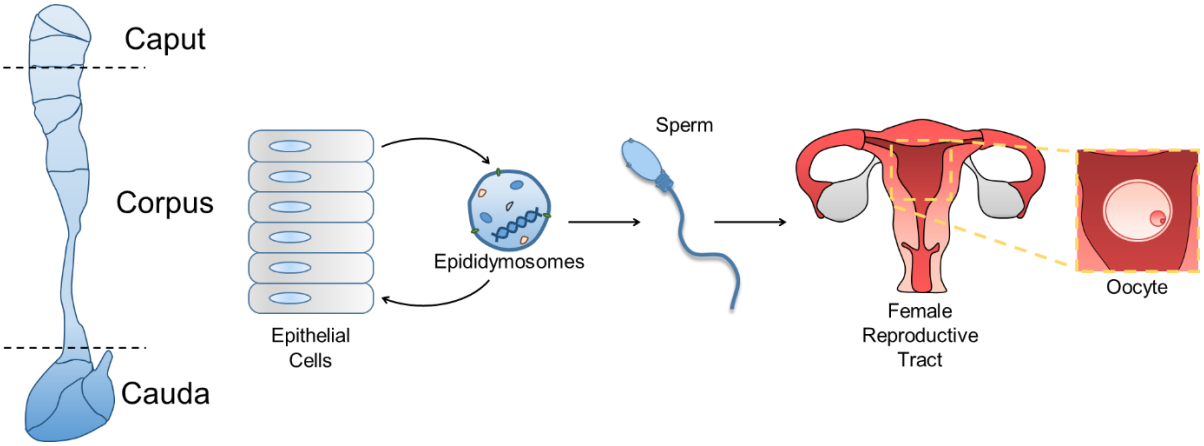

Figure 1.2: Model for miRNA control of epididymal function and sperm maturation. As sperm progress through the intraluminal milieu of the mammalian epididymis they gain functional competence in a process that is driven entirely by extrinsic factors. Emerging evidence indicates that these factors include a suite of macromolecules (of which proteins and sRNA appear to predominate) whose genesis within the epididymal epithelium is highly coordinated via segment specific patterns of gene expression. One potential mechanism for the bulk delivery of epididymal protein and sRNA to the maturing spermatozoa is via epididymosomes, small membrane bound vesicles that are secreted from the lining soma. Following delivery, the protein and/or sRNA cargo promote the functional maturation of spermatozoa and may also influence the peri-conception environment and/or early embryonic development. Conversely, epididymosomes may also participate in the paracrine regulation of gene expression profiles following uptake into the epithelial cells of downstream epididymal segments [168].

Based on our research, the current working model for an epididymal contribution of miRNAs to sperm suggests that the epithelium of each epididymal segment possesses a unique miRNA profile that forms an important tier of regulation to control specific gene expression patterns throughout the epididymis. An important feature of this model is that, in addition to their putative role in regulating epithelial cell function, a portion of the epididymal miRNAs are selectively released to the lumen of the tract whereupon they have the ability to be incorporated into the maturing spermatozoa. Our favoured mechanism for this form of intracellular communication is via the packaging of miRNAs, along with other macromolecular cargo, into small membrane bound vesicles known as epididymosomes. These entities are, in turn, released into the intraluminal milieu via apocrine secretion whereupon they from intimate associations with the sperm head and mid-piece, ultimately delivering their payload to these sperm domains. Based on independent research, it is also hypothesised that epididymosomes can facilitated a reciprocal transfer of miRNAs to the epididymal epithelium of downstream segments of the tract,

where they may exert a form of paracrine over gene expression. Finally, our model posits that a least a portion of the miRNA cargo that spermatozoa convey into the female reproductive tract may participate in modulating the receptivity of the peri-conceptual environment in the female tract and/or influence the trajectory of early embryonic development (Figure 1.2). Given the relatively high degree of species conservation among identified epididymal miRNAs, it is likely that this proposed model is of relevance to a wide range of mammalian species, including our own [161, 162].

1.9 Conclusion

With the documented evidence of declining reproductive health, new avenues of research are required to improve fertility and overcome issues surrounding our current reliance on assisted reproductive technologies [198]. Through exploration of the molecular mechanisms governing the maturation of male gametes, it has become increasingly apparent that regulatory RNAs, and in particular miRNAs, play a crucial role in the regulating the physiological status of the male reproductive system. Indeed, miRNA-directed gene expression regulation has proven to be essential for normal germ cell development during spermatogenesis [67]. Similarly, miRNAs appear to hold a pivotal role in the regulation of post-testicular maturational events that occur in the extragonadal tissues of the male reproductive tract. Indeed, miRNAs have now been implicated in the extragonadal control of segment specific gene expression profiles, protein secretion and unique physiological compartments that collectively drive sperm maturation as the cells descend through the tubule [143]. Epididymal microenvironments may also be influenced by a sophisticated signalling network involving epididymosomes, which are able to convey miRNA and protein cargo to sperm progressing through the tract. Analysis of the roles of this novel form of intracellular communication in accounting for the plasticity of the sperm miRNA profile represents an exciting new avenue for mammalian reproductive research.

1.10 Project Aims and Rationale

In view of recent findings, the overall goal of this project was to document the full complement of known miRNAs from the various components sourced from the three gross

anatomical segments of mammalian epididymis, using the mouse as a model. Furthermore, this project sought to provide a basis for the trafficking of miRNAs to sperm during epididymal transit, as well as identify any novel miRNAs present throughout the tract. In order to achieve this, the following hypotheses were tested in accordance with the aims listed below.

Hypotheses

1. miRNAs are responsible for modulating the epididymal microenvironments responsible for driving the acquisition of functional characteristics during sperm maturation.
2. Epididymal extracellular vesicles are responsible for delivering miRNA cargo to sperm as they progress through the tract.

Aims

1. Document the complement of miRNAs present in the epithelial cells, spermatozoa and epididymosomes of each epididymal segment.
2. Investigate the trafficking of miRNAs to spermatozoa during epididymal transit.
3. Identify the presence of novel miRNAs throughout the epididymis.

Chapter 2: Materials and Methods

2.1 General

Centrifugation of 1.5 mL Eppendorf tubes at maximum speed (20,000 x *g*) was performed using an Eppendorf 5417R Centrifuge.

2.2 Chemicals and solutions

The chemicals used throughout this study were all of analytical grade. Details of solutions used are contained within the Appendix section. Unless specified, each reagent used was sourced from Sigma Aldrich (St. Louise, Mo, USA) or ThermoFisher Scientific (Waltham, MA, USA).

2.3 Ethics statement

All experimental procedures with the approval of the University of Newcastle's Animal Care and Ethics Committee (approval number A-2013-322) Inbred Swiss mice were used throughout the project in accordance with international guidelines. Mice were supplied with food and water *ad libitum* and housed under a controlled lighting system (16 hours light: 8 hours dark) at 21–22°C. All mice were humanely euthanized by CO_2 asphyxiation prior to dissection.

2.4 Dissection of euthanized Swiss mice

The vasculature of adult male mice (8 weeks old) was perfused with pre-warmed (37°C) Phosphate Buffered Saline (PBS) immediately after euthanasia to minimise blood-borne contamination of samples. All whole tissues (brain, heart, liver, testes, ovaries, spleen, kidneys, thymus, uterus and epididymis) were stored at -80°C immediately after harvesting.

2.5 Isolation of epididymal epithelial cells

Following isolation of epididymal segments, caput and corpus tissues were pooled in a pre-warmed (37°C) 1.0 mL droplet of Biggers, Whitten and Whittingham media (BWW, Appendix 1). Multiple incisions were made with a razor blade and samples were incubated for 30 minutes to allow epididymal sperm to separate from the surrounding tissue. In the case of caudal segments, tissues were cleared of contaminating sperm via retrograde perfusion with sterile PBS. All tissue segments were subjected to further washing via three rounds of submersion and

agitation in warm sterile PBS. Following this, epididymal tissues were resuspended in 100 µg/mL trypsin and incubated with vigorous shaking using a POCD Scientific Intelli-Mixer RM-2M at 37°C for 30 minutes. Tissue clumps and cells were isolated via centrifugation at 800 x *g* for 5 minutes, resuspended in a solution of 1 mg/mL of collagenase type II and incubated for further digestion at 37°C with vigorous shaking for 30 minutes. An equal amount of DMEM was added to each sample in order to halt the digestion reaction. Cell-containing samples were then filtered through a 70 µm cell strainer, made up to 2.0 mL with DMEM and incubated in 6-well plates for four hours at 32°C in order to allow all non-epithelial cells to attach to the bottom of the wells. The epithelial cell-containing supernatants were carefully removed from wells, subjected to centrifugation at 800 x *g* for 5 minutes and cell pellets were stored at -80°C for downstream analyses. Epididymal epithelial cells sourced from 9 – 12 animals were pooled to generate sufficient material for each biological replicate of downstream analyses. Enrichment of epididymal epithelial cells (>95%) was assessed by immunocytochemistry, as detailed in Nixon 2015a [161]. Immunofluorescence imaging confirmed that the only cells present in epithelial cell preparations were those expressing androgen receptor, while a counterstain for a sperm acrosome marker, PNA, resulted in no additional fluorescence. Western blotting confirmed the presence of Androgen receptor and Cytokeratin 8 in both whole tissue and epithelial cell lysate preparations, as well as a distinct absence of the intrinsic sperm protein, IZUMO1.

2.6 Isolation of epididymal spermatozoa

Caput and corpus segments were pooled in pairs in a 1.0 mL pre-warmed droplet of BWW. Small incisions were made with a razor blade, and epididymal sperm were separated from the surrounding tissue via gentle agitation at 37°C for 20 minutes. Samples were filtered with a 70 µm cell strainer in order to remove tissue chunks. The resulting tissue-free liquid was carefully placed atop a continuous 27 % Percoll gradient and centrifuged using a Hercaeus Megafuge 1.0R at 500 x *g* with a swinging bucket rotor for 15 minutes without brake. After discarding the supernatant, enriched sperm pellets were combined and washed twice by resuspension in 1.0 mL sterile PBS and centrifugation at 500 x *g* for 3 minutes. For isolation of highly enriched

populations of caudal sperm, distal epididymal segments were immersed in water-saturated mineral oil and sperm was isolated via retrograde perfusion of the lumen. Isolated sperm were expelled into BWW (1.0 mL per cauda) and allowed to disperse throughout the media for 30 minutes at 37°C. Following this, samples were subjected to centrifugation at 500 x *g* for 3 minutes to pellet sperm. Isolated cells were washed twice in sterile PBS as described above. Each sperm sample was assessed for the presence of somatic cells, as outlined in Nixon 2015b [162]. All pellets of isolated sperm were immediately stored at -80°C for downstream analyses. Sperm sourced from 9 – 12 animals were pooled to generate sufficient material for each biological replicate of downstream analyses.

2.7 Isolation of epididymosomes

The pairs of the appropriate epididymal segments from each mouse were pooled into a 500 µL droplet of BWW. Multiple incisions were made with a razor blade, tissues were subjected to mild agitation and incubated for 30 minutes at 37°C in order to allow the luminal contents to be released. The resulting samples were passed through a 70 µm to remove tissue pieces. Samples were then cleansed of cellular debris by way of sequential centrifugation at 4°C (Appendix 2). Cleansed suspensions were subsequently placed carefully atop a discontinuous OptiPrep density gradient (Appendix 3) and subjected to ultracentrifugation at 100,000 x *g* for 18 hours at 4°C using a Beckman Coulter Optima MAX Ultracentrifuge with a TLS-55 swinging rotor. Samples were then split into twelve 185 µL fractions, each of which was diluted with 2.0 mL of sterile PBS, and subjected to ultracentrifugation at 100,000 x *g* for 4 hours at 4°C using a TLA 100.4 fixed rotor. Epididymosome pellets were dissolved into solution for downstream analyses and stored at -80°C. Fractions 9 and 10 were utilized in future analyses as they reported the highest enrichment of epididymosomes. Epididymosomes sourced from 9 – 12 animals were pooled to generate sufficient material for each biological replicate of downstream analyses.

2.8 Epididymosome bead binding

Due to their small size, visualization of epididymosomes via fluorescent microscopy requires an initial binding of these vesicles *en masse* to latex beads. For this purpose, 20 µL of

4 µm aldehyde/sulphate latex beads (ThermoFisher Scientific) was added to a solution of epididymosomes promptly after sonication. This solution was made up to 200 µL with sterile PBS and incubated for 2.5 hours with gentle agitation at room temperature to allow epididymosomes to bind to the beads. In order to block the unbound areas of the latex beads, 110 µL of 1M glycine was added to each sample and prior to incubation for a further 30 minutes. Beads were washed twice with 1.0 mL of 0.5 % Bovine Serum Albumin (BSA) in PBS via centrifugation at 1,500 x *g* for 3 minutes. Samples were then incubated with primary antibodies (CD9 and FLOT1, 1:100 dilution in 1 % BSA/PBS) overnight at 4°C. Samples were washed as previously stated, and sequentially exposed to goat anti-rabbit 488 Alexa Fluor and goat anti-rat 594 Alexa Flour (1:400 dilution in 1 % BSA/PBS) for 1 hour at room temperature with gentle agitation. After washing, beads were allowed to settle onto 12-well slides and epididymosomes bound to the beads were viewed by fluorescence microscopy.

2.9 Co-incubation of epididymosomes with sperm

A co-incubation protocol to assess delivery of miRNA cargo was designed based on an optimised procedure used for the transfer of proteins from bovine epididymosomes to sperm. After isolation, caput and corpus epididymosomes of three animals were resuspended in 250 µL of pre-chilled (4°C), modified BWW (pH 6.5) supplemented with 1 mM $ZnCl_2$ (Zn-BWW) via sonication. This solution was warmed to 37°C prior to being used to gently resuspend a caput sperm cell pellet (2 x 10^6) sourced from three animals. The co-incubation reaction was allowed to take place over 3 hours at 37°C in 5 % CO_2 with gentle agitation. After pelleting cells via centrifugation at 500 x *g* for 3 minutes, sperm were washed three times via centrifugation in 1.0 mL of pre-warmed, sterile PBS to remove any unbound epididymosomes. Pelleted sperm were then stored at -80°C prior to RNA extraction and downstream analyses. A number of measures were taken in an effort to validate this approach of epididymosome-mediated delivery of miRNAs to sperm. First, epididymosomes were loaded with a non-fluorescent membrane dye, CFSE (carboxyfluorescein diacetate succinimidyl ester), which is modified upon entry into a cell to a non-membrane permeable label that emits substantial fluorescence. This was achieved by

incubating isolated epididymosomes in a solution of 1.25 µL of CFSE for 30 minutes at 37°C in a dark environment. After loading, samples were diluted with 2.0 mL of sterile PBS and subjected to ultracentrifugation at 100,000 x *g* for 3 hours in order to wash epididymosomes of excess CFSE. The resulting epididymosomes were then either utilised in the co-incubation protocol described above in combination with a Live/Dead co-label to determine sperm vitality, or bound to beads (as described in 2.8).

2.10 RNA extraction

Two distinct protocols were employed to isolate RNA from material of interest depending on downstream analyses. A Direct-zol RNA MiniPrep Kit (Zymo Research Corporation, Irvine, CA, USA) was used to generate RNA for Next Generation Sequencing according to manufacturer's instructions. Briefly, cells were macerated in 500 µL TRI Reagent with a sterile plastic pestle, diluted with an equal volume of 100 % ethanol and mixed by vortex. Mixtures were loaded into a Zymo-Spin IIC Column and centrifuged for 30 seconds at 18,000 x *g*. 400 µL of Direct-zol RNA PreWash, was run through the columns via 30 seconds of centrifugation, before washing with 700 µL of RNA Wash Buffer. Following this, RNA was eluted into 50 µL of DEPC H_2O and samples were incubated with 1 % DNase (Promega) to eliminate genomic DNA contamination. RNA was stored indefinitely at -80°C.

'Solution D' RNA extractions, based on a guanidinium thiocyanate-phenol-chloroform protocol designed in 1987 [199, 200], were utilised to isolate RNA for use in downstream qPCR reactions. Tissues/cells were macerated in 500 µL of Solution D (Appendix 4) using a sterilised plastic pestle. After the addition of 50 µL of 2M CH_3COONa, samples were vortexed briefly and supplemented with 500 µL of phenol/chloroform/isoamyl alcohol. After this, samples were vortexed for 1 minute prior to being centrifuged at 18,000 x *g* for 20 minutes at 4°C. The resulting solution separated into a supernatant, interphase and organic phase, the former of which was carefully removed, diluted in an equal volume of 100 % isopropanol and incubated at -20°C for a minimum of 1 hour before further processing. In order to extract additional RNA from the remaining solutions, the interphase and organic phase were reconstituted with 500 µL of

Solution D, as well as 50 µL of 2M CH_3COONa, prior to being incubated for 1 hour at -20°C. Reconstituted samples were then subjected to centrifugation at 13,000 x *g* for 20 minutes at 4°C and supernatants were removed and diluted as specified previously. After 1 hour of incubation at -20°C, precipitated RNA was separated from solution via centrifugation at 18,000 x *g* for 20 minutes at 4°C. Pellets were resuspended in 100 µL of Solution D, like samples were pooled and samples were diluted in an equal volume of 100 % isopropanol prior to being incubated for a further 1 hour at -20°C. Precipitates were removed from solution and washed with 70 % EtOH via centrifugation. Cleaned pellets were allowed to air-dry, after which they were resuspended in 20 µL of sterile diethylpyrocarbonate (DEPC) H_2O. Total RNA of sperm, epithelial cells and epididymosomes sourced from each epididymal segment (caput, corpus, cauda) was pooled from a minimum of nine animals to generate a single biological replicate. Purity of RNA samples was determined through the use of a Shimadzu UV-2501PC with the Shimadzu UVPC v3.9 software and concentration was calculated as per the following equation: Concentration = $Absorbance_{260}$ x Dilution Factor x 40. All samples were stored indefinitely at -80°C immediately after quantification.

2.11 DNase treatment of RNA samples

In order to remove any DNA contamination, RNA samples were DNase treated prior to performing downstream analyses. First, 3.0 µL of RQ1 RNase-Free DNase and 3.0 µL of RQ1 DNase 10x reaction buffer were added to each RNA sample and incubated at 37°C for 1 hour. Following a 10 minute heat-inactivation of the DNase enzyme at 70°C, sample volumes were made up to 200 µL with DEPC H_2O and combined with 200 µL of phenol/chloroform/isoamyl alcohol and vortexed for 1 minute. Samples where then subjected to centrifugation at 18,000 x *g* for 20 minutes at 4°C, the top aqueous layer was carefully removed and diluted in 1/10 volume of 3M CH_3COONa and 2.5 volumes of 100 % ethanol prior to being incubated for 1 hour at -20°C. RNA was pelleted from solution and washed with 70 % ethanol via centrifugation. Pellets were reconstituted in 20 µL of DEPC H_2O and RNA concentration and purity was determined as previously outlined.

2.12 Reverse transcription and PCR for RNA quality control

In order to confirm RNA quality, samples were reverse transcribed and the resulting cDNA was screened for housekeeping genes via conventional PCR. To begin the reverse transcription process, 2.0 µg of RNA was combined with 1.0 µL of Oligo $(dT)_{15}$ Primer and made up to a final volume of 11 µL with DEPC H_2O prior to incubation at 70°C for 5 minutes. After cooling on ice for 5 minutes, 11 µL of reverse transcription master mix (Appendix 5) was added to each sample. Following this, 1.0 µL of M-MLV reverse transcriptase enzyme was added to '+RT' samples, while 1.0 µL of DEPC H_2O was added to '-RT' reverse transcription control samples. Reactions took place over 1 hour at 42°C, following which each sample was diluted with 80 µL of DEPC H_2O. cDNA samples were stored indefinitely at -20°C. cDNA was screened for the housekeeping genes, Beta-2 Microglobulin (B2M) and Cyclophilin (Appendix 6), via both conventional and quantitative Polymerase Chain Reactions (PCRs). Specific examples of each protocol performed are highlighted in (Appendices 6, 7, 8 and 9). DNA agarose gel electrophoresis for the evaluation of conventional PCR products was carried out using a BioRad PowerPac 200 system in 1.5 % agarose gels containing 0.3 µg/mL ethidium bromide. Products were run alongside either a Promega 1 kb DNA ladder or a Bioline 100 bp HyperLadder and gels were submerged in 1 x TAE prior to electrophoresis at 100 V for 60 minutes. Resolved DNA fragments were visualised using a Kodak EDAS290 system with the Kodak 1D v3.6 software.

2.13 Next Generation Sequencing

Three biological replicates of epididymal samples were subjected to Illumina TruSeq small RNA sample preparation protocol as per the manufacturers' instructions (Illumina Inc. San Diego, CA, USA) at the Australian Genome Research Facility (AGRF, Melbourne, VIC, Australia). The miRNA libraries generated from the three biological replicates were analysed in duplicate and sequenced using an Illumina Hiseq-2000 RNA-seq platform as 50 bp single end chemistry at AGRF as previously described [161-163]. Briefly, the sequence reads from all samples were analysed for quality control on an Agilent 2100 Bioanalyser (Agilent Technologies, Santa Clara, CA, USA) and screened for the presence of contaminants by matching against the

contaminant database (containing PhiX, ChrM, rDNA and Illumina small RNA adaptor sequences) using cutadapt [201] and bowtie aligner. Cleaned sequence reads were processed through a quantification module pipeline in miRDEEP2 ver2.0.0.7 to determine miRNA expression profiles or previously identified miRNAs [202].

miRNA read counts were normalised in accordance with RNAseq library sizes, and a threshold of detection (count value of > 10 counts per million) was applied to determine presence/absence of miRNAs. Sample diagnostics and differential expression analyses were conducted using the edgeR [203] and limma Bioconductor package in conjunction with an identification filters set to a ≥ 2-fold difference and a false discovery rate (FDR) of 0.05. The relationship between miRNA accumulation between each biological replicate in this study were visualized via multi-dimension scaling (MDS) plots [204], where the leading log-fold change was plotted for dimensions 1 and 2 using all miRNA counts within a read library. Data discussed in this thesis are readily accessible from NCBI's Gene Expression Omnibus through the following GEO accession numbers: GSE70197 (epithelial cells), GSE70198 (spermatozoa) and GSE79500 (epididymosomes).

2.14 Taqman reverse transcription and real time PCR confirmation of selected miRNAs

Validation of miRNA profiles was conducted using quantitative real-time PCR (RT-qPCR) with (non-locked nucleic acid modified) TaqMan miRNA assay reagents (ThermoFisher Scientific) as per the manufacturer's instructions. In short, a reverse transcription master mix (Appendix 11) was mixed with ~1.0 µg of RNA in a total reaction volume of 15 µL and subjected to thermocycling (Appendix 12). The resulting cDNA was diluted with an equal volume of DEPC H_2O and utilised in the Taqman RT-qPCR protocol (Appendices 13 and 14). The mature forms of miRNAs selected for analysis were are presented in Table 2.1.

Table 2.1: Identification codes of miRNA Taqman Assays.

miRNA Assay	Assay ID
U6 sRNA	001973
let-7b-5p	002619
let-7c-5p	000379
miR-9-5p	000583
miR-34b-5p	002617
miR-34c-5p	000428
miR-127-3p	000452
miR-139-5p	002689
miR-145-5p	002278
miR-151	001190
miR-181b-5p	001098
miR-191-5p	002299
miR-196b-5p	002215

miRNA Assay	Assay ID
miR-200c-3p	002300
miR-375	000564
miR-410-3p	001274
miR-465a-5p	001826
miR-467d	002518
miR-467e	002568
miR-470-5p	002588
miR-486-5p	001278
*Nov-miR*13	CSN1ETO
*Nov-miR*37	CSPACZW
*Nov-miR*42	CST95OS
*Nov-miR*101	CSRR9CC
*Nov-miR*127	CSS07IK

RT-qPCR was performed using a Light Cycler 96 SW 1.1 (Roche, Castle Hill, Australia). All RT-qPCR data was normalised against the evenly expressed, endogenous U6 small nuclear RNA. Relative expression was calculated using the $2^{-\Delta Ct}$ method as previously described [205]. All miRNA RT-qPCR analyses were performed in triplicate using pooled biological samples distinct from those samples employed in next generation sequencing analyses.

2.15 *In silico* analysis of previously identified miRNAs and target prediction

A number of *in silico* methodologies were employed to analyse miRNA profiles. In order to ensure consistency across a range of biological replicates, abundance values of miRNAs in counts per million (CPM) were log transformed and subject to hierarchical median gene clustering using Cluster3, (Stanford University, Palo Alto, CA, USA) prior to being examined using heatmaps generated through the use of Java Treeview (Stanford University). Total numbers of miRNAs characterised by significant fold changes between each epididymal segment were calculated and plotted in the form of column graphs, while volcano plots were employed in order to visualise trends associated with differentially accumulating miRNAs in epididymal samples.

Gene targets of known miRNAs exhibiting significant fold changes in accumulation between epididymal segments were identified with Ingenuity Pathway Analysis (IPA) software (v8.8, Ingenuity Systems, Redwood City, CA, USA). Experimentally validated filters were applied when identifying targets, and a number of miRNAs were mapped to several genes within biological pathways of interest.

2.16 *In silico* identification of putative novel miRNAs

All 21 FASTQ files resulting from the RNAseq analysis performed by AGRF were interrogated for the presence of potentially novel miRNA sequences using UEA sRNA Workbench v 3.2 (University of East Anglia, Norwich, UK) [206]. First, the adapter sequence (LMN_3; TGGAATTCTCGGGTGCCAAGG) was trimmed from sequencing reads and size distributions of reads were recorded. To narrow our search to miRNA molecules, each of the 21 trimmed files were filtered for reads with abundance ≥ 10 and sequence length of 20 – 25. At this point, each sequence file was merged into one master file for streamlined high throughput processing. Potentially novel miRNA sequences were identified from this file through use of the UEA 'miRCat' tool, with tRNA filters applied, which generated a list comprised of several hundred candidates. In short, miRCat works to map sequence reads to an input genome (in this case, mouse genome assembly GRCm38) and searches for sRNA loci that match specific criteria (no more than four sRNAs can overlap, each sRNA must be within 200 nt of each other, and sRNAs within the locus must be oriented in the same direction). The sRNA in the locus with the highest abundance is nominated by miRCat as a candidate novel miRNA and surrounding sequence windows of various lengths are folded to determine a > 50 nt pre-miRNA secondary structure that is free of mismatches. Various filters were applied to the resulting dataset to narrow down potentially novel miRNA candidates; > 2 genome matches, sRNA length 21 - 23, abundance > 10, $p < 0.05$. Remaining sequences were then blasted in miRBase and several NCBI databases to ensure that false-positive sequences documented in prior studies had been eliminated. As a final point of exclusion, secondary structures of novel pre-miRNA molecules were generated using RNAfold [207] and visualised using VARNA [208]. Candidate novel miRNAs were

selected based on hairpin structure, whereby hairpins containing bulges of > 5 nt, or forked structures, were excluded from subsequent analyses.

2.17 Statistical analysis

Statistical analyses were performed using JMP Software (v12.2.0). Multivariate correlation analyses and Student T-tests were utilised to determine statistical significance between datasets with a significance threshold of $P < 0.05$. 'R' was used to generate linear regression models. Each dataset was made up of three biological replicates and all data are presented as mean ± SEM.

Chapter 3: Profiling the complement of miRNAs present throughout the mammalian epididymis

3.1 Introduction

Reproductive health is a growing concern worldwide, with defective sperm functionality in the form of an idiopathic failure of sperm-egg recognition being identified as a prime cause of human infertility [2, 3]. Functional competence of sperm is acquired, not during their initial differentiation in the testis, but in their subsequent transit through an accessory organ of the male reproductive tract: the epididymis [143]. This long and convoluted tract is characterised by segments that are defined by unique gene expression profiles. This in turn results in differential secretion of proteins in the epididymal lumen, which constitute the microenvironments responsible for bestowing fertilising ability and progressive motility upon sperm during their transit of the tract [144]. Previously, several studies have implicated miRNAs as playing a key role establishing and maintaining epididymal microenvironments by providing an additional tier of gene expression regulation. In order to investigate the role that miRNAs play in mammalian sperm maturation, our research group sought to methodically analyse the miRNA profiles of specific elements that comprise the dominant segments of the epididymis. The experimental design employed by our research group to achieve this goal is shown in Figure 3.1.

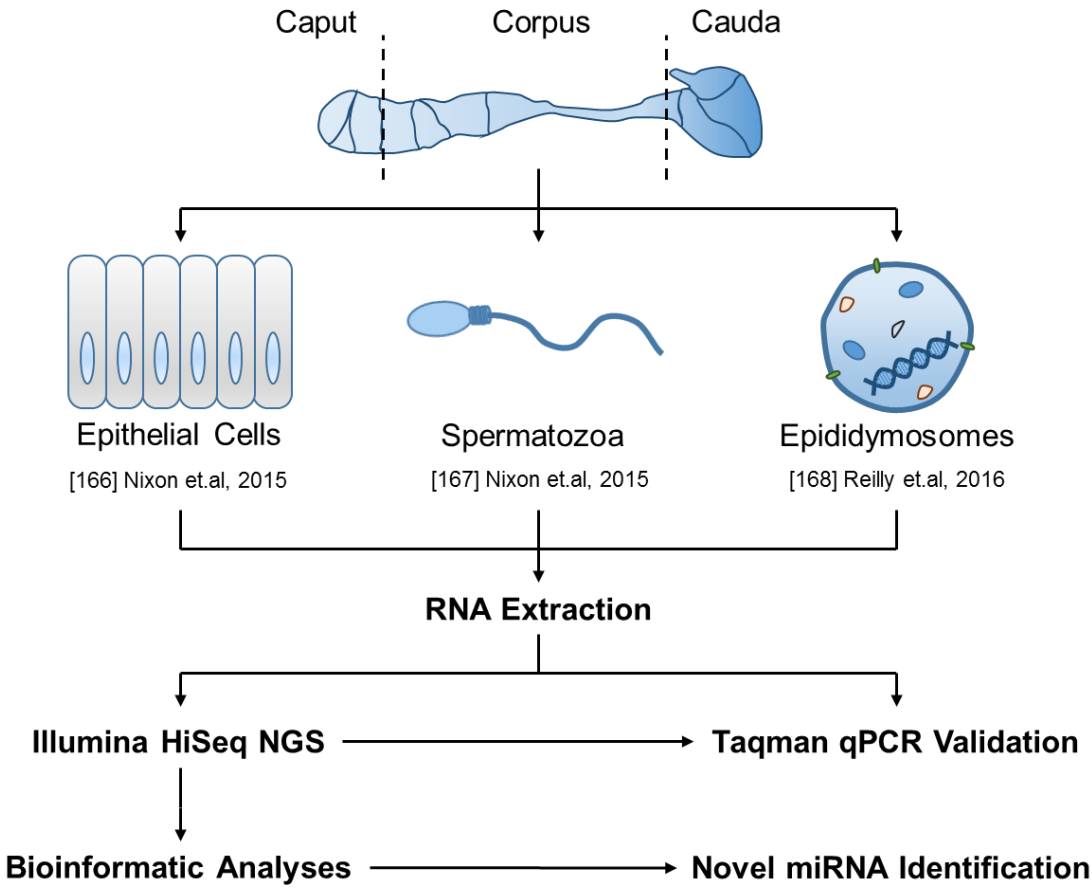

Figure 3.1: Experimental plan for sequencing miRNA profiles of the mammalian epididymis. Epididymides of adult mice were split into the archetypical anatomical segments: the caput, corpus and cauda. Three components (epithelial cells, spermatozoa and epididymosomes) were then isolated from each segment via rigorously validated methods. The RNA extracted from each component was analysed via next generation sequencing at AGRF in order to generate full profiles of known miRNAs accumulated in each sample. Taqman qPCR validations were employed to confirm the accuracy of reported profiles while bioinformatic analyses detailed the extent to which miRNA profiles are altered throughout the epididymis and identified the role that differentially accumulated miRNAs may play within the tract. Initial bioinformatic analyses then paved the way for the identification of novel miRNAs.

The experimental plan detailed in Figure 3.1 was employed in an effort to provide evidence for the model suggested in Figure 1.2. In short, this involved the isolation of pure populations of epithelial cells, spermatozoa and epididymosomes from the three archetypical segments of the epididymis. Following this, RNA was isolated from large and distinct biological pools of these samples and used as a starting point for NGS analyses. After generation of miRNA libraries at AGRF, accuracy of such libraries was assessed utilising Taqman RT-qPCR and a number of bioinformatics analyses. Subsequently, a variety of bioinformatics tools were used to demonstrate the miRNA profiles of each epididymal region in terms of epithelial cells, sperm and

epididymosomes. In order to tease apart the roles that miRNAs play in each epididymal component, each of these analyses was undertaken systematically in three separate studies published throughout 2015/16.

3.2 Next Generation Sequencing Analysis Reveals Segmental Patterns of microRNA Expression in Mouse Epididymal Epithelial Cells

The initial study, titled "Next Generation Sequencing Analysis Reveals Segmental Patterns of microRNA Expression in Mouse Epididymal Epithelial Cells" (published in PLoS ONE in 2015 and attached at the end of this document), sought to investigate the segment-segment expression changes of epididymal miRNAs. Several aspects of this study were underway prior to my involvement in the project, including; the identification of localisation and abundance of two key components of miRNA processing pathways (the DICER1 endonuclease and the AGO2 catalytic component of RISC), collection of RNA from whole epididymal tissue and pure epithelial cells populations, NGS sequence analyses and miRNA library generation, heat map and RT-PCR validation of NGS data, and the identification of targeted pathways through interrogation of IPA.

My contribution to this body work laid in the performance of additional bioinformatics analyses [see Figure 7]. Primarily, this involved the investigation of the functional significance of miRNAs characterised by dynamic expression profiles that were altered between epididymal segments. A reproductive genetic database with records of mouse epididymal gene expression was searched for experimentally validated targets of differentially accumulated miRNAs highlighted in this study. The expression of number of these genes, including *Hdac9*, *Smad3*, and *E2f3* was aligned with the abundance of miRNAs listed as targets by the online database miRTar, showing a close correlation between the spatial abundance of these miRNAs and their gene targets, as displayed in Figure 9 of the attached manuscript.

Further bioinformatics analyses were performed using data from a number of independent studies, order to calculate the level of species conservation between miRNAs sourced from whole epididymal tissue, and these analyses are documented in S3 and S4 Table of the attached

manuscript. Surprisingly, only 21 % of miRNAs identified were conserved across mouse, rat, and human datasets, the vast majority of which (81 %) were present in each epididymal segment, suggesting that these conserved miRNAs may play key regulatory roles in maintaining this reproductive tissue. An important caveat of this analysis was that differing sequencing strategies (i.e. microarrays vs NGS) were employed, a variance that could contribute to the relatively poor abundance observed in this study. However, what this analysis did provide was evidence of dynamic epididymal miRNA accumulation that can be observed across a range of species.

This initial study sought to provide the basis of the project detailed within this thesis. The identification of some 218 miRNAs in pure epididymal epithelial populations and the determination of their abundance in each segment of the tract reinforced the notion that a small population of these appear to regulate the protein production within the tract that is responsible for segment specific microenvironments, and therefore sperm maturation. The data within this study also served to identify additional contributions to the overall epididymal miRNA signatures, prompting investigation into the miRNA content of sperm within the tract.

3.3 The MicroRNA Signature of Mouse Spermatozoa Is Substantially Modified During Epididymal Maturation

The following study, titled "The MicroRNA Signature of Mouse Spermatozoa Is Substantially Modified During Epididymal Maturation" (published in Biology of Reproduction and attached at the end of this document), sought to investigate the changes in abundance of miRNAs accumulated within sperm of the epididymis. Similar to the previous publication, several aspects of this study were underway prior to my involvement in the project, including; the identification of localisation of miRNA processing machinery within testicular germ cells and epididymal sperm, isolation of sperm and RNA from these cells, NGS sequence analyses and miRNA library generation, heat map and RT-PCR validation of NGS data, and the identification of targeted pathways through interrogation of IPA.

Again, similar to the previous study on epididymal epithelial cell miRNAs, my

contribution to this publication involved bioinformatics analyses supplementary to the main body of text. Primarily, this involved conducting analyses to determine the level of conservation between miRNAs sourced from the highly enriched population of epididymal epithelial cells in our previous publication, and the sperm-borne miRNAs herein. This analysis confirmed that a most of the miRNAs identified in epithelial cells (213 / 218) were also present in our sperm dataset, though a portion of miRNAs (52) were found to be unique to sperm (Table 2 of the attached manuscript). The complex and dynamic profile of miRNAs identified in the analysis of epididymal sperm begs the question: Given these cells are transcriptionally and translationally quiescent, how are miRNAs being delivered to sperm during epididymal maturation? The leading hypothesis for such a phenomenon, documented in Figure 1.1 of this thesis, was that exosome-like vesicles of epididymal origins, titled 'epididymosomes' are produced by the epithelium with a specific set of cargo which is then delivered to the sperm via interactions between the vesicles and the sperm head. In order to provide a bioinformatic basis for this model, the level of conservation between mouse sperm miRNAs listed in our own study, and the content of bovine epididymosomes was determined (S1 table of the attached manuscript). Indeed, it was determined that most of the miRNAs held by bovine epididymosomes were represented in our own datasets, despite the limitations of differing sequencing technologies and the fact that this is a cross species analysis, therefore providing support that these molecules may be highly conserved across species, and there could be bestowed upon sperm by epididymosomes during epididymal transit. However, prior to 2016, direct evidence of the delivery of miRNAs to sperm had not yet been provided, and thus this phenomenon, as well as the full characterisation of epididymosome miRNA profiles, was explored in the third analysis of this study.

3.4 Characterisation of Mouse Epididymosomes Reveals a Complex Profile Of microRNAs and a Potential Mechanism for Modification of the Sperm Epigenome

The final study used to provide evidence for the role of miRNAs throughout the epididymis, titled "Characterisation of Mouse Epididymosomes Reveals a Complex Profile of

microRNAs and a Potential Mechanism for Modification of the Sperm Epigenome" (published in Scientific Reports in 2016 and attached at the end of this document), sought to investigate both the content of miRNAs harboured by these vesicles, as well as the ability of epididymosomes to bestow miRNA payload upon sperm in direct support of our proposed model. Prior to my commencement, a number of aspects of this study were already underway; these included the optimisation and validation of epididymosome isolation as depicted in Figure 1 of the manuscript, as well as the generation of the first replicate of RNA used for NGS analyses. Material used for the remaining two replicates were generated by myself, and AGRF worked to perform NGS and miRNA library assembly.

From here, I was directly responsible for generating the remaining bioinformatic analyses (Figure 2, Figure 3, Figure 4 A and C, Figure S2, and Tables S1 to S5). Additionally, I was responsible for generating material for, and performing analysis on two replicates of RNA used in RT-qPCR validation of NGS profiles. Further, I worked to conceive the sperm and epididymosome co-incubation protocol utilized throughout this study, and was responsible for generating the first two replicates used to document the transfer of miRNAs from the former to the latter *in vitro*, as well as producing a first draft of the initial manuscript.

The study of epididymosome miRNAs detailed an impressive of cohort of sRNAs within these vesicles, and worked to demonstrate that these miRNAs are largely characterised by significant fold changes in abundance between epididymal segments. Bioinformatics analyses determined that a number of miRNAs represented in epididymosome populations were absent from analyses of their parent cells, suggesting selective packaging epididymosome of cargo. More importantly, this study provided the first empirical evidence to support the notion that epididymosomes are capable of endowing sperm with a selection of miRNAs during the cell's transit through the epididymis. This finding effectively tied together the model previously described in Figure 1.1 that suggests that the miRNA cargo of sperm is altered via a sophisticated mechanism involving the production and shuttling of these molecules from the epididymal epithelium, to maturing gametes via specialised microvesicles. Importantly this has implications

for future research, as perturbations of epididymal miRNA profiles could result in altered sperm miRNA content and influence the trajectory offspring developmental. Such implications, as well as several other concepts pertaining to the body of work detailed in this chapter, are discussed further in Chapter 5 and 6 of this thesis.

Chapter 4: Identification and characterisation of novel miRNAs in the mouse epididymis

4.1 Introduction

The previous studies conducted by our research group, as well as those performed by independent researchers, have highlighted the importance that miRNAs hold within the male reproductive tract, in particular the epididymis. Given the vast number of miRNAs identified within this tract, and the high abundance of these regulatory molecules, it is likely that lowly abundant and yet to be characterised novel miRNA species may exist within this tract. Indeed, the epididymis presents a unique model for novel miRNA identification owing to the degree of segment-segment transcriptome, proteome and miRNA profile variations. Identification of additional miRNAs that have the potential to contribute to the regulation of epididymal microenvironments could provide further insight into the functional maturation of sperm as they progress through this tract. Moreover, as our previous work has provided evidence that these regulatory molecules may be delivered to sperm during epididymal transit, and it has been suggested that sRNAs are able to subsequently influence embryo health and developmental trajectory, the investigation of novel epididymal miRNAs is of high importance, and has therefore formed the basis of the second half of this project. As opposed to Chapter 3 of this study, the work captured within this section of the present study is yet to be published.

Varied approaches to miRNA discovery have resulted in the identification of an inventory consisting of thousands of miRNA species, with new entries being added to miRBase (www.mirbase.org), the principle online catalogue of miRNAs, on a daily basis [209]. The miRBase database comprises sequences and annotation of all previously experimentally validated miRNAs, while the miRBase registry houses data characterising novel miRNAs yet to be published, and each entry in miRBase details precursor hairpin structure, mature sequences,

genome coordinates, transcript information, deep sequencing data, and references [209]. The discovery and annotation of novel miRNAs has been both accelerated and streamlined through the development of improved NGS technologies. As a result, deep sequencing, in combination with several widely available bioinformatics tools, are now able to be employed by research groups to provide evidence for the existence of novel miRNA molecules with sufficient confidence that even predicted miRNA molecules are beginning to feature in the miRBase miRNA database. Many bioinformatic tools are available for the identification of novel miRNAs including miRDeep [202], miRanalyzer [210], miRScan [211, 212] and miRCat [206]. Typically, tools such as these first predict a putative miRNA in genome sequences according to the structural characteristics of each putative miRNA. This is accomplished by identifying sequences with hairpin structures similar to those of known miRNA precursors, specifically pre-miRNAs. A number of ancillary tools can then be utilised to filter candidate novel miRNAs, including the analysis of the stem-loop and mature sequences, miRNA* sequences, abundance (read count), encoding loci number and p-values. Further analyses, extending to observation of proposed stem-loop structures and BLAST searches against several databases to distinguish between true predictions, false positives and other types of sRNA molecules [202, 206, 210-212]. After prediction, various experimental techniques can be utilised to validate the existence of putative novel miRNAs, among the most popular of which are Northern blot hybridisation and RT-qPCR [213]. The current release of miRBase, release 21, (26-06-2014) details miRNAs in 223 species, with a total of 28,645 hairpin precursor and 35,828 mature miRNA molecule sequences housed in this release [209]. This is a significant addition to the 206 species, 24,521 precursors and 30,424 mature miRNAs detailed in the previous release (release 20; 24-06-2014) [209]. Generation of an impressively large number of molecules in such a short period of time calls into question their presence in cells, as well as the means and extent to which they influence biological pathways. Further, the burgeoning number of miRNAs being discovered has acted as a catalyst for the development of bioinformatic tools capable of predicting miRNA:mRNA interactions associated with each of these molecules.

As described in Section 1.4, miRNAs regulate gene expression at a post-transcriptional level via interactions with the 3' UTR of mRNAs [53-57]. This interaction is governed primarily by perfect Watson-Crick base pairing between the mRNA 3' UTR and the 5' located 'seed sequence' of the miRNA, which spans nucleotides 2 – 8, and can be supplemented by additional base pairing within the 3' end of the miRNA sRNA [57]. Further, it is well documented that a single transcript can contain several potential target sites for an individual miRNA, as well as target sites for many different miRNAs. Likewise, any one miRNA has the potential to regulate a number of genes via interactions with the 3' UTR, adding to the complexity of the regulatory networks governed by miRNAs [53, 55]. Many computational analysis tools have been developed in order to rapidly predict putative miRNA gene targets in lieu of large scale biological methods. Algorithms such as DIANA miR-microT [214, 215], miRDB [216, 217], RNAhybrid [218], PITA [219], and miRanda [220] were designed to tackle the immense task of identifying targets of the thousands of new miRNAs discovered each year and have been used extensively throughout research projects in the past [221-224].

Due to several modifications in algorithms resulting in different criteria of target identification, including base-pairing, target site accessibility (measured as the amount of energy required to unfold mRNA secondary structures to allow for miRNA:mRNA hybridisation) and evolutionary conservation of the site, recent studies often turn to the use of a suite of target prediction analyses, in an effort to increase scope and confidence of target selection [224-226]. These discrepancies in detection methods also result in a number of limitations, with studies directing their attention to the documentation of high false positive and false negative rates when identifying targets [227, 228]. Further, a number of target identification tools often function without providing the user with the ability to modify and restrict searches, limiting the ability to tailor analyses to a higher degree of discrimination. Though a small selection of identification tools simply require the input of a custom miRNA sequence and parameters of selection to deliver an extensive list of > 1,000 targets (such as miRDB and DIANA miR micro-T), the majority of analysis tools require the user to identify and input the sequence of the 3' UTRs of specific genes

of interest into the software one by one. This has resulted in researchers opting to utilise a pipeline of tools that results in the progressive narrowing of the scope of putative miRNA targets, as each gene is screened for target potential through subsequent analysis tools.

4.2 Identification of Novel miRNAs

After having documented the full complement of known miRNAs present in epididymal epithelial cells, spermatozoa and epididymosomes, the attention of this project was turned to the discovery of novel miRNA species. These studies were undertaken with the goal of identifying a cohort of previous unidentified miRNAs that may contribute to the regulation of the epididymal microenvironments responsible for driving sperm maturation. The impetus for such studies stems from previous studies conducted by both our own research group, as well as independent researchers, which suggest that miRNAs form a key regulatory network in the epididymis, and that these molecules may also be distributed to sperm where they can work to influence downstream biological processes in the female reproductive tract.

Using a suite of well documented tools and techniques, a bioinformatic workflow was designed in order to confidently identify and characterise novel miRNAs, and this is presented in Figure 4.1.

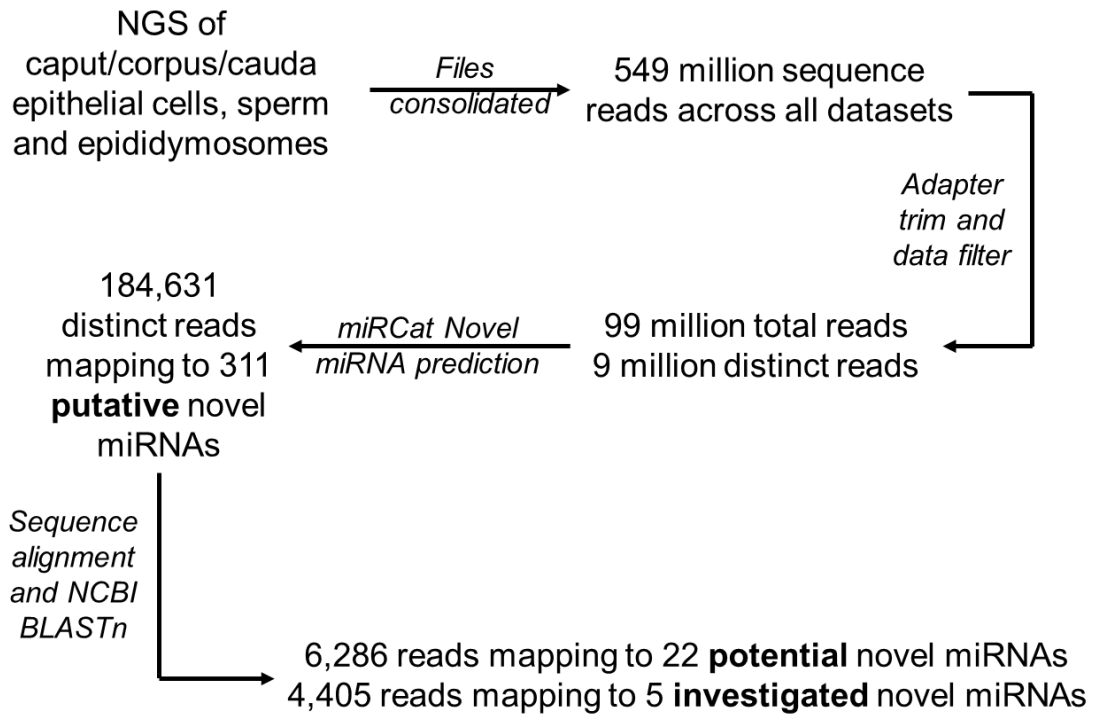

Figure 4.1: Bioinformatic workflow for identifying novel miRNAs. Small RNA libraries resulting from next generation sequencing analyses conducted in previous studies [161-163] were interrogated in an effort to identify potentially novel miRNAs. After all 21 files were consolidated into a master FASTA file and adapter sequences were trimmed, the UEA sRNA workbench tool, "miRCat", was employed to identify putative novel miRNAs. Each of these sequences were screened via NCBI BLASTn searches to eliminate false positive, resulting in a number of putative novel miRNAs. From these, 5 hypothetical miRNAs were selected for further investigation, based on total read abundance and differential read values between epididymal segments.

The Illumina HiSeq sRNA sequencing files (FASTQ format) generated by AGRF as part of our group's previous studies (Appendix 15), in combination with UEA sRNA Workbench v 3.2 [206], were used as the foundation of the identification of novel miRNAs in the mammalian epididymis. Initially, the 549 million total reads detected across all libraries were compiled into a master file (FASTA format). Subsequently, adapter sequences (5' - TGGAATTCTCGGGTGCCAAGG) were trimmed from sequences and reads were filtered for sizes of 20 – 25 nt. The miRCat tool was then used to probe the master file for the presence of putative novel miRNAs resulting in ~184,631 reads being mapped to 311 putative novel miRNAs (*Nov-miR*s), listed as *Nov-miR*s 1 to 311. Several data filters were applied and , rigorous BLASTn searches [229] against various databases were conducted to remove false positives and

narrow the list of novel miRNAs down before further evaluation.

Secondary structures of potential novel miRNA stem-loops were visualised as a means of further assessing each candidate. The folding structure of precursor for each putative novel miRNA stem-loop was generated using the RNAfold software [207] in conjunction with the RNA visualisation tool VARNA [230]. Stem-loops were assessed for several key standard miRNA features, including; (1) the start and end position of the mature novel miRNA; (2) less than 5-nt bulges within the miRNA/miRNA* duplex (i.e., 5 consecutive mismatched dsRNA base-pairings); (3) abnormal (forked or branched) dsRNA structures within the overall stem-loop structure, and; (4) a minimum free energy (MFE) of less than -15 kcal/mol. Using this criteria set, the precursors of 22 *Nov-miR*s were determined to have folding structure properties corresponding to those of the folding structures adopted by the precursor transcripts of canonical pre-miRNAs, and the predicted stem-loop structures of *Nov-miR*13, *Nov-miR*37, *Nov-miR*42, *Nov-miR*101 and *Nov-miR*12 have been visualised in Figure 4.5.

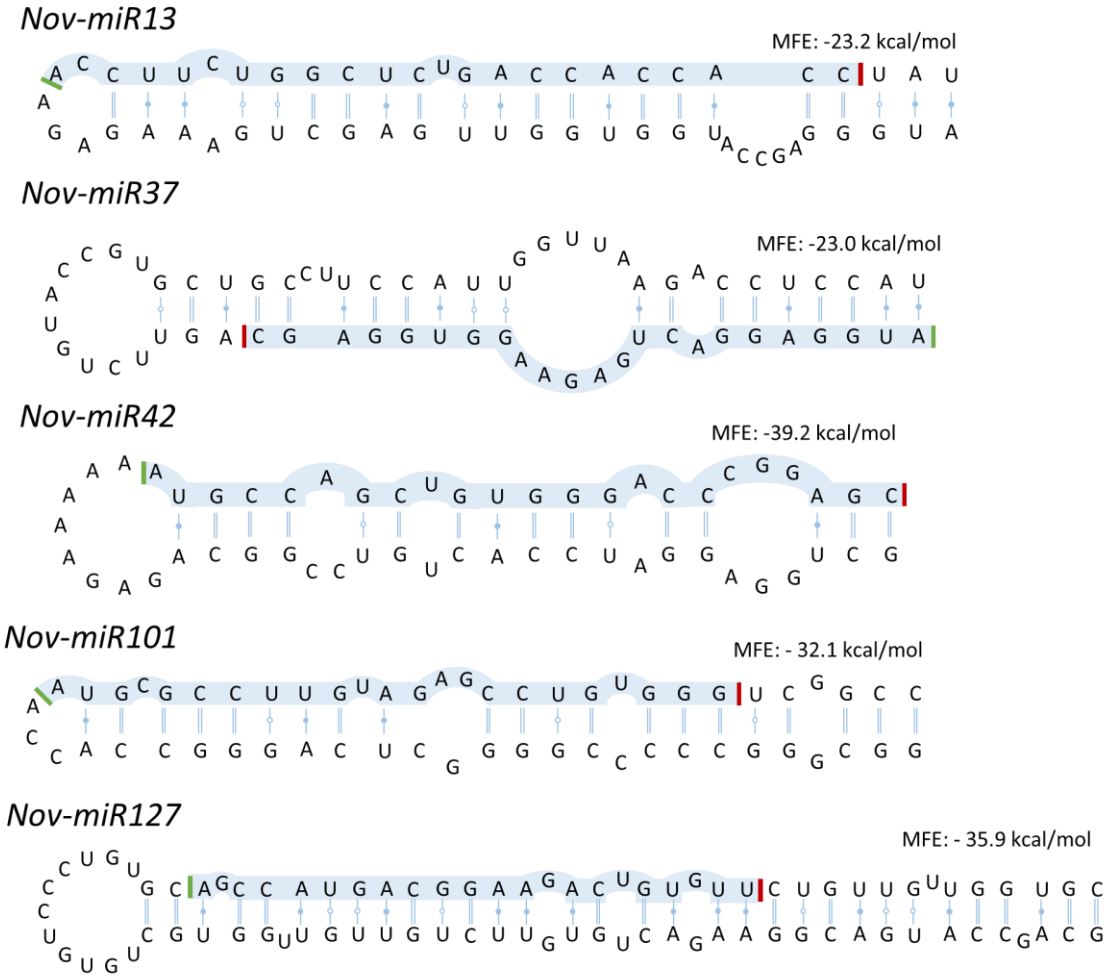

Figure 4.2: Predicted secondary structure of putative novel precursor stem-loops for the five investigated miRNAs. Mature miRNA sequences as detected by next generation sequencing analyses are denoted in blue. Start and end positions of the mature product are marked with green and red bars, respectively. MFE, minimum free energy of the stem-loop structure.

A number of novel miRNAs were removed from the total list of potential novel miRNAs based on inappropriate precursor stem-loop structures, leaving the 22 *Nov-miR*s listed in Appendix 16. The predicted secondary structure of all remaining novel miRNAs stem-loops investigated further are shown in Appendices 23 – 26. Ultimately, each stem-loop sequence presented is quite standard, possessing typical stem-loop structures that are free of bulges at the site of the mature miRNA, and are characterised by low MFE (i.e. < -15 kcal/mol; the lower the free energy, the more likely the structure will form). Sizes of stem-loop structures varied greatly, ranging from 93- to 55-nt, with an average of 68-nt. Similarly, MFE values for stem-loop secondary structures showed a high degree of variation, spanning from -15.6 kcal/mol to

- 39.2 kcal/mol and an average of -25.3 kcal/mol, as expected of miRNA stem-loops.

The sequences of each of the 22 potential novel miRNAs mentioned previously were aligned back against each of the original FASTQ sequencing files in order to determine abundance of each putative novel miRNA in each dataset. The resulting sequence reads were normalised as counts per million (CPM) against the number of reads mapping to 22-nt sequences remaining in each sRNA library after adapter trimming using the following equation:

$$CPM = \frac{Raw\ abundance\ of\ novel\ miRNA}{Mapped\ 22nt\ reads} \text{ x } 1{,}000{,}000$$

Of the remaining 22 potential novel miRNAs, five putative miRNAs (Figure 4.2) were selected for further analysis, including identification of targets and biological validation. Summary tables of bioinformatics output generated by miRCat, as well as abundance (in number of reads) of novel miRNAs (*Nov-miR*s) are depicted in Tables 4.1 and 4.2 respectively, while more extensive lists are included in Appendices 16, 20-23.

Table 4.1: Summary of putative novel miRNAs selected for further analysis.

Novel miRNA ID	Chromosome	Sequence	sRNA Length	Stem-Loop Length	Genomic Hits
Nov-miR13	2 dna_sm:chromosome chromosome:GRCm38:2:1:182113224:1	ACCTTCTGGCTCTGACCACCACC	23	57	1
Nov-miR37	13 dna_sm:chromosome chromosome:GRCm38:13:1:120421639:1	ATGGAGGACTGAGAAGGTGGAGC	23	62	1
Nov-miR42	13 dna_sm:chromosome chromosome:GRCm38:13:1:120421639:1	ATGCCAGCTGTGGGACCCGGAGC	23	75	2
Nov-miR101	17 dna_sm:chromosome chromosome:GRCm38:17:1:94987271:1	ATGCGCCTTGTAGAGCCTGTGGG	23	57	1
Nov-miR127	16 dna_sm:chromosome chromosome:GRCm38:16:1:98207768:1	AGCCATGACGGAAGACTGTGTT	22	92	1

Table 4.2: Abundance of putative novel miRNAs selected for further analyses.

Novel miRNA	Spermatozoa			Epithelial Cells			Epididymosomes		
	Caput	Corpus	Cauda	Caput	Corpus	Cauda	Caput	Corpus	Cauda
Nov-miR13	29	822	0	14	179	13	18	503	39
Nov-miR37	22	48	5	10	24	40	2	13	62
Nov-miR42	2	39	1	2	17	10	3	15	11
Nov-miR101	3	32	0	0	4	3	1	4	0
Nov-miR127	1	0	23	0	0	0	0	0	1

*Grey highlighted cells indicates that the average read counts were below threshold of detection.

As described above, a total of 22 putative novel miRNAs remained to which 6,286 were confidently aligned after several filters were applied to the dataset. While the majority of these were detected at low abundance that approached that of the threshold set for positive detection (10 CPM), several *Nov-miR*s appeared to be relatively abundant within epididymal samples, including those chosen for further validation. In total, 19, 4 and 10 *Nov-miR*s were detected in spermatozoa, epithelial cells and epididymosomes, respectively. In fact, 11 *Nov-miR*s were found to be unique to sperm, 3 *Nov-miR*s were unique to epididymosomes (with a total of 7 *Nov-miR*s detected in epididymosomes being absent from epithelial cell analyses), while none of the filtered list of 22 *Nov-miR*s were unique to epithelial cells. The average length of mature *Nov-miR* sRNA was 22-nt (with 4 / 5 of the *Nov-miR*s selected for further analysis being 23-nt in length), with an average G/C content of 55.2 % and the majority of *Nov-miR*s being present at only one chromosomal location. Several putative *Nov-miR*s were found to map to common chromosomes, with five of the putative novel miRNAs being located on chromosome 2, while chromosomes 7 and 13 each had three novel miRNAs mapped to them.

4.2 Potential Targets of Novel miRNAs

Genes with the potential to be regulated by the five putative novel miRNAs were identified using a rigorous screening process. This included utilising several well-established bioinformatic tools documented in a range of previous studies focussing on the identification of miRNA targets [221-224]. The workflow utilised for putative target gene identification is illustrated below in Figure 4.6.

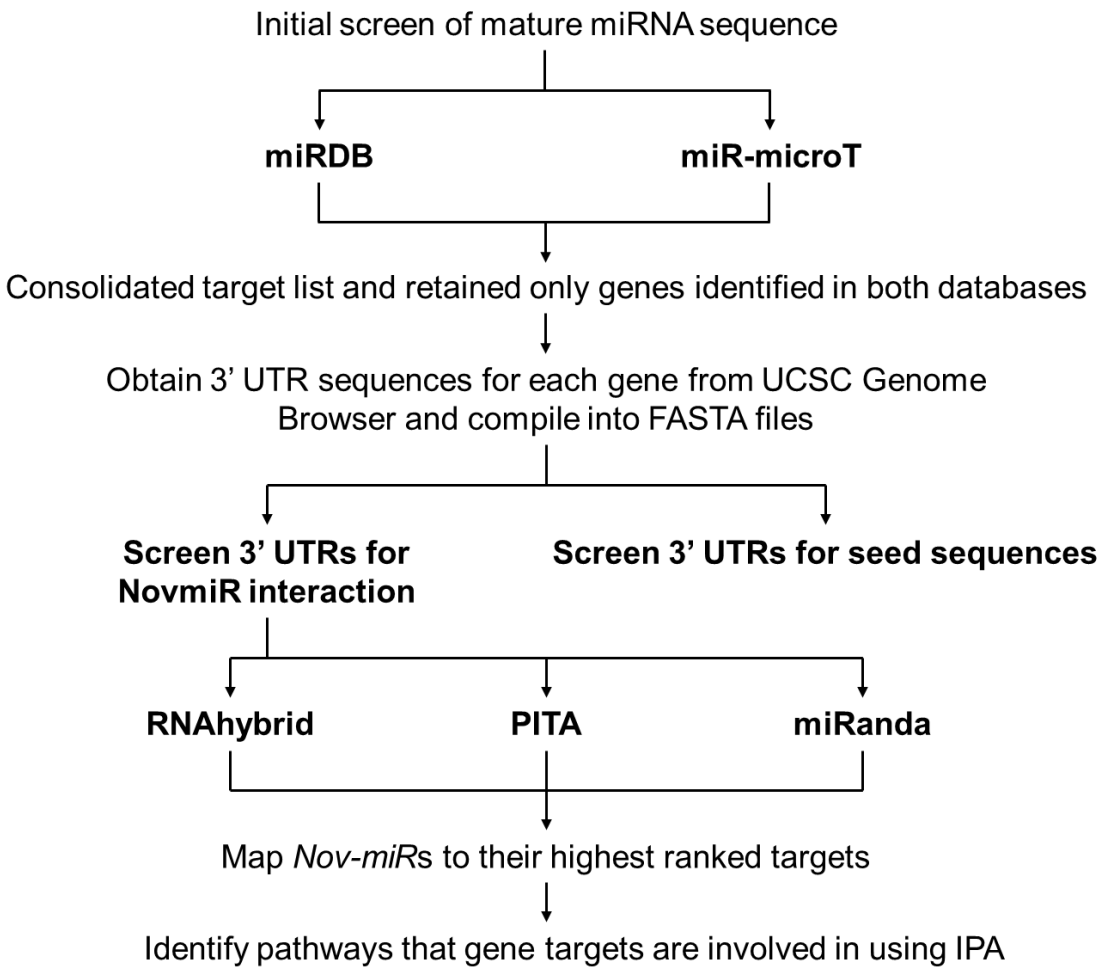

Figure 4.3: Flowchart illustrating target identification of novel miRNAs. Novel miRNA sequences were first screened for potential targets using two algorithms: miRDB and miR-microT. The 3' UTR of genes flagged by both analyses were then checked for the presence of miRNA seed sequences and screened using three additional algorithms: RNAhybrid, PITA and miRanda. Potential target genes of each of the five analysed putative novel miRNAs were ranked as per an average weight across each analysis (see accompanying text) and the duplexes of the top five target genes and the corresponding putative novel miRNA were aligned. Subsequently, the pathways potentially under miRNA-directed gene expression regulation by these five putative novel miRNAs were identified using Ingenuity Pathway Analysis software.

Initially, sRNA sequences of the five putative novel miRNAs identified in miRCat analyses were used to screen for potential target genes using the established miRDB [216, 217] and miR-microT [214, 215] tools. Both of the applied tools allow for the prediction of potential target genes for miRNA sRNAs solely based on the seed sequence of the molecule. After compiling the 300 most likely predicted genes (based on confidence scoring) identified by each database, 50, 78, 50, 5 and 41 target gene mRNAs were identified as putative targets of

*Nov-miR*13, *Nov-miR*37, *Nov-miR*42, *Nov-miR*101 and *Nov-miR*127 respectively, in both analyses. The 3ˈUTR of each of each these putative target genes were then obtained via interrogation of the UCSC Genome Browser. Each sequence was subsequently formatted as a FASTA file in preparation for further target gene interrogation. First, seed sequences of *Nov-miR*s were identified in the 3ˈUTRs of their respective targets and tallied. Approximately 96 % of *Nov-miR* seed sequences were found in their corresponding 3ˈ UTRs equal to, or greater than 5 times. Interestingly, *Card10*, a potential target of *Nov-miR37* was found to contain 31 target sequences for the *Nov-miR37* seed sequence. Subsequently, the aforementioned FASTA files were employed in combination with the corresponding novel miRNA sequences in order to screen for potential miRNA:mRNA interactions using either tools that required sequences to be screened one-by-one (RNAhybrid [218] and PITA [219]) or those that allowed for input of gene sequences *en masse* (miRanda [220]). Default thresholds of prediction confidence were used for each analysis, and genes were required to be identified by at least three of the total five databases in order to be considered for further analyses. The vast majority of gene targets were identified across all five prediction tools, with only four genes being identified in < 3 of the five analysis tools used and ~98 % of the remaining miRNAs being identified in each analysis approach. Potential target genes of *Nov-miR*s were then assigned a rank according to the score provided by each prediction tool. Overall confidence ranks for each target gene was then determined by averaging confidence ranks across each dataset and the subsequent generation of a final list in descending order. A summary of the top 5 ranked target genes potentially regulated by each of the five analysed putative novel miRNAs is presented in Table 4.3, while a more comprehensive table of candidate genes is provided in Appendix 27.

Table 4.3: Summary of novel miRNA targets identified with the highest level of confidence across several analysis tools.

Targeted Gene	Analysis Tool					# of Seed in 3'UTR
	miRDB[1,2]	miR-microT[3,4]	RNAhybrid[5]	PITA[6]	miRanda[7]	
Nov-miR13						
Atp6v1c1	+	+	+	+	+	1
Ccnj	+	+	+	+	+	3
Traf3	+	+	+	+	+	2
Cdh20	+	+	+	+	+	2
Dgkk	+	+	+	+	+	4
Nov-miR37						
Ankrd45	+	+	+	+	+	10
Card10	+	+	+	+	+	31
Sbk3	+	+	+	+	+	5
Tnfrsf11a	+	+	+	+	+	2
Clvs1	+	+	+	+	+	3
Nov-miR42						
Mfrp	+	+	+	+	+	3
Rbx1	+	+	+	+	+	2
Trip12	+	+	+	+	+	1
Slc6a6	+	+	+	+	+	2
2810403A07Rik	+	+	+	+	+	1
Nov-miR101						
Tctn3	+	+	+	+	+	2
Tgoln1	+	+	+	+	+	1
Apc2	+	+	+	+	+	1
Obfc1	+	+	+	+	+	1
Tenm2	+	+	+	+	+	1
Nov-miR127						
Cenpo	+	+	+	+	+	3
Rapgef2	+	+	+	+	+	1
Ptbp3	+	+	+	+	+	2
Adamts5	+	+	+	+	+	1
Foxp2	+	+	+	+	+	3

After having identified the gene targets with the highest confidence predictions across each analysis tool, the duplexes formed via interactions between the 3' UTR and *Nov-miR* molecules were predicted using an extension of the RNAhybrid tool. Internal loops were constricted to ≥ 6 nt, while a perfect match between the *Nov-miR* seed sequence and the target 3' UTR was required (with G/U wobble allowed). Interactions between *Nov-miR*s and gene targets predicted with the highest confidence across databases, along with the MFE (within

a -15 kcal/mol threshold) associated with the respective duplex is illustrated in Figures 4.7 through 4.11.

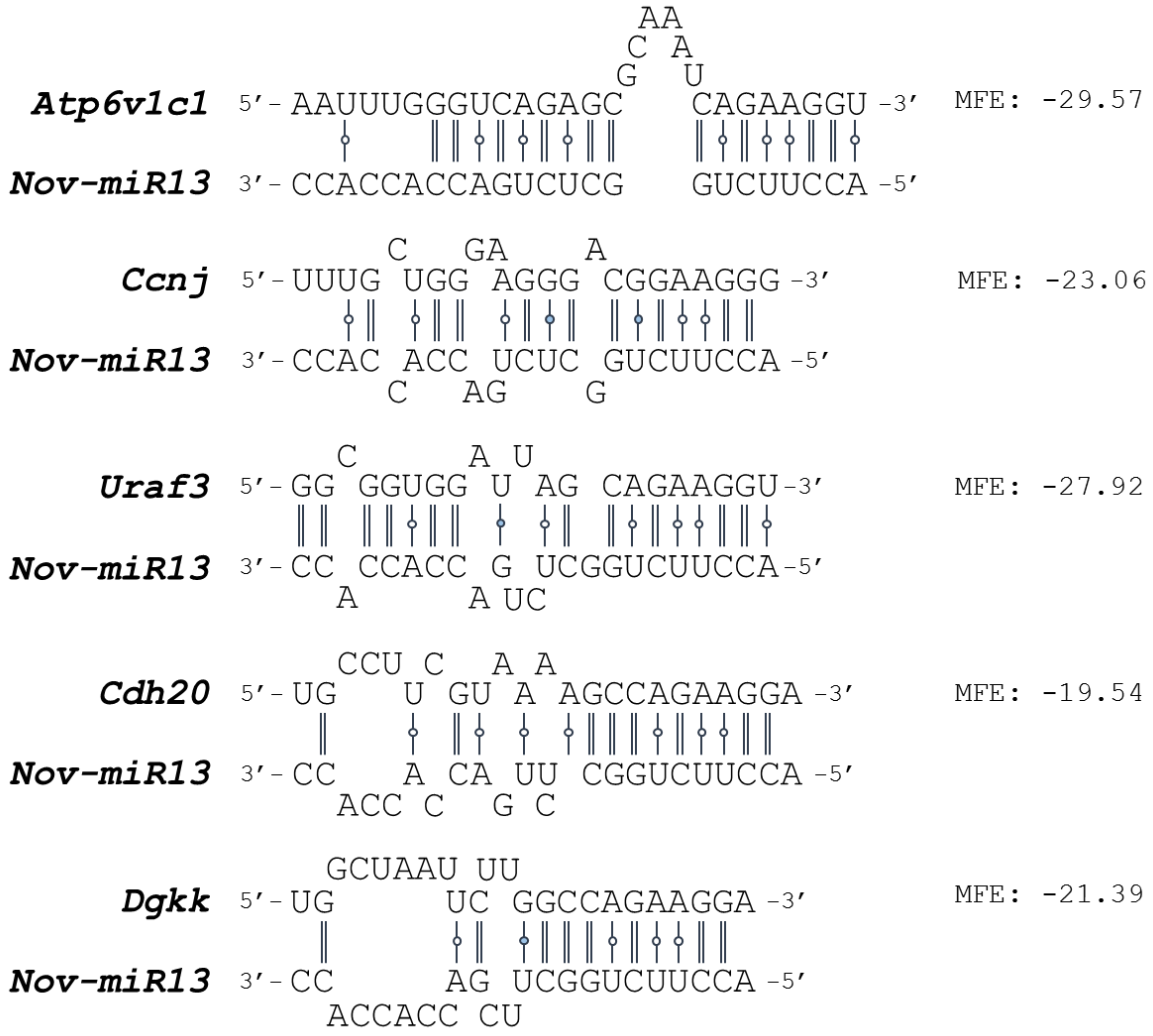

Figure 4.4: Duplexes formed at potential sites of interaction between *Nov-miR13* and putative target genes. Duplexes formed between *Nov-miR*13 and the five most confidently predicted gene targets identified in this study (*Atp6v1c1*, *Ccnj*, *Traf3*, *Cdh20*, and *Dgkk*) were generated with the aid of RNAhybrid.

The five most highly ranked predicted mRNA targets of *Nov-miR13* were *Atp6v1c1*, *Ccnj*, *Traf3*, *Cdh20*, and *Dgkk*. The interactions between *Nov-miR13* and the top five predicted genes were characterised by an MFE range of -29.57 kcal/mol to -19.54 kcal/mol. Further, each interaction displayed imperfect binding downstream of the seed sequence, with *Dgkk* and *Atp6v1c1* each containing a 6-nt bulge in the miRNA/mRNA target duplex; the maximum allowed by these analyses. Finally, each of the interactions visualised possessed between 2- to 4-nt of complementary binding within the 'centred site' spanning between miRNA nt 13 – 16, with

Atp6v1c1 displaying perfect homology to the centred site of *Nov-miR13*.

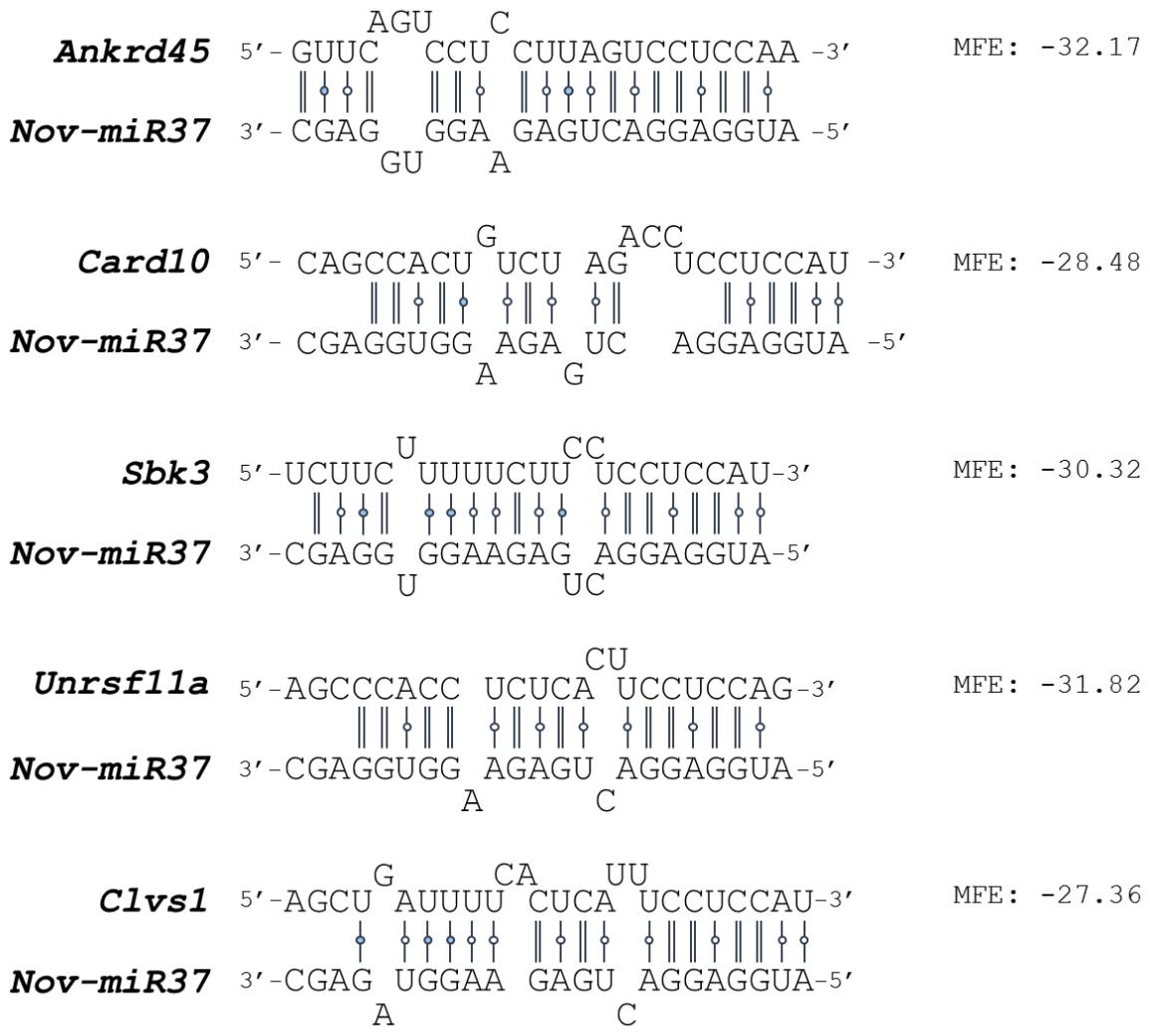

Figure 4.5: Duplexes formed at potential target sites of between *Nov-miR37* and putative target genes. Duplexes formed between *Nov-miR37* and the five most confidently predicted target genes, *Ankrd45*, *Card10*, *Sbk3*, *Tnrsf11a*, and *Clvs1*, identified in this study. Each miRNA/target mRNA schematic was generated with the aid of RNAhybrid.

The five highest ranked predicted targets of *Nov-miR37* were *Ankrd45*, *Card10*, *Sbk3*, *Tnrsf11a*, and *Clvs1*. The MFE characterising the interactions between the *Nov-miR37* sRNA and the 3' UTR of each predicted target genes were well below the applied threshold, with a range of -32.17 kcal/mol to -28.48 kcal/mol. Further, imperfect binding downstream of the seed sequence was apparent in each interaction, with the maximum bulge within the duplex of 3-nt being observed for the *Nov-miR*37 sRNA interactions with the *Ankrd45* and *Card10* putative target transcripts. Each of the visualised interactions possessed either 3- or 4-nt of base-pairing

within the ‘centred site’, with both the *Clvs1* and *Sbk3* putative target transcripts showing perfect homology to the centred site of the *Nov-miR37* sRNA.

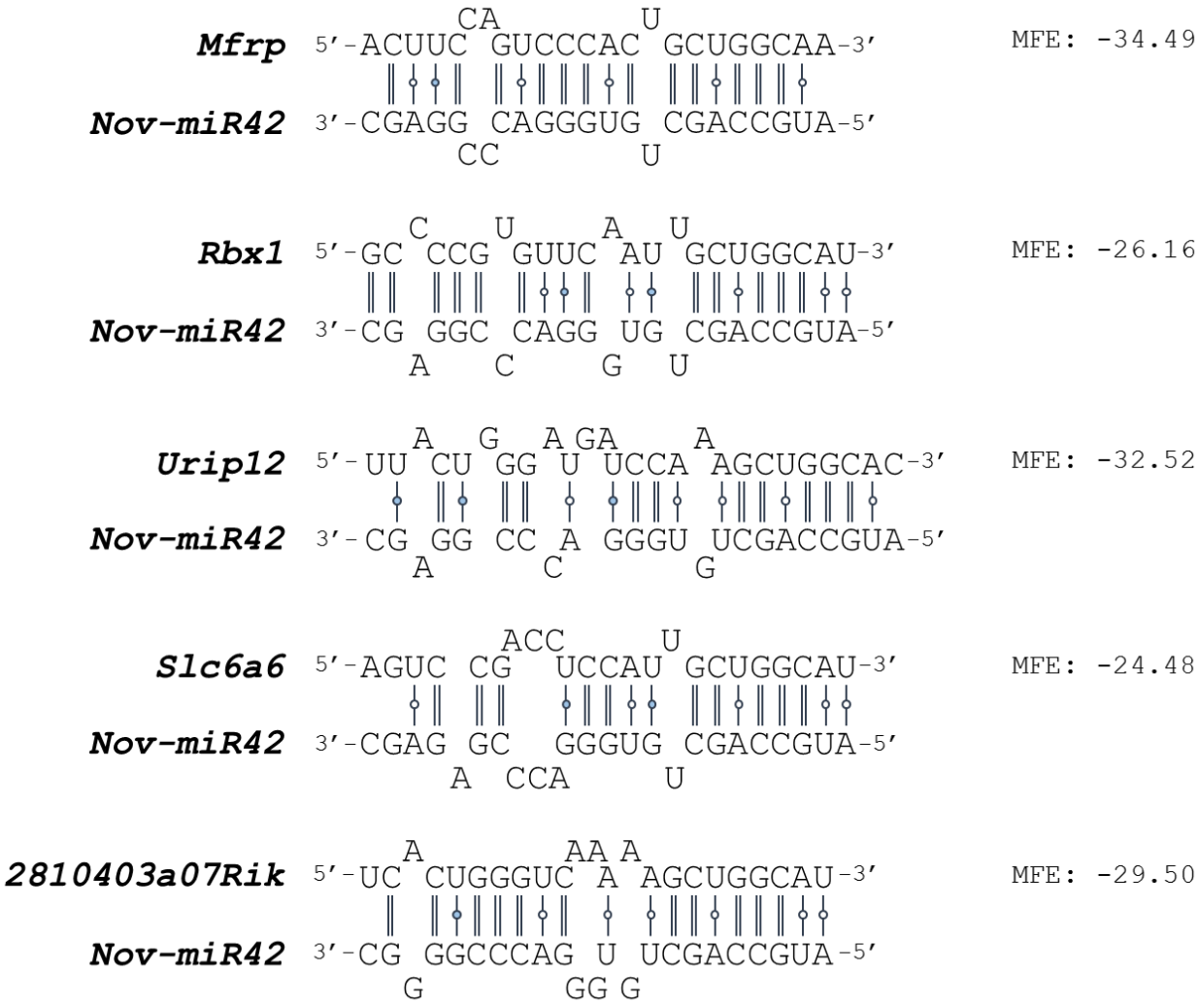

Figure 4.6: Duplexes formed at potential sites of interaction between *Nov-miR42* and putative target genes. Duplexes formed between *Nov-miR42* and the five most confidently predicted gene targets identified in this study (*Mfrp*, *Rbx1*, *Trip12*, *Slca6*, and *2810403a07Rik*) were generated with the aid of RNAhybrid.

Interactions between the 3' UTRs of *Mfrp*, *Rbx1*, *Trip12*, *Slc6a6*, and *2810403a07Rik* and *Nov-miR42* were characterised by an MFE range of -34.49 kcal/mol to -24.48 kcal/mol, with the *Nov-miR42:Mfrp* interaction reporting the lowest MFE score encountered throughout this study. Each duplex contained imperfect Watson-crick binding downstream of the miRNA seed sequence, with the maximum bulge within the duplex again being of 3 nts and observed within *Slc6a6*. Interactions visualised possessed 2 – 4 nts of complementary binding to the *Nov-miR42* centred site spanning between nts 13 – 16, with *Mfrp* and *Rbx1* showing perfect homology.

Figure 4.7: Duplexes formed at potential sites of interaction between *Nov-miR101* and putative target genes. Duplexes formed between *Nov-miR101* and the five most confidently predicted gene targets identified in this study (*Apc3*, *Tctn3*, *Tgoln1*, *Obfc1*, and *Tenm2*) were generated with the aid of RNAhybrid.

The mature sequence of *Nov-miR101* was found to most likely align to the 3' UTRs of *Apc3*, *Tctn3*, *Tgoln1*, *Obfc1*, and *Tenm2*. These interactions were characterised by an MFE range of -27.07 kcal/mol to -18.65 kcal/mol, with the *Nov-miR101:Tgoln1* interaction being the closest to the threshold of all interactions studied. Each duplex contained several mismatches downstream of the miRNA seed sequence, with the maximum bulge within the duplex again being of 4 nts and observed within *Tgoln1*. Interactions visualised possessed 1 – 4 nts of complementary binding to the *Nov-miR101* centred site spanning between nts 13 – 16, with *Apc3* and *Obfc1* showing perfect homology and *Tgoln1* demonstrating just 1 nt of homology within the site.

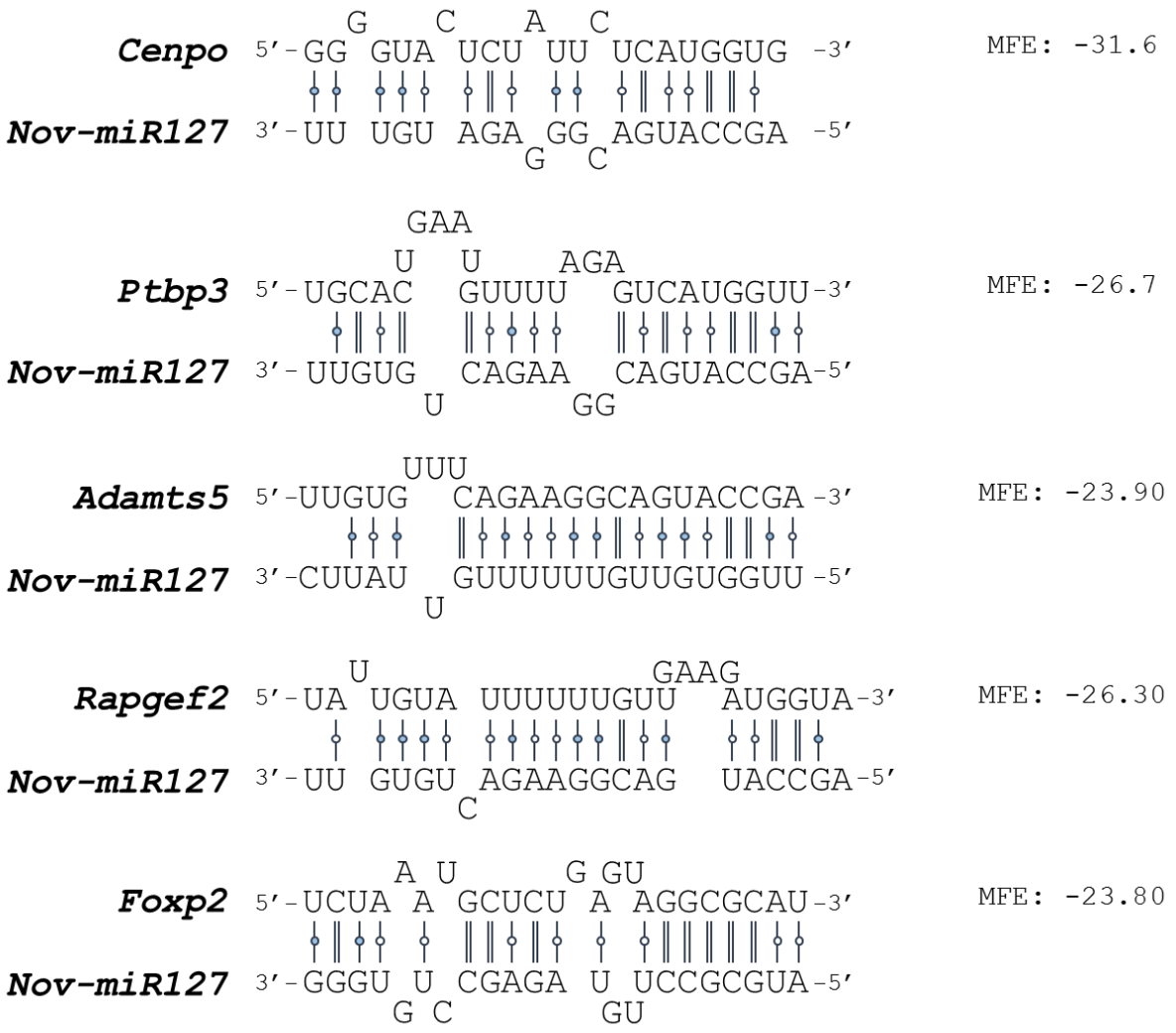

Figure 4.8: Duplexes formed at potential sites of interaction between *Nov-miR127* and putative target genes. Duplexes formed between *Nov-miR127* and the five most confidently predicted gene targets identified in this study (*Cenpo*, *Ptbp3*, *Adamts5*, *Rapgef2*, and *Foxp2*) were generated with the aid of RNAhybrid.

Nov-miR127 was found to most likely bind to the 3' UTRs of *Cenpo*, *Ptbp3*, *Adamts5*, *Rapgef2*, and *Foxp2*. The interactions between *Nov-miR127* and each of these genes were characterised by an MFE range of -31.60 kcal/mol to -23.80 kcal/mol, while each duplex displayed imperfect binding downstream of the seed sequence, with *Rapgef2* containing a 4 nts bulge in the duplex – the maximum allowed by these analyses. The interactions visualised possessed either 3 or 4 nts of complementary binding within the 'centred site' spanning between nts 13 – 16, with *Ptbp3*, *Adamts5*, and *Foxp2* displaying perfect homology to the centred site of *Nov-miR127*.

After identifying potential targets for each of the five putative novel miRNAs, bioinformatics analyses were conducted to determine the biological pathways that each miRNA potentially indirectly influences via target genes expression regulation. Through interrogation of datasets using Ingenuity Pathway Analysis (IPA) software with experimentally validated filters, several pathways governing a number of key biological processes were identified. The processes potentially influenced by the five putative novel miRNAs are illustrated in Figure 4.12.

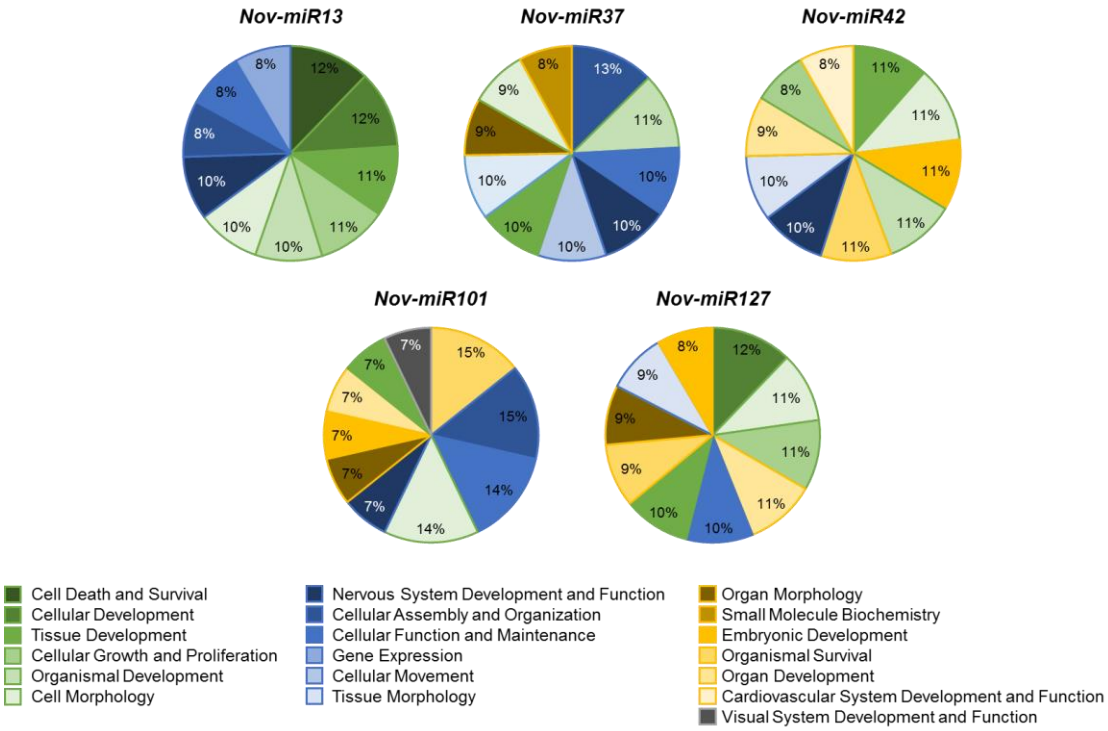

Figure 4.9: Significant biological pathways potentially regulated by identified *Nov-miR*s. Biological functions of potential novel miRNA gene targets were predicted using Ingenuity Pathway Analysis software. The percentage of genes involved in the top 10 processes identified were plotted in pie charts. Common pathways identified were involved in biological processes including; cell death and survival, cellular assembly and organisation, tissue development, cellular development, and organismal survival.

Genes with the potential to be regulated by *Nov-miR*s are involved in a wide range of biological processes and pathways with 19 different processes being highlighted by IPA analyses across all *Nov-miR*s. Among the most commonly identified processes across all *Nov-miR*s were cellular development, cell death and survival, cellular growth and proliferation, and cellular movement, processes that featured among the most frequently mapped-to pathways in our previous analysis performed on known mouse epididymal miRNAs. However, a number of

pathways, (including nervous system development and function, cellular assembly and organisation, tissue morphology, and organ morphology), were identified as prominent pathways influenced by *Nov-miR* target gene proteins, despite not being detected in prior analyses of known miRNAs. *Nov-miR13* primarily mapped to the cell death and survival, cellular development, and tissue development biological processes, with a total of 15 pathways being identified in this analysis. Similar numbers of pathways were recorded for *Nov-miRs 37* (cellular assembly, organismal development, and cell function and maintenance, 12 total identified), *42* (tissue development, cell morphology, and embryonic development, 10 identified in total), and *101* (organismal development, cellular assembly and organisation, and cell function and maintenance, 10 total). *Nov-miR127* mapped to the most biological processes (23) with the highest ranked processes being cellular development, cell morphology, and cellular growth and proliferation.

4.3 Validation of Novel miRNAs

A final point of previous studies identifying novel miRNAs is the experimental validation of proposed molecules in a biological setting using a variety of different approaches. In order to provide a line of biological evidence to confirm the validity of the putative novel miRNAs analysed here, RT-qPCR in conjunction with customised Taqman primers was employed. As epididymosomes lack the capacity for a functional miRNA processing pathway, validation of novel miRNAs was directed at distinct biological pools of RNA that differed from those used for NGS analyses, and were sourced from epididymal epithelial cells and spermatozoa. RT-qPCR generated data is presented in Figures 4.13 and 4.14, while raw counts and amplification curves for each biological replicate are presented in Appendices 28 – 51, and formatted analyses of each biological replicate are shown in Appendices 52 and 53.

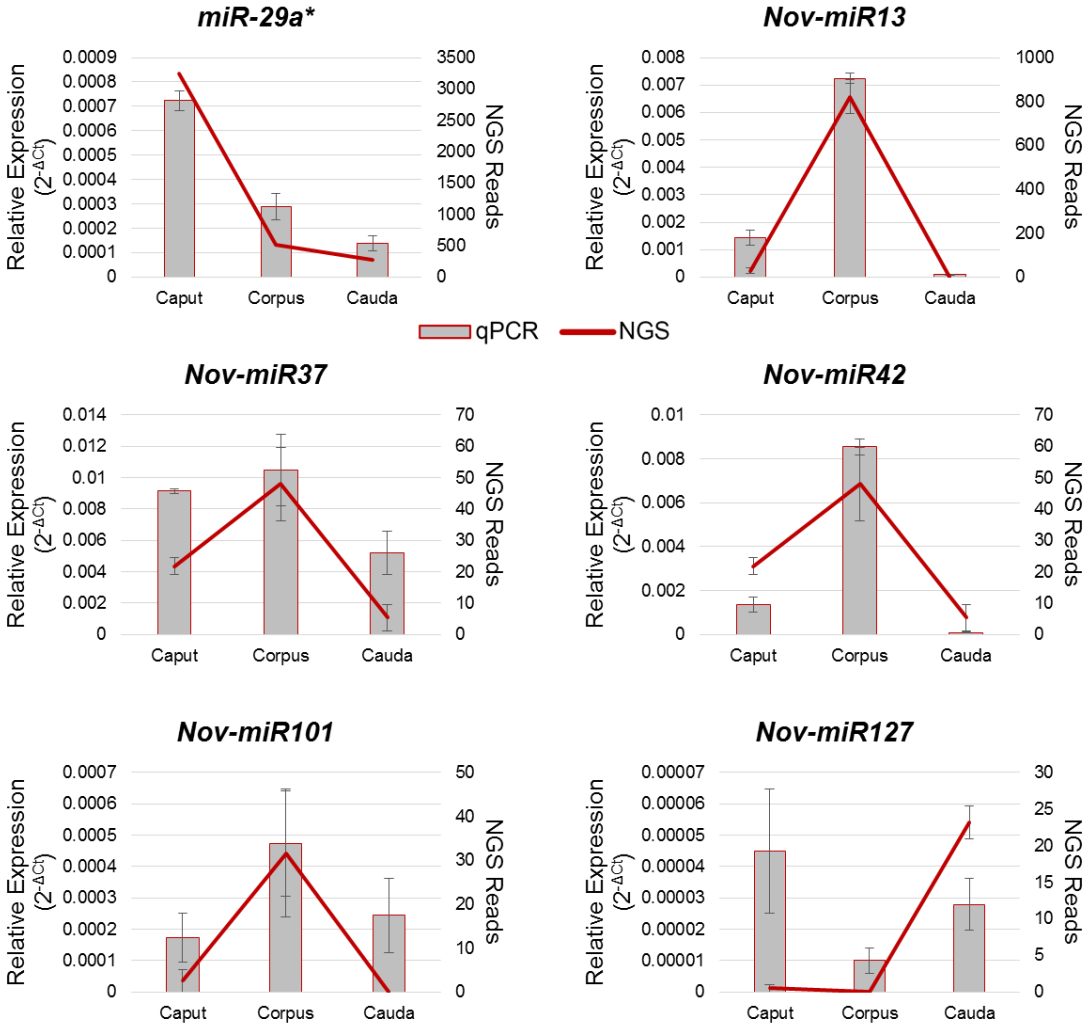

Figure 4.10: TaqMan RT-qPCR validation of novel miRNAs in epididymal spermatozoa. Pooled biological samples (n = 9-12 mice), differing to those employed in NGS analyses, were analysed in triplicate in order to verify the presence of novel miRNAs. All data were normalized against the U6 sRNA internal control. Quantitative PCR data is expressed as grey columns while NGS reads are overlaid as dark red lines.

In order to confirm that next generation sequencing data is faithfully reporting the dynamic accumulation of novel miRNAs in the epididymis, an initial screen of the highly accumulated and differentially expressed molecule, *miR-29a**, was also performed. As shown in Figure 4.13, the RT-qPCR data for *miR-29a** mirrors that of the NGS data, a trend observed across each of the three biological replicates analysed (Appendix 28 – 41). Similar trends were observed when analysing the presence of the novel miRNAs, *Nov-miR13* and *Nov-miR42*, across each assessed biological replicate. However, it should be noted that, although the RT-qPCR data for *Nov-miR101* appears to mirror that of the NGS data across epididymal segments, differences

in abundance between biological replicates have resulted in substantial standard error. Furthermore, only the third biological replicate for assessment of *Nov-miR37* and *Nov-miR101* levels showed an accumulation profile similar to the NGS reads when analysed by RT-qPCR. Validations of *Nov-miR*s was also performed on isolated epididymal epithelial cells.

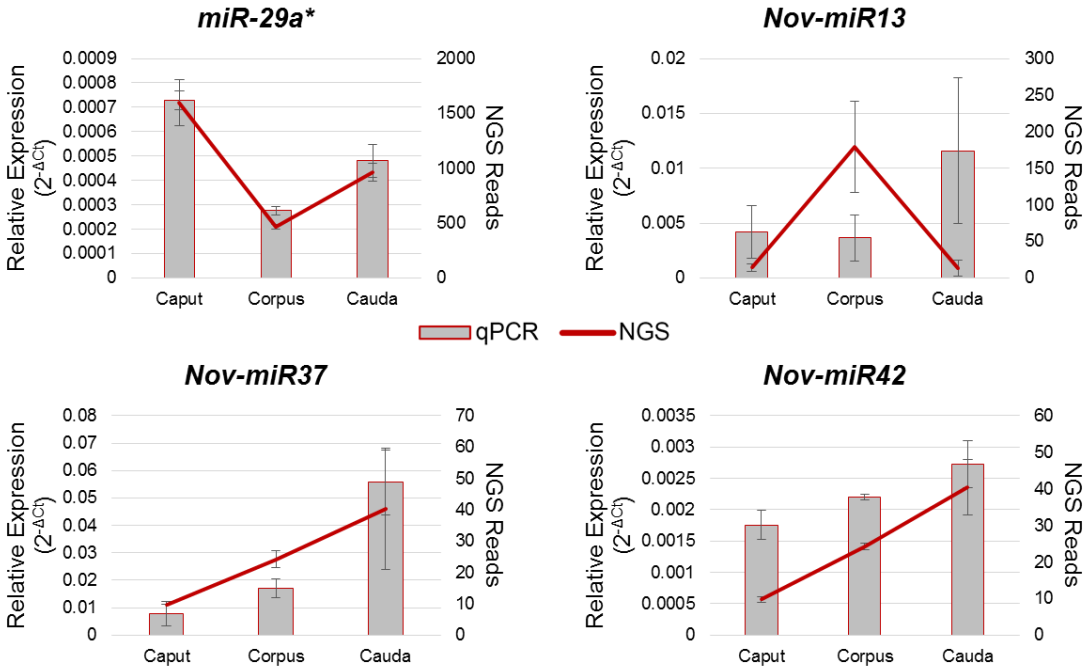

Figure 4.11: TaqMan RT-qPCR validation of novel miRNAs in epididymal epithelial cells. Pooled biological samples (n = 9-12 mice), differing to those employed in NGS analyses, were analysed in triplicate in order to verify the presence of novel miRNAs. All data were normalized against the U6 sRNA internal control. Quantitative PCR data is expressed as grey columns while NGS reads are overlaid as dark red lines.

The known miRNA, *miR-29a**, was again employed in order to confirm the accuracy of NGS sequencing data of epithelial cells. As shown in Appendices 42 – 51, the first replicate for each miRNA in epithelial cell analyses does not match the NGS data. Therefore, this data has been omitted from the analysis depicted in Figure 4.14 and as such, statistical analyses were not performed. As Figure 4.14 demonstrates, the second two biological replicates of the *miR-29a** RT-qPCR analysis closely matched the NGS read counts across each epididymal segment and a similar trend to this was seen for *Nov-miR37*. However, RT-qPCR analysis of *Nov-miR*13 and *Nov-miR*42 differs from that denoted by the NGS read counts, with inconsistencies between biological replicates being observed across epididymal segments (Appendices 46/47 an 50/51).

Chapter 5: Discussion

5.1 Introduction

Nascent spermatozoa released from the germinal epithelium of the testes require additional maturation in order to acquire the forward motility and functional competence required to fertilise an oocyte, and these maturational events take place as the cells travel through the luminal environment of the epididymis. Epididymal maturation operates in the distinct absence of transcription and translation within the sperm cells, and is therefore driven solely by extrinsic factors produced and secreted by the epididymal epithelium. Furthermore, maturation of these cells occurs progressively as they transit the several highly specialised microenvironments of the tract, with the distal segment of the tract providing sperm with an environment optimised for their prolonged storage in a quiescent state prior to ejaculation. The studies presented in this chapter, as well as a number of studies conducted by independent research groups, point to the importance of functional sRNA regulatory networks in the generation of nascent sperm, as well as the regulation of the microenvironments responsible for driving their maturation [82, 89, 158, 159, 231]. As robust and thorough as the studies detailed in this chapter are, a number of elements of these studies are worthy of further discussion. Indeed, these studies presented a number of advantages over previous research. However, they are not without their limitations, and several avenues could be employed as a means of improving these works.

5.2 Epididymal miRNA Discussion

Ultimately, each of the studies in Chapter 3 bring forward significant and novel findings that improve our understanding of the epididymis and mammalian sperm maturation: comprehensive and accurate miRNA profiles for epididymal epithelial cells, sperm and epididymosomes were generated, the extent to which sperm miRNAs are altered between epididymal regions was documented, and a mechanism by which sperm gain miRNAs during their progression through the epididymis was identified [161-163]. Epididymal epithelial cells, spermatozoa and epididymosomes were found to possess 218, 295, and 358 unique species of

mature miRNAs, respectively, across each epididymal region. Surprisingly, just 46 % of the miRNAs identified across each analysis were conserved between epididymal epithelial cells, sperm and epididymosomes, with several miRNA families being conserved between each sample. Though the miRNA profile of epididymal epithelial cells appeared to be relatively stable, a small portion (~24 %) of all miRNAs identified were differentially expressed between epididymal segments. Contrasting to this, the sperm miRNAome was found to fluctuate greatly in both total number of miRNAs, and abundance of conserved miRNAs, as these cells progressed from the caput to the cauda of the tract, with approximately 78 % of the total miRNA count being characterised by significant fold changes in accumulation and a large cohort of molecules exhibiting extreme increases in abundance as the cells entered the distal region of the epididymis. Epididymosome miRNA profiles demonstrated similarly diverse abundance across epididymal segments, with approximately 46 % of the total miRNAs identified within the vesicles being characterised by dramatic fold changes. Curiously, each study highlighted the fact that the corpus epididymis possesses few unique miRNAs. In fact, in the cases of epididymal epithelial cells and spermatozoa, epididymal components sourced from the corpus possessed the lowest total miRNA reads. These findings are consistent with previous work in the rat and human models [157, 166]. Intriguingly, this appears to stand in contrast to the well-established paradigm for epididymal sperm maturation, which states that specific changes to sperm functional competence are largely driven during the transit of these cells through the proximal regions of the tract (the caput and corpus) [190]. These changes include the addition, and post-translational modification, of several proteins within the maturing sperm proteome as they leave the caput epididymis [232]. This serves to posit that the miRNA signature of sperm is not directly linked with the maturation of these cells, and this is bolstered by the fact that a nascent sperm sourced from the testes can be injected directly into an oocyte to form viable embryos [233]. Therefore it is most likely that the sperm miRNA payload plays a more discrete role in the transfer of paternal epigenetic signatures to progeny.

Given that sperm are considered to be incapable of transcription and translation [234], it

has been suggested that the tailoring of their epigenome is primarily performed by epididymosomes, and that this delivery of cargo has the potential to influence the function of these cells in downstream developmental events [163, 177, 235]. In fact, the role of these vesicles in altering epididymal miRNA profiles, particularly in the cauda epididymis where sperm are stored for an extended period of time, may be far more significant than previously thought. In a recent study performed by Gapp et al [170], it was determined that the introduction of total sperm-borne sRNAs into oocytes fertilised by control sperm imbues progeny with paternal behavioural and metabolic anomalies [170]. Though it is possible to fertilise an oocyte with an immature sperm isolated from the testes, these findings would suggest that the epididymis plays a role in shaping the payload of sperm to prevent epigenetic syndromes that may manifest later in life. It would therefore be expected that the dysregulation of epididymosome miRNA profiles could have profound implications for offspring health.

Despite the strong evidence for epididymosome transfer of miRNAs to sperm, a point of curiosity is the fact that sperm harbor some 30 miRNAs that were not identified in the expansive list of epithelial cell or epididymosome-borne miRNAs. Even more curious, is the fact that a number of these miRNAs are characterised by changes in abundance as the cells progress through the epididymis. Indeed, it was evident that sperm lost 13 of their unique miRNAs during epididymal transit, with miRNAs such as *miR-27a-5p*, *miR-142-3p* and *miR-92a-1-5p* featuring among those with the highest abundance in the caput. Though the mechanism by which sperm lose miRNAs during epididymal maturation is not understood, the leading hypothesis suggests that this takes place during the shedding of the cytoplasmic droplet, a remnant of the germ cell cytoplasm that is lost as these cells progress through the epididymis [236]. Several studies have documented the presence of RNAs within the cytoplasmic droplet and, though these analyses have not yet extended to the analysis of miRNAs within this structure, it is certainly possible miRNAs may be shed through the loss of this structure as the final stages of miRNA processing occurs within the cytoplasm in mammals [237-239].

Curiously, spermatozoa appeared to gain 14 miRNAs as they entered the caudal segment,

including *miR-130b-5p*, *miR-743a-5p* and *miR-471-3p*. This suggests that epididymosomes may not account for the total transfer of miRNAs to sperm and that other mechanisms of miRNA acquisition may be at play within the epididymis. Notably, the epididymal intraluminal milieu that sperm are harboured in during post-testicular maturation is replete with a suite of proteins that drive maturational events. Though the mechanism by which luminal DNA or RNA molecules may be delivered to the sperm in the absence of shuttling vectors, such as epididymosomes, has not been a point of study in this project, several studies have documented the uptake of DNA by sperm cells using *in vitro* methods [240-242]. In accordance with this, it is tempting to speculate that any non-protein-bound DNA and RNA within the epididymis may be taken on by sperm transiting the tract, and that these could then influence the epigenetic signature of these cells. Further, it is possible that exogenous vesicles produced elsewhere in the body are capable of delivering their cargo to maturing sperm, a phenomenon recently observed in the context of somatic cells delivering RNA to sperm via exosomes [243]. Alternatively, it is possible that sperm cells, although transcriptionally and translationally inert, may possess the protein machinery required to generate their own miRNAs from pre-miRNA precursors: a hypothesis bolstered by the detection of core miRNA pathway machinery proteins, DICER1 and AGO2, within the sperm proteome. Though the investigation of such phenomena lie outside of the scope of this project, it stands as an avenue of future research, particularly as several of the sperm miRNAs uniquely detected in the caudal cells are present in relatively high abundance (for example, *miR-130b-5p* with 158 reads).

Interestingly, miRNA profiles of epididymosomes revealed that these vesicles possess a more expansive repertoire of miRNAs, many of which appear in far higher abundance, than their parent epithelial cells. Indeed, 164 of the miRNAs identified in epididymosomes (46 %) were not detected at equivalent analyses of epithelial cells, while 112 miRNAs (31 % of the total epididymosome miRNA population) were uniquely identified within the extracellular vesicles. Several of these unique epididymosome miRNAs were characterised by relatively high read counts, with the abundance of several of these miRNAs peaking in the cauda

epididymis (e.g. *miR-21a-5p*: >20,000 reads, *miR-126a*: > 1,500 reads, *miR-145a* > 1,800 reads, *miR-486a/b*: >1,700 reads, *miR-195a*: > 600, *let-7j*: > 500 reads). The functional significance of these miRNAs may lie beyond the epididymis. The female reproductive tract is also replete with extracellular vesicles, and a particular class of these (uterosomes) have been studied in regard to their interactions with ejaculated sperm upon entering the tract [181, 244]. Uterosomes are thought to be produced in a similar fashion as epididymosomes – via apocrine secretion – and share a number of characteristics with their epididymal counterparts, including population heterogeneity and their ability to deliver proteins to sperm [233]. In fact, it has been suggested that the latter of these is performed in order to facilitate capacitation of male gametes after ejaculation, a role similar to that of epididymosomes in driving the functional competence of sperm progressing through the epididymis [181, 244]. Further, uterosomes are implicated in epithelial cell signalling within the female reproductive tract and it has been suggested that CD9 positive and CD9 negative populations may exist, another similarity drawn between these vesicles and epididymosomes [181, 244]. Though empirical evidence is yet to be provided for such speculation, given the wide range of similarities between extracellular vesicles produced by the male and female tracts, it is reasonable to posit that epididymosomes released in seminal fluid may be able to play a regulatory role via interactions with the epithelium of the female reproductive tract in order to modulate the surrounding environment to promote sperm viability within the region. An expanding body of literature detailing the influence that seminal fluid has on the female reproductive tract has been afforded by the work of the Robertson Research Institute. The research performed by this group has led to the conclusion that interactions between seminal fluid and the endometrial epithelium results in the induction, or suppression, of several mRNAs and miRNAs, which in turn causes the initiation of processes firmly linked to immune responses [168, 245].

Given that seminal fluid comprises several microvesicles, including epididymosomes, it is possible that encapsulated miRNAs may be delivered to the female reproductive tract upon insemination in order to condition the tract for optimal fertilisation [163, 245-247]. The most

abundant of the miRNAs unique to epididymosomes, *miR-21*, has been shown to play an active role in the female reproductive tract, via regulation of the transforming growth factor beta (TGFβ) pathway, which is well documented as a key modulator of the immunological responses of the tract [143, 248]. Indeed, this miRNA is heavily implicated in the control of the TGFβ signalling pathway, targeting several key genes including *Tgfbr2, Pten, Pdcd4* and *Tap63*, suggesting that this miRNA possesses the ability regulate the responsiveness of female tract epithelial cells to TGFβ [249]. Additionally, *miR-21* has been shown to interact with the *Smad7* mRNA [250], which produces a protein that interacts with several other members of the SMAD family in order to competitively bind to TGFB1 [251], further emphasising the significance that this miRNA holds regulating the TGFβ signalling responsible for inducing a leukocytic response in the female reproductive tract post-coitus, as well as the tailoring of the tract for optimal embryo implantation [143, 168, 248, 252, 253]. Interestingly, *miR-21* plays an additional role in cellular proliferation and differentiation at sites of implantation, where it is substantially accumulated in sub-luminal stroma surrounding blastocysts [254]. Here, *miR-21* works to catalyse the degradation of *Reck*, an inhibitor of matrix metalloproteinases that are responsible for remodelling the extracellular matrix after conception [255, 256]. Other highly abundant and unique epididymosome miRNAs have the potential to perform regulatory roles in the female tract: *miR-126* regulates various inflammatory mediators [257], *miR-145* is responsible for regulating tumour suppression in response to TGFβ signalling [258], *miR-486a/b* could play a role in embryonic stress resistance by disrupting NF-κB negative feedback loops [259, 260], and *miR-195* may play similar roles to *miR-21* via regulation of *Smad7* [261]. The roles highlighted here lead to the suggestion that the introduction of epididymosomes harbouring substantial quantities of these miRNAs, particularly *miR-21*, into the female reproductive tract upon ejaculation has the potential to influence the trajectory of environmental modelling within the tract, in order to prepare for implantation and embryogenesis.

Indeed, with more than 17,000 mRNA transcripts having been identified in the mouse epididymis, it is feasible that an elaborate network of miRNAs operate throughout the tubule to

maintain the epididymal tissue and thereby promote the microenvironments required for sperm maturation [147]. The studies presented throughout this chapter, in combination with a myriad of previous studies, provide further evidence for the theory that miRNAs provide an addition tier of regulation within male reproductive tract.

A factor with the potential to distort the results obtained throughout the studies documented in this chapter is the separation of epididymal segments. While the epididymis has been divided into three major segments throughout these studies, this accessory organ of the male reproductive tract is led by a region called the initial segment [262]. The initial segment of the epididymis is well documented throughout the literature, with several studies being dedicated to the characterisation of this segment. Indeed, the epithelial cells lining the initial segment have been documented as the tallest of all epididymal segments and plays a role in the removal of testicular fluids entering the tract [263]. Indeed, the blood flow to this section is greater than remainder of the tract [264-266], and the initial segment of the epididymis is surrounded by a profuse arrangement of perforated capillaries, which spans underneath the epithelium, while subsequent segments are characterised by sparse non-fenestrated capillaries [267, 268]. Further, the initial segment plays significant roles in the production of mature gametes, with one particular study demonstrating that genetic modification causing a lack of the epididymal initial segment results in sterility [269].

In addition to the identification of the initial segment of the epididymis, articles documenting variation between regions of the mouse epididymis, in the context of up to 10 segments as opposed to three, are quite common [147, 177, 262, 270-274]. Though it is possible to consolidate gene expression values afforded by these studies into three segments equivalent in size to the caput, corpus and cauda, in order to compare our own data with transcriptomic data, it would have been advantageous to mirror the separation of epididymal segments documented in these studies. Given that transcriptomic data reveals an incredibly complex arrangement of gene expression throughout each segment of the tubule, a similar arrangement of miRNAs regulating these genes throughout the tract would provide stronger evidence for the role that these small

molecules play in regulating epididymal function, and therefore sperm maturation. Obviously, this kind of analysis would be subject to two caveats: accuracy of segment separation, and isolation of sufficient material for detailed NGS analyses. Despite harvesting material from animals of the same ages, the length of the entire epididymis would still be subject to small variations between specimens and distinguishing between each of the 10 segments, as opposed to the visually-defined caput, corpus and cauda, would prove difficult. Additionally, biological pools of 9 – 12 animals (depending on sample type and segment) were used throughout the analyses performed in this chapter, not only to determine miRNA profiles in samples resembling all physiologically normal mice, but also to generate an amount of cells/vesicles to produce sufficient quantities of RNA to perform sequencing and RT-qPCR analyses. Clearly, employing this strategy would necessitate the use of many more animals, in order to generate adequate material for downstream experiments, as well as additional time in order to process such samples. Given that the corpus region has been determined to possess low variation of miRNAs (with little to no miRNAs being unique to this segment of the epididymis being identified within the three studies conducted in this chapter), it could be suggested that breaking this segment down further would be redundant, while breaking down the highly complex caput and cauda regions into proximal and distal sub-sections (as well as isolating an initial segment) would provide an increased understanding of the nuances of miRNA abundance within these segments.

A further limitation of the analyses performed throughout this chapter involves the comparison of miRNA profiles between separate strains of mice. A myriad of previous studies have employed strains of mice differing from those employed in the analyses of this project. The majority of studies analysing the sRNA content of the male reproductive system have employed the C57BL [154, 275-283] mouse strain, with other strains being used less frequently; Swiss (CD1) [284], BALB/c [89, 285], and FVB/NJ [235]. Given the paradigm set by previous studies, a logical starting point of this project would be the investigation of sRNA species in C57BL strains of mice, in order to ensure consistency with existing data. This is further enforced by a study published almost a decade ago by Parsons and colleagues [286]. This study analysed

miRNA expression in the hippocampus of A/J, BALB/c, C57BL, and DBA strains of mice and determined that ~12 % of all miRNAs analysed demonstrated marked differences in accumulation between strains [286]. As this analysis was restricted to the hippocampus one may suggest that this trend is exclusive to a specific tissue. However, the possibility remains that artefacts of phenotypic variation between strains of mice may serve to distort analyses attempting to make comparisons between epididymal studies. Indeed, this was evident when comparisons were drawn between the sperm miRNAs identified in the third portion of this project and the sperm miRNAs identified by Sharma and colleagues in 2016 [163, 235]. In fact, of the miRNAs identified across these two studies only 57 % conservation was observed between caput sperm datasets, while 62 % conservation was found between caudal sperm analyses. Furthermore, this comparison did not take into account the magnitude of differential miRNA accumulation within these cells (only presence or absence were recorded), and it is therefore likely that statistical analyses of levels of expression within these datasets would highlight further differences in miRNA abundance [229, 287]. Additionally, it would be expected that such differences would also be observed across a range of ncRNAs, including other classes of sRNA. While the use of Swiss (CD1) served to aid in the relation of these studies with a broad range of other studies performed by our own group and focussing on wider biological processes, inconsistencies documented between mice strains used as model organisms in epigenetic studies of the epididymis, as well as other tissues, begs the questions as to which strain is most appropriate for use in these experiments, and suggests that a consensus strain is required to be nominated in order to increase reproducibility of results across a range of institutions.

An advantage of the analyses performed in the present set of studies over previous work, is the application of NGS technologies over the previously favoured microarrays [161-163]. In fact, several independent studies have highlighted both the advantages and disadvantages of each of these techniques, with NGS technologies being highlighted as the preferred strategy for large scale sRNA surveys, such as those reported herein [288-290]. A marked advance in sequencing approaches occurred in 1977 when Sanger and colleagues were the first to document rapid DNA

sequencing by characterising the complete genome of bacteriophage ϕX174 [291]. This accomplishment is widely referred to as the pioneer 'first generation' DNA sequencing technology, acting as a foundation for several subsequent techniques. However, this technology was decidedly insufficient for the sequencing of the human genome, due to relatively low throughput and high cost. For this purpose, a technique developed by Hood and colleagues, which relied on fluorescent detection for specific bases, was employed, allowing for the concurrent sequencing of numerous samples and the completion of the Human Genome Project in the early 2000's [292, 293]. Since then, microarrays have grown in popularity as the primary tool for analysing gene expression. However, with the further development of next generation sequencing technologies, the applicability of microarrays in gene expression quantification has been called into question, which numerous whole studies being dedicated to highlighting differences between sequencing approaches [294-298].

Microarrays typically work by employing nucleic acid probes several dozen nucleotides in length bound to glass slides. Target sequences, which are fluorescently labelled, are then hybridized to the bound probes, prior to a washing step which limits analyses to strands that are strongly paired. Fluorescence signal intensities are directly related to the amount of material hybridized to a probe, and are processed by software that generates relative expression values in comparison to the intensity of a similar feature under different conditions [299, 300]. Because microarray analyses are limited to transcripts that have successfully bound to the arrays, the quality of these analyses are directly reliant upon the bioinformatic information of the genome and transcriptome of the organism of interest. A review published by Jaksik in 2015 proposed eight phases of microarray experiments and each of the factors within each of these phases that could potentially influence the final measurement of gene expression [301]. Among these were; a difference in efficiency of amplification and labelling of different structures of RNAs, bias in hybridization efficiency between probes, removal of non-specific hybridization after washing processes, and artefacts of background correction and normalization arising from using similar means of processing each probe during data analysis [301]. Despite their intrinsic limitations, the

quality, coverage and specificity of microarrays is constantly evolving to match newer sequencing technologies and, in fact, these strategies have been used extensively in previous studies to analyse and reliably report the RNA composition of various elements relating to reproduction in both the male and female tracts [255, 302, 303]. Notably, these studies provided a novel insight in to the production of functionally competent gametes. However, in order to unmask the intricacies and extent to which sRNA molecules influence these key biological processes, a more advanced approach to sequencing would be required. Given the constantly falling price of operation, RNA-seq is the NGS technology that is quickly becoming favoured for obtaining accurate measurements of transcript abundance in place of microarrays. In short, RNA-seq works by converting an isolated sample of RNA into a population of fragmented cDNA with adapters ligated to either one or both ends of the molecule, followed immediately by PCR amplification and gel purification of the cDNA. An additional step of size exclusion can be integrated by running samples through a polyacrylamide gel and purifying via ethanol precipitation. Using high-throughput sequencing technology, short sequences are obtained for each cDNA and aligned with a reference genome or transcriptome [304-308]. A number of advantages for employing RNA-seq over microarrays in transcriptome and sRNA sequencing analyses have been highlighted across several studies. Though both techniques allow for high-throughput sequencing, as well as the ability to sequence without a reference genome, RNA-seq has many clear advantages: background noise is markedly lower than that encountered in microarray analyses [309], RNA-seq can confidently detect gene expression from 1.25 fold-changes upward of 8,000-fold [310], and it is able to distinguish between different isoforms and allelic expression [311]. On top of this, RNA-seq can be performed with significantly less starting RNA, and the cost of mapping reads to large genomes is relatively low, in comparison to microarray analyses [309]. NGS was employed in the studies documented throughout this chapter in an effort to generate complete miRNA profiles of sample types sourced from each epididymal segment with a high degree of specificity, accuracy and reliability [161-163]. Indeed, a wider coverage of miRNAs was documented in these studies, in comparison to those performed in studies utilising

microarrays [157, 158, 164, 247]. However, despite the vast improvements RNA-seq has made on microarray technologies, these technologies do not come without their own limitations. In particular, GC or AT enriched regions in the full DNA fragment can result in underrepresentation of read counts originating from these sequences [312, 313]. Furthermore, distribution of RNA-seq base level read counts can be altered by local dinucleotide frequencies and total gene length [312]. A number of biases can also be introduced by steps common with those used in microarray analyses, such as those introduced in cDNA preparation of PCR amplification steps.

Further advances have been made in the world of sequencing, with the production of several techniques categorised as "third generation sequencing" technologies. For example, the single molecule real time (SMRT) platform produced by Pacific Biosciences, which utilises an eloquent system that works to sequence nucleotides at the same rate as the endogenous polymerase, is capable of detecting single modified bases in real time, while sequencing reads exceeding 10 kb in length [314]. Further, it has been shown that the SMRT platform is capable of performing real time analyses of RNA sequencing, while also providing evaluations of modifications and structural arrangements [315]. Additional technologies, such as those produced by Oxford Nanopore Technologies (ONT), offer the potential for incredibly fast, and far lower cost sequencing; and with the added feature of only being roughly the size of a mobile phone and therefore remarkably portable, so much so that sequencing can now be performed in the field [316, 317]. Admittedly, current nanopore technologies suffer a significant draw back in the form of poor quality profile generation. However, that is not to say these technologies do not have their place in third generation sequencing; their low cost, rapid processing, and frequent improvements presents a revolution to the sequencing field, such that the ability to undertake sequencing has been expanded to the point where researchers in remote regions are able to determine genome composition of disease causing microbes shortly after collecting samples [318]. Similar to the SMRT platform, Nanopore technology also offers the ability to perform direct RNA sequencing in real time, along with analyses of RNA structure [319, 320]. It would be feasible to utilise nanopore technologies as a 'first pass' for investigations as a means

of quickly and cheaply determining whether to invest in more expensive technologies. Further, it is certainly possible to use initial screening with nanopore technology to generate genome reference sequences or to compose a scaffold against which RNA-seq data may be mapped – merging the sizeable read length of this technology with the accuracy and high read depth of short read sequencing [317, 321-323]. Such experimental design could have been employed in the three miRNA studies highlighted in this chapter in order to further strengthen the quality and reliability of sequencing results, as well as provide an initial overview of the dynamic miRNA profiles of epididymal epithelial cells, sperm and epididymosomes. Additionally, this proposed strategy would provide useful in sequencing the sRNA composition of sperm across a wide range of mammals in the field to determine the similarities and differences between the mouse profiles documented in this study in an effort to uncover evolutionary conservation of epididymal maturation events.

As mentioned previously, an increasing number of miRNAs were identified between each study documented in Chapter 3. At face value, one possible explanation that could account for the apparent differences in the total number of miRNAs identified from study to study is that of a varying depth of sequence coverage for each of these analyses. However, such an issue has been combatted through the use of normalisation and bioinformatics tools. Indeed, the total number of library reads in epithelial cells averaged at 14.9M, 14.3M and 13.2M for the caput, corpus and cauda respectively (Appendix 15, [161]), while spermatozoa total read counts averaged at 15.8M, 15.8M and 14.3M in each of the same segments (Appendix 15, [162]). Interestingly, a marked increase in total library reads was also observed within the epididymosome datasets, with the caput, corpus and cauda segments yielding an average of 52.1M, 50.4M, and 18.9M reads respectively (Appendix 15, [163]). Though it has been suggested in the past that NGS analyses do not require elaborate methods of normalisation [324], it has been noted that differences between the depth of coverage in each analysis can lead to biases within data sets [325, 326], and therefore strict normalisation of data, similar to that which was employed throughout these studies, is required to allow for comparison of data between biological samples. Indeed, the

EdgeR and limma Bioconductor package [204, 327, 328] utilised in the normalisation of datasets across each of the analyses presented in this project have been employed extensively in previous studies analysing an array of RNA-seq datasets generated using material sourced from a range of different organisms [329, 330]. Therefore, despite differences in raw library sizes across biological replicates and biological samples, it is unlikely that the increasing number of total miRNAs in normalised datasets produced in these studies are an artefact of sequencing depth – rather, the total number of miRNAs identified throughout epididymal epithelial cells, sperm and epididymosomes is a result of the miRNA profiles of these samples being naturally and progressively complex. This claim is reinforced by the robust bioinformatics performed throughout this body of work to ensure consistency each NGS dataset. These analyses, in the form of heat maps and a multi-dimension scaling plot, have confirmed that our normalised data for each biological replicate is consistent and that each biological sample is comparable, Further, the strength of our NGS data presented in each study has been reinforced through the use of RT-qPCR validations of differentially expressed miRNAs.

In summary, the studies documented throughout this chapter emphasise the extent and the significance of the miRNA profile in terms of regulating the epididymal microenvironments that are key to ensuring male gametes reach functional competence prior to their entry into the female reproductive tract. Through the systematic profiling strategies employed in these studies, it was determined that mouse epididymal epithelial cells are primarily characterised by static miRNA profiles, while a small portion of these molecules appear to perform significant roles in regulating differential gene expression throughout the tubule [161]. This revealed profiles that were incredibly plastic, with a vast overhaul of the sperm miRNAome being observed as these cells progress through the epididymis. Complementary empirical identification implicating epididymosomes as vectors with the potential to transport their miRNA cargo to sperm was achieved via the extended co-incubation of epididymosomes with spermatozoa *in vitro*. This provided unique evidence for a long suggested mechanism for the introduction of modifications to the sperm epigenome, and it is apparent that these modifications have the potential to alter the

course of embryogenesis via the transmission of paternal epigenetic signatures [163]. Finally, the results detailed throughout these studies afford a markedly increased insight and understanding of the factors influencing male fertility as a whole and provides the potential for a number of future avenues of research. Of course, the studies presented here open a number of exciting avenues of research, the specifics of which are detailed in Chapter 6.

5.3 Novel miRNA Discussion

The studies described in this chapter focused on the detection and characterisation of putative novel miRNA molecules in the mouse epididymis. Using a well-documented workflow for detection of novel miRNAs (*Nov-miR*s), several hundred putative *Nov-miR*s were initially identified. However, this number was significantly reduced by the application of several stringent selection criteria and removal of false positives via NCBI BLASTn searches. The remaining 22 *Nov-miR*s accounted for over 6,200 reads across all 21 samples analysed throughout the course of this project, with five promising candidate novel miRNAs selected *Nov-miR*s or further target gene identification and *in vitro* validation. Indeed, each of these molecules were characterised by stem-loop secondary structures that closely resemble those previously described for validated miRNAs. Further, 49, 78, 50, 5 and 41 potential targets were identified for the five analysed novel miRNAs, including's *Nov-miR13*, *Nov-miR37*, *Nov-miR42*, *Nov-miR101* and *Nov-miR127*, respectively.

At the start of this study, a disadvantage of the analysis tool employed in this study, miRCat, was encountered in the form of the evidently high false-positive rate a novel miRNA identification. Though 311 putative novel miRNAs were initially listed by the miRCat analyses performed on a master file comprising of all 21 sequencing files, the majority of these (93 %) were removed by various screening steps of differing stringency. Each candidate *Nov-miR* was subjected to BLASTn searches against several NCBI databases, resulting in the removal of 74 sequences which had previously been identified as a different species of sRNA. The miRCat tool of the UEA sRNA workbench allows users to input several parameters that work to restrict the scope of candidate novel miRNAs to a manageable set of molecules that are likely to exist [206],

those which filter results for tRFs and other sRNAs not characteristic of canonical miRNAs. Although this filter was applied throughout these analyses, a number of the sequences removed as a result of the BLASTn searches conducted were highlighted as tRFs. A possibility remains that the latest release of miRBase and tRF database used for miRCat analyses had not yet been updated to include miRNA molecules already present in the NCBI, resulting in the flagging of many molecules which had previously been identified. Despite this limitation, the UEA sRNA Workbench presented several advantages throughout this study, namely the ability to identify potentially novel miRNAs from a large master files comprising all 21 RNA-seq files produced in the studies documented in Chapter 3 of this work. The output data produced from this analysis was incredibly comprehensive, forming a solid foundation for the range of further analyses that were performed in order to evaluate highlighted potential novel miRNAs.

Interestingly, the abundance of the five assessed novel miRNAs was highest in the corpus epididymis across all samples, with 16 / 18, 4 / 4 and 9 / 10 *Nov-miR*s identified as having the highest abundance in this segment in the sperm, epithelial cells and epididymosomes respectively. Further, the majority of these (14 in sperm, 3 in epithelial cells, and 6 in epididymosomes) were unique to the corpus segment, a finding that stands in contrast to the distinct lack of known miRNAs identified within this segment of the track described in Chapter 3 of this thesis [161-163]. Additionally, the aforementioned previous studies determined that, in the case of sperm and epithelial cells, enrichment of total known miRNAs was lowest in the corpus, while epididymosome datasets ranked the corpus as the segment second least replete with miRNAs, a trend that does not match the abundance of *Nov-miR*s throughout the epididymis [161-163]. Of interest is the abundance of *Nov-miR13* in the corpus epididymis, where it was determined to have 822, 179 and 503 sRNA reads in the sperm, epithelial cell and epididymosomes samples respectively, placing this novel miRNA within the top 30 % most abundant miRNAs found in sperm and epididymosomes.

Curiously though, the abundance of *Nov-miR13* in the cauda epididymis was lower than the corpus, with a complete absence of this molecule within the caudal sperm samples tested.

Such changes in abundance may point to two mechanisms at play within the maturing gametes. Firstly, the accumulation of large quantities of *Nov-miR*s could be attributed to *in-situ* processing of miRNA precursors, or to epididymosome mediated delivery. As mentioned previously, these cells appear to possess the machinery required for the production of mature miRNAs and thus there remains a possibility that sperm progressing through the epididymis are able to process harboured precursor molecules into both known and novel miRNAs alike [162]. Additionally, given that epididymosomes are replete with *Nov-miR*s in the corpus, it is possible that these vesicles are responsible for delivering these molecules to maturing gametes. Secondly, though puzzling, the apparent loss of the vast majority of *Nov-miR*s as sperm enter the caudal epididymis may suggest a mechanism by which these cells selectively shed their miRNA cargo as they traverse the epididymis [162]. Indeed, this is a trend observed throughout the studies conducted on known miRNAs, with approximately 91 / 295 of these miRNAs being characterised by a marked reduction in abundance between corpus and cauda segments, with 41 miRNAs (~45 %) demonstrated to be completely lost in these segments, despite having previously been enriched in the corpus. As miRNAs have the potential to target a wide range of mRNAs, it is possible that the miRNAs shed by the sperm during their epididymal transit may be able to influence downstream biological processes, subsequent to ejaculation [15, 16]. Though further data is required to establish the selective removal of miRNAs from maturing male gametes, such a mechanism would ensure that the epigenetic profile conveyed to the oocyte and female reproductive tract is one that will play a positive role in directing implantation and embryogenesis. Indeed, removal of the excess cytoplasm from epididymal sperm is evident through shedding of the cytoplasmic droplet, and this process has been linked to male fertility in a number of species [236]. In fact, it has previously been shown that lifestyle factors, such as smoking, stress, diet, and infection, can have a distinct impact on the retention of residual cytoplasm in sperm cells as well as the viability of sperm [331-335], and similar observations apply to patients with varicocele, a common complication that results in a marked reduction of male fertility [336-338].

Of course, the enrichment of *Nov-miR*s and several known miRNAs in the corpus region

could point to the type of role that these molecules may play in driving sperm maturation. Previous studies have documented interactions between maturing sperm and the epididymal epithelium, suggesting that male gametes may indeed perform a role as vectors for transmission of miRNA signatures from one epididymal segment to another [339]. Though not yet experimentally validated, several hundred potential targets for each *Nov-miR* were identified in initial *in silico* surveys, with *Nov-miR13* (the novel molecule with consistently high abundance in the corpus) retaining 49 putative target genes after strict removal of candidates following several dataset interrogations. These target gene mRNAs were found to be involved a number of key biological pathways, including cell death and survival, cellular development, and tissue development, with at least 37 % of the predicted mRNA targets being associated with adipose tissue of epididymal fat pads. Additional targets were found to be involved in sperm capacitation, development of primordial germ cells, testicular transcriptional repression, and the establishment of important signalling units in sperm, suggesting that this molecule may play additional roles outside of the epididymis. Interestingly, the putative target genes of the sperm-specific molecule, *Nov-miR101*, were found to be involved in organismal development, cell assembly and organisation, and cell function and maintenance, while the second sperm-specific miRNA, *Nov-miR127,* was found to potentially target genes involved in cellular development, cell morphology and organismal development. The latter of these is of particular interest as the abundance of *Nov-miR127* in sperm is characterised by a significant increase in the caudal region, after having being determined absent in cells sourced from the proximal epididymis. As the caudal sperm population represents the cells that will enter the female reproductive tract and potentially the oocyte, it is possible that *Nov-miR127* may play a role in these downstream processes.

A point of improvement for this study could be the application of several additional novel miRNA identification tools. Although a single tool for the identification of novel miRNAs (miRCat) was employed in this study (due to computing power, technical know-how and operating system capabilities), a number of additional tools are widely available and have been extensively reviewed throughout the literature [340-342]. Among the most common tools are

miRDeep2 [343], and miRanalyzer [344], each of which use differing algorithms and mapping tools to predict novel molecules. The analysis tool miRDeep2 works by first evaluating all candidates and uses the popular Bowie alignment tool [345], coupled with Bayesian statistical models, to score and remove those sequences with structural signatures that differ from those expected to be formed after Drosha and Dicer processing [202]. Sequences are allocated scores based on number of reads, identification of a conserved seed sequence, and the minimum free energy associated with predicted secondary structures of the precursor transcripts from which the novel miRNAs are putative processed from. This tool has been used extensively throughout the literature and output results have been thoroughly validated via wet-lab experimentation [202, 346, 347]. Further, miRDeep2 and its predecessors have formed the basis of several additional analysis tools, including the increasingly popular tool, miRDeep* [348]. Another common tool, miRanalyzer, utilises a different strategy for novel miRNA identification. This tool begins searching for reads that do not align with known miRNAs or other transcripts and analyses these using a machine learning approach based on the random forest method, whereby various classifiers trained on a group of known miRNAs are employed in unison to produce a wide range of potentially novel miRNAs [210, 345, 349]. miRanalyzer has also been validated via wet-lab experimentation [350, 351]. Though a strategy employing several novel miRNA identification tools in tandem is yet to be featured in published studies to date, utilising several additional tools for novel miRNA identification would work to reduce the number of false-positives encountered throughout this study, could be used to narrow the scale of novel molecules identified, and provide additional bioinformatical evidence for the existence of the *Nov-miR*s identified within this study, thereby increasing a user's confidence in the existence of molecules before performing subsequent analyses.

Though the bioinformatics analyses performed throughout this study were thorough and robust, potentially novel miRNAs require wet-lab validation in order to confirm the existence of these molecules. By far the most common form of novel miRNA validation is RT-qPCR of the candidate sequence. This approach was used in this study and analyses were performed on

samples of RNA that differed from those used for NGS. A highly abundant and known miRNA, *miR-29a** , was initially analysed utilising the U6 sRNA as a normalisation control, in order to confirm that each biological replicate of RNA sourced from sperm and epithelial cells was able to faithfully represent the NGS data obtained. Indeed, for the spermatozoa datasets, this was observed as the RT-qPCR generated expression data of this miRNA in each biological replicate represented the NGS reads previously obtained. Subsequent RT-qPCR analyses of *Nov-miR13*, *Nov-miR42* and *Nov-miR101* demonstrated relative expression that followed trends closely resembling those observed in the NGS data output determined by the miRCat analysis tool, thereby providing empirical evidence for the existence of these molecules within the epididymis. However, these results were confounded when analyses were turned to the interrogation of epididymal epithelial cells. Firstly, only the RT-qPCR analysis of *miR-29a** in replicates two and three of the epithelial cell analyses were true to bioinformatic data, calling into question the validity of replicate one, which was subsequently removed from further analyses. When analysing the latter two replicates, it was clear that the data pertaining to *Nov-miR13* and *Nov-miR42* did not align with the bioinformatic data: two novel miRNAs determined to be true to the NGS reads in sperm. Further, *Nov-miR37*, which was found not to agree with NGS data in sperm, was characterised by a relative expression corresponding to the NGS reads detected in epithelial cells. Such confounding results present a number of concerns regarding the data, though a number of possible scenarios may account for these data. Firstly, the confounding results could have been influenced by the read count of the *Nov-miR*s identified. Given that the highest read count is *Nov-miR*13 in sperm sourced from the corpus epididymis, and that the abundance of all other *Nov-miR*s in all other samples is significantly lower, it is possible that these molecules are simply too few to detect accurately via standard RT-qPCR. A concern that needs to be taken into consideration is the "Monte Carlo" effect – an intrinsic drawback of amplifying from small quantities of template RNA, as each sequence used as a template for the reverse transcription reaction possesses a unique probability of being either amplified or lost during the reaction, resulting in variation between the relative abundance determined by RT-qPCR analyses [352-

354]. As such, templates with a lower abundance are less likely to have their real quantities reflected in the final amplicon. An additional factor that could introduce issues when detecting sequences of such low abundance could lie within the content of the RT-qPCR reaction. In conditions of with a surplus of primers, the probability of a primer annealing to any one strand of template requires several precise factors, including annealing time and temperature, as well as the availability of template sequences [352-354]. Though difficult to resolve, a number of steps may be employed in order to improve upon the protocols used throughout this study in an effort to validate *Nov-miR*s by RT-qPCR. First of all, it would be worth experimenting on lowly abundant and already characterised miRNAs within the epididymis, to determine if reaction efficiency can be increased via alterations to primer concentrations. This would serve to reduce the issues documented with primer efficiency when amplifying from small quantities of template, although with the caveat that this would then introduce speculation into the relatability of these data with those pertaining to already known and more greatly abundant miRNAs.

Given the discrepancies observed between *Nov-miR* RT-qPCR data in the epithelial cells and sperm of the epididymis, it would be worth exploring a number of the additional validation methods frequently employed in other studies. [355]. Such discrepancies in *Nov-miR* validation data make it difficult to firmly state that there is empirical evidence to support the existence of these molecules. However, if data pertaining to the abundance of *Nov-miR*s in epididymal epithelial cells is discounted due to the lower abundance documented in these cells in addition to speculation surrounding validity and reliability, and therefore if analyses are restricted to the RNA samples taken from epididymal sperm, it is within reason to suggest that *Nov-miR13*, *Nov-miR42* and *Nov-miR101* are indeed three novel miRNA species. Indeed, additional validation of such findings, focussing solely on sperm samples, would be required in order to provide further empirical evidence – extending to the use of an additional replicate in conjunction with other methods of validation.

In summary, this body of work has provided bioinformatical evidence for several novel miRNA species. An extensive list of potential targets of five selected candidate *Nov-miR*s was

established using a suit of target prediction tools, and a number of these targets were involved in pathways similar to those regulated but previously known epididymal miRNAs. Experimental validation by way of RT-qPCR provided evidence to support the presence of *Nov-miR13*, *Nov-miR42* and *Nov-miR101*, while further validation is required to suggest these molecules exist within the epididymal epithelium. Given the exceptional sequencing depth achieved by the NGS analyses employed throughout these studies, we are confident that we are close to having compiled a complete list of all species of miRNAs present within the epididymis. Indeed, as the miRCat tool utilised in this study to identify novel miRNAs has been able to flag a number of candidates close to the threshold of detection (≥ 10 reads), it is not likely that future use of additional bioinformatics tools for novel miRNA identification will yield any further candidates.

Chapter 6: Future Directions and Final Conclusions

6.1 Introduction

The results presented in this thesis provide evidence for the importance of miRNAs throughout the epididymis, a pivotal accessory organ of the male reproductive tract. Indeed, it is evident that the sperm miRNA signature is modified extensively as these cells transit the epididymis and a key method by which the male gametes acquire new miRNA molecules lies in the interaction with epididymosomes. As documented in previous studies, epididymosomes differ in miRNA cargo from their parent epithelial cells, such that these vesicles are comprised of highly dynamic and regionalised miRNA profiles while epididymal epithelial cells possess similar miRNA profiles throughout the tract. This suggests selective packaging of molecules into these vesicles in order to tailor the cargo harboured by recipient cells, a phenomenon that draws parallels with that of several other cells types throughout the body. In addition to the known miRNAs identified in these analyses, it was determined that several putative novel miRNA molecules also exist within epididymal samples, with several of these being identified in significant abundance, though with the caveat that further experimental validation of these molecules is required. Each of the findings presented herein scratch the surface of the role that sRNAs play within the epididymis, and thus pave the way for a number of exciting avenues of future research into the functional significance of these molecules in the context of male reproduction.

6.2 Future Work

An interesting focus for future study would be further bioinformatic investigation of miRNAs throughout the epididymis. A number of different avenues of research could be explored in order to expand and improve upon the three studies outlined in Chapter 3 of this document. As a starting point, it would be advantageous to examine the genomic locations of the known

miRNAs identified in the mouse epididymis throughout this study in an effort to determine localisation of specific clusters. Approximately 40 % of miRNAs across species such as the mouse and human are found in genomic clusters [356], with 51 and 55 unique clusters existing in the genome of each of these species, respectively [357]. Intriguingly, miRNA clusters often contain sequences originating from several different families at a time, suggesting that each cluster can target a broad range of mRNAs. Further, it has been suggested that genes coding for proteins that interact with each other in order to perform their biological function, are each targeted by a single cluster of miRNAs, suggesting that regulatory networks directed by these molecules are more elegant than previously thought [357]. By mapping known miRNAs identified throughout this study, the scope of epididymal target genes may be narrowed, presenting a unique and detailed insight into the functional significance of epididymal miRNAs [358-360].

During the course of these studies we demonstrated that epididymal sperm possess crucial miRNA processing machinery. In tandem with this analysis was the examination of these machinery within male gametes at differing stages of development, with spermatogonial stem cells (Spg), meiotic pachytene spermatocytes (PS), post meiotic round spermatids (RS), and testicular sperm forming the basis of this analysis. The role of miRNAs during spermatogenesis has been documented previously, with several studies having identified a number of miRNAs that are preferentially expressed in specific testicular cells (as documented in Table 1.1). However, one drawback of these analyses is the inconsistencies involving miRNA detection technologies. Further, microarrays, a technology becoming increasingly outdated in favour of NGS, has featured in many of these studies, leaving room for significant improvement by way of more advanced sequencing technologies. Though this lies well-outside of the scope or this thesis or the studies documented herein, the evaluation of miRNA profiles by NGS within the progressively changing cells involved in spermatogenesis could shed additional light onto the role that these small molecules play in the generation of physiologically normal nascent sperm. Indeed, our laboratory already possesses the capacity to perform the isolation of highly enriched populations of testicular germ cells, an established bioinformatic toolkit for analysis of this dataset as well as

downstream wet-lab validation methodology. Studies involving the study of sncRNAs in these cell lines via NGS would ultimately build on our current understanding of the reproductive process in mammalian males.

Another avenue for future research effort centres on further optimization of epididymosome co-incubation strategies with spermatozoa. The protocol employed in this study was based on those used to achieve protein transfer from the microvesicles to gametes in previous studies [197]. As a starting point, the protocol for co-incubation of these two epididymal components could be further optimised in order to promote transfer of molecules *in vitro*. The temperature selected for use in the protocol employed in this study was 37°C, which is above that of the physiological temperature in which epididymosomes and spermatozoa are produced in most mammals. Though a wealth of studies detailing exosome mediated transfer of protein and RNAs to a range of cells is available, studies exploring a range of temperatures in order to achieve greater transfer of molecules to recipient cells are lacking. Exploration of several other conditions of the co-incubation protocol could work to enhance transfer to recipient sperm. For example, several studies have employed co-incubation between somatic cells and exosomes for up to 72 hours [361], while other studies have allowed reactions to take place for just 35 minutes [362]. If sufficient and measurable transfer of RNA molecules to sperm can be achieved in a shorter time period than that used in this project, it would greatly assist in downstream experiments as sperm would be exposed to an exogenous environment for a shorter period of time and thereby be more likely to retain vitality at the end point of the experiment.

Another potentially important factor influencing epididymosome fusion with sperm could lie in the supplementation of the reaction media. In this study, media was adjusted to pH 6.5 and supplemented with $ZnCl_2$. The pH of the bull epididymis ranges between 6.0 and 6.5 [363], conditions which were matched by a number of studies investigating epididymosome and sperm co-incubation conducted in the same species. Interestingly, though the present study conformed to these conditions, a previous study investigating the transfer of proteins to sperm in the murine model did not alter pH of media used for their reaction (PBS: pH 7.4) [181]. This begs the question

as to whether the low pH utilised in the present study served to improve the interactions between epididymosomes and sperm, or instead simply resulted in a decrease in sperm vitality. Emphasizing this point, a recent study investigating the impact of a range of pH conditions on the progressive motility, hypo-osmotic swelling rate, sperm penetration and ATPase activity has suggested that lower pH (5.2 – 6.2) results in declined fertility, while higher there was no difference observed between the higher pH values tested (7.2 – 8.2) [364]. Despite co-incubation of epididymosomes with sperm using material sourced from the bull being optimised for pH 6.5 conditions, pH optimisation of this protocol for use with mouse material was not performed in this study. Given that mouse sperm are notoriously susceptible to high mortality *in vitro* culture, it would be favourable to determine whether an efficient reaction can take place in a medium with a pH more suited to these cells, and allow sperm cells to retain vitality during co-incubation with epididymosomes. This would prove beneficial for future studies involving the *in vitro* fertilisation of oocytes with sperm harbouring tailored miRNA cargo.

It has been documented across a number of species, including the mouse, that the epididymis is replete in a number of divalent cations, especially zinc [365-369]. As a result of this, several divalent cations, including Mg^{2+}, Ca^{2+}, and Zn^{2+} have been tested for the ability to increase efficiency of protein delivery to sperm following co-incubation with epididymosomes using the bull as a model, with only the latter of these exhibiting any kind of benefit. Though supplementation of co-incubation media with zinc was utilised in the current study, it was not outlined as method used in previous studies centring on murine models [181]. Further, in an analysis performed by Sharma and colleagues (who pioneered the protocol for these specific co-incubation experiments), zinc supplementation was omitted from the materials and methods [184], suggesting it may not play as influential a role as previously thought. In fact, it is possible that the presence of the zinc in these reactions could inhibit the functional competence of sperm. For example, excessive amounts of zinc, comparable to this utilised in the current study have been documented as having inhibitory effects on sperm acrosome reactions, as well as sperm motility [370]. Though this complication is not regarded as an issue for studies analysing the

content bestowed upon sperm, this does leads one to speculate whether the addition of zinc to epididymosome and sperm co-incubation reactions, in an effort to improve interaction efficiency, is a worthy trade-off for optimal sperm function if future end-point experiments involve the incubation of these sperm with oocytes *in vitro*, as this may elicit significant declination of fertilisation success.

A final point of optimization required for the co-incubation protocol highlighted in this project would be the alteration of epididymal sperm and epididymosome concentrations. Previous studies documenting exosome-mediated transfer of RNA and proteins to recipient cells have used a myriad of concentrations of vesicles in the final reaction volume, with no apparent consensus of proportion of cells to vesicles documented across the field of research. Further, several studies conducted on the bovine model within the same research group have shown varying ratios of epididymosomes to sperm; the proportion of epididymosome protein to number of sperm in a the 2016 study [184] being extended to 12 times the amount used in 2013 [195], and an 80 fold increase on that originally reported in 2012 [371]. The analyses presented in this study, as well as those documented in the mouse previously [181], did not account for concentration of epididymosomes used in co-incubation experiments. Rather, epididymosomes were sourced in these studies from an equivalent number of mice. This ensures that transfer of molecules documented in this study more closely resembles the physiological uptake of RNA and protein in the epididymis when compared to previous studies, as each of these are relying on progressively increased saturation of cells with vesicles during these experiments that could work to convey an unrealistic model for natural delivery. Indeed, it would be advantageous to document the impact of increasing epididymosome concentration in these reactions, and to optimise this for maximum delivery of RNA and protein to living cells. In particular, this would prove useful in experiments seeking to tailor the payload of sperm for specific functions in downstream analyses as it may allow for greater transfer of miRNAs of interest.

Additional experiments investigating the transfer of molecules to sperm could prove useful in highlighting the mechanisms by and extent to which this elegant process occurs. One

such experiment could involve the tracking of a miRNA from a cell line into sperm through a number of steps. First, a 'miRNA mimic' (an artificial molecule containing a double stranded miRNA-like structure) incorporating a fluorescent tag, could be transfected into cultured epididymal epithelial cells grown in exosome depleted media, and this process could be confirmed via fluorescence microscopy and RT-qPCR for the miRNA. Exosomes produced by these cells could then be subjected to several lines of validation; transfected exosomes could be compared with controls again via bead binding fluorescence microscopy and RT-qPCR, while Western blotting and particle sizing could be performed as additional lines of evidence for the production of these vesicles. Providing fluorescence could be detected within the vesicles, exosomes from transfected cultured cells could then be co-incubated with purified epididymal sperm in a similar fashion as described throughout this project. As the exosomes produced by cultured cells may differ in composition, and therefore function, to those produced *in vivo*, co-incubation protocols may need to be optimised in order to ensure the efficient transfer of material to sperm cells. Overall, optimisation of such protocols would allow for a greater understanding of the way in which the sophisticated process of delivering RNAs to male gametes occurs, opening up several avenues for the manipulation of this process for the treatment of male fertility.

An additional point that would serve to complete the investigation of epididymal sRNAs would be a study focussing on the bulk transfer of miRNAs to sperm during epididymal transit. During the studies presented herein, the first evidence of miRNA transfer from epididymosomes elaborated by the epididymal epithelium to sperm was documented, while a 2016 study by Rando and colleagues provided the first evidence of tRF transfer to sperm via these microvesicles [235]. However, in the former study the transfer of only 9 miRNAs was detailed [163], while in the latter study documented over a dozen tRFs transferred. Additionally, the trafficking of piRNAs to epididymal sperm is yet to be elucidated. Given the complex and thorough datasets obtained throughout the studies documented in this thesis, an advantage of performing this analysis is that a firm basis already exists that would allow for a comparison between consistently produced datasets. The study of bulk transfer of sRNAs to sperm would form a solid foundation for future

studies investigating the therapeutic options for restoration of the epigenetic landscape of defective spermatozoa, and ultimately aid in determining the role that miRNAs play in male fertility.

After having determined the extent to which sRNAs can be trafficked *in vitro* using the mouse as a model, it would be worth investigating whether fusion between epididymosomes and sperm of differing species can be achieved. Cross species analyses are becoming more prominent throughout the area of reproductive biology, with a prime example of this being the use of the more readily available bovine oocytes in the assessment of the ability of equine sperm to bind to a zona pellucida (ZP) [372]. With this approach being used as an industry standard to obtain sufficient oocytes for zona pellucida binding assays, it is feasible to suggest that this approach may also be used to overcome the issue of large specimen numbers required for the isolation of large quantities of epididymosomes from small animals. For example, in the aforementioned study investigating the bulk delivery of sRNAs to sperm, large numbers of animals would be required to harvest sufficient epididymosomes to produce adequate samples for biological replication. However, if bovine epididymosomes sourced from animals already being processed at abattoirs are able to fuse with mice sperm, they could replace the use of murine epididymosomes and thus reduce the number of animals sacrificed. Of course, the analysis of cross species interactions between sperm and epididymosomes would require extensive experimentation employing the co-incubation protocol dictated within this thesis - though it is likely that, due to sperm sourced from differing species possessing different needs in culture, this protocol would need to be altered in order to ensure efficient binding of, and transfer of cargo from, epididymosomes to sperm. Beyond a reduction in the number of animals utilised, such an approach could be exploited in an effort to determine the level of conservation of the receptors harboured by sperm and epididymosomes that may facilitate their interactions, and therefore serve to aid in the identification of these molecules. Further, if a transfer of RNAs is observed during these cross-species studies, it would be feasible to suggest that membrane proteins of epididymosomes may be conserved between species – a topic that could form the basis of future

studies focussing on the proteomic content of these vesicles.

The final point of interest for this study lies within the alteration of epididymal sRNA signatures. Though it is possible to source a functionally immature sperm from the testes and use it to fertilize an egg, ICSI and other assisted reproductive technologies can result in a variety of offspring epigenetic syndromes, with functionally immature sperm being highlighted as a potential contributor to this phenomenon [4]. Such findings implicate the post-testicular maturation of sperm in the epididymis as a crucial point for the epigenetic modification of male gametes prior to fertilisation. An interesting point of further research for this project, would be the investigation of the impact that several other well-documented environmental insults that have been documented to have an adverse effect on the viability of sperm (including testicular heating [373], dietary acrylamide exposure [374], and electromagnetic radiation [375]) have on epididymal sRNA profiles. Providing these insults result in alteration of the sRNA content of the epididymis, it would then be worth investigating whether these insults, as well as cigarette smoke which has been previously shown to influence sperm miRNA profiles [171], are able to convey transgenerational effects to offspring. The investigation of such a phenomenon could be broken down into several stages to elucidate the mechanisms by which these insults effect sperm. Of particular interest would be the trafficking of altered miRNA profiles from epididymal epithelial cells to epididymosomes, and subsequently from epididymosomes to spermatozoa. Should this be the mechanism by which epigenetic changes are bestowed upon maturing sperm, and if these changes are not observed within testicular cells, it would firmly implicate the epididymis as an important region of the male reproductive tract for epigenetic modification of the male germ cell. Such findings would also prompt the investigation into a new avenue of research: the treatment of sperm via tailored vesicles prior to IVF. Though it would be beneficial to gain a greater understanding of epididymosome-sperm interactions in order to tailor exosomes to have an affinity for these cells, a previous study has already documented that an artificially manufactured liposome harbouring exogenous DNA was able to interact with, and deliver its contents to, the sperm head [252]. Such findings suggest that vesicles loaded with specific repertoires of sRNAs

may, at some point in the future, be used as a vector to help restore typical epigenetic profiles of mammalian sperm prior to the use of pre-existing assisted reproductive technologies.

6.3 Final conclusions

Within the context of this project, we have investigated the comprehensive profiles of miRNAs in epithelial cells, spermatozoa and epididymosomes sourced from the three dominant anatomical segments of the mouse epididymis. The results produced throughout the course of this project provide evidence for a pivotal role of miRNAs play in the regulation of epididymal physiology and function. Indeed, it is highly likely that these small molecules form an integral part of the regulatory network that governs the segment specific secretion of proteins and, in turn, forms the unique microenvironments the drive the acquisition of functional competence in the maturing male gametes. An impressive 218, 295, and 358 miRNAs were found in epithelial cells, sperm, and epididymosomes respectively via systematic screening of samples using NGS. The miRNA profile of mouse epithelial cells contains fewer miRNAs characterised by significant fold changes in abundance between segments, suggesting that these molecules play roles in modulating segment specific microenvironments, while the majority are involved in housekeeping roles. The analyses also lead to the discovery that sperm miRNA profiles are subjected to substantial modification as the cells traverse the tract, with the majority of molecules held by sperm being characterised by significant fold changes in abundance; a finding that extends the potential roles that miRNAs play during downstream biological processes associated with fertilisation and/or embryo development. Finally, the study of epididymosomes revealed that they possess a complex selection of miRNA cargo. Perhaps the most exciting finding of this project was the demonstration that epididymosomes can as vectors to deliver miRNA cargo to spermatozoa *in vitro*, suggesting that the extended exposure of these cells to the intraluminal milieu of the epididymis is responsible for establishing an optimal epigenome for sperm to take forward to the female reproductive tract during coitus.

Complementary analysis of novel miRNAs (*Nov-miR*s) expressed in the mouse epididymis led to the identification of 22 potentially novel molecules, of which five were

subjected to detailed validation and *in silico* target prediction. This strategy confirmed that three of the *Nov-miR*s were present in epididymal sperm, including the highly abundant *Nov-miR13*. Though additional work in now necessary to confirm the presence of these molecules, as well as experimental evidence to support their ability to regulate predicted target genes, it appears that the epididymis may host a number of novel miRNA species.

Finally, the findings presented herein provide a strong platform for a number of important future studies. These include; optimization of the *in vitro* sperm-epididymosome co-incubation strategy, the detection of additional species of sRNAs (such as piRNAs and tRFs) within the epididymis, investigation into the scope of sRNA delivery to sperm during epididymal transit, and the effects of environmental insults on the sRNA profile of sperm and on future generations.

References

1. Skakkebaek, N.E., et al., *Is human fecundity declining?* Int J Androl, 2006. **29**(1): p. 2-11.
2. McLachlan, R.I. and D.M. de Kretser, *Male infertility: the case for continued research.* Med J Aust, 2001. **174**(3): p. 116-7.
3. Liu, D.Y. and H.W. Baker, *Defective sperm-zona pellucida interaction: a major cause of failure of fertilization in clinical in-vitro fertilization.* Hum Reprod, 2000. **15**(3): p. 702-8.
4. Odom, L.N. and J. Segars, *Imprinting disorders and assisted reproductive technology.* Current opinion in endocrinology, diabetes, and obesity, 2010. **17**(6): p. 517-522.
5. Niemitz, E.L. and A.P. Feinberg, *Epigenetics and Assisted Reproductive Technology: A Call for Investigation.* American Journal of Human Genetics, 2004. **74**(4): p. 599-609.
6. Maher, E.R., M. Afnan, and C.L. Barratt, *Epigenetic risks related to assisted reproductive technologies: epigenetics, imprinting, ART and icebergs?* Hum Reprod, 2003. **18**(12): p. 2508-11.
7. Pinborg, A., et al., *Epigenetics and assisted reproductive technologies.* Acta Obstet Gynecol Scand, 2016. **95**(1): p. 10-5.
8. Iliadou, A.N., P.C. Janson, and S. Cnattingius, *Epigenetics and assisted reproductive technology.* J Intern Med, 2011. **270**(5): p. 414-20.
9. Hale, B.J., C.X. Yang, and J.W. Ross, *Small RNA regulation of reproductive function.* Mol Reprod Dev, 2014. **81**(2): p. 148-59.
10. Bartel, D.P., *MicroRNAs: genomics, biogenesis, mechanism, and function.* Cell, 2004. **116**(2): p. 281-97.

11. Lee, C.T., T. Risom, and W.M. Strauss, *MicroRNAs in mammalian development.* Birth Defects Res C Embryo Today, 2006. **78**(2): p. 129-39.

12. Chawla, G. and N.S. Sokol, *MicroRNAs in Drosophila development.* Int Rev Cell Mol Biol, 2011. **286**: p. 1-65.

13. Flynt, A.S. and E.C. Lai, *Biological principles of microRNA-mediated regulation: shared themes amid diversity.* Nature reviews. Genetics, 2008. **9**(11): p. 831-842.

14. Li, C. and B. Zhang, *MicroRNAs in Control of Plant Development.* J Cell Physiol, 2016. **231**(2): p. 303-13.

15. Peter, M.E., *Targeting of mRNAs by multiple miRNAs: the next step.* Oncogene, 2010. **29**(15): p. 2161-4.

16. Erson-Bensan, A.E., *Introduction to microRNAs in biological systems.* Methods Mol Biol, 2014. **1107**: p. 1-14.

17. Liu, X., K. Fortin, and Z. Mourelatos, *MicroRNAs: biogenesis and molecular functions.* Brain Pathol, 2008. **18**(1): p. 113-21.

18. Williams, A.E., *Functional aspects of animal microRNAs.* Cell Mol Life Sci, 2008. **65**(4): p. 545-62.

19. Ha, M. and V.N. Kim, *Regulation of microRNA biogenesis.* Nat Rev Mol Cell Biol, 2014. **15**(8): p. 509-524.

20. Ardekani, A.M. and M.M. Naeini, *The Role of MicroRNAs in Human Diseases.* Avicenna Journal of Medical Biotechnology, 2010. **2**(4): p. 161-179.

21. Kawahara, Y., *Human diseases caused by germline and somatic abnormalities in microRNA and microRNA-related genes.* Congenit Anom (Kyoto), 2014. **54**(1): p. 12-21.

22. Meola, N., V.A. Gennarino, and S. Banfi, *microRNAs and genetic diseases.* Pathogenetics, 2009. **2**(1): p. 7.

23. Tan, L., J.T. Yu, and L. Tan, *Causes and Consequences of MicroRNA Dysregulation in Neurodegenerative Diseases.* Mol Neurobiol, 2015. **51**(3): p. 1249-62.

24. Sassen, S., E.A. Miska, and C. Caldas, *MicroRNA—implications for cancer.* Virchows Archiv, 2008. **452**(1): p. 1-10.

25. Kye, M.J. and I.d.C.G. Gonçalves, *The role of miRNA in motor neuron disease.* Frontiers in Cellular Neuroscience, 2014. **8**: p. 15.

26. Maes, O.C., et al., *MicroRNA: Implications for Alzheimer Disease and other Human CNS Disorders.* Current Genomics, 2009. **10**(3): p. 154-168.

27. Lee, Y., et al., *The nuclear RNase III Drosha initiates microRNA processing.* Nature, 2003. **425**(6956): p. 415-9.

28. Han, J., et al., *The Drosha-DGCR8 complex in primary microRNA processing.* Genes & Development, 2004. **18**(24): p. 3016-3027.

29. Faller, M., et al., *DGCR8 recognizes primary transcripts of microRNAs through highly cooperative binding and formation of higher-order structures.* RNA, 2010. **16**(8): p. 1570-1583.

30. Auyeung, V.C., et al., *Beyond secondary structure: primary-sequence determinants license pri-miRNA hairpins for processing.* Cell, 2013. **152**(4): p. 844-858.

31. Barr, I. and F. Guo, *Primary microRNA processing assay reconstituted using recombinant Drosha and DGCR8.* Methods Mol Biol, 2014. **1095**: p. 73-86.

32. Quick-Cleveland, J., et al., *The DGCR8 RNA-binding heme domain recognizes primary microRNAs by clamping the hairpin.* Cell reports, 2014. **7**(6): p. 1994-2005.

33. Han, J., et al., *The Drosha-DGCR8 complex in primary microRNA processing.* Genes Dev, 2004. **18**(24): p. 3016-27.

34. Macrae, I.J., et al., *Structural basis for double-stranded RNA processing by Dicer.* Science, 2006. **311**(5758): p. 195-8.

35. Abdelfattah, A.M., C. Park, and M.Y. Choi, *Update on non-canonical microRNAs.* Biomolecular concepts, 2014. **5**(4): p. 275-287.

36. Havens, M.A., et al., *Biogenesis of mammalian microRNAs by a non-canonical processing pathway.* Nucleic Acids Research, 2012. **40**(10): p. 4626-4640.

37. Okamura, K., et al., *The mirtron pathway generates microRNA-class regulatory RNAs in Drosophila.* Cell, 2007. **130**(1): p. 89-100.

38. Ruby, J.G., C.H. Jan, and D.P. Bartel, *Intronic microRNA precursors that bypass Drosha processing.* Nature, 2007. **448**(7149): p. 83-6.

39. Bohnsack, M.T., K. Czaplinski, and D. Gorlich, *Exportin 5 is a RanGTP-dependent dsRNA-binding protein that mediates nuclear export of pre-miRNAs.* RNA, 2004. **10**(2): p. 185-91.

40. Yi, R., et al., *Exportin-5 mediates the nuclear export of pre-microRNAs and short hairpin RNAs.* Genes Dev, 2003. **17**(24): p. 3011-6.

41. Carmell, M.A. and G.J. Hannon, *RNase III enzymes and the initiation of gene silencing.* Nat Struct Mol Biol, 2004. **11**(3): p. 214-8.

42. Park, J.E., et al., *Dicer recognizes the 5' end of RNA for efficient and accurate processing.* Nature, 2011. **475**(7355): p. 201-5.

43. Lau, P.-W., et al., *The Molecular Architecture of Human Dicer.* Nature structural & molecular biology, 2012. **19**(4): p. 436-440.

44. Lee, H.Y. and J.A. Doudna, *TRBP alters human precursor microRNA processing in vitro.* RNA, 2012. **18**(11): p. 2012-2019.

45. Chakravarthy, S., et al., *Substrate-specific kinetics of Dicer-catalyzed RNA processing.* J Mol Biol, 2010. **404**(3): p. 392-402.

46. Nykanen, A., B. Haley, and P.D. Zamore, *ATP requirements and small interfering RNA structure in the RNA interference pathway.* Cell, 2001. **107**(3): p. 309-21.

47. Iwasaki, S., et al., *Hsc70/Hsp90 chaperone machinery mediates ATP-dependent RISC loading of small RNA duplexes.* Mol Cell, 2010. **39**(2): p. 292-9.

48. Hu, H.Y., et al., *Sequence features associated with microRNA strand selection in humans and flies.* BMC Genomics, 2009. **10**: p. 413.

49. Ro, S., et al., *Tissue-dependent paired expression of miRNAs.* Nucleic Acids Research, 2007. **35**(17): p. 5944-5953.

50. Bhayani, M.K., G.A. Calin, and S.Y. Lai, *Functional relevance of miRNA* sequences in human disease.* Mutation Research/Fundamental and Molecular Mechanisms of Mutagenesis, 2012. **731**(1–2): p. 14-19.

51. Meijer, H.A., E.M. Smith, and M. Bushell, *Regulation of miRNA strand selection: follow the leader?* Biochem Soc Trans, 2014. **42**(4): p. 1135-40.

52. Yekta, S., I.H. Shih, and D.P. Bartel, *MicroRNA-directed cleavage of HOXB8 mRNA.* Science, 2004. **304**(5670): p. 594-6.

53. Lewis, B.P., et al., *Prediction of mammalian microRNA targets.* Cell, 2003. **115**(7): p. 787-98.

54. Brennecke, J., et al., *Principles of microRNA-target recognition.* PLoS Biol, 2005. **3**(3): p. e85.

55. Krek, A., et al., *Combinatorial microRNA target predictions.* Nat Genet, 2005. **37**(5): p. 495-500.

56. Lewis, B.P., C.B. Burge, and D.P. Bartel, *Conserved seed pairing, often flanked by adenosines, indicates that thousands of human genes are microRNA targets.* Cell, 2005. **120**(1): p. 15-20.

57. Grimson, A., et al., *MicroRNA targeting specificity in mammals: determinants beyond seed pairing.* Mol Cell, 2007. **27**(1): p. 91-105.

58. Hutvagner, G. and P.D. Zamore, *A microRNA in a multiple-turnover RNAi enzyme complex.* Science, 2002. **297**(5589): p. 2056-60.

59. Elbashir, S.M., W. Lendeckel, and T. Tuschl, *RNA interference is mediated by 21- and 22-nucleotide RNAs.* Genes Dev, 2001. **15**(2): p. 188-200.

60. Tang, G., et al., *A biochemical framework for RNA silencing in plants.* Genes Dev, 2003. **17**(1): p. 49-63.

61. Valencia-Sanchez, M.A., et al., *Control of translation and mRNA degradation by miRNAs and siRNAs.* Genes Dev, 2006. **20**(5): p. 515-24.

62. Pillai, R.S., *MicroRNA function: multiple mechanisms for a tiny RNA?* RNA, 2005. **11**(12): p. 1753-61.

63. Pillai, R.S., et al., *Inhibition of translational initiation by Let-7 MicroRNA in human cells.* Science, 2005. **309**(5740): p. 1573-6.

64. Kiriakidou, M., et al., *An mRNA m7G cap binding-like motif within human Ago2 represses translation.* Cell, 2007. **129**(6): p. 1141-51.

65. Moretti, F., et al., *PABP and the poly(A) tail augment microRNA repression by facilitated miRISC binding.* Nat Struct Mol Biol, 2012. **19**(6): p. 603-8.

66. Chendrimada, T.P., et al., *MicroRNA silencing through RISC recruitment of eIF6.* Nature, 2007. **447**(7146): p. 823-8.

67. de Mateo, S. and P. Sassone-Corsi, *Regulation of spermatogenesis by small non-coding RNAs: role of the germ granule.* Semin Cell Dev Biol, 2014. **29**: p. 84-92.

68. Oatley, J.M. and R.L. Brinster, *THE GERMLINE STEM CELL NICHE UNIT IN MAMMALIAN TESTES.* Physiological reviews, 2012. **92**(2): p. 577-595.

69. De Rooij, D.G. and L.D. Russell, *All You Wanted to Know About Spermatogonia but Were Afraid to Ask.* Journal of Andrology, 2000. **21**(6): p. 776-798.

70. de Rooij, D., *Proliferation and differentiation of spermatogonial stem cells.* Reproduction, 2001. **121**(3): p. 347-354.

71. Hess, R.A. and L. Renato de Franca, *Spermatogenesis and cycle of the seminiferous epithelium.* Adv Exp Med Biol, 2008. **636**: p. 1-15.

72. de Kretser, D.M., et al., *Spermatogenesis.* Hum Reprod, 1998. **13 Suppl 1**: p. 1-8.

73. Phillips, B.T., K. Gassei, and K.E. Orwig, *Spermatogonial stem cell regulation and spermatogenesis.* Philos Trans R Soc Lond B Biol Sci, 2010. **365**(1546): p. 1663-78.

74. Kimmins, S., et al., *Testis-specific transcription mechanisms promoting male germ-cell differentiation.* Reproduction, 2004. **128**(1): p. 5-12.

75. Kimmins, S. and P. Sassone-Corsi, *Chromatin remodelling and epigenetic features of germ cells.* Nature, 2005. **434**(7033): p. 583-589.

76. Jan, S.Z., et al., *Molecular control of rodent spermatogenesis.* Biochimica et Biophysica Acta (BBA) - Molecular Basis of Disease, 2012. **1822**(12): p. 1838-1850.

77. Tanaka, H. and T. Baba, *Gene expression in spermiogenesis.* Cellular and Molecular Life Sciences CMLS, 2005. **62**(3): p. 344-354.

78. Marcon, E., et al., *miRNA and piRNA localization in the male mammalian meiotic nucleus.* Chromosome Res, 2008. **16**(2): p. 243-60.

79. Ro, S., et al., *Cloning and expression profiling of testis-expressed microRNAs.* Developmental biology, 2007. **311**(2): p. 592-602.

80. Smorag, L., et al., *MicroRNA signature in various cell types of mouse spermatogenesis: Evidence for stage-specifically expressed miRNA-221, -203 and -34b-5p mediated spermatogenesis regulation.* Biology of the Cell, 2012. **104**(11): p. 677-692.

81. Barad, O., et al., *MicroRNA expression detected by oligonucleotide microarrays: system establishment and expression profiling in human tissues.* Genome Res, 2004. **14**(12): p. 2486-94.

82. Kotaja, N., *MicroRNAs and spermatogenesis.* Fertil Steril, 2014. **101**(6): p. 1552-62.

83. Bao, J., et al., *MicroRNA-449 and microRNA-34b/c function redundantly in murine testes by targeting E2F transcription factor-retinoblastoma protein (E2F-pRb) pathway.* J Biol Chem, 2012. **287**(26): p. 21686-98.

84. Bouhallier, F., et al., *Role of miR-34c microRNA in the late steps of spermatogenesis.* RNA, 2010. **16**(4): p. 720-731.

85. Dai, L., et al., *Testis-specific miRNA-469 up-regulated in gonadotropin-regulated testicular RNA helicase (GRTH/DDX25)-null mice silences transition*

protein 2 and protamine 2 messages at sites within coding region: implications of its role in germ cell development. J Biol Chem, 2011. **286**(52): p. 44306-18.

86. Liu, T., et al., *MicroRNA-122 influences the development of sperm abnormalities from human induced pluripotent stem cells by regulating TNP2 expression.* Stem Cells Dev, 2013. **22**(12): p. 1839-50.

87. Bjorkgren, I. and P. Sipila, *The role of Dicer1 in the male reproductive tract.* Asian J Androl, 2015. **17**(5): p. 737-41.

88. Korhonen, H.M., et al., *Dicer Is Required for Haploid Male Germ Cell Differentiation in Mice.* PLoS ONE, 2011. **6**(9): p. e24821.

89. Yan, N., et al., *A microarray for microRNA profiling in mouse testis tissues.* Reproduction, 2007. **134**(1): p. 73-9.

90. Wu, J., et al., *MicroRNA-184 downregulates nuclear receptor corepressor 2 in mouse spermatogenesis.* BMC Developmental Biology, 2011. **11**(1): p. 1-10.

91. Romero, Y., et al., *Dicer1 depletion in male germ cells leads to infertility due to cumulative meiotic and spermiogenic defects.* PLoS One, 2011. **6**(10): p. e25241.

92. Tanaka, H. and T. Baba, *Gene expression in spermiogenesis.* Cell Mol Life Sci, 2005. **62**(3): p. 344-54.

93. Hayashi, K., et al., *MicroRNA Biogenesis Is Required for Mouse Primordial Germ Cell Development and Spermatogenesis.* PLoS ONE, 2008. **3**(3): p. e1738.

94. Dyce, P.W., D. Toms, and J. Li, *Stem cells and germ cells: microRNA and gene expression signatures.* Histol Histopathol, 2010. **25**(4): p. 505-13.

95. Rosa, A. and A.H. Brivanlou, *A regulatory circuitry comprised of miR-302 and the transcription factors OCT4 and NR2F2 regulates human embryonic stem cell differentiation.* EMBO J, 2011. **30**(2): p. 237-48.

96. Lichner, Z., et al., *The miR-290-295 cluster promotes pluripotency maintenance by regulating cell cycle phase distribution in mouse embryonic stem cells.* Differentiation, 2011. **81**(1): p. 11-24.

97. Novotny, G.W., et al., *Analysis of gene expression in normal and neoplastic human testis: new roles of RNA.* Int J Androl, 2007. **30**(4): p. 316-26; discussion 326-7.

98. Novotny, G.W., et al., *Translational repression of E2F1 mRNA in carcinoma in situ and normal testis correlates with expression of the miR-17-92 cluster.* Cell Death Differ, 2007. **14**(4): p. 879-82.

99. Lian, J., et al., *Altered microRNA expression in patients with non-obstructive azoospermia.* Reproductive Biology and Endocrinology : RB&E, 2009. **7**: p. 13-13.

100. Luo, L., et al., *Microarray-based approach identifies differentially expressed microRNAs in porcine sexually immature and mature testes.* PLoS One, 2010. **5**(8): p. e11744.

101. Zhong, X., et al., *Identification of microRNAs regulating reprogramming factor LIN28 in embryonic stem cells and cancer cells.* J Biol Chem, 2010. **285**(53): p. 41961-71.

102. Tian, H., et al., *The targeting and functions of miRNA-383 are mediated by FMRP during spermatogenesis.* Cell Death & Disease, 2013. **4**(5): p. e617.

103. Buchold, G.M., et al., *Analysis of microRNA expression in the prepubertal testis.* PLoS One, 2010. **5**(12): p. e15317.

104. Eades, G., et al., *miR-200a regulates SIRT1 expression and epithelial to mesenchymal transition (EMT)-like transformation in mammary epithelial cells.* J Biol Chem, 2011. **286**(29): p. 25992-6002.

105. Hu, M., et al., *MicroRNA-141 regulates Smad interacting protein 1 (SIP1) and inhibits migration and invasion of colorectal cancer cells.* Dig Dis Sci, 2010. **55**(8): p. 2365-72.

106. Radisky, D.C., *miR-200c at the nexus of epithelial-mesenchymal transition, resistance to apoptosis, and the breast cancer stem cell phenotype.* Breast Cancer Research : BCR, 2011. **13**(3): p. 110-110.

107. Song, L., et al., *Cellular microRNAs inhibit replication of the H1N1 influenza A virus in infected cells.* J Virol, 2010. **84**(17): p. 8849-60.

108. Li, C., et al., *MicroRNA-16 Modulates Melatonin-Induced Cell Growth in the Mouse-Derived Spermatogonia Cell Line GC-1 spg Cells by Targeting Ccnd1.* Biology of Reproduction, 2016.

109. Niu, Z., et al., *MicroRNA-21 regulates the self-renewal of mouse spermatogonial stem cells.* Proceedings of the National Academy of Sciences, 2011. **108**(31): p. 12740-12745.

110. He, Z., et al., *MiRNA-20 and mirna-106a regulate spermatogonial stem cell renewal at the post-transcriptional level via targeting STAT3 and Ccnd1.* Stem Cells, 2013. **31**(10): p. 2205-17.

111. Huszar, J.M. and C.J. Payne, *MicroRNA 146 (Mir146) Modulates Spermatogonial Differentiation by Retinoic Acid in Mice.* Biology of Reproduction, 2013. **88**(1): p. 15.

112. Yang, Q.E., et al., *MicroRNAs 221 and 222 regulate the undifferentiated state in mammalian male germ cells.* Development, 2013. **140**(2): p. 280-90.

113. Rong, Z., et al., *Screening for miRNAs and their potential targets in response to TGF-beta1 based on miRNA microarray and comparative proteomics analyses in a mouse GC-1 spg germ cell line.* Int J Mol Med, 2015. **35**(3): p. 821-8.

114. Liang, X., et al., *MicroRNA-34c enhances murine male germ cell apoptosis through targeting ATF1.* PLoS One, 2012. **7**(3): p. e33861.

115. Bjork, J.K., et al., *miR-18, a member of Oncomir-1, targets heat shock transcription factor 2 in spermatogenesis.* Development, 2010. **137**(19): p. 3177-84.

116. Yu, Z., T. Raabe, and N.B. Hecht, *MicroRNA Mirn122a Reduces Expression of the Posttranscriptionally Regulated Germ Cell Transition Protein 2 (Tnp2) Messenger RNA (mRNA) by mRNA Cleavage.* Biology of Reproduction, 2005. **73**(3): p. 427-433.

117. Bouhallier, F., et al., *Role of miR-34c microRNA in the late steps of spermatogenesis.* RNA, 2010. **16**(4): p. 720-31.

118. Nagaraja, A.K., et al., *A link between mir-100 and FRAP1/mTOR in clear cell ovarian cancer.* Mol Endocrinol, 2010. **24**(2): p. 447-63.

119. Ito, T., S. Yagi, and M. Yamakuchi, *MicroRNA-34a regulation of endothelial senescence.* Biochem Biophys Res Commun, 2010. **398**(4): p. 735-40.

120. Vogt, M., et al., *Frequent concomitant inactivation of miR-34a and miR-34b/c by CpG methylation in colorectal, pancreatic, mammary, ovarian, urothelial, and renal cell carcinomas and soft tissue sarcomas.* Virchows Arch, 2011. **458**(3): p. 313-22.

121. Kong, K.L., et al., *MicroRNA-375 inhibits tumour growth and metastasis in oesophageal squamous cell carcinoma through repressing insulin-like growth factor 1 receptor.* Gut, 2012. **61**(1): p. 33-42.

122. Yan, N., et al., *Microarray profiling of microRNAs expressed in testis tissues of developing primates.* J Assist Reprod Genet, 2009. **26**(4): p. 179-86.

123. Marcet, B., et al., *Control of vertebrate multiciliogenesis by miR-449 through direct repression of the Delta/Notch pathway.* Nat Cell Biol, 2011. **13**(6): p. 693-9.

124. Tang, D., et al., *Up-Regulation of microRNA-210 is Associated with Spermatogenesis by Targeting IGF2 in Male Infertility.* Medical Science Monitor : International Medical Journal of Experimental and Clinical Research, 2016. **22**: p. 2905-2910.

125. Tamminga, J., et al., *DNA damage-induced upregulation of miR-709 in the germline downregulates BORIS to counteract aberrant DNA hypomethylation.* Cell Cycle, 2008. **7**(23): p. 3731-6.

126. Guan, Y., et al., *Roles of small RNAs in the effects of nutrition on apoptosis and spermatogenesis in the adult testis.* Scientific Reports, 2015. **5**: p. 10372.

127. Bar-Eli, M., *Searching for the 'melano-miRs': miR-214 drives melanoma metastasis.* The EMBO Journal, 2011. **30**(10): p. 1880-1881.

128. Yang, H., et al., *MicroRNA expression profiling in human ovarian cancer: miR-214 induces cell survival and cisplatin resistance by targeting PTEN.* Cancer Res, 2008. **68**(2): p. 425-33.

129. Zhu, W., et al., *miR-181b modulates multidrug resistance by targeting BCL2 in human cancer cell lines.* International Journal of Cancer, 2010. **127**(11): p. 2520-2529.

130. Wu, Q., et al., *MicroRNA-200a inhibits CD133/1+ ovarian cancer stem cells migration and invasion by targeting E-cadherin repressor ZEB2.* Gynecol Oncol, 2011. **122**(1): p. 149-54.

131. Tome, M., et al., *miR-335 orchestrates cell proliferation, migration and differentiation in human mesenchymal stem cells.* Cell Death Differ, 2011. **18**(6): p. 985-95.

132. Hashimoto, Y., et al., *Involvement of epigenetically silenced microRNA-181c in gastric carcinogenesis.* Carcinogenesis, 2010. **31**(5): p. 777-84.

133. Haenisch, S., et al., *Down-regulation of ATP-binding cassette C2 protein expression in HepG2 cells after rifampicin treatment is mediated by microRNA-379.* Mol Pharmacol, 2011. **80**(2): p. 314-20.

134. Bhaskaran, M., et al., *MicroRNA-127 modulates fetal lung development.* Physiol Genomics, 2009. **37**(3): p. 268-78.

135. Wang, C., et al., *miR-29b regulates migration of human breast cancer cells.* Mol Cell Biochem, 2011. **352**(1-2): p. 197-207.

136. Wang, F., et al., *Regulation of erythroid differentiation by miR-376a and its targets.* Cell Res, 2011. **21**(8): p. 1196-209.

137. Williams, A.E., et al., *Maternally imprinted microRNAs are differentially expressed during mouse and human lung development.* Dev Dyn, 2007. **236**(2): p. 572-80.

138. Buechner, J., et al., *Tumour-suppressor microRNAs let-7 and mir-101 target the proto-oncogene MYCN and inhibit cell proliferation in MYCN-amplified neuroblastoma.* Br J Cancer, 2011. **105**(2): p. 296-303.

139. Lee, M.R., J.S. Kim, and K.S. Kim, *miR-124a is important for migratory cell fate transition during gastrulation of human embryonic stem cells.* Stem Cells, 2010. **28**(9): p. 1550-9.

140. Vaira, V., et al., *miR-296 regulation of a cell polarity-cell plasticity module controls tumor progression.* Oncogene, 2012. **31**(1): p. 27-38.

141. Hunt, S., et al., *MicroRNA-124 suppresses oral squamous cell carcinoma motility by targeting ITGB1.* FEBS Lett, 2011. **585**(1): p. 187-92.

142. Hermo, L., et al., *Surfing the wave, cycle, life history, and genes/proteins expressed by testicular germ cells. Part 1: background to spermatogenesis, spermatogonia, and spermatocytes.* Microsc Res Tech, 2010. **73**(4): p. 241-78.

143. Aitken, R.J., et al., *Proteomic changes in mammalian spermatozoa during epididymal maturation.* Asian J Androl, 2007. **9**(4): p. 554-64.

144. Dacheux, J.L., et al., *Epididymal cell secretory activities and the role of proteins in boar sperm maturation.* Theriogenology, 2005. **63**(2): p. 319-41.

145. Dacheux, J.L., et al., *Mammalian epididymal proteome.* Mol Cell Endocrinol, 2009. **306**(1-2): p. 45-50.

146. Buffone, M.G., et al., *Heads or Tails? Structural Events and Molecular Mechanisms That Promote Mammalian Sperm Acrosomal Exocytosis and Motility.* Molecular reproduction and development, 2012. **79**(1): p. 4-18.

147. Johnston, D.S., et al., *The mouse epididymal transcriptome: transcriptional profiling of segmental gene expression in the epididymis.* Biol Reprod, 2005. **73**(3): p. 404-13.

148. Robaire, B. and M. Hamzeh, *Androgen action in the epididymis.* J Androl, 2011. **32**(6): p. 592-9.

149. Hu, S.G., et al., *Androgenic regulation of beta-defensins in the mouse epididymis.* Reprod Biol Endocrinol, 2014. **12**: p. 76.

150. O'Hara, L., et al., *Androgen receptor expression in the caput epididymal epithelium is essential for development of the initial segment and epididymal spermatozoa transit.* Endocrinology, 2011. **152**(2): p. 718-29.

151. Xu, B., et al., *Testicular lumicrine factors regulate ERK, STAT, and NFKB pathways in the initial segment of the rat epididymis to prevent apoptosis.* Biol Reprod, 2011. **84**(6): p. 1282-91.

152. Ungefroren, H., R. Ivell, and S. Ergun, *Region-specific expression of the androgen receptor in the human epididymis.* Mol Hum Reprod, 1997. **3**(11): p. 933-40.

153. Viger, R.S. and B. Robaire, *The mRNAs for the steroid 5 alpha-reductase isozymes, types 1 and 2, are differentially regulated in the rat epididymis.* J Androl, 1996. **17**(1): p. 27-34.

154. Björkgren, I., et al., *Dicer1 Ablation in the Mouse Epididymis Causes Dedifferentiation of the Epithelium and Imbalance in Sex Steroid Signaling.* PLOS ONE, 2012. **7**(6): p. e38457.

155. Bjorkgren, I., et al., *Imbalanced lipid homeostasis in the conditional Dicer1 knockout mouse epididymis causes instability of the sperm membrane.* FASEB J, 2015. **29**(2): p. 433-42.

156. Ni, M.-J., et al., *Identification and Characterization of a Novel Non-Coding RNA Involved in Sperm Maturation.* PLoS ONE, 2011. **6**(10): p. e26053.

157. Belleannee, C., et al., *microRNA signature is altered in both human epididymis and seminal microvesicles following vasectomy.* Hum Reprod, 2013. **28**(6): p. 1455-67.

158. Belleannee, C., et al., *Epididymosomes convey different repertoires of microRNAs throughout the bovine epididymis.* Biol Reprod, 2013. **89**(2): p. 30.

159. Belleannée, C., et al., *Role of MicroRNAs in Controlling Gene Expression in Different Segments of the Human Epididymis.* PLoS ONE, 2012. **7**(4): p. e34996.

160. Ma, W., et al., *MicroRNA-29a Inhibited Epididymal Epithelial Cell Proliferation by Targeting Nuclear Autoantigenic Sperm Protein (NASP).* The Journal of Biological Chemistry, 2012. **287**(13): p. 10189-10199.

161. Nixon, B., et al., *Next Generation Sequencing Analysis Reveals Segmental Patterns of microRNA Expression in Mouse Epididymal Epithelial Cells.* PLoS One, 2015. **10**(8): p. e0135605.

162. Nixon, B., et al., *The microRNA signature of mouse spermatozoa is substantially modified during epididymal maturation.* Biol Reprod, 2015. **93**(4): p. 91.

163. Reilly, J.N., et al., *Characterisation of mouse epididymosomes reveals a complex profile of microRNAs and a potential mechanism for modification of the sperm epigenome.* Sci Rep, 2016. **6**: p. 31794.

164. Zhang, J., et al., *Comparative profiling of genes and miRNAs expressed in the newborn, young adult, and aged human epididymides.* Acta Biochim Biophys Sin (Shanghai), 2010. **42**(2): p. 145-53.

165. Landgraf, P., et al., *A mammalian microRNA expression atlas based on small RNA library sequencing.* Cell, 2007. **129**(7): p. 1401-14.

166. Chu, C., et al., *Epididymal Region-Specific miRNA Expression and DNA Methylation and Their Roles in Controlling Gene Expression in Rats.* PLoS One, 2015. **10**(4): p. e0124450.

167. Anderson, A.L., et al., *Assessment of microRNA expression in mouse epididymal epithelial cells and spermatozoa by next generation sequencing.* Genom Data, 2015. **6**: p. 208-11.

168. Schjenken, J.E. and S.A. Robertson, *Seminal fluid and immune adaptation for pregnancy--comparative biology in mammalian species.* Reprod Domest Anim, 2014. **49 Suppl 3**: p. 27-36.

169. Rodgers, A.B., et al., *Paternal stress exposure alters sperm microRNA content and reprograms offspring HPA stress axis regulation.* J Neurosci, 2013. **33**(21): p. 9003-12.

170. Gapp, K., et al., *Implication of sperm RNAs in transgenerational inheritance of the effects of early trauma in mice.* Nature neuroscience, 2014. **17**(5): p. 667-669.

171. Marczylo, E.L., et al., *Smoking induces differential miRNA expression in human spermatozoa: a potential transgenerational epigenetic concern?* Epigenetics, 2012. **7**(5): p. 432-9.

172. McPherson, N.O., et al., *Preconception diet or exercise intervention in obese fathers normalizes sperm microRNA profile and metabolic syndrome in female offspring.* Am J Physiol Endocrinol Metab, 2015. **308**(9): p. E805-21.

173. Fullston, T., et al., *Paternal obesity induces metabolic and sperm disturbances in male offspring that are exacerbated by their exposure to an "obesogenic" diet.* Physiological Reports, 2015. **3**(3): p. e12336.

174. Rando, O.J., *Daddy Issues: Paternal Effects on Phenotype.* Cell. **151**(4): p. 702-708.

175. Carone, B.R., et al., *Paternally induced transgenerational environmental reprogramming of metabolic gene expression in mammals.* Cell, 2010. **143**(7): p. 1084-96.

176. Ng, S.F., et al., *Chronic high-fat diet in fathers programs beta-cell dysfunction in female rat offspring.* Nature, 2010. **467**(7318): p. 963-6.

177. Sullivan, R., G. Frenette, and J. Girouard, *Epididymosomes are involved in the acquisition of new sperm proteins during epididymal transit.* Asian J Androl, 2007. **9**(4): p. 483-91.

178. Sullivan, R., *Epididymosomes: a heterogeneous population of microvesicles with multiple functions in sperm maturation and storage.* Asian J Androl, 2015. **17**(5): p. 726-9.

179. Suryawanshi, A.R., et al., *Epididymosome-mediated acquisition of MMSDH, an androgen-dependent and developmentally regulated epididymal sperm protein.* J Androl, 2012. **33**(5): p. 963-74.

180. Girouard, J., G. Frenette, and R. Sullivan, *Comparative proteome and lipid profiles of bovine epididymosomes collected in the intraluminal compartment of the caput and cauda epididymidis.* Int J Androl, 2011. **34**(5 Pt 2): p. e475-86.

181. Griffiths, G.S., et al., *Investigating the role of murine epididymosomes and uterosomes in GPI-linked protein transfer to sperm using SPAM1 as a model.* Mol Reprod Dev, 2008. **75**(11): p. 1627-36.

182. Sullivan, R. and F. Saez, *Epididymosomes, prostasomes, and liposomes: their roles in mammalian male reproductive physiology.* Reproduction, 2013. **146**(1): p. R21-35.

183. Frenette, G., et al., *Characterization of two distinct populations of epididymosomes collected in the intraluminal compartment of the bovine cauda epididymis.* Biol Reprod, 2010. **83**(3): p. 473-80.

184. Sharma, U., et al., *Biogenesis and function of tRNA fragments during sperm maturation and fertilization in mammals.* Science, 2016. **351**(6271): p. 391-6.

185. Farkas, R., *Apocrine secretion: New insights into an old phenomenon.* Biochim Biophys Acta, 2015. **1850**(9): p. 1740-50.

186. Sullivan, R., *Epididymosomes: a heterogeneous population of microvesicles with multiple functions in sperm maturation and storage.* Asian Journal of Andrology, 2015. **17**(5): p. 726-729.

187. Jones, R., T. Mann, and R.J. Sherins, *Adverse Effects of Peroxidized Lipid on Human Spermatozoa.* Proceedings of the Royal Society of London B: Biological Sciences, 1978. **201**(1145): p. 413-417.

188. Davis, B.K., *Interaction of lipids with the plasma membrane of sperm cells. I. The antifertilization action of cholesterol.* Arch Androl, 1980. **5**(3): p. 249-54.

189. Frenette, G., J. Girouard, and R. Sullivan, *Comparison between epididymosomes collected in the intraluminal compartment of the bovine caput and cauda epididymidis.* Biol Reprod, 2006. **75**(6): p. 885-90.

190. Yanagimachi, R., et al., *Maturation of spermatozoa in the epididymis of the Chinese hamster.* Am J Anat, 1985. **172**(4): p. 317-30.

191. Thimon, V., et al., *Protein composition of human epididymosomes collected during surgical vasectomy reversal: a proteomic and genomic approach.* Human Reproduction, 2008. **23**(8): p. 1698-1707.

192. Rejraji, H., et al., *Lipid Remodeling of Murine Epididymosomes and Spermatozoa During Epididymal Maturation.* Biology of Reproduction, 2006. **74**(6): p. 1104-1113.

193. Fornes, M.W., A. Barbieri, and J.C. Cavicchia, *Morphological and enzymatic study of membrane-bound vesicles from the lumen of the rat epididymis.* Andrologia, 1995. **27**(1): p. 1-5.

194. Ecroyd, H., et al., *Compartmentalization of Prion Isoforms Within the Reproductive Tract of the Ram.* Biology of Reproduction, 2004. **71**(3): p. 993-1001.

195. Caballero, J.N., et al., *CD9-positive microvesicles mediate the transfer of molecules to Bovine Spermatozoa during epididymal maturation.* PLoS One, 2013. **8**(6): p. e65364.

196. D'Amours, O., et al., *Evidences of Biological Functions of Biliverdin Reductase A in the Bovine Epididymis.* J Cell Physiol, 2016. **231**(5): p. 1077-89.

197. Frenette, G., C. Lessard, and R. Sullivan, *Selected Proteins of "Prostasome-Like Particles" from Epididymal Cauda Fluid Are Transferred to Epididymal Caput Spermatozoa in Bull.* Biology of Reproduction, 2002. **67**(1): p. 308-313.

198. Lawrence, L.T. and K.H. Moley, *Epigenetics and assisted reproductive technologies: human imprinting syndromes.* Semin Reprod Med, 2008. **26**(2): p. 143-52.

199. Chomczynski, P. and N. Sacchi, *Single-step method of RNA isolation by acid guanidinium thiocyanate-phenol-chloroform extraction.* Anal Biochem, 1987. **162**(1): p. 156-9.

200. Chomczynski, P. and N. Sacchi, *The single-step method of RNA isolation by acid guanidinium thiocyanate-phenol-chloroform extraction: twenty-something years on.* Nat Protoc, 2006. **1**(2): p. 581-5.

201. Martin, M., *Cutadapt removes adapter sequences from high-throughput sequencing reads.* EMBnet.journal, 2011. **17**: p. 10-12.

202. Friedlander, M.R., et al., *Discovering microRNAs from deep sequencing data using miRDeep.* Nat Biotechnol, 2008. **26**(4): p. 407-15.

203. McCarthy, D.J., Y. Chen, and G.K. Smyth, *Differential expression analysis of multifactor RNA-Seq experiments with respect to biological variation.* Nucleic Acids Res, 2012. **40**(10): p. 4288-97.

204. Ritchie, M.E., et al., *limma powers differential expression analyses for RNA-sequencing and microarray studies.* Nucleic Acids Res, 2015. **43**(7): p. e47.

205. Schmittgen, T.D. and K.J. Livak, *Analyzing real-time PCR data by the comparative C(T) method.* Nat Protoc, 2008. **3**(6): p. 1101-8.

206. Stocks, M.B., et al., *The UEA sRNA workbench: a suite of tools for analysing and visualizing next generation sequencing microRNA and small RNA datasets.* Bioinformatics, 2012. **28**(15): p. 2059-61.

207. Gruber, A.R., et al., *The Vienna RNA Websuite.* Nucleic Acids Research, 2008. **36**(Web Server issue): p. W70-W74.

208. Darty, K., A. Denise, and Y. Ponty, *VARNA: Interactive drawing and editing of the RNA secondary structure.* Bioinformatics, 2009. **25**(15): p. 1974-5.

209. Griffiths-Jones, S., et al., *miRBase: tools for microRNA genomics.* Nucleic Acids Research, 2008. **36**(Database issue): p. D154-D158.

210. Hackenberg, M., et al., *miRanalyzer: a microRNA detection and analysis tool for next-generation sequencing experiments.* Nucleic Acids Res, 2009. **37**(Web Server issue): p. W68-76.

211. Lim, L.P., et al., *The microRNAs of Caenorhabditis elegans.* Genes & Development, 2003. **17**(8): p. 991-1008.

212. Lim, L.P., et al., *Vertebrate microRNA genes.* Science, 2003. **299**(5612): p. 1540.

213. Kuhn, D.E., et al., *Experimental Validation of miRNA Targets.* Methods (San Diego, Calif.), 2008. **44**(1): p. 47-54.

214. Kanellos, I., et al., *MR-microT: a MapReduce-based MicroRNA target prediction method*, in *Proceedings of the 26th International Conference on Scientific and Statistical Database Management*. 2014, ACM: Aalborg, Denmark. p. 1-4.

215. Reczko, M., et al., *Functional microRNA targets in protein coding sequences.* Bioinformatics, 2012. **28**(6): p. 771-776.

216. Wang, X., *miRDB: A microRNA target prediction and functional annotation database with a wiki interface.* RNA, 2008. **14**(6): p. 1012-1017.

217. Wang, X., *Improving microRNA target prediction by modeling with unambiguously identified microRNA-target pairs from CLIP-ligation studies.* Bioinformatics, 2016. **32**(9): p. 1316-22.

218. Rehmsmeier, M., et al., *Fast and effective prediction of microRNA/target duplexes.* RNA, 2004. **10**(10): p. 1507-17.

219. Kertesz, M., et al., *The role of site accessibility in microRNA target recognition.* Nat Genet, 2007. **39**(10): p. 1278-1284.

220. John, B., et al., *Human MicroRNA targets.* PLoS Biol, 2004. **2**(11): p. e363.

221. Le Guen, C.L., J.R. Friedman, and N.J. Hand, *Novel targets of miR-30, a microRNA required for biliary development.* F1000Research, 2013. **2**: p. 197.

222. Liao, Q., et al., *Identification of miRNA-mRNA crosstalk in CD4+ T cells during HIV-1 infection by integrating transcriptome analyses.* J Transl Med, 2017. **15**(1): p. 41.

223. Bizuayehu, T.T., et al., *Characterization of Novel Precursor miRNAs Using Next Generation Sequencing and Prediction of miRNA Targets in Atlantic Halibut.* PLoS ONE, 2013. **8**(4): p. e61378.

224. Witkos, T.M., E. Koscianska, and W.J. Krzyzosiak, *Practical Aspects of microRNA Target Prediction.* Current Molecular Medicine, 2011. **11**(2): p. 93-109.

225. Dweep, H. and N. Gretz, *miRWalk2.0: a comprehensive atlas of microRNA-target interactions.* Nat Methods, 2015. **12**(8): p. 697.

226. Peterson, S.M., et al., *Common features of microRNA target prediction tools.* Frontiers in Genetics, 2014. **5**: p. 23.

227. Baek, D., et al., *The impact of microRNAs on protein output.* Nature, 2008. **455**(7209): p. 64-71.

228. Ritchie, W., S. Flamant, and J.E. Rasko, *Predicting microRNA targets and functions: traps for the unwary.* Nat Methods, 2009. **6**(6): p. 397-8.

229. Johnson, M., et al., *NCBI BLAST: a better web interface.* Nucleic Acids Res, 2008. **36**(Web Server issue): p. W5-9.

230. Darty, K., A. Denise, and Y. Ponty, *VARNA: Interactive drawing and editing of the RNA secondary structure.* Bioinformatics, 2009. **25**(15): p. 1974-1975.

231. Belleannée, C., *Extracellular microRNAs from the epididymis as potential mediators of cell-to-cell communication.* Asian Journal of Andrology, 2015. **17**(5): p. 730-736.

232. van Der Horst, G., et al., *The maturation of sperm motility in the epididymis and vas deferens of the vervet monkey, Cercopithecus aethiops.* Int J Androl, 1999. **22**(3): p. 197-207.

233. Loutradi, K.E., et al., *The effects of sperm quality on embryo development after intracytoplasmic sperm injection.* Journal of Assisted Reproduction and Genetics, 2006. **23**(2): p. 69-74.

234. Ward, W.S. and A.O. Zalensky, *The unique, complex organization of the transcriptionally silent sperm chromatin.* Crit Rev Eukaryot Gene Expr, 1996. **6**(2-3): p. 139-47.

235. Sharma, U., et al., *Biogenesis and function of tRNA fragments during sperm maturation and fertilization in mammals.* Science (New York, N.Y.), 2016. **351**(6271): p. 391-396.

236. Cooper, T.G., *The epididymis, cytoplasmic droplets and male fertility.* Asian Journal of Andrology, 2011. **13**(1): p. 130-138.

237. Cooper, T.G. and C.H. Yeung, *Acquisition of volume regulatory response of sperm upon maturation in the epididymis and the role of the cytoplasmic droplet.* Microsc Res Tech, 2003. **61**(1): p. 28-38.

238. Cortadellas, N. and M. Durfort, *Fate and composition of cytoplasmic droplet of hamster epididymal spermatozoa.* J Morphol, 1994. **221**(2): p. 199-210.

239. Graves, P. and Y. Zeng, *Biogenesis of Mammalian MicroRNAs: A Global View.* Genomics, Proteomics & Bioinformatics, 2012. **10**(5): p. 239-245.

240. Hoseini Pajooh, K., et al., *Techniques for augmentation of exogenous DNA uptake by ovine spermatozoa.* Iranian Journal of Veterinary Research, 2016. **17**(1): p. 25-30.

241. Lavitrano, M., et al., *Sperm cells as vectors for introducing foreign DNA into eggs: genetic transformation of mice.* Cell, 1989. **57**(5): p. 717-23.

242. Zani, M., et al., *The mechanism of binding of exogenous DNA to sperm cells: factors controlling the DNA uptake.* Exp Cell Res, 1995. **217**(1): p. 57-64.

243. Cossetti, C., et al., *Soma-to-Germline Transmission of RNA in Mice Xenografted with Human Tumour Cells: Possible Transport by Exosomes.* PLOS ONE, 2014. **9**(7): p. e101629.

244. Martin-DeLeon, P.A., *Uterosomes: Exosomal cargo during the estrus cycle and interaction with sperm.* Front Biosci (Schol Ed), 2016. **8**: p. 115-22.

245. Schjenken, J.E. and S.A. Robertson, *Seminal Fluid Signalling in the Female Reproductive Tract: Implications for Reproductive Success and Offspring Health.* Adv Exp Med Biol, 2015. **868**: p. 127-58.

246. Sharkey, D.J., et al., *Seminal fluid factors regulate activin A and follistatin synthesis in female cervical epithelial cells.* Mol Cell Endocrinol, 2015. **417**: p. 178-90.

247. Belleannée, C., et al., *microRNA signature is altered in both human epididymis and seminal microvesicles following vasectomy.* Human Reproduction, 2013. **28**(6): p. 1455-1467.

248. Schoysman, R., et al., *Pregnancy after fertilisation with human testicular spermatozoa.* Lancet, 1993. **342**(8881): p. 1237.

249. Wang, T., et al., *TGF-beta-induced miR-21 negatively regulates the antiproliferative activity but has no effect on EMT of TGF-beta in HaCaT cells.* Int J Biochem Cell Biol, 2012. **44**(2): p. 366-76.

250. Li, Q., et al., *MiR-21/Smad 7 signaling determines TGF-beta1-induced CAF formation.* Sci Rep, 2013. **3**: p. 2038.

251. Yan, X., Z. Liu, and Y. Chen, *Regulation of TGF-beta signaling by Smad7.* Acta Biochim Biophys Sin (Shanghai), 2009. **41**(4): p. 263-72.

252. Bachiller, D., et al., *Liposome-mediated DNA uptake by sperm cells.* Mol Reprod Dev, 1991. **30**(3): p. 194-200.

253. Schoysman, R., et al., *Assisted fertilization with epididymal spermatozoa.* Acta Eur Fertil, 1993. **24**(1): p. 7-12.

254. Hu, S.J., et al., *MicroRNA expression and regulation in mouse uterus during embryo implantation.* J Biol Chem, 2008. **283**(34): p. 23473-84.

255. Carletti, M.Z. and L.K. Christenson, *MicroRNA in the ovary and female reproductive tract.* Journal of animal science, 2009. **87**(14 Suppl): p. E29-E38.

256. Dammer, E.B. and M.B. Sewer, *Phosphorylation of CtBP1 by cAMP-dependent protein kinase modulates induction of CYP17 by stimulating partnering of CtBP1 and 2.* J Biol Chem, 2008. **283**(11): p. 6925-34.

257. Marques-Rocha, J.L., et al., *Noncoding RNAs, cytokines, and inflammation-related diseases.* FASEB J, 2015. **29**(9): p. 3595-611.

258. Mayorga, M.E. and M.S. Penn, *miR-145 is differentially regulated by TGF-beta1 and ischaemia and targets Disabled-2 expression and wnt/beta-catenin activity.* J Cell Mol Med, 2012. **16**(5): p. 1106-13.

259. Torchinsky, A. and V. Toder, *To die or not to die: the function of the transcription factor NF-kappaB in embryos exposed to stress.* Am J Reprod Immunol, 2004. **51**(2): p. 138-43.

260. Song, L., et al., *miR-486 sustains NF-kappaB activity by disrupting multiple NF-kappaB-negative feedback loops.* Cell Res, 2013. **23**(2): p. 274-89.

261. Duan, Y. and Q. Chen, *TGF-β1 regulating miR-205/miR-195 expression affects the TGF-β signal pathway by respectively targeting SMAD2/SMAD7.* Oncology Reports, 2016. **36**(4): p. 1837-1844.

262. Cornwall, G.A., *New insights into epididymal biology and function.* Human Reproduction Update, 2009. **15**(2): p. 213-227.

263. Levine, N. and D.J. Marsh, *Micropuncture studies of the electrochemical aspects of fluid and electrolyte transport in individual seminiferous tubules, the epididymis and the vas deferens in rats.* J Physiol, 1971. **213**(3): p. 557-70.

264. Brown, P.D. and G.M. Waites, *Regional blood flow in the epididymis of the rat and rabbit: effect of efferent duct ligation and orchidectomy.* J Reprod Fertil, 1972. **28**(2): p. 221-33.

265. Setchell, B.P., G.M. Waites, and A.R. Till, *VARIATIONS IN FLOW OF BLOOD WITHIN THE EPIDIDYMIS AND TESTIS OF THE SHEEP AND RAT.* Nature, 1964. **203**: p. 317-8.

266. Markey, C.M. and G.T. Meyer, *A quantitative description of the epididymis and its microvasculature: an age-related study in the rat.* J Anat, 1992. **180 (Pt 2)**: p. 255-62.

267. Takano, H., *[Qualitative and quantitative histology and histogenesis of the mouse epididymis, with special emphasis on the regional difference (author's transl)]*. Kaibogaku Zasshi, 1980. **55**(6): p. 573-87.

268. Suzuki, F., *Microvasculature of the mouse testis and excurrent duct system.* Am J Anat, 1982. **163**(4): p. 309-25.

269. Sonnenberg-Riethmacher, E., et al., *The c-ros tyrosine kinase receptor controls regionalization and differentiation of epithelial cells in the epididymis.* Genes Dev, 1996. **10**(10): p. 1184-93.

270. Skerget, S., et al., *Sperm Proteome Maturation in the Mouse Epididymis.* PLoS ONE, 2015. **10**(11): p. e0140650.

271. Trasler, J., et al., *Characterization of the testis and epididymis in mouse models of human Tay Sachs and Sandhoff diseases and partial determination of accumulated gangliosides.* Endocrinology, 1998. **139**(7): p. 3280-8.

272. Ramos-Ibeas, P., et al., *Most regions of mouse epididymis are able to phagocytose immature germ cells.* Reproduction, 2013. **146**(5): p. 481-9.

273. Yeung, C.-H. and T.G. Cooper, *Acquisition and Development of Sperm Motility Upon Maturation in the Epididymis*, in *The Epididymis: From Molecules to Clinical Practice: A Comprehensive Survey of the Efferent Ducts, the Epididymis and the Vas Deferens*, B. Robaire and B.T. Hinton, Editors. 2002, Springer US: Boston, MA. p. 417-434.

274. Johnston, D.S., et al., *Identification of epididymis-specific transcripts in the mouse and rat by transcriptional profiling.* Asian J Androl, 2007. **9**(4): p. 522-7.

275. Rodgers, A.B., et al., *Paternal stress exposure alters sperm microRNA content and reprograms offspring HPA stress axis regulation.* The Journal of

neuroscience : the official journal of the Society for Neuroscience, 2013. **33**(21): p. 9003-9012.

276. Fullston, T., et al., *Sperm microRNA Content Is Altered in a Mouse Model of Male Obesity, but the Same Suite of microRNAs Are Not Altered in Offspring's Sperm.* PLoS ONE, 2016. **11**(11): p. e0166076.

277. Rodgers, A.B., et al., *Transgenerational epigenetic programming via sperm microRNA recapitulates effects of paternal stress.* Proceedings of the National Academy of Sciences, 2015. **112**(44): p. 13699-13704.

278. Tang, F., et al., *Maternal microRNAs are essential for mouse zygotic development.* Genes Dev, 2007. **21**(6): p. 644-8.

279. Kawano, M., et al., *Novel Small Noncoding RNAs in Mouse Spermatozoa, Zygotes and Early Embryos.* PLoS ONE, 2012. **7**(9): p. e44542.

280. Zhang, P., et al., *MIWI and piRNA-mediated cleavage of messenger RNAs in mouse testes.* Cell Research, 2015. **25**(2): p. 193-207.

281. Rico-Leo, E.M., et al., *piRNA-associated proteins and retrotransposons are differentially expressed in murine testis and ovary of aryl hydrocarbon receptor deficient mice.* Open Biology, 2016. **6**(12): p. 160186.

282. Carmell, M.A., et al., *MIWI2 Is Essential for Spermatogenesis and Repression of Transposons in the Mouse Male Germline.* Developmental Cell, 2007. **12**(4): p. 503-514.

283. Björkgren, I., et al., *Imbalanced lipid homeostasis in the conditional Dicer1 knockout mouse epididymis causes instability of the sperm membrane.* The FASEB Journal, 2015. **29**(2): p. 433-442.

284. Peng, H., et al., *A novel class of tRNA-derived small RNAs extremely enriched in mature mouse sperm.* Cell Res, 2012. **22**(11): p. 1609-1612.

285. Mishima, T., et al., *MicroRNA (miRNA) cloning analysis reveals sex differences in miRNA expression profiles between adult mouse testis and ovary.* Reproduction, 2008. **136**(6): p. 811-22.

286. Parsons, M.J., et al., *Using hippocampal microRNA expression differences between mouse inbred strains to characterise miRNA function.* Mammalian Genome, 2008. **19**(7-8): p. 552-560.

287. Chuma, S. and T. Nakano, *piRNA and spermatogenesis in mice.* Philosophical Transactions of the Royal Society B: Biological Sciences, 2013. **368**(1609): p. 20110338.

288. Heather, J.M. and B. Chain, *The sequence of sequencers: The history of sequencing DNA.* Genomics, 2016. **107**(1): p. 1-8.

289. Gut, I.G., *New sequencing technologies.* Clin Transl Oncol, 2013. **15**(11): p. 879-81.

290. Shendure, J., *The beginning of the end for microarrays?* Nat Methods, 2008. **5**(7): p. 585-7.

291. Sanger, F., et al., *Nucleotide sequence of bacteriophage phi X174 DNA.* Nature, 1977. **265**(5596): p. 687-95.

292. Smith, L.M., et al., *Fluorescence detection in automated DNA sequence analysis.* Nature, 1986. **321**(6071): p. 674-9.

293. Lander, E.S., et al., *Initial sequencing and analysis of the human genome.* Nature, 2001. **409**(6822): p. 860-921.

294. Willenbrock, H., et al., *Quantitative miRNA expression analysis: Comparing microarrays with next-generation sequencing.* RNA, 2009. **15**(11): p. 2028-2034.

295. Kelly, A.D., et al., *Next-generation sequencing and microarray-based interrogation of microRNAs from formalin-fixed, paraffin-embedded tissue: Preliminary assessment of cross-platform concordance.* Genomics, 2013. **102**(1): p. 8-14.

296. Git, A., et al., *Systematic comparison of microarray profiling, real-time PCR, and next-generation sequencing technologies for measuring differential microRNA expression.* RNA, 2010. **16**(5): p. 991-1006.

297. Leshkowitz, D., et al., *Differences in microRNA detection levels are technology and sequence dependent.* RNA, 2013. **19**(4): p. 527-38.

298. Chatterjee, A., et al., *A cross comparison of technologies for the detection of microRNAs in clinical FFPE samples of hepatoblastoma patients.* Sci Rep, 2015. **5**: p. 10438.

299. Jaksik, R., et al., *Microarray experiments and factors which affect their reliability.* Biology Direct, 2015. **10**: p. 46.

300. Draghici, S., et al., *Reliability and reproducibility issues in DNA microarray measurements.* Trends in genetics : TIG, 2006. **22**(2): p. 101-109.

301. Jaksik, R., et al., *Microarray experiments and factors which affect their reliability.* Biology Direct, 2015. **10**(1): p. 46.

302. Son, C.G., et al., *Database of mRNA gene expression profiles of multiple human organs.* Genome research, 2005. **15**(3): p. 443-450.

303. Snyder, E.M., et al., *Gene Expression in the Efferent ducts, Epididymis, and Vas deferens during Embryonic Development of the Mouse.* Developmental dynamics : an official publication of the American Association of Anatomists, 2010. **239**(9): p. 2479-2491.

304. Eminaga, S., et al., *Quantification of microRNA Expression with Next-Generation Sequencing.* Current protocols in molecular biology / edited by Frederick M. Ausubel ... [et al.], 2013. **0 4**: p. Unit-4.17.

305. Liu, L., et al., *Comparison of Next-Generation Sequencing Systems.* Journal of Biomedicine and Biotechnology, 2012. **2012**: p. 251364.

306. Liu, J., et al., *Next generation sequencing for profiling expression of miRNAs: technical progress and applications in drug development.* Journal of biomedical science and engineering, 2011. **4**(10): p. 666-676.

307. Tang, H.M., et al., *[Application of next generation sequencing in microRNA detection]*. Yi Chuan, 2012. **34**(6): p. 784-92.

308. Motameny, S., et al., *Next Generation Sequencing of miRNAs – Strategies, Resources and Methods.* Genes, 2010. **1**(1): p. 70-84.

309. Wang, Z., M. Gerstein, and M. Snyder, *RNA-Seq: a revolutionary tool for transcriptomics.* Nature reviews. Genetics, 2009. **10**(1): p. 57-63.

310. Mantione, K.J., et al., *Comparing Bioinformatic Gene Expression Profiling Methods: Microarray and RNA-Seq.* Medical Science Monitor Basic Research, 2014. **20**: p. 138-141.

311. Han, Y., et al., *Advanced Applications of RNA Sequencing and Challenges.* Bioinformatics and Biology Insights, 2015. **9**(Suppl 1): p. 29-46.

312. Zheng, W., L.M. Chung, and H. Zhao, *Bias detection and correction in RNA-Sequencing data.* BMC Bioinformatics, 2011. **12**: p. 290-290.

313. Benjamini, Y. and T.P. Speed, *Summarizing and correcting the GC content bias in high-throughput sequencing.* Nucleic Acids Res, 2012. **40**(10): p. e72.

314. McCarthy, A., *Third generation DNA sequencing: pacific biosciences' single molecule real time technology.* Chem Biol, 2010. **17**(7): p. 675-6.

315. Vilfan, I.D., et al., *Analysis of RNA base modification and structural rearrangement by single-molecule real-time detection of reverse transcription.* J Nanobiotechnology, 2013. **11**: p. 8.

316. Lu, H., F. Giordano, and Z. Ning, *Oxford Nanopore MinION Sequencing and Genome Assembly.* Genomics Proteomics Bioinformatics, 2016. **14**(5): p. 265-279.

317. Laver, T., et al., *Assessing the performance of the Oxford Nanopore Technologies MinION.* Biomol Detect Quantif, 2015. **3**: p. 1-8.

318. Check Hayden, E., *Pint-sized DNA sequencer impresses first users.* Nature, 2015. **521**(7550): p. 15-6.

319. Ayub, M., et al., *Nanopore-based identification of individual nucleotides for direct RNA sequencing.* Nano Lett, 2013. **13**(12): p. 6144-50.

320. Henley, R.Y., S. Carson, and M. Wanunu, *Studies of RNA Sequence and Structure Using Nanopores.* Progress in molecular biology and translational science, 2016. **139**: p. 73-99.

321. Park, D., et al., *Uncovering the novel characteristics of Asian honey bee, Apis cerana, by whole genome sequencing.* BMC Genomics, 2015. **16**: p. 1.

322. Ashton, P.M., et al., *MinION nanopore sequencing identifies the position and structure of a bacterial antibiotic resistance island.* Nat Biotechnol, 2015. **33**(3): p. 296-300.

323. Karlsson, E., et al., *Scaffolding of a bacterial genome using MinION nanopore sequencing.* Sci Rep, 2015. **5**: p. 11996.

324. Wang, Z., M. Gerstein, and M. Snyder, *RNA-Seq: a revolutionary tool for transcriptomics.* Nat Rev Genet, 2009. **10**(1): p. 57-63.

325. Mortazavi, A., et al., *Mapping and quantifying mammalian transcriptomes by RNA-Seq.* Nat Methods, 2008. **5**(7): p. 621-8.

326. Dillies, M.A., et al., *A comprehensive evaluation of normalization methods for Illumina high-throughput RNA sequencing data analysis.* Brief Bioinform, 2013. **14**(6): p. 671-83.

327. Huber, W., et al., *Orchestrating high-throughput genomic analysis with Bioconductor.* Nat Methods, 2015. **12**(2): p. 115-21.

328. Robinson, M.D., D.J. McCarthy, and G.K. Smyth, *edgeR: a Bioconductor package for differential expression analysis of digital gene expression data.* Bioinformatics, 2010. **26**(1): p. 139-40.

329. Conesa, A., et al., *A survey of best practices for RNA-seq data analysis.* Genome Biology, 2016. **17**: p. 13.

330. Law, C.W., et al., *RNA-seq analysis is easy as 1-2-3 with limma, Glimma and edgeR.* F1000Research, 2016. **5**: p. 1408.

331. Mak, V., et al., *Smoking is associated with the retention of cytoplasm by human spermatozoa.* Urology, 2000. **56**(3): p. 463-6.

332. Kovac, J.R., A. Khanna, and L.I. Lipshultz, *The effects of cigarette smoking on male fertility.* Postgrad Med, 2015. **127**(3): p. 338-41.

333. Harlev, A., et al., *Smoking and Male Infertility: An Evidence-Based Review*. The World Journal of Men's Health, 2015. **33**(3): p. 143-160.

334. Dai, J.-B., Z.-X. Wang, and Z.-D. Qiao, *The hazardous effects of tobacco smoking on male fertility.* Asian Journal of Andrology, 2015. **17**(6): p. 954-960.

335. Gaur, D.S., M. Talekar, and V.P. Pathak, *Effect of cigarette smoking on semen quality of infertile men.* Singapore Med J, 2007. **48**(2): p. 119-23.

336. Baazeem, A., et al., *Varicocele and male factor infertility treatment: a new meta-analysis and review of the role of varicocele repair.* Eur Urol, 2011. **60**(4): p. 796-808.

337. Kantartzi, P.D., et al., *Male infertility and varicocele: myths and reality.* Hippokratia, 2007. **11**(3): p. 99-104.

338. Zini, A., et al., *Varicocele is associated with abnormal retention of cytoplasmic droplets by human spermatozoa.* Fertil Steril, 2000. **74**(3): p. 461-4.

339. Chen, S., et al., *Sperm storage and spermatozoa interaction with epithelial cells in oviduct of Chinese soft-shelled turtle, Pelodiscus sinensis.* Ecology and Evolution, 2015. **5**(15): p. 3023-3030.

340. Mendes, N.D., A.T. Freitas, and M.F. Sagot, *Current tools for the identification of miRNA genes and their targets.* Nucleic Acids Research, 2009. **37**(8): p. 2419-2433.

341. Akhtar, M.M., et al., *Bioinformatic tools for microRNA dissection.* Nucleic Acids Research, 2016. **44**(1): p. 24-44.

342. Kang, W. and M.R. Friedländer, *Computational Prediction of miRNA Genes from Small RNA Sequencing Data.* Frontiers in Bioengineering and Biotechnology, 2015. **3**: p. 7.

343. Friedländer, M.R., et al., *miRDeep2 accurately identifies known and hundreds of novel microRNA genes in seven animal clades.* Nucleic Acids Research, 2012. **40**(1): p. 37-52.

344. Hackenberg, M., et al., *miRanalyzer: a microRNA detection and analysis tool for next-generation sequencing experiments.* Nucleic Acids Research, 2009. **37**(Web Server issue): p. W68-W76.

345. Langmead, B., et al., *Ultrafast and memory-efficient alignment of short DNA sequences to the human genome.* Genome Biol, 2009. **10**(3): p. R25.

346. Friedlander, M.R., et al., *High-resolution profiling and discovery of planarian small RNAs.* Proc Natl Acad Sci U S A, 2009. **106**(28): p. 11546-51.

347. Metpally, R.P., et al., *Comparison of Analysis Tools for miRNA High Throughput Sequencing Using Nerve Crush as a Model.* Front Genet, 2013. **4**: p. 20.

348. An, J., et al., *miRDeep*: an integrated application tool for miRNA identification from RNA sequencing data.* Nucleic Acids Research, 2013. **41**(2): p. 727-737.

349. Hackenberg, M., N. Rodriguez-Ezpeleta, and A.M. Aransay, *miRanalyzer: an update on the detection and analysis of microRNAs in high-throughput sequencing experiments.* Nucleic Acids Res, 2011. **39**(Web Server issue): p. W132-8.

350. Smith, L.K., et al., *Deep sequencing identification of novel glucocorticoid-responsive miRNAs in apoptotic primary lymphocytes.* PLoS One, 2013. **8**(10): p. e78316.

351. Mayoral, J.G., et al., *Wolbachia infection modifies the profile, shuttling and structure of microRNAs in a mosquito cell line.* PLoS One, 2014. **9**(4): p. e96107.

352. Bustin, S.A. and T. Nolan, *Pitfalls of Quantitative Real-Time Reverse-Transcription Polymerase Chain Reaction.* Journal of Biomolecular Techniques : JBT, 2004. **15**(3): p. 155-166.

353. Karrer, E.E., et al., *In situ isolation of mRNA from individual plant cells: creation of cell-specific cDNA libraries.* Proc Natl Acad Sci U S A, 1995. **92**(9): p. 3814-8.

354. Curry, J., C. McHale, and M.T. Smith, *Low efficiency of the Moloney murine leukemia virus reverse transcriptase during reverse transcription of rare t(8;21) fusion gene transcripts.* Biotechniques, 2002. **32**(4): p. 768, 770, 772, 754-5.

355. Marchuk, D., et al., *Construction of T-vectors, a rapid and general system for direct cloning of unmodified PCR products.* Nucleic Acids Res, 1991. **19**(5): p. 1154.

356. Griffiths-Jones, S., et al., *miRBase: tools for microRNA genomics.* Nucleic Acids Res, 2008. **36**(Database issue): p. D154-8.

357. Yuan, X., et al., *Clustered microRNAs' coordination in regulating protein-protein interaction network.* BMC Syst Biol, 2009. **3**: p. 65.

358. Lee, Y., et al., *MicroRNA maturation: stepwise processing and subcellular localization.* EMBO J, 2002. **21**(17): p. 4663-70.

359. Lau, N.C., et al., *An abundant class of tiny RNAs with probable regulatory roles in Caenorhabditis elegans.* Science, 2001. **294**(5543): p. 858-62.

360. Lagos-Quintana, M., et al., *Identification of novel genes coding for small expressed RNAs.* Science, 2001. **294**(5543): p. 853-8.

361. Guay, C., et al., *Horizontal transfer of exosomal microRNAs transduce apoptotic signals between pancreatic beta-cells.* Cell Communication and Signaling, 2015. **13**(1): p. 17.

362. Montecalvo, A., et al., *Mechanism of transfer of functional microRNAs between mouse dendritic cells via exosomes.* Blood, 2012. **119**(3): p. 756-766.

363. Wales, R.G., J.C. Wallace, and I.G. White, *Composition of bull epididymal and testicular fluid.* J Reprod Fertil, 1966. **12**(1): p. 139-44.

364. Zhou, J., et al., *The Semen pH Affects Sperm Motility and Capacitation.* PLOS ONE, 2015. **10**(7): p. e0132974.

365. Mawson, C.A. and M.I. Fischer, *Zinc content of the genital organs of the rat.* Nature, 1951. **167**(4256): p. 859.

366. Muntzing, J., et al., *Hormonal control of zinc uptake and binding in the rat dorsolateral prostate.* Invest Urol, 1977. **14**(6): p. 492-5.

367. Srivastava, A., A.R. Chowdhury, and B.S. Setty, *Zinc content in the epididymis, vas deferens, prostate, and seminal vesicles of juvenile rhesus monkey (Macaca mulatta): effect of androgen and estrogen.* Prostate, 1984. **5**(2): p. 153-8.

368. Srivastava, A., A.R. Chowdhury, and B.S. Setty, *Testicular regulation and sub-cellular distribution of zinc in the epididymis and vas deferens of rhesus monkey (Macaca mulatta).* Acta Endocrinol (Copenh), 1986. **113**(3): p. 440-9.

369. Zalewski, P.D., et al., *Changes in distribution of labile zinc in mouse spermatozoa during maturation in the epididymis assessed by the fluorophore Zinquin.* Reprod Fertil Dev, 1996. **8**(7): p. 1097-105.

370. Riffo, M., S. Leiva, and J. Astudillo, *Effect of zinc on human sperm motility and the acrosome reaction.* Int J Androl, 1992. **15**(3): p. 229-37.

371. D'Amours, O., et al., *Epididymosomes Transfer Epididymal Sperm Binding Protein 1 (ELSPBP1) to Dead Spermatozoa During Epididymal Transit in Bovine1.* Biology of Reproduction, 2012. **87**(4): p. 94, 1-11-94, 1-11.

372. Coutinho da Silva, M.A., et al., *Effects of components of semen extenders on the binding of stallion spermatozoa to bovine or equine zonae pellucidae.* Reproduction, 2012. **143**(5): p. 577-85.

373. Hamilton, T.R.d.S., et al., *Evaluation of Lasting Effects of Heat Stress on Sperm Profile and Oxidative Status of Ram Semen and Epididymal Sperm.* Oxidative Medicine and Cellular Longevity, 2016. **2016**: p. 1687657.

374. Pourentezari, M., et al., *Effects of acrylamide on sperm parameters, chromatin quality, and the level of blood testosterone in mice.* Iranian Journal of Reproductive Medicine, 2014. **12**(5): p. 335-342.

375. Wdowiak, A., L. Wdowiak, and H. Wiktor, *Evaluation of the effect of using mobile phones on male fertility.* Ann Agric Environ Med, 2007. **14**(1): p. 169-72.

Appendices

Appendix 1: Biggers, Whitten and Whittingham media (BWW) Composition

Component	Final Concentration
NaCl	91.5 mM
KCl	4.6 mM
$CaCl_2 \cdot 2H_2O$	1.7 mM
KH_2PO_4	1.2 mM
$MgSO_4 \cdot 7H_2O$	1.2 mM
$NaHCO_3$	25 mM
D-glucose	5.6 mM
Sodium pyruvate	0.27 mM
Sodium lactate	44 mM
Penicillin	5 U/mL
Streptomycin	5 µg/mL
Hepes buffer	20 mM
BSA	3 mg/mL
pH	**7.4**
Osmolarity	**300 mOsm/kg**

Appendix 2: Sequential centrifugation steps employed to cleanse epididymosome samples of sperm

No. Spins	Speed	Time
3	500 x *g*	5 mins
1	2,000 x *g*	
1	4,000 x *g*	
1	8,000 x *g*	
1	17,000 x *g*	10 mins
3	20,000 x *g*	

Appendix 3: Composition of Discontinuous Optiprep density gradient used to isolate epididymosomes

Layer	60 % Optiprep	0.25M Sucrose/10mM Tris
40 %	667 µL	333 µL
20 %	333 µL	667 µL
10 %	167 µL	833 µL
5 %	83 µL	917 µL

Appendix 4: Composition of 'Solution D' reagent used in RNA extractions

Component	Amount
Guanidine Thiocyanate	23.63g
0.75 Sodium Citrate	1.66mL
Lauroylsarcosine sodium salt	1.25mL
0.72 % B-Mercaptoethanol	360 µL
H_2O	Up to 50mL

Appendix 5: Composition of reverse transcription master mix

Reagent	Volume (µL)
M-MLV Reverse Transcription 5x Buffer	5
100mM DTT in DEPC H_2O	2
Recombinant RNAsin Ribonuclease Inhibitor	1
10mM dNTPs	1
25mM $MgCl_2$	2
Total	**11**

Appendix 6: Composition of SYBR green qPCR master mix

Component	Volume (µL)
GoTaq qPCR Master Mix	10
Fwd/Rev Primer Mix	0.2
H_2O	8.8
Total	**19**

Appendix 7: qPCR protocol for housekeeping genes

Stage	Step 1	Step 2	Step 3	Cycles
Pre-incubation	95°C / 5 mins			1
2 Step Amplification*	95°C / 10 sec	56°C / 30 sec		50
Melting	95°C / 10 sec	65°C / 60 sec	95°C / 1 sec	1
Cooling	37°C / 30 sec			1

*Measurements were acquired after each cycle of 2 Step Amplification.

Appendix 8: Composition of Taqman reverse transcription master mix

Reagent	Volume (µL)
RT Primer Pool	6.00
dNTPs with dTTP (100mM)	0.30
MultiScribe Reverse Transcriptate (50U/ µL)	3.00
10x RT Buffer	1.50
RNase Inhibitor (20U/ µL)	0.19
Nuclease Free Water	1.01
RNA (300-1000µg)	3
Total	**15**

Appendix 9: Thermocycler protocol used for Taqman reverse transcription

Step	Time (mins)	Temperature
Hold	30	15°C
Hold	30	42°C
Hold	5	85°C
Hold	Infinite	4°C

Appendix 10: Composition of Taqman RT-qPCR reactions

Component	Volume (µL)
Taqman MM	10
H_2O	8.5
Taqman Assay	1
cDNA	0.5
Total	**20**

Appendix 11: Thermocycler protocol used for Taqman RT-qPCR

Stage	Step 1	Step 2	Cycles
Pre-incubation	95°C / 5 mins		1
2 Step Amplification*	95°C / 15 sec	60°C / 60 sec	50
Cooling	37°C / 30 sec		1

*Measurements were acquired after each cycle of 2 Step Amplification.

Appendix 12: Details of each miR-seq file generated in prior NGS analyses.

Sample and GEO Accession #	Segment	Replicate	Sample Code	Library Reads	22nt Reads
Epithelial Cells ***GSE70197***	Caput	1	*GSM1720694*	15,133,362	1,045,96
		2	*GSM1720695*	14,620,058	982,66
	Corpus	1	*GSM1720696*	13,556,570	468,19
		2	*GSM1720697*	15,018,277	368,52
	Cauda	1	*GSM1720698*	13,213,955	785,78
		2	*GSM1720699*	13,162,248	622,48
Spermatozoa ***GSE70198***	Caput	1	*GSM1720708*	15,420,966	1,437,11
		2	*GSM1720709*	16,099,162	1,444,32
	Corpus	1	*GSM1720710*	16,603,751	372,74
		2	*GSM1720711*	14,923,859	333,23
	Cauda	1	*GSM1720712*	13,890,643	418,74
		2	*GSM1720713*	14,755,798	284,81
Epididymosomes ***GSE79500***	Caput	1	*GSM2096405*	95,821,564	6,407,48
		2	*GSM2096406*	29,229,900	5,015,12
		3	*GSM2096407*	31,275,980	4,596,92
	Corpus	1	*GSM2096408*	95,433,795	3,235,59
		2	*GSM2096409*	32,198,568	1,418,01
		3	*GSM2096410*	23,638,623	894,35
	Cauda	1	*GSM2096411*	15,045,156	748,94
		2	*GSM2096412*	13,475,652	830,86
		3	*GSM2096413*	28,382,821	2,301,45

Appendix 13: Details of all potentially novel miRNAs.

Novel miRNA ID	Chromosome	Sequence	sRNA Length	Hairpin Length	Genomic Hits
Nov-miR13	*2 dna_sm:chromosome chromosome:GRCm38:2:1:182113224:1*	*ACCTTCTGGCTCTGACCACCACC*	*23*	*57*	*1*
Nov-miR31	13 dna_sm:chromosome chromosome:GRCm38:13:1:120421639:1	CTGCATGTGGACATGTCTGCCCT	23	57	1
Nov-miR37	*13 dna_sm:chromosome chromosome:GRCm38:13:1:120421639:1*	*ATGGAGGACTGAGAAGGTGGAGC*	*23*	*62*	*1*
Nov-miR38	2 dna_sm:chromosome chromosome:GRCm38:2:1:182113224:1	TGTGGACCTGTACGTGCCGCGGA	23	61	2
Nov-miR42	*13 dna_sm:chromosome chromosome:GRCm38:13:1:120421639:1*	*ATGCCAGCTGTGGGACCCGGAGC*	*23*	*75*	*2*
Nov-miR50	1 dna_sm:chromosome chromosome:GRCm38:1:1:195471971:1	TTCCACTGTTGGTAGAGAGCTG	22	63	1
Nov-miR52	16 dna_sm:chromosome chromosome:GRCm38:16:1:98207768:1	TCAAGGTCACTGAGACACAGTCT	23	60	1
Nov-miR61	11 dna_sm:chromosome chromosome:GRCm38:11:1:122082543:1	ACCCAGGACTGAAAGAGGCTC	21	64	1
Nov-miR63	X dna_sm:chromosome chromosome:GRCm38:X:1:171031299:1	TTGAGTCAGTAGTACTGAGCC	21	93	1
Nov-miR80	7 dna_sm:chromosome chromosome:GRCm38:7:1:145441459:1	ACAGTGGCCAGGTGCCAGGGC	21	58	1
Nov-miR89	2 dna_sm:chromosome chromosome:GRCm38:2:1:182113224:1	ATAGGCTCAGAAGACATTAGGCT	23	58	1
Nov-miR101	*17 dna_sm:chromosome chromosome:GRCm38:17:1:94987271:1*	*ATGCGCCTTGTAGAGCCTGTGGG*	*23*	*57*	*1*
Nov-miR123	2 dna_sm:chromosome chromosome:GRCm38:2:1:182113224:1	ATGTGTCCCTGCTGTGACATG	21	55	1
Nov-miR125	1 dna_sm:chromosome chromosome:GRCm38:1:1:195471971:1	ACAGGAGTGTGCCTTGGGGCTG	22	91	1
Nov-miR127	*16 dna_sm:chromosome chromosome:GRCm38:16:1:98207768:1*	*AGCCATGACGGAAGACTGTGTT*	*22*	*92*	*2*
Nov-miR196	7 dna_sm:chromosome chromosome:GRCm38:7:1:145441459:1	AAATCGAGAGAGACTTGGGTTG	22	74	1
Nov-miR210	15 dna_sm:chromosome chromosome:GRCm38:15:1:104043685:1	TCTGCTAGCACTCCAGACTCAC	22	64	1
Nov-miR243	2 dna_sm:chromosome chromosome:GRCm38:2:1:182113224:1	ACACGTGACATAGGCGCCCAGC	22	85	1
Nov-miR293	X dna_sm:chromosome chromosome:GRCm38:X:1:171031299:1	ATGAGATTAGTCATTCTGGCC	21	70	1
Nov-miR295	7 dna_sm:chromosome chromosome:GRCm38:7:1:145441459:1	AAATTGAGTGTCGGGCAGAGA	21	55	1
Nov-miR307	4 dna_sm:chromosome chromosome:GRCm38:4:1:156508116:1	TTCAGGCTGTTAGAGAGGAGCC	22	85	1
Nov-miR311	9 dna_sm:chromosome chromosome:GRCm38:9:1:124595110:1	TGGGAGACTGACTGAAGAAGCCT	23	57	1

Appendix 14: Raw abundance of all potentially novel miRNAs in spermatozoa.

Nov-miR Number	Spermatozoa						Average Raw Counts		
	Caput		Corpus		Cauda		Spermatozoa		
	Replicate 1	Replicate 2	Replicate 1	Replicate 2	Replicate 1	Replicate 2	Caput	Corpus	Cauda
Nov-miR13	43	16	348	332	0	0	30	340	0
Nov-miR31	17	13	4	0	0	1	15	2	1
Nov-miR37	20	24	17	22	1	6	22	20	4
Nov-miR38	10	7	9	11	0	0	9	10	0
Nov-miR42	1	3	11	20	0	1	2	16	1
Nov-miR50	1	8	2	4	0	0	5	3	0
Nov-miR52	0	0	1	1	0	0	0	1	0
Nov-miR61	2	4	4	6	0	0	3	5	0
Nov-miR63	5	4	2	2	0	0	5	2	0
Nov-miR80	2	0	7	4	0	0	1	6	0
Nov-miR89	3	0	6	9	0	0	2	8	0
Nov-miR101	0	5	8	17	0	0	3	13	0
Nov-miR123	0	1	4	7	0	0	1	6	0
Nov-miR125	1	1	2	6	0	0	1	4	0
Nov-miR127	0	1	0	0	20	13	1	0	17
Nov-miR196	1	0	13	5	0	0	1	9	0
Nov-miR210	1	0	0	0	10	5	1	0	8
Nov-miR243	0	1	4	6	0	0	1	5	0
Nov-miR293	0	0	4	7	0	0	0	6	0
Nov-miR295	1	2	8	5	0	0	2	7	0
Nov-miR307	0	1	9	5	0	0	1	7	0
Nov-miR311	2	1	7	4	0	0	2	6	0

Appendix 15: Raw abundance of all potentially novel miRNAs in epithelial cells.

Nov-miR Number	Epithelial Cells						Average Raw Counts		
	Caput		Corpus		Cauda		Epithelial Cells		
	Replicate 1	Replicate 2	Replicate 1	Replicate 2	Replicate 1	Replicate 2	Caput	Corpus	Cauda
Nov-miR13	28	13	90	39	1	7	21	65	4
Nov-miR31	3	5	1	0	0	2	4	1	1
Nov-miR37	14	14	8	9	25	6	14	9	16
Nov-miR38	2	1	6	4	1	0	2	5	1
Nov-miR42	4	2	6	6	1	5	3	6	3
Nov-miR50	2	0	2	0	0	0	1	1	0
Nov-miR52	1	0	1	0	0	0	1	1	0
Nov-miR61	0	0	1	2	0	1	0	2	1
Nov-miR63	1	1	1	1	0	0	1	1	0
Nov-miR80	0	0	1	1	0	0	0	1	0
Nov-miR89	1	1	2	0	0	0	1	1	0
Nov-miR101	0	0	3	0	1	1	0	2	1
Nov-miR123	0	0	2	2	0	1	0	2	1
Nov-miR125	0	1	3	2	1	0	1	3	1
Nov-miR127	0	0	0	0	0	0	0	0	0
Nov-miR196	0	0	0	0	0	0	0	0	0
Nov-miR210	0	0	0	0	0	0	0	0	0
Nov-miR243	1	0	1	0	0	2	1	1	1
Nov-miR293	0	0	0	0	0	1	0	0	1
Nov-miR295	0	0	1	0	0	0	0	1	0
Nov-miR307	0	0	0	0	0	0	0	0	0
Nov-miR311	1	0	4	0	0	0	1	2	0

Appendix 16: Raw abundance of all potentially novel miRNAs in epididymosomes.

Nov-miR Number	Epididymosomes									Average Raw Counts		
	Caput			Corpus			Cauda			Epididymosomes		
	Replicate 1	Replicate 2	Replicate 3	Replicate 1	Replicate 2	Replicate 3	Replicate 1	Replicate 2	Replicate 3	Caput	Corpus	Cauda
Nov-miR13	112	69	107	691	834	632	0	0	271	96	719	90
Nov-miR31	72	35	167	45	21	6	4	5	9	91	24	6
Nov-miR37	16	5	10	39	21	11	90	35	56	10	24	60
Nov-miR38	43	0	31	39	3	1	4	4	22	25	14	10
Nov-miR42	7	25	12	30	24	16	4	11	30	15	23	15
Nov-miR50	22	21	26	20	25	22	1	0	4	23	22	2
Nov-miR52	24	13	36	162	67	22	0	0	9	24	84	3
Nov-miR61	28	3	5	67	15	12	0	2	3	12	31	2
Nov-miR63	16	4	42	30	8	19	0	0	8	21	19	3
Nov-miR80	0	0	0	18	18	9	0	0	5	0	15	2
Nov-miR89	8	3	6	44	16	11	0	0	2	6	24	1
Nov-miR101	4	4	1	7	10	2	1	0	0	3	6	0
Nov-miR123	3	0	4	9	2	7	2	0	3	2	6	2
Nov-miR125	3	3	3	5	46	4	0	0	0	3	18	0
Nov-miR127	1	0	0	1	1	0	0	1	2	0	1	1
Nov-miR196	4	1	0	17	3	1	0	0	2	2	7	1
Nov-miR210	0	0	0	0	0	0	0	0	0	0	0	0
Nov-miR243	1	0	1	11	3	2	0	0	1	1	5	0
Nov-miR293	0	0	0	0	0	2	0	0	0	0	1	0
Nov-miR295	0	0	0	1	1	1	0	0	0	0	1	0
Nov-miR307	1	0	0	0	0	1	0	1	0	0	0	0
Nov-miR311	1	0	0	1	0	2	0	0	0	0	1	0

Appendix 17: Normalised abundance of all potentially novel miRNAs in spermatozoa.

Nov-miR Number	Spermatozoa						Average Counts		
	Caput		Corpus		Cauda		Spermatozoa		
	Replicate 1	Replicate 2	Replicate 1	Replicate 2	Replicate 1	Replicate 2	Caput	Corpus	Cauda
Nov-miR13	41.1	16.3	743.3	900.9	0.0	0.0	28.7	822.1	0.0
Nov-miR31	16.3	13.2	8.5	0.0	0.0	1.6	14.7	4.3	0.8
Nov-miR37	19.1	24.4	36.3	59.7	1.3	9.6	21.8	48.0	5.5
Nov-miR38	9.6	7.1	19.2	29.8	0.0	0.0	8.3	24.5	0.0
Nov-miR42	1.0	3.1	23.5	54.3	0.0	1.6	2.0	38.9	0.8
Nov-miR50	1.0	8.1	4.3	10.9	0.0	0.0	4.5	7.6	0.0
Nov-miR52	0.0	0.0	2.1	2.7	0.0	0.0	0.0	2.4	0.0
Nov-miR61	1.9	4.1	8.5	16.3	0.0	0.0	3.0	12.4	0.0
Nov-miR63	4.8	4.1	4.3	5.4	0.0	0.0	4.4	4.8	0.0
Nov-miR80	1.9	0.0	15.0	10.9	0.0	0.0	1.0	12.9	0.0
Nov-miR89	2.9	0.0	12.8	24.4	0.0	0.0	1.4	18.6	0.0
Nov-miR101	0.0	5.1	17.1	46.1	0.0	0.0	2.5	31.6	0.0
Nov-miR123	0.0	1.0	8.5	19.0	0.0	0.0	0.5	13.8	0.0
Nov-miR125	1.0	1.0	4.3	16.3	0.0	0.0	1.0	10.3	0.0
Nov-miR127	0.0	1.0	0.0	0.0	25.5	20.9	0.5	0.0	23.2
Nov-miR196	1.0	0.0	27.8	13.6	0.0	0.0	0.5	20.7	0.0
Nov-miR210	1.0	0.0	0.0	0.0	12.7	8.0	0.5	0.0	10.4
Nov-miR243	0.0	1.0	8.5	16.3	0.0	0.0	0.5	12.4	0.0
Nov-miR293	0.0	0.0	8.5	19.0	0.0	0.0	0.0	13.8	0.0
Nov-miR295	1.0	2.0	17.1	13.6	0.0	0.0	1.5	15.3	0.0
Nov-miR307	0.0	1.0	19.2	13.6	0.0	0.0	0.5	16.4	0.0
Nov-miR311	1.9	1.0	15.0	10.9	0.0	0.0	1.5	12.9	0.0

Appendix 18: Normalised abundance of all potentially novel miRNAs in epithelial cells.

Nov-miR Number	Epithelial Cells						Average Counts		
	Caput		Corpus		Cauda		Epithelial Cells		
	Replicate 1	Replicate 2	Replicate 1	Replicate 2	Replicate 1	Replicate 2	Caput	Corpus	Cauda
Nov-miR13	19.5	9.0	241.5	117.0	2.4	24.6	14.2	179.2	13.5
Nov-miR31	2.1	3.5	2.7	0.0	0.0	7.0	2.8	1.3	3.5
Nov-miR37	9.7	9.7	21.5	27.0	59.7	21.1	9.7	24.2	40.4
Nov-miR38	1.4	0.7	16.1	12.0	2.4	0.0	1.0	14.1	1.2
Nov-miR42	2.8	1.4	16.1	18.0	2.4	17.6	2.1	17.1	10.0
Nov-miR50	1.4	0.0	5.4	0.0	0.0	0.0	0.7	2.7	0.0
Nov-miR52	0.7	0.0	2.7	0.0	0.0	0.0	0.3	1.3	0.0
Nov-miR61	0.0	0.0	2.7	6.0	0.0	3.5	0.0	4.3	1.8
Nov-miR63	0.7	0.7	2.7	3.0	0.0	0.0	0.7	2.8	0.0
Nov-miR80	0.0	0.0	2.7	3.0	0.0	0.0	0.0	2.8	0.0
Nov-miR89	0.7	0.7	5.4	0.0	0.0	0.0	0.7	2.7	0.0
Nov-miR101	0.0	0.0	8.0	0.0	2.4	3.5	0.0	4.0	2.9
Nov-miR123	0.0	0.0	5.4	6.0	0.0	3.5	0.0	5.7	1.8
Nov-miR125	0.0	0.7	8.0	6.0	2.4	0.0	0.3	7.0	1.2
Nov-miR127	0.0	0.0	0.0	0.0	0.0	0.0	0.0	0.0	0.0
Nov-miR196	0.0	0.0	0.0	0.0	0.0	0.0	0.0	0.0	0.0
Nov-miR210	0.0	0.0	0.0	0.0	0.0	0.0	0.0	0.0	0.0
Nov-miR243	0.7	0.0	2.7	0.0	0.0	7.0	0.3	1.3	3.5
Nov-miR293	0.0	0.0	0.0	0.0	0.0	3.5	0.0	0.0	1.8
Nov-miR295	0.0	0.0	2.7	0.0	0.0	0.0	0.0	1.3	0.0
Nov-miR307	0.0	0.0	0.0	0.0	0.0	0.0	0.0	0.0	0.0
Nov-miR311	0.7	0.0	10.7	0.0	0.0	0.0	0.3	5.4	0.0

Appendix 19: Normalised abundance of all potentially novel miRNAs in epididymosomes.

Nov-miR Number	Epididymosomes									Average Counts		
	Caput			Corpus			Cauda			Epididymosomes		
	Replicate 1	Replicate 2	Replicate 3	Replicate 1	Replicate 2	Replicate 3	Replicate 1	Replicate 2	Replicate 3	Caput	Corpus	Cauda
Nov-miR13	17.5	13.8	23.3	213.6	588.1	706.7	0.0	0.0	117.8	18.2	502.8	39.3
Nov-miR31	11.2	7.0	36.3	13.9	14.8	6.7	5.3	6.0	3.9	18.2	11.8	5.1
Nov-miR37	2.5	1.0	2.2	12.1	14.8	12.3	120.2	42.1	24.3	1.9	13.1	62.2
Nov-miR38	6.7	0.0	6.7	12.1	2.1	1.1	5.3	4.8	9.6	4.5	5.1	6.6
Nov-miR42	1.1	5.0	2.6	9.3	16.9	17.9	5.3	13.2	13.0	2.9	14.7	10.5
Nov-miR50	3.4	4.2	5.7	6.2	17.6	24.6	1.3	0.0	1.7	4.4	16.1	1.0
Nov-miR52	3.7	2.6	7.8	50.1	47.2	24.6	0.0	0.0	3.9	4.7	40.6	1.3
Nov-miR61	4.4	0.6	1.1	20.7	10.6	13.4	0.0	2.4	1.3	2.0	14.9	1.2
Nov-miR63	2.5	0.8	9.1	9.3	5.6	21.2	0.0	0.0	3.5	4.1	12.1	1.2
Nov-miR80	0.0	0.0	0.0	5.6	12.7	10.1	0.0	0.0	2.2	0.0	9.4	0.7
Nov-miR89	1.2	0.6	1.3	13.6	11.3	12.3	0.0	0.0	0.9	1.1	12.4	0.3
Nov-miR101	0.6	0.8	0.2	2.2	7.1	2.2	1.3	0.0	0.0	0.5	3.8	0.4
Nov-miR123	0.5	0.0	0.9	2.8	1.4	7.8	2.7	0.0	1.3	0.4	4.0	1.3
Nov-miR125	0.5	0.6	0.7	1.5	32.4	4.5	0.0	0.0	0.0	0.6	12.8	0.0
Nov-miR127	0.2	0.0	0.0	0.3	0.7	0.0	0.0	1.2	0.9	0.1	0.3	0.7
Nov-miR196	0.6	0.2	0.0	5.3	2.1	1.1	0.0	0.0	0.9	0.3	2.8	0.3
Nov-miR210	0.0	0.0	0.0	0.0	0.0	0.0	0.0	0.0	0.0	0.0	0.0	0.0
Nov-miR243	0.2	0.0	0.2	3.4	2.1	2.2	0.0	0.0	0.4	0.1	2.6	0.1
Nov-miR293	0.0	0.0	0.0	0.0	0.0	2.2	0.0	0.0	0.0	0.0	0.7	0.0
Nov-miR295	0.0	0.0	0.0	0.3	0.7	1.1	0.0	0.0	0.0	0.0	0.7	0.0
Nov-miR307	0.2	0.0	0.0	0.0	0.0	1.1	0.0	1.2	0.0	0.1	0.4	0.4
Nov-miR311	0.2	0.0	0.0	0.3	0.0	2.2	0.0	0.0	0.0	0.1	0.8	0.0

Appendix 20: Secondary hairpin structure of *Nov-miR*s 13 – 52

NovmiR13

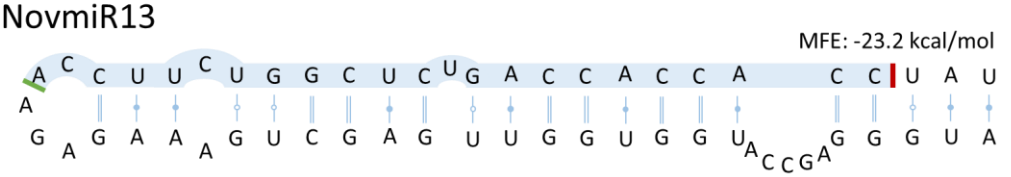

NovmiR31

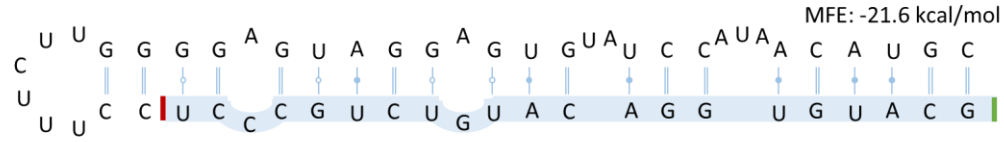

NovmiR37

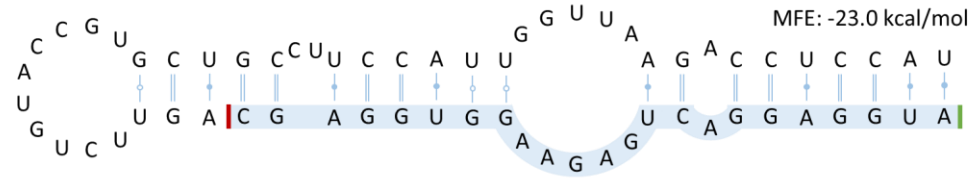

NovmiR38

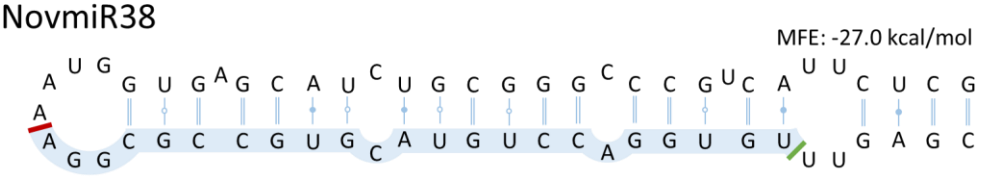

NovmiR42

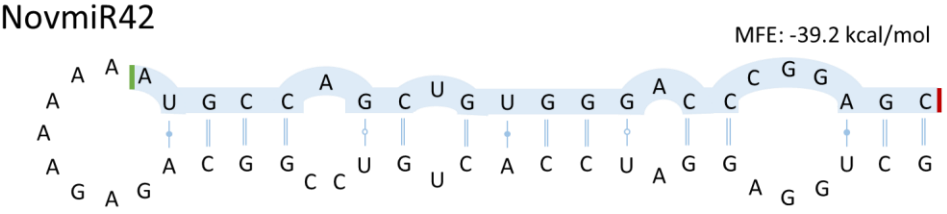

NovmiR50

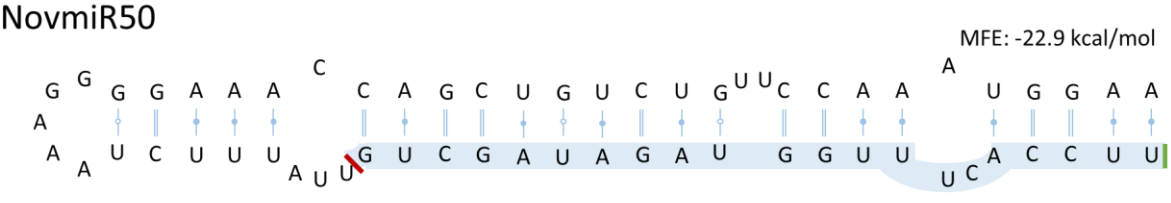

NovmiR52

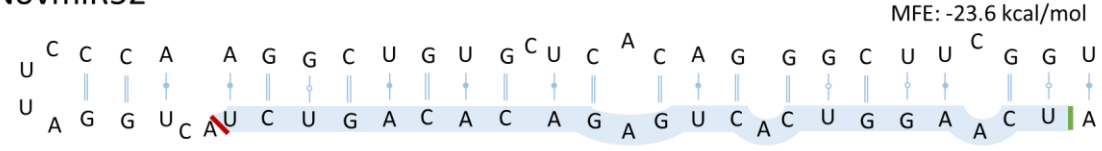

Appendix 21: Secondary hairpin structure of *Nov-miR*s 61 – 125

NovmiR61

MFE: -25.1 kcal/mol

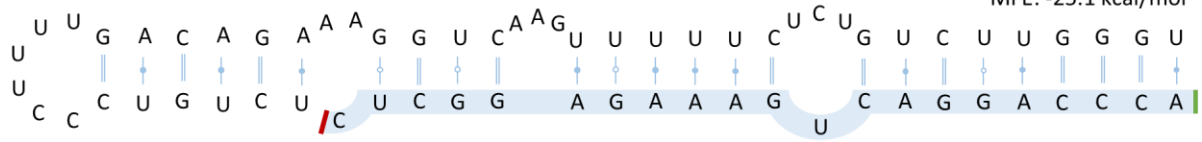

NovmiR63

MFE: -23.7 kcal/mol

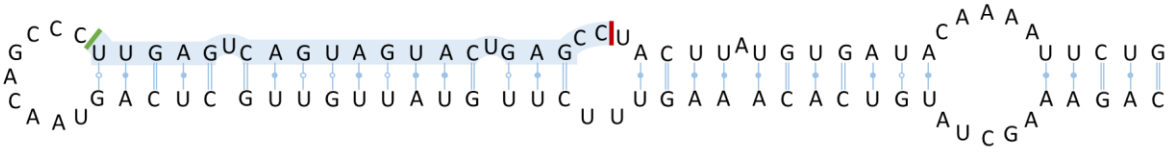

NovmiR80

MFE: - 20.9 kcal/mol

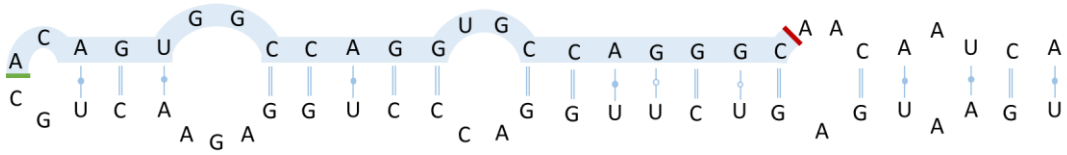

NovmiR89

MFE: - 20.7 kcal/mol

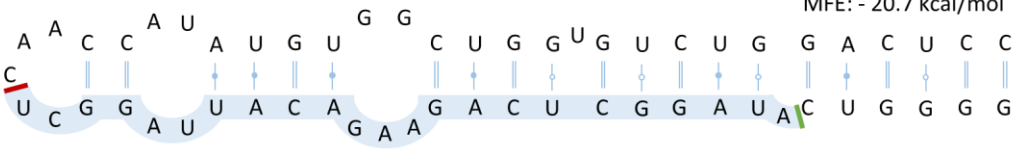

NovmiR101

MFE: - 32.1 kcal/mol

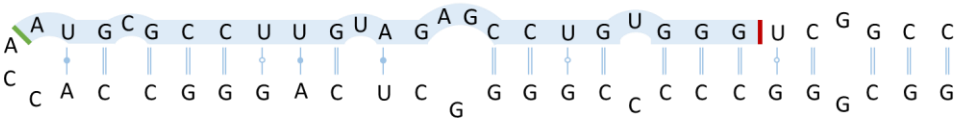

NovmiR123

MFE: - 15.6 kcal/mol

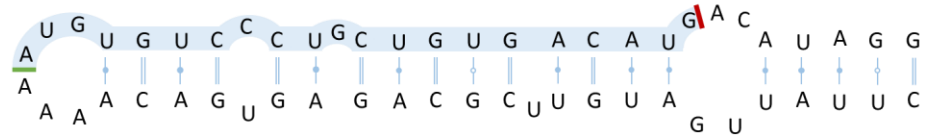

NovmiR125

MFE: - 30.6 kcal/mol

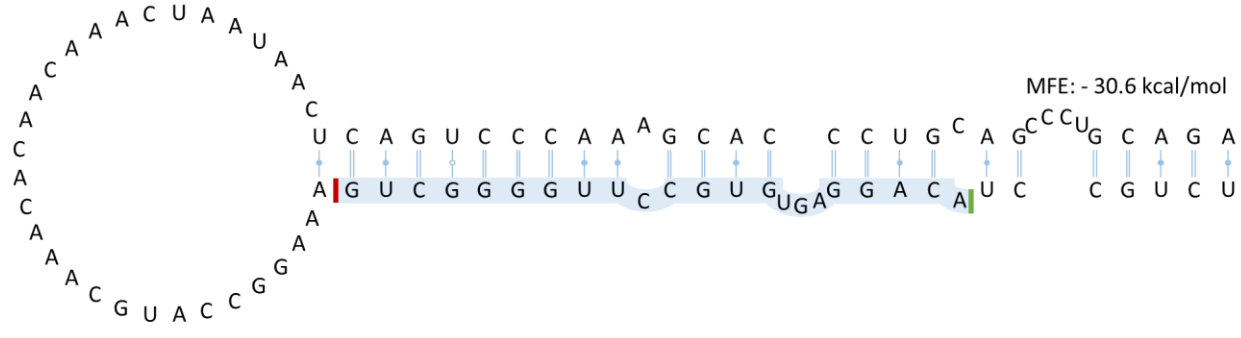

Appendix 22: Secondary hairpin structure of *Nov-miR*s 127 – 311

NovmiR127

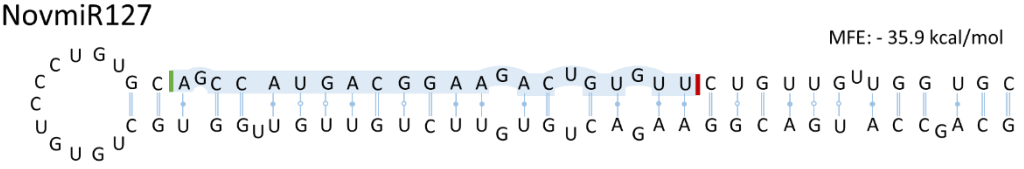

NovmiR196

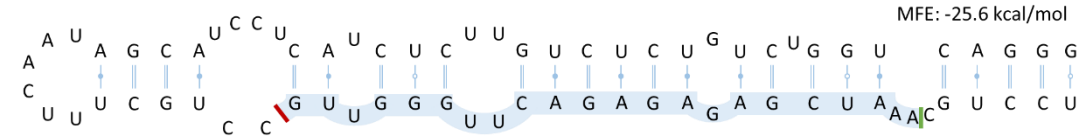

NovmiR210

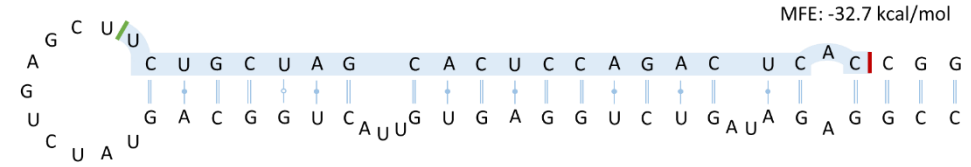

NovmiR243

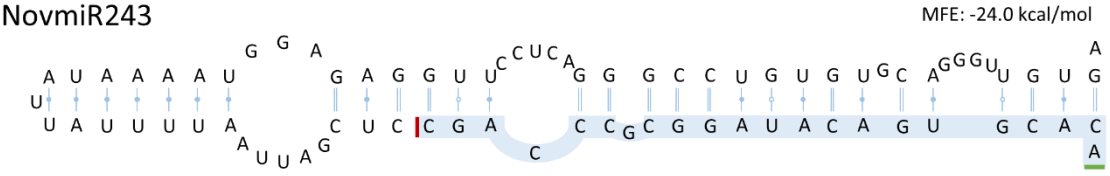

NovmiR293

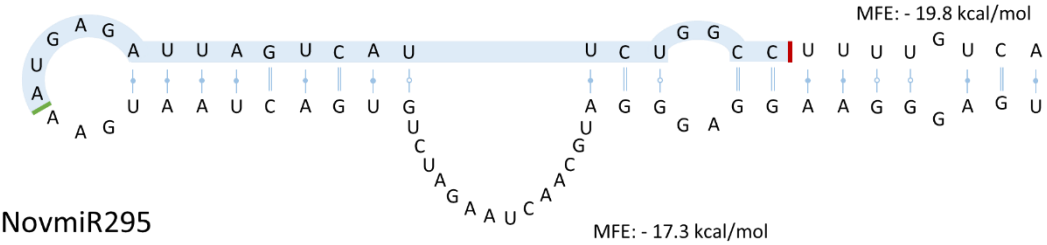

NovmiR295

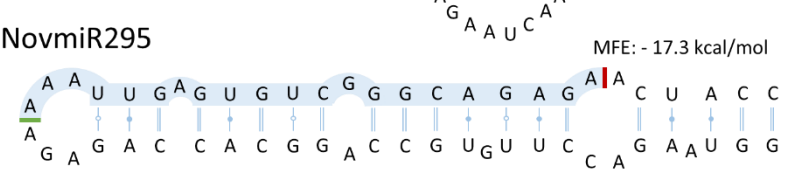

NovmiR307

NovmiR311

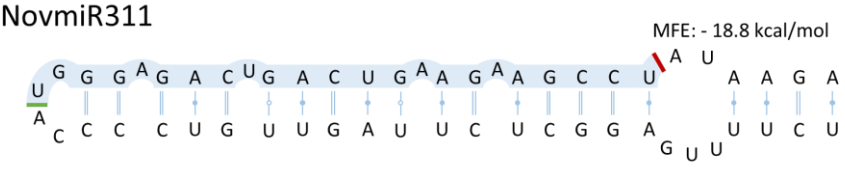

Appendix 23: Putative Targets of *Nov-miR*s as Identified by Several Analysis Tools

Targetted Gene	Analysis Tool					# of Seed in 3'UTR
	miRDB[1,2]	miR-microT[3,4]	RNAhybrid[5]	PITA[6]	miRanda[7]	
			***Nov-miR*13**			
Atad5	+	+	+	+	+	1
Atp6v1c1	+	+	+	+	+	1
Ccnj	+	+	+	+	+	3
Cdh20	+	+	+	+	+	2
Ckap2l	+	+	+	+	+	2
Clptm1l	+	+	+	+	+	1
Cpeb4	+	+	+	+	+	1
Ctbp2	+	+	+	+	+	1
D17Wsu92e	+	+	+	+	+	2
Dgkk	+	+	+	+	+	4
Dhx40	+	+	+	+	+	2
Dyrk1a	+	+	+	+	+	2
Eef1a1	+	+	+	+	+	1
Eif4g3	+	+	+	+	+	1
Fam178a	+	+	+	+	+	1
Fbxo32	+	+	+	+	+	1
Fign	+	+	+	+	+	1
Fli1	+	+	+	+	+	1
Foxc1	+	+	+	+	+	2
Igf2bp2	+	+	+	+	+	2
Ktn1	+	+	+	+	+	1
Lhcgr	+	+	+	+	+	1
Lhfpl3	+	+	+	+	+	1
Lif	+	+	+	+	+	2
Mapk9	+	+	+	+	+	2
Nfib	+	+	+	+	+	2
Pabpc4	+	+	+	+	+	1
Pak7	+	+	+	+	+	1
Plcb1	+	+	+	+	+	3
Ptprt	+	+	+	+	+	2
Rab3c	+	+	+	+	+	2
Slc25a19	+	+	+	+	+	3
Stxbp5	+	+	+	+	+	1
Sugp2	+	+	+	+	+	1

Tardbp	+	+	+	+	+	3
Tcf7l2	+	+	+	+	+	1
Tifab	+	+	+	+	+	5
Tnik	+	+	+	+	+	2
Traf3	+	+	+	+	+	2
Trim10	+	+	+	+	+	1
Ube2e3	+	+	+	+	+	1
Vps13d	+	+	+	+	+	1
Wasf1	+	+	+	+	+	1
Wdr82	+	+	+	+	+	3
Xrn1	+	+	+	+	+	4
Zfp36l1	+	+	+	+	+	1
Zfp518a	+	+	+	+	+	2
Zfp871	+	+	+	+	+	3
Zswim6	+	+	+	+	+	1
Targetted Gene	**Analysis Tool**					**# of Seed in 3'UTR**
	miRDB[1,2]	miR-microT[3,4]	RNAhybrid[5]	PITA[6]	miRanda[7]	

***Nov-miR*37**

2610002M06Rik	+	+	+	+	+	3
4921501E09Rik	+	+	+	+	+	1
Acr	+	+	+	+	+	1
AI593442	+	+	+	+	+	1
Ankrd45	+	+	+	+	+	10
Ankrd50	+	+	+	+	+	2
Aqp3	+	+	+	+	+	4
Arnt2	+	+	+	+	+	2
Ash2l	+	+	+	+	+	2
Atad1	+	+	+	+	+	2
Camk1d	+	+	+	+	+	7
Card10	+	+	+	+	+	31
Ccdc125	+	+	+	+	+	1
Cep170b	+	+	+	+	+	1
Chd1	+	+	+	+	+	1
Clvs1	+	+	+	+	+	3
Cntn2	+	+	+	+	+	7
Ctbs	+	+	+	+	+	2
Dach1	+	+	+	+	+	1
Dock5	+	+	+	+	+	2

Drp2	+	+	+	+	+	2
Eml4	+	+	+	+	+	1
Fam134c	+	+	+	+	+	3
Fam49b	+	+	+	+	+	1
Fbxo28	+	+	+	+	+	7
Fxr1	+	+	+	+	+	1
Gatad2a	+	+	+	+	+	2
Gigyf1	+	+	+	+	+	7
Gramd2	+	+	+	+	+	1
Gria2	+	+	+	+	+	3
Khdrbs1	+	+	+	+	+	1
Kpna3	+	+	+	+	+	1
Man1a2	+	+	+	+	+	4
Map1a	+	+	+	+	+	4
Map1b	+	+	+	+	+	1
Mapre2	+	+	+	+	+	2
Mat2a	+	+	+	+	+	1
Matn1	+	+	+	+	+	1
Mfhas1	+	+	+	+	+	1
Mgat4a	+	+	+	+	+	2
Myh15	+	+	+	+	+	1
Nav3	+	+	+	+	+	1
Necap1	+	+	+	+	+	1
Nono	+	+	+	+	+	2
Nrk	+	+	+	+	+	2
Pate2	+	+	+	+	+	3
Pcyt1b	+	+	+	+	+	5
Peli1	+	+	+	+	+	3
Pianp	+	+	+	+	+	4
Picalm	+	+	+	+	+	1
Prelp	+	+	+	+	+	4
Prlr	+	+	+	+	+	7
Ranbp10	+	+	+	+	+	4
Rbm33	+	+	+	+	+	5
Rictor	+	+	+	+	+	2
Sbk3	+	+	+	+	+	5
Sesn1	+	+	+	+	+	2
Shisa6	+	+	+	+	+	10

Sidt2	+	+	+	+	+	1
Slmap	+	+	+	+	+	1
Sptb	+	+	+	+	+	4
Timp3	+	+	+	+	+	2
Tnfrsf11a	+	+	+	+	+	2
Tns4	+	+	+	+	+	3
Ttc9c	+	+	+	+	+	1
Txnrd1	+	+	+	+	+	2
Vsig1	+	+	+	+	+	1
Wasf1	+	+	+	+	+	1
Ywhab	+	+	+	+	+	3
Zfp157	+	+	+	+	+	1
Adrb3	+	+	+	+	-	2
Cgnl1	+	+	+	+	-	1
Dcp1b	+	+	+	+	-	1
Rasal2	+	+	+	+	-	4
Anks1b	+	+	+	-	-	2
Targetted Gene	**Analysis Tool**					**# of Seed in 3'UTR**
	miRDB[1,2]	miR-microT[3,4]	RNAhybrid[5]	PITA[6]	miRanda[7]	
			***Nov-miR*42**			
2810403A07Rik	+	+	+	+	+	1
4921517D22Rik	+	+	+	+	+	1
5730409E04Rik	+	+	+	+	+	2
Ackr3	+	+	+	+	+	5
Actg1	+	+	+	+	+	1
Arhgap26	+	+	+	+	+	2
Bcr	+	+	+	+	+	1
Car12	+	+	+	+	+	2
Cbfa2t2	+	+	+	+	+	1
Cdt1	+	+	+	+	+	2
Chml	+	+	+	+	+	1
Cntnap1	+	+	+	+	+	1
Cops7b	+	+	+	+	+	1
Csmd1	+	+	+	+	+	2
Cstf2	+	+	+	+	+	1
Dap3	+	+	+	+	+	2
Dzank1	+	+	+	+	+	1
Edaradd	+	+	+	+	+	2

Eif4e2	+	+	+	+	+	1
Fam134b	+	+	+	+	+	1
Gda	+	+	+	+	+	2
Gipc1	+	+	+	+	+	1
Gm597	+	+	+	+	+	1
Hspa9	+	+	+	+	+	1
Itga3	+	+	+	+	+	2
Iyd	+	+	+	+	+	2
Map4k3	+	+	+	+	+	1
Mfrp	+	+	+	+	+	3
Naa25	+	+	+	+	+	1
Nphp3	+	+	+	+	+	2
Nqo2	+	+	+	+	+	2
Prkcg	+	+	+	+	+	1
Rbx1	+	+	+	+	+	2
Robo1	+	+	+	+	+	1
Secisbp2l	+	+	+	+	+	1
Slc18a2	+	+	+	+	+	2
Slc6a6	+	+	+	+	+	2
Slc9a8	+	+	+	+	+	2
Sos1	+	+	+	+	+	1
Triap1	+	+	+	+	+	2
Trip12	+	+	+	+	+	1
Usp11	+	+	+	+	+	1
Vezf1	+	+	+	+	+	2
Wdr76	+	+	+	+	+	1
Zfhx4	+	+	+	+	+	1
Targetted Gene	**Analysis Tool**					**# of Seed in 3'UTR**
	miRDB[1,2]	miR-microT[3,4]	RNAhybrid[5]	PITA[6]	miRanda[7]	

***Nov-miR*101**

Tenm2	+	+	+	+	+	1
Tctn3	+	+	+	+	+	2
Tgoln1	+	+	+	+	+	1
Apc2	+	+	+	+	+	1
Obfc1	+	+	+	+	+	1
Targetted Gene	**Analysis Tool**					**# of Seed in 3'UTR**
	miRDB[1,2]	miR-microT[3,4]	RNAhybrid[5]	PITA[6]	miRanda[7]	

***Nov-miR*127**

A230046K03Rik	+	+	+	+	+	1
Abca1	+	+	+	+	+	2
Adamts5	+	+	+	+	+	1
Agpat5	+	+	+	+	+	2
Bzw1	+	+	+	+	+	1
Ccdc96	+	+	+	+	+	1
Cenpo	+	+	+	+	+	3
Cep41	+	+	+	+	+	1
Cux1	+	+	+	+	+	4
Dgkk	+	+	+	+	+	1
Ermp1	+	+	+	+	+	2
Fem1b	+	+	+	+	+	1
Foxp2	+	+	+	+	+	3
Fyn	+	+	+	+	+	1
Htr3a	+	+	+	+	+	1
Kcnv2	+	+	+	+	+	3
Kdm5c	+	+	+	+	+	2
Mbd5	+	+	+	+	+	2
Mgea5	+	+	+	+	+	1
Mpzl2	+	+	+	+	+	1
Nfib	+	+	+	+	+	2
Npr3	+	+	+	+	+	2
Nup210	+	+	+	+	+	2
Opa1	+	+	+	+	+	1
Otud5	+	+	+	+	+	1
Pappa	+	+	+	+	+	1
Ptbp3	+	+	+	+	+	2
Rapgef2	+	+	+	+	+	1
Rbpj	+	+	+	+	+	2
Rdh19	+	+	+	+	+	2
Rfk	+	+	+	+	+	1
Rrm2	+	+	+	+	+	1
Sema3a	+	+	+	+	+	2
Slc19a2	+	+	+	+	+	2
Slc4a4	+	+	+	+	+	2
Suv39h2	+	+	+	+	+	1
Tbx18	+	+	+	+	+	2
Thbs4	+	+	+	+	+	1

Tnik	+	+	+	+	+	1
Txnip	+	+	+	+	+	1
Zcchc6	+	+	+	+	+	2

Appendix 24: Ranking of Putative Targets of *Nov-miR*s as Identified by Several Analysis Tools

Targetted Gene	Database Ranking					Assigned Rank
	miRDB[1,2]	miR-microT[3,4]	RNAhybrid[5]	PITA[6]	miRanda[7]	
			***Nov-miR*13**			
Atp6v1c1	29	7	4	1	3	**1**
Ccnj	4	15	11	5	9	**2**
Traf3	36	1	7	2	2	**3**
Cdh20	2	4	22	17	8	**4**
Dgkk	9	11	19	6	15	**5**
Tifab	48	3	10	15	4	**6**
D17Wsu92e	20	46	6	3	7	**7**
Zswim6	6	32	2	19	28	**8**
Rab3c	15	38	17	12	6	**9**
Ckap2l	30	24	15	9	11	**10**
Nfib	13	13	13	34	20	**11**
Fli1	5	12	36	25	18	**12**
Pabpc4	26	20	29	7	17	**13**
Wdr82	7	19	21	44	12	**14**
Tnik	45	25	9	11	14	**15**
Lif	43	30	14	10	13	**16**
Tardbp	22	9	34	14	33	**17**
Pak7	17	42	12	4	37	**18**
Ptprt	39	35	1	49	1	**19**
Ube2e3	3	36	30	8	48	**20**
Zfp871	46	16	20	23	21	**21**
Xrn1	47	29	5	33	16	**22**
Zfp36l1	16	22	31	31	30	**23**
Lhcgr	28	21	27	29	26	**24**
Slc25a19	18	48	3	39	24	**25**
Ktn1	41	5	37	18	31	**26**
Tcf7l2	42	28	32	26	5	**27**
Fam178a	32	47	18	13	23	**28**
Dhx40	8	8	43	32	42	**29**
Dyrk1a	27	31	16	24	36	**30**

Mapk9	1	27	33	30	43	**31**
Vps13d	40	14	26	37	19	**32**
Plcb1	11	40	35	28	22	**33**
Igf2bp2	14	44	28	16	34	**34**
Sugp2	12	10	38	41	44	**35**
Foxc1	33	2	39	48	25	**36**
Stxbp5	23	34	25	20	46	**37**
Fbxo32	24	49	8	21	47	**38**
Fign	38	6	23	45	40	**39**
Lhfpl3	35	17	44	35	29	**40**
Cpeb4	21	26	40	47	27	**41**
Trim10	44	39	46	27	10	**42**
Zfp518a	31	43	41	22	32	**43**
Eef1a1	10	37	47	43	39	**44**
Wasf1	19	23	49	40	45	**45**
Atad5	25	18	48	38	49	**46**
Clptm1l	34	33	45	36	38	**47**
Ctbp2	37	45	24	46	41	**48**
Eif4g3	49	41	42	42	35	**49**

Targetted Gene	**Database Ranking**					**Assigned Rank**
	miRDB[1,2]	miR-microT[3,4]	RNAhybrid[5]	PITA[6]	miRanda[7]	
Nov-miR37						
Ankrd45	1	51	1	1	2	**1**
Card10	6	3	8	8	35	**2**
Sbk3	39	12	5	4	5	**3**
Tnfrsf11a	5	59	2	2	1	**4**
Clvs1	9	15	3	12	30	**5**
Pcyt1b	12	19	32	16	4	**6**
Man1a2	3	10	10	28	38	**7**
Necap1	4	21	18	11	40	**8**
Camk1d	2	25	15	10	48	**9**
Nav3	11	6	6	7	76	**10**
Prelp	16	20	26	36	11	**11**
Myh15	15	38	24	13	31	**12**
Kpna3	25	4	21	15	61	**13**
Mapre2	24	45	12	21	28	**14**
Pianp	76	24	14	9	9	**15**
Fxr1	10	31	27	6	62	**16**

Rbm33	55	29	7	38	12	**17**
Mgat4a	49	52	11	20	14	**18**
Prlr	63	16	4	46	17	**19**
Sptb	34	65	17	33	3	**20**
Ranbp10	35	13	50	41	13	**21**
Cntn2	36	22	16	51	27	**22**
Matn1	30	23	23	44	32	**23**
Pate2	26	72	20	31	6	**24**
Shisa6	70	56	19	5	7	**25**
Fam49b	43	49	28	18	23	**26**
Fam134c	29	63	9	17	45	**27**
Dock5	37	5	39	35	47	**28**
Arnt2	33	7	13	42	70	**29**
Gramd2	7	1	53	55	51	**30**
Timp3	17	34	57	47	16	**31**
Peli1	62	43	34	25	10	**32**
Map1a	18	46	37	32	41	**33**
Ankrd50	31	50	31	30	37	**34**
Ccdc125	42	14	40	40	44	**35**
Mfhas1	46	9	46	65	20	**36**
Khdrbs1	51	2	49	62	24	**37**
Tns4	19	73	22	19	56	**38**
Ywhab	20	28	54	37	53	**39**
Sidt2	47	77	60	3	8	**40**
Aqp3	45	40	33	22	57	**41**
AI593442	57	44	36	14	50	**42**
Map1b	61	41	41	23	36	**43**
Slmap	14	37	73	58	22	**44**
Ctbs	28	26	45	45	60	**45**
4921501E09Rik	56	27	55	43	25	**46**
Acr	32	48	67	39	26	**47**
Wasf1	8	8	74	67	59	**48**
Drp2	54	71	25	26	42	**49**
Fbxo28	40	74	29	48	29	**50**
Gria2	77	76	30	34	15	**51**
2610002M06Rik	50	30	35	64	55	**52**
Dach1	72	18	47	73	34	**53**
Nono	38	35	72	68	33	**54**

Sesn1	22	36	75	72	46	**55**
Atad1	67	60	44	27	54	**56**
Cgnl1	60	53	43	24	75	**57**
Txnrd1	48	32	48	60	69	**58**
Picalm	68	55	58	56	21	**59**
Ppp2r3a	13	11	78	79	79	**60**
Mat2a	44	69	69	63	18	**61**
Nrk	65	68	59	52	19	**62**
Vsig1	41	39	71	75	39	**63**
Rasal2	21	67	51	54	73	**64**
Gatad2a	74	75	42	29	52	**65**
Cep170b	75	57	38	53	58	**67**
Ttc9c	27	78	68	71	43	**68**
Chd1	64	61	52	69	49	**69**
Eml4	58	42	70	59	68	**70**
Zfp157	73	47	65	57	63	**71**
Zcchc11	59	17	77	77	77	**72**
Rictor	69	70	62	49	65	**73**
Adrb3	52	58	64	70	74	**74**
Syn1	23	64	79	78	78	**75**
Gigyf1	71	79	56	50	67	**76**
Anks1b	53	62	61	76	71	**77**
Ash2l	78	33	76	74	64	**78**
Dcp1b	79	54	63	61	72	**79**

Targetted Gene	**Database Ranking**					**Assigned Rank**
	miRDB[1,2]	miR-microT[3,4]	RNAhybrid[5]	PITA[6]	miRanda[7]	
Nov-miR42						
Mfrp	19	25	1	1	1	**1**
Rbx1	3	5	20	8	19	**2**
Trip12	50	1	3	3	2	**3**
Slc6a6	8	7	14	25	8	**4**
2810403A07Rik	13	6	13	23	9	**5**
Nphp3	17	4	24	4	16	**6**
Slc9a8	11	43	8	2	7	**7**
Car12	24	26	2	19	5	**8**
Slc18a2	1	9	35	15	23	**9**
Iyd	12	20	27	9	20	**10**
Ackr3	6	48	4	24	12	**11**

Itga3	4	32	11	27	22	**12**
Usp11	47	17	18	5	11	**13**
Prkcg	30	23	23	10	18	**14**
Dzank1	29	30	7	36	4	**15**
Chml	31	44	5	22	6	**16**
Vezf1	21	10	37	7	41	**17**
Sos1	2	14	31	41	31	**18**
Zfhx4	5	2	42	31	40	**19**
Dap3	42	46	10	20	3	**20**
Cntnap1	34	39	9	29	10	**21**
Arhgap26	9	29	19	39	27	**22**
5730409E04Rik	33	18	12	34	28	**23**
Gipc1	48	16	25	16	21	**24**
Csmd1	10	8	41	45	24	**25**
Secisbp2l	18	41	33	11	25	**26**
Fam134b	14	21	39	28	29	**27**
Edaradd	41	38	6	33	14	**28**
Actg1	22	37	15	43	17	**29**
Cdt1	45	15	17	46	13	**30**
Gm597	25	13	38	38	26	**31**
Eif4e2	35	11	28	32	34	**32**
Nqo2	46	24	22	6	43	**33**
Triap1	26	47	26	12	36	**34**
Cops7b	49	28	16	42	15	**35**
Cbfa2t2	32	40	21	26	32	**36**
Robo1	16	45	40	18	35	**37**
Cstf2	43	22	29	35	30	**38**
Wdr76	37	42	36	13	33	**39**
Bcr	20	35	34	37	37	**40**
Map4k3	44	34	30	14	42	**41**
Gda	15	50	32	30	38	**42**
Naa25	23	33	45	21	44	**43**
Hspa9	36	3	44	40	45	**44**
Tulp4	40	19	47	17	46	**45**
Agap1	28	12	46	47	47	**46**
4921517D22Rik	39	27	43	44	39	**47**
Spag11b	27	31	48	48	48	**48**
Lrrc8c	7	49	50	50	50	**49**

Meaf6	38	36	49	49	49	**50**
Targetted Gene	**Database Ranking**					**Assigned Rank**
	miRDB[1,2]	miR-microT[3,4]	RNAhybrid[5]	PITA[6]	miRanda[7]	
			***Nov-miR*101**			
Apc2	2	4	3	2	1	1
Tctn3	4	2	1	4	2	2
Tgoln1	1	3	5	1	5	3
Obfc1	3	5	2	3	3	4
Tenm2	5	1	4	5	4	5
Targetted Gene	**Database Ranking**					**Assigned Rank**
	miRDB[1,2]	miR-microT[3,4]	RNAhybrid[5]	PITA[6]	miRanda[7]	
			***Nov-miR*127**			
Rapgef2	6	3	8	3	31	1
Cenpo	2	7	1	6	41	2
Ptbp3	13	18	7	8	14	3
Adamts5	26	4	17	10	6	4
Foxp2	3	1	19	31	17	5
Mpzl2	38	5	3	5	29	6
Mgea5	5	24	26	7	20	7
Abca1	14	30	2	1	40	8
Fem1b	8	13	37	22	8	9
Rdh19	19	11	28	19	11	10
Sema3a	1	6	35	35	13	11
Tnik	34	15	6	13	22	12
Nup210	4	26	10	17	36	13
Tbx18	29	23	14	9	21	14
Pappa	30	20	5	4	38	15
Bzw1	9	12	33	40	5	16
Nfib	36	2	34	15	12	17
Cep41	22	27	16	11	25	18
Rrm2	20	39	4	2	39	19
Npr3	17	16	31	38	4	20
Otud5	11	35	36	24	1	21
Kdm5c	18	9	20	34	27	22
Cux1	27	17	9	20	37	23
Dgkk	33	21	15	32	10	24
Mbd5	16	22	22	33	18	25
A230046K03Rik	12	38	41	21	3	26

Htr3a	15	37	18	12	33	27
Rbpj	7	33	11	30	35	28
Suv39h2	25	14	25	25	28	29
Ermp1	10	32	29	28	19	30
Ccdc96	21	28	24	23	24	31
Fyn	24	34	13	18	32	32
Thbs4	37	8	40	29	9	33
Zcchc6	32	25	23	14	30	34
Agpat5	35	19	39	36	2	35
Slc4a4	39	10	27	41	15	36
Txnip	31	41	12	27	26	37
Opa1	28	40	21	16	34	38
Slc19a2	41	36	38	26	7	39
Rfk	23	31	32	39	23	40
Kcnv2	40	29	30	37	16	41

Appendix 25: Amplification cycles of the U6 sRNA internal control in cDNA and reverse transcription control samples generated from biological pools of epididymal spermatozoa.

Replicate	**Segment**	**+RT**			**-RT**
Rep 1	Caput	21.99	21.81	21.89	31.46
	Corpus	20.36	20.32	20.3	26.82
	Cauda	18.22	18.23	18.33	25.14
Rep 2	Caput	21.69	21.6	21.4	35.26
	Corpus	21.02	20.84	21.14	37.12
	Cauda	21.4	21.62	21.66	32.12
Rep 3	Caput	21.79	22.01	22.02	-
	Corpus	22.5	22.47	22.36	36.14
	Cauda	22.22	22.08	21.21	-

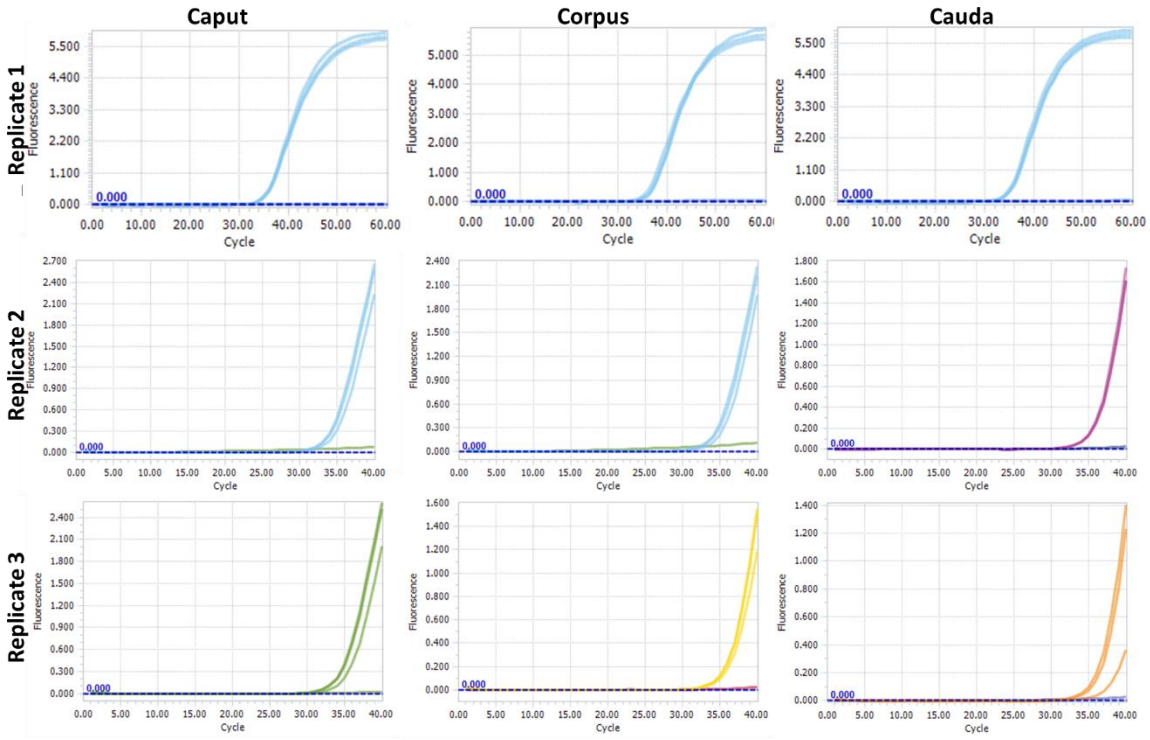

Appendix 26: Amplification curves of the U6 sRNA internal control in cDNA and reverse transcription control samples generated from biological pools of epididymal spermatozoa.

Appendix 27: Amplification cycles of *miR-29a in cDNA and reverse transcription control samples generated from biological pools of epididymal spermatozoa.**

Replicate	Segment	+RT			-RT
Rep 1	Caput	32.61	32.65	32.65	-
	Corpus	33.09	33.78	33.92	-
	Cauda	32.32	31.85	32.36	-
Rep 2	Caput	31.73	31.5	32.26	-
	Corpus	31.91	32.81	32.21	-
	Cauda	33.52	33.53	33.6	-
Rep 3	Caput	31.88	32.02	32.92	-
	Corpus	34.12	33.72	33.71	-
	Cauda	36.59	34	34.48	-

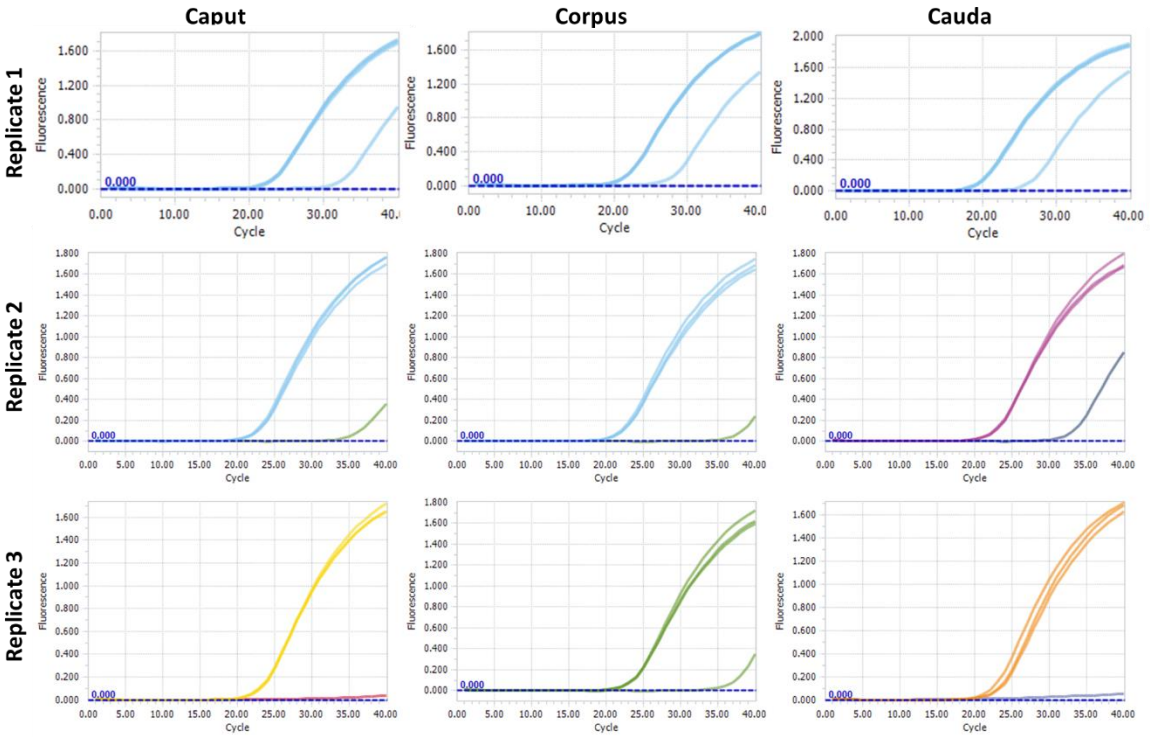

Appendix 28: Amplification curves of *miR-29a in cDNA and reverse transcription control samples generated from biological pools of epididymal spermatozoa.**

Appendix 29: Amplification cycles of *Nov-miR*13 in cDNA and reverse transcription control samples generated from biological pools of epididymal spermatozoa.

Replicate	Segment	+RT			-RT
Rep 1	Caput	31.23	32.7	32.28	-
	Corpus	27.5	27.63	27.42	-
	Cauda	33.58	34.05	33.23	-
Rep 2	Caput	31.17	31.37	32	-
	Corpus	28.01	28.39	28.1	-
	Cauda	34.04	34.28	34.42	-
Rep 3	Caput	30.5	30.63	30.74	-
	Corpus	29.44	29.52	29.33	-
	Cauda	34.83	35.17	35.61	-

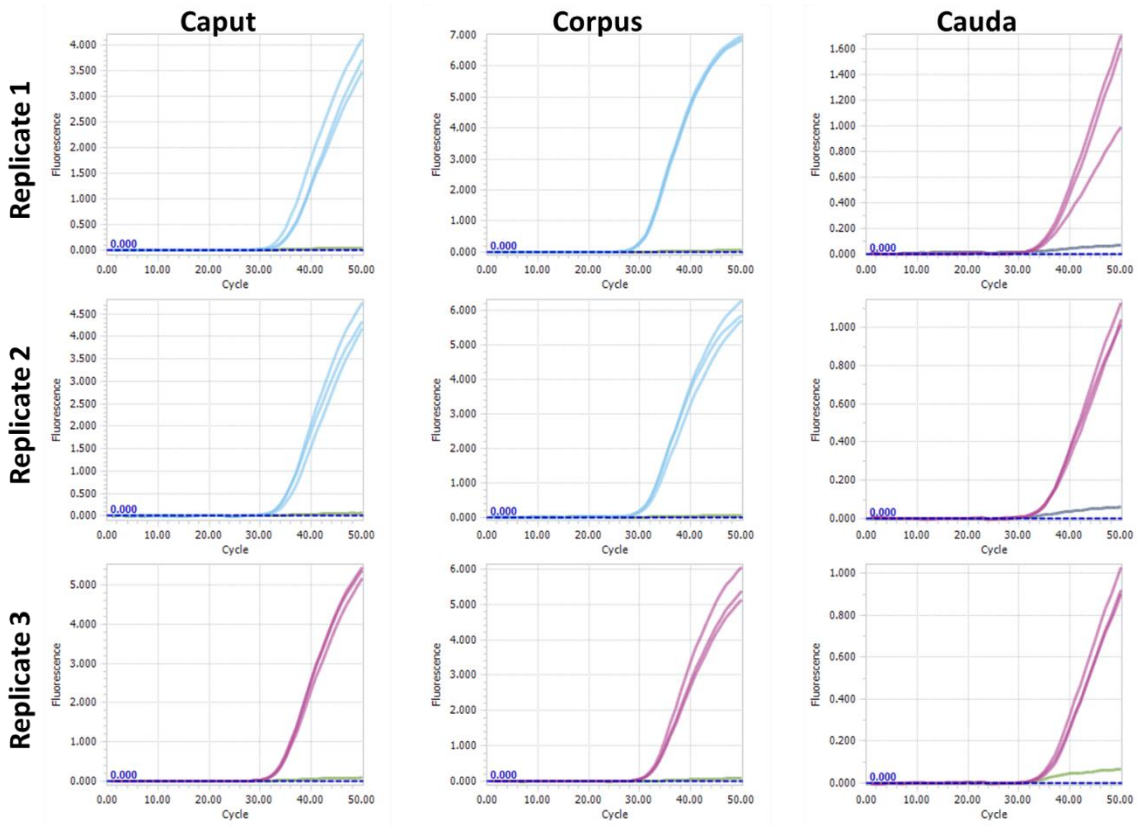

Appendix 30: Amplification curves of *Nov-miR*13 in cDNA and reverse transcription control samples generated from biological pools of epididymal spermatozoa.

Appendix 31: Amplification cycles of *Nov-miR*37 in cDNA and reverse transcription control samples generated from biological pools of epididymal spermatozoa.

Replicate	Segment	+RT			-RT
Rep 1	Caput	28.67	28.51	28.58	-
	Corpus	27.62	27.47	27.28	-
	Cauda	28.91	29.74	29.8	-
Rep 2	Caput	28.46	28.29	28.35	-
	Corpus	28.22	28.54	28.41	-
	Cauda	28.62	28.72	28.49	-
Rep 3	Caput	28.99	28.45	28.86	-
	Corpus	28.11	28.38	28.15	-
	Cauda	28.71	28.99	28.93	-

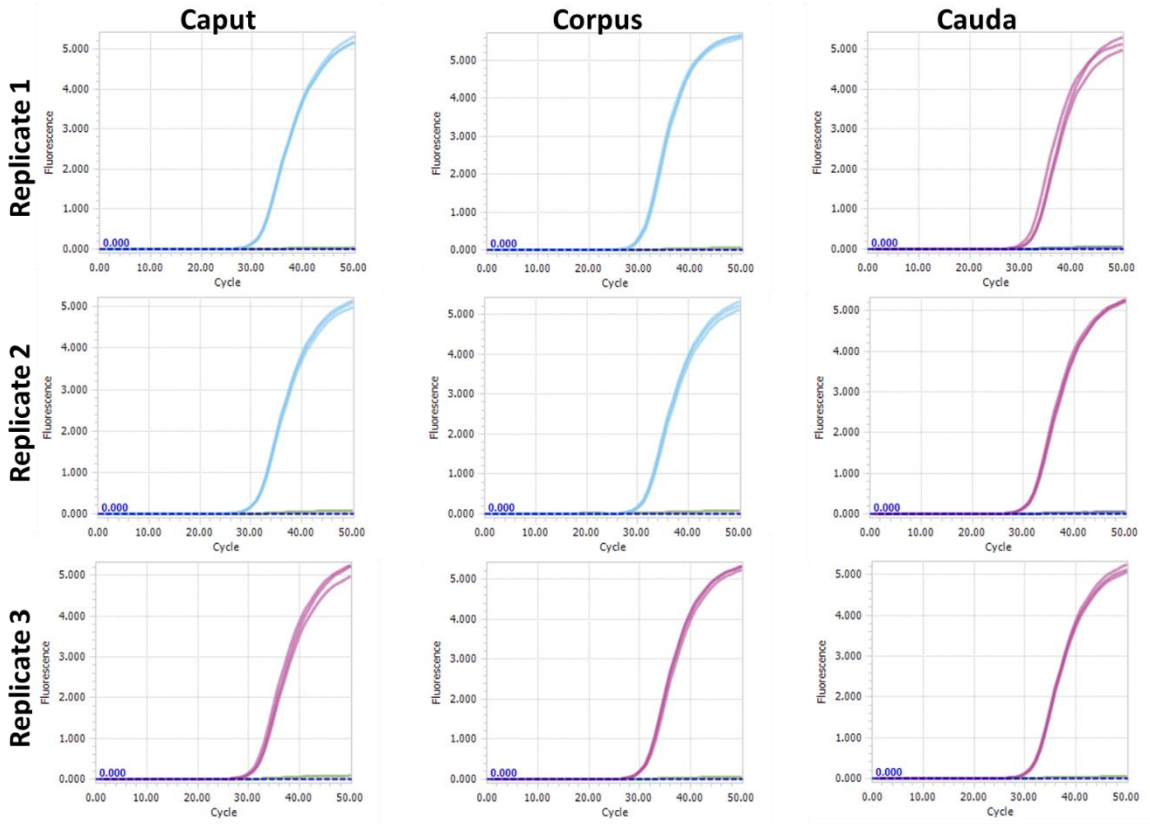

Appendix 32: Amplification curves of *Nov-miR*37 in cDNA and reverse transcription control samples generated from biological pools of epididymal spermatozoa.

Appendix 33: Amplification cycles of *Nov-miR*42 in cDNA and reverse transcription control samples generated from biological pools of epididymal spermatozoa.

Replicate	**Segment**	**+RT**			**-RT**
Rep 1	Caput	33.3	33.11	32.34	-
	Corpus	27	27.06	27.19	-
	Cauda	34.56	34.42	33.99	-
Rep 2	Caput	31.2	31.52	31.5	-
	Corpus	28.07	27.98	28.27	-
	Cauda	35.14	34.51	34.46	-
Rep 3	Caput	30.52	30.55	30.63	-
	Corpus	29.3	29.12	29.23	-
	Cauda	34.14	35.19	34.69	-

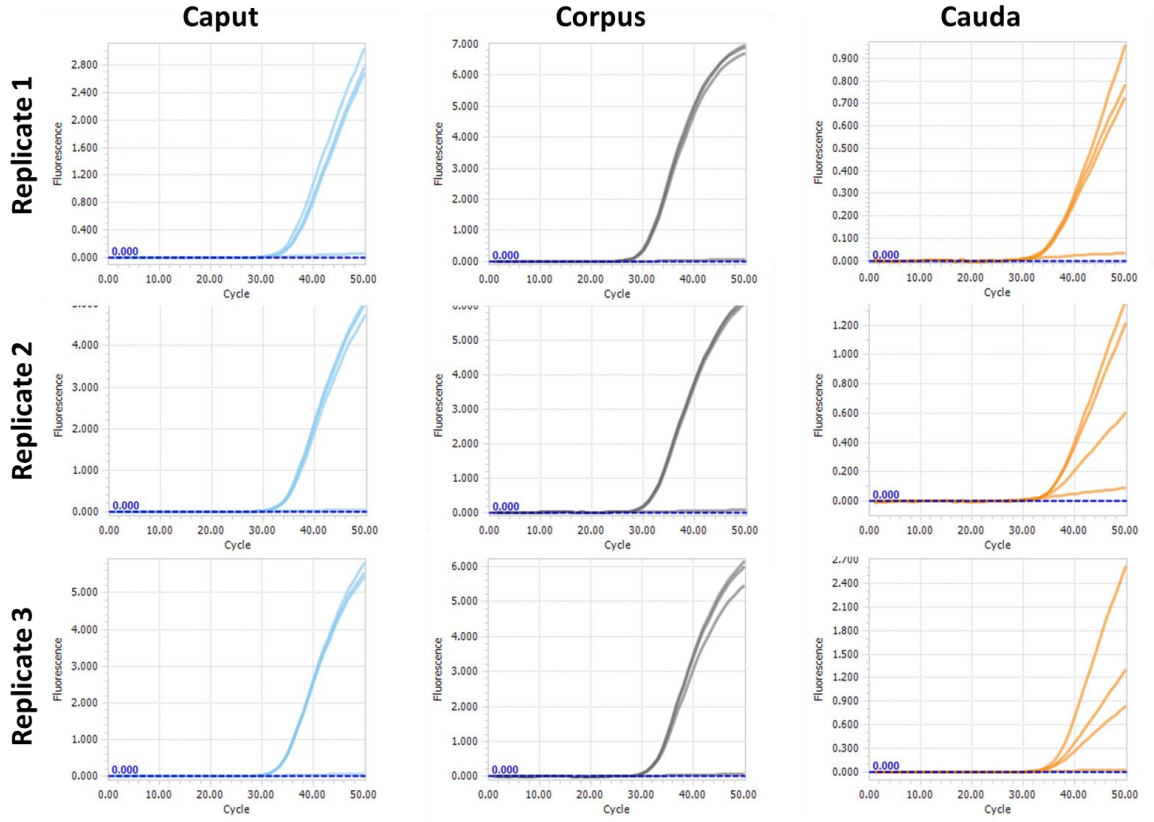

Appendix 34: Amplification cycles of *Nov-miR*42 in cDNA and reverse transcription control samples generated from biological pools of epididymal spermatozoa.

Appendix 35: Amplification cycles of *Nov-miR*101 in cDNA and reverse transcription control samples generated from biological pools of epididymal spermatozoa.

Replicate	Segment	+RT			-RT
Rep 1	Caput	50	50	34.37	-
	Corpus	32.53	32.75	33.07	-
	Cauda	33.43	35.69	34.23	-
Rep 2	Caput	35.8	33.74	36.19	-
	Corpus	33	34.09	33.04	-
	Cauda	34.33	35.63	36.6	-
Rep 3	Caput	33.3	32.59	33.35	-
	Corpus	31.79	32.66	32.54	-
	Cauda	32.07	32.44	32.72	-

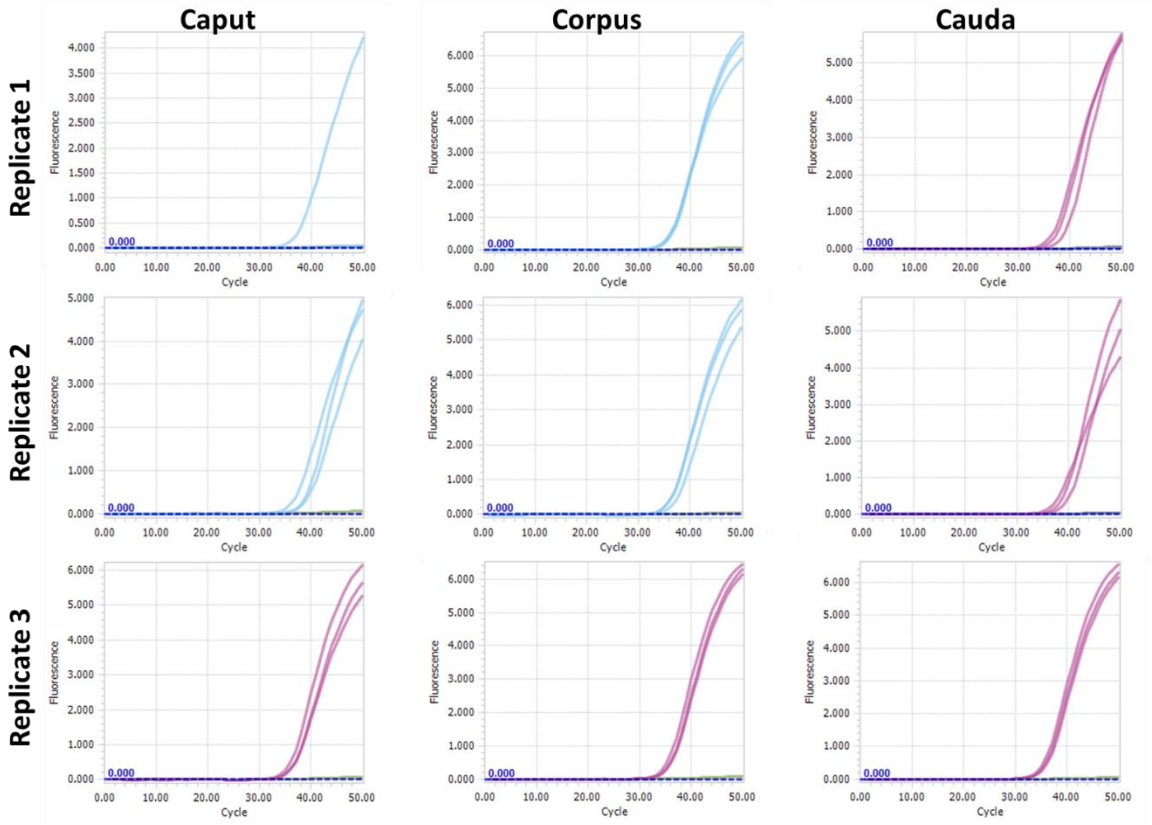

Appendix 36: Amplification curves of *Nov-miR*101 in cDNA and reverse transcription control samples generated from biological pools of epididymal spermatozoa.

Appendix 37: Amplification cycles of *Nov-miR*127 in cDNA and reverse transcription control samples generated from biological pools of epididymal spermatozoa.

Replicate	Segment	+RT			-RT
Rep 1	Caput	34.72	35.22	35.09	-
	Corpus	38.71	37.28	36.43	-
	Cauda	36.2	36.71	36.83	-
Rep 2	Caput	36.46	38.1	36.88	-
	Corpus	36.26	37.64	35.31	-
	Cauda	36.83	36.94	36.23	-
Rep 3	Caput	36.32	37.21	50	-
	Corpus	-	-	-	-
	Cauda	36.39	35.92	35.86	-

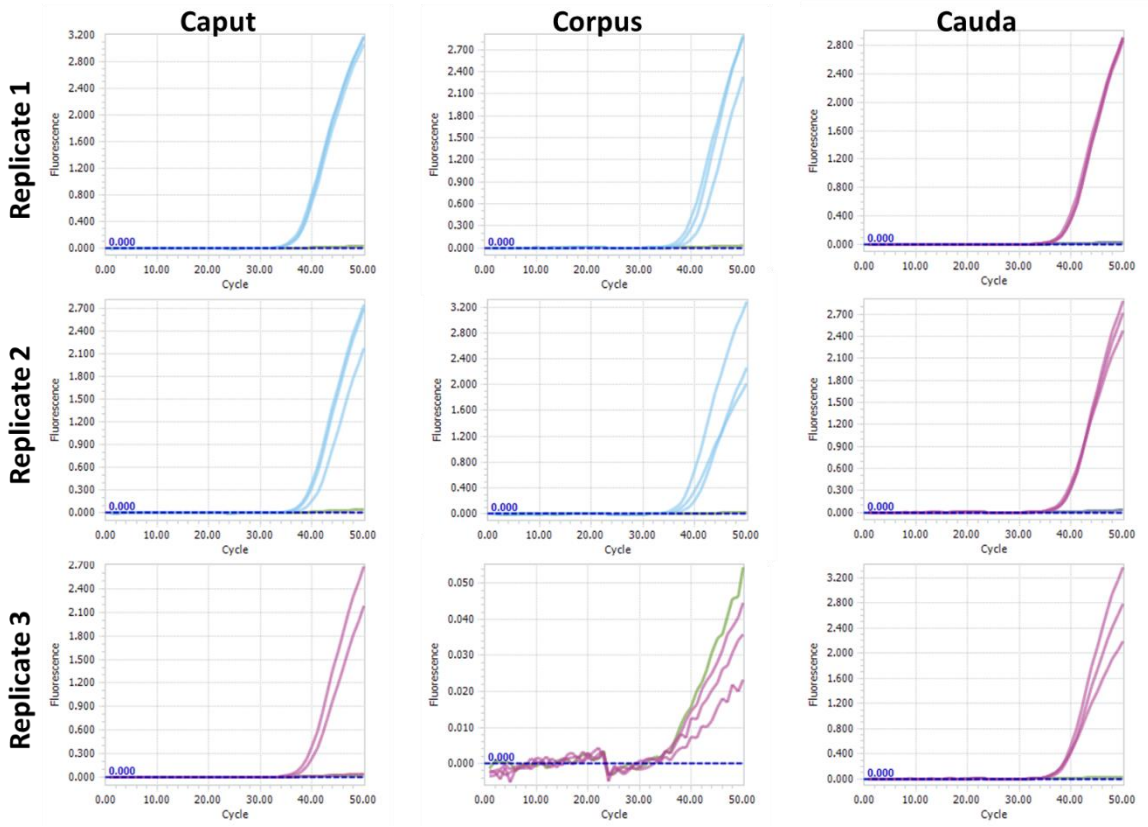

Appendix 38: Amplification curves of *Nov-miR*127 in cDNA and reverse transcription control samples generated from biological pools of epididymal spermatozoa.

Appendix 39: Amplification cycles of the U6 sRNA internal control in cDNA and reverse transcription control samples generated from biological pools of epididymal epithelial cells.

Replicate	Segment	+RT			-RT
Rep 1	Caput	28.08	23	22.88	-
	Corpus	23.28	22.04	23.34	37.39
	Cauda	19.93	17.73	17.4	40.72
Rep 2	Caput	22.85	22.62	22.98	37.62
	Corpus	21.76	22.81	22.07	38.6
	Cauda	24.96	23.6	23.58	-
Rep 3	Caput	22.76	22.25	22.25	-
	Corpus	23.24	22.46	21.51	39.44
	Cauda	23.79	24.37	23.83	35.31

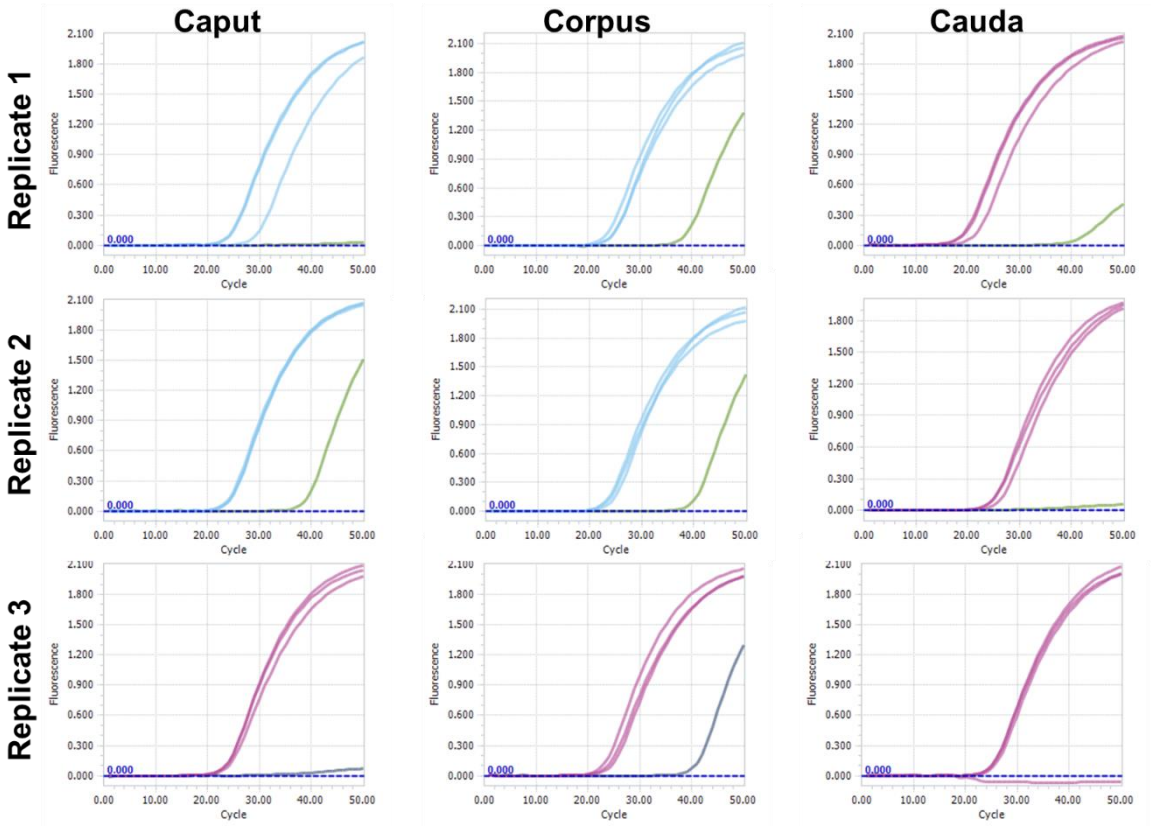

Appendix 40: Amplification curves of the U6 sRNA internal control in cDNA and reverse transcription control samples generated from biological pools of epididymal epithelial cells.

Appendix 41: Amplification cycles of *miR-29a in cDNA and reverse transcription control samples generated from biological pools of epididymal epithelial cells.**

Replicate	Segment	+RT			-RT
Rep 1	Caput	35.07	34.39	35.11	-
	Corpus	33.35	33.17	32.77	-
	Cauda	34.39	33.41	34.76	-
Rep 2	Caput	33.17	33.12	33.86	-
	Corpus	33.9	33.88	34.84	-
	Cauda	36.42	35.09	34.91	-
Rep 3	Caput	32.9	32.71	32.54	-
	Corpus	34.02	34.79	33.4	-
	Cauda	34.39	34.96	34.76	-

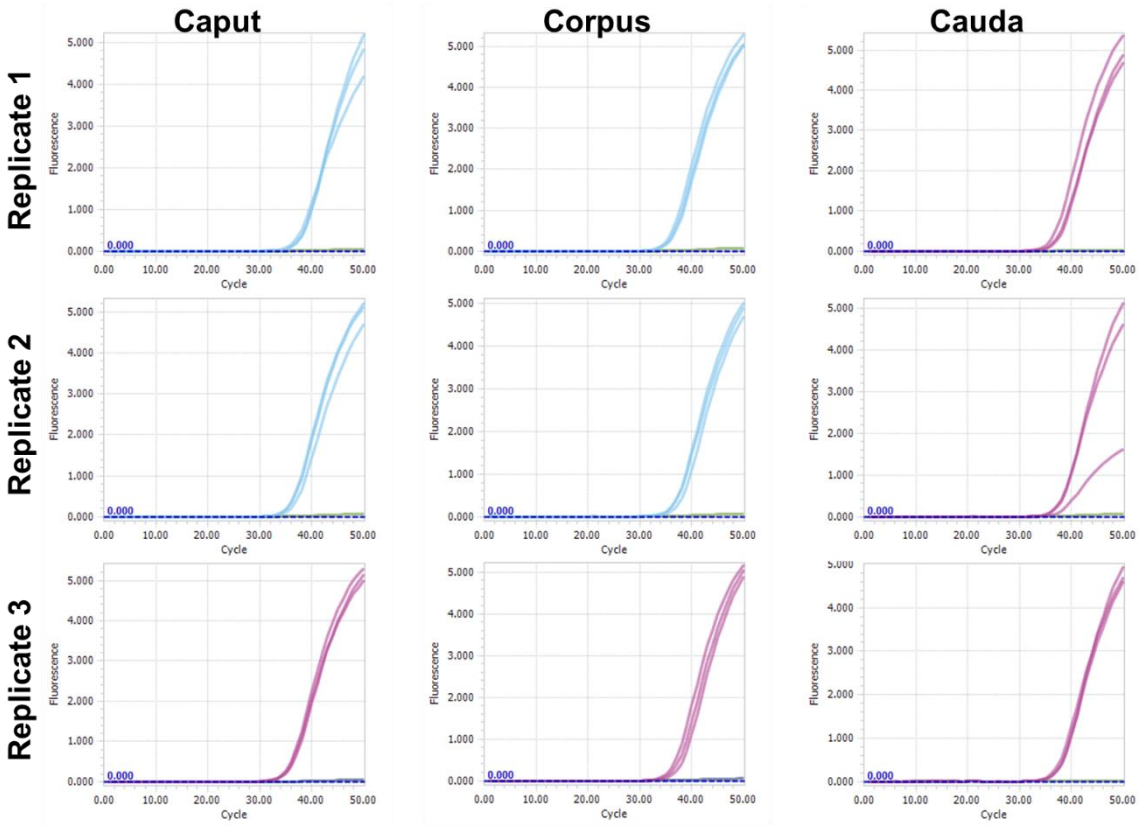

Appendix 42: Amplification curves of *miR-29a** **in cDNA and reverse transcription control samples generated from biological pools of epididymal epithelial cells.**

Appendix 43: Amplification cycles of *Nov-miR*13 in cDNA and reverse transcription control samples generated from biological pools of epididymal epithelial cells.

Replicate	**Segment**	**+RT**			**-RT**
Rep 1	Caput	32.85	32.15	32.03	-
	Corpus	31.32	31.46	31.11	-
	Cauda	31.38	31.42	31.42	-
Rep 2	Caput	29.43	29.58	30.13	-
	Corpus	29.57	29.2	29.19	-
	Cauda	29.39	29.37	29.69	-
Rep 3	Caput	35.8	37.68	50	-
	Corpus	37.06	37.13	36.21	-
	Cauda	38.25	37.35	37.7	-

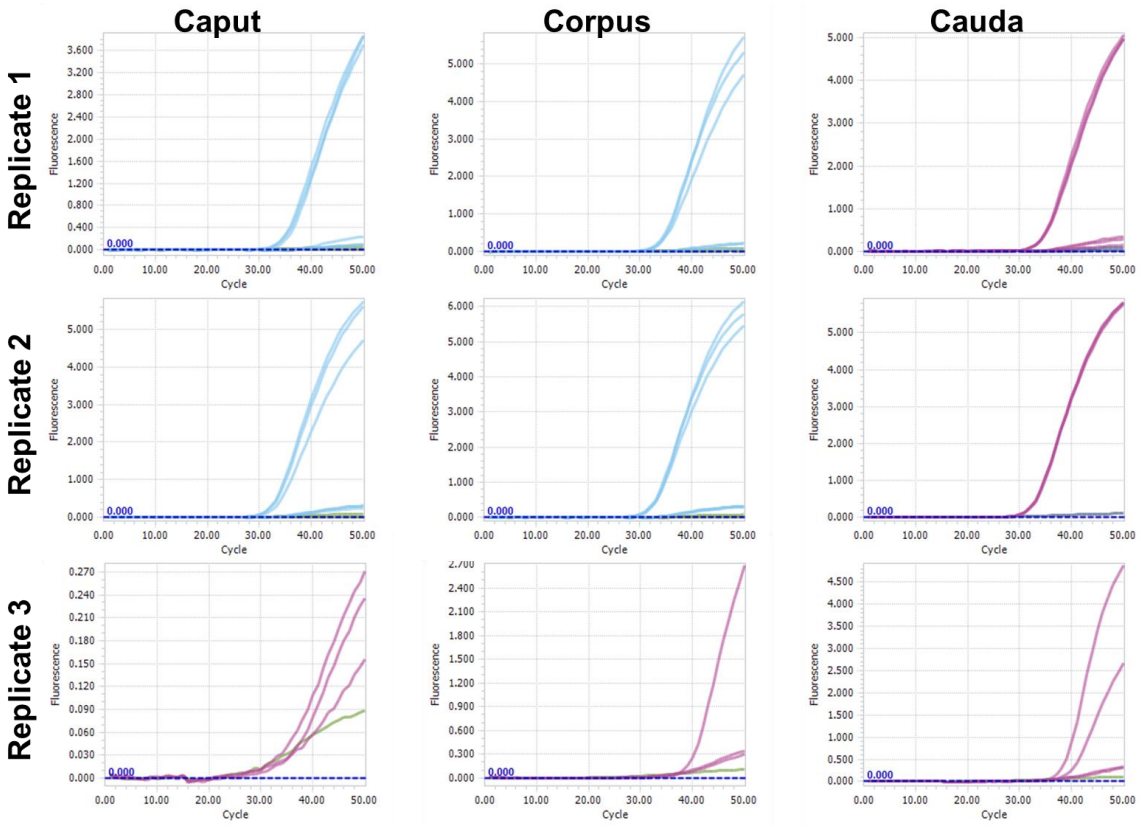

Appendix 44: Amplification curves of *Nov-miR*13 in cDNA and reverse transcription control samples generated from biological pools of epididymal epithelial cells.

Appendix 45: Amplification cycles of *Nov-miR*37 in cDNA and reverse transcription control samples generated from biological pools of epididymal epithelial cells.

Replicate	**Segment**	**+RT**			**-RT**
Rep 1	Caput	29.27	29.17	29.06	-
	Corpus	27.16	27.04	27.53	-
	Cauda	28.52	28.51	29.01	-
Rep 2	Caput	29.03	28.86	28.65	-
	Corpus	27.49	27.89	27.57	-
	Cauda	27.87	27.75	27.68	-
Rep 3	Caput	32.28	36.73	35.55	-
	Corpus	29	29.02	28.59	-
	Cauda	29.05	28.78	28.62	-

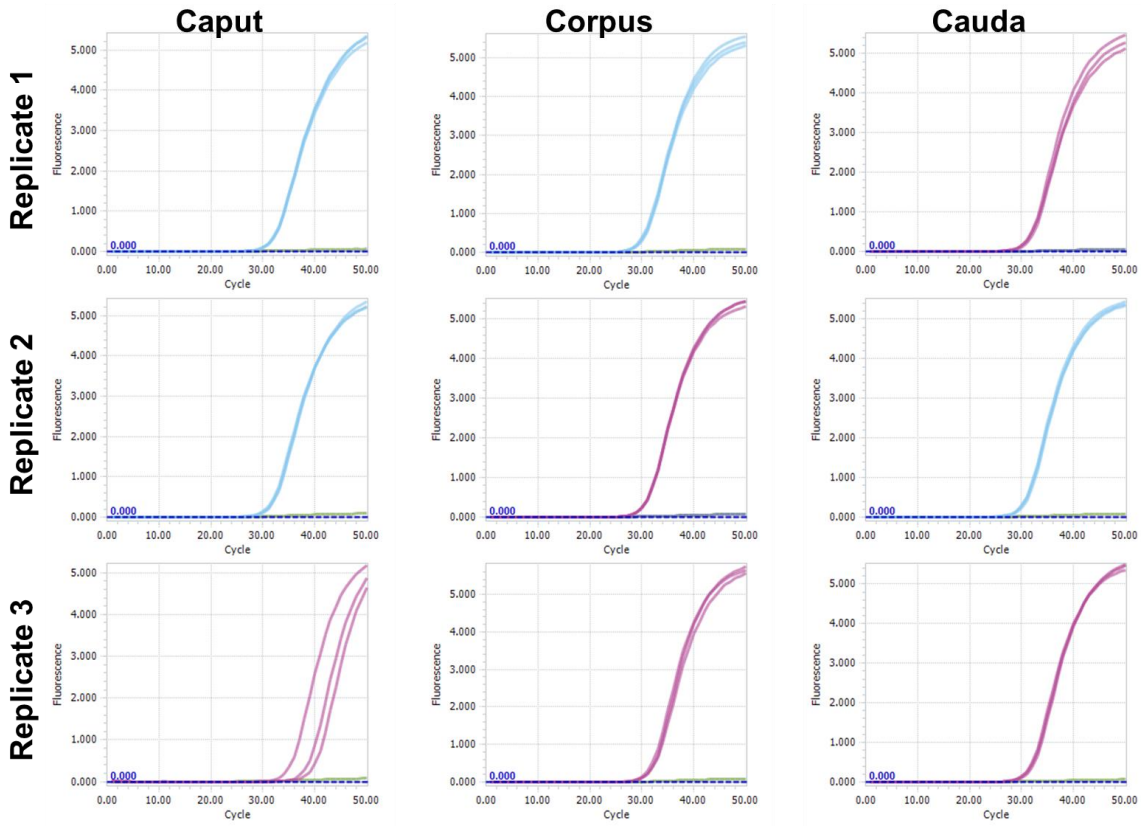

Appendix 46: Amplification curves of *Nov-miR*37 in cDNA and reverse transcription control samples generated from biological pools of epididymal epithelial cells.

Appendix 47: Amplification cycles of *Nov-miR*42 in cDNA and reverse transcription control samples generated from biological pools of epididymal epithelial cells.

Replicate	Segment	+RT			-RT
Rep 1	Caput	32.15	33.24	32.88	-
	Corpus	30.78	30.85	30.89	-
	Cauda	33.83	44.55	50	-
Rep 2	Caput	31.68	32.01	31.32	-
	Corpus	30.6	30.99	31.39	-
	Cauda	32.57	32.64	33.65	-
Rep 3	Caput	31.78	32.06	32.02	-
	Corpus	31.31	31.55	31	-
	Cauda	32.19	32.11	32.32	-

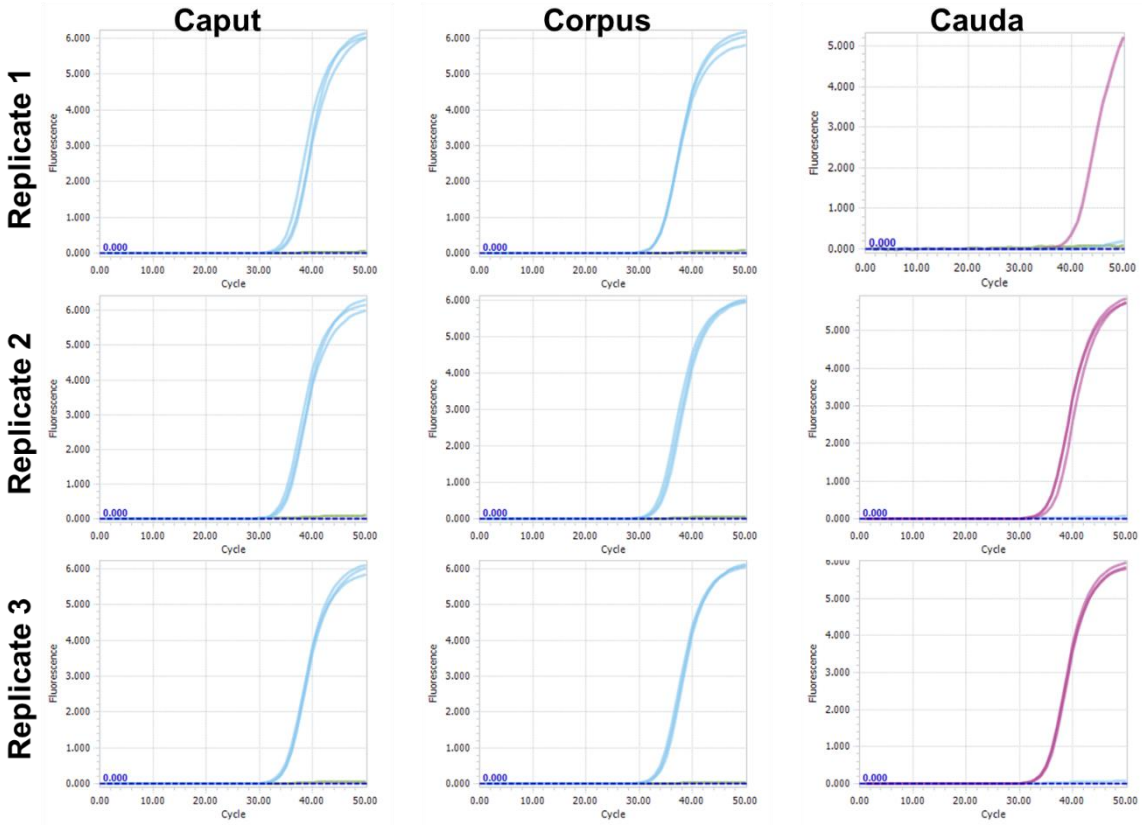

Appendix 48: Amplification curves of *Nov-miR*42 in cDNA and reverse transcription control samples generated from biological pools of epididymal epithelial cells.

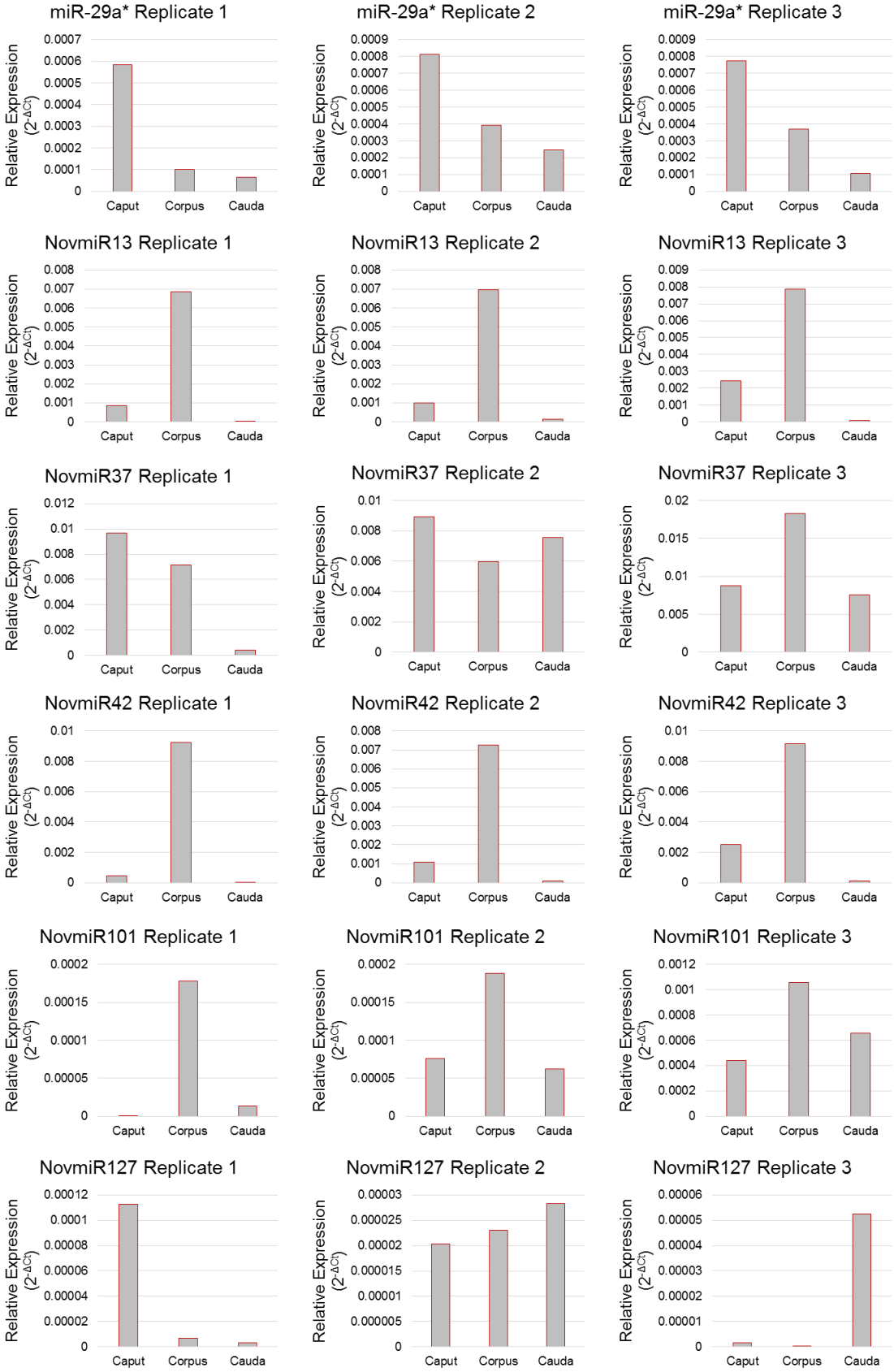

Appendix 49: TaqMan RT-qPCR validation of novel miRNAs in epididymal spermatozoa across each biological pool. Pooled biological samples differing to those employed in NGS analyses (n = 9-12

mice) were analysed in triplicate in order to verify the presence of novel miRNAs. All data were normalized against the U6 sRNA internal control.

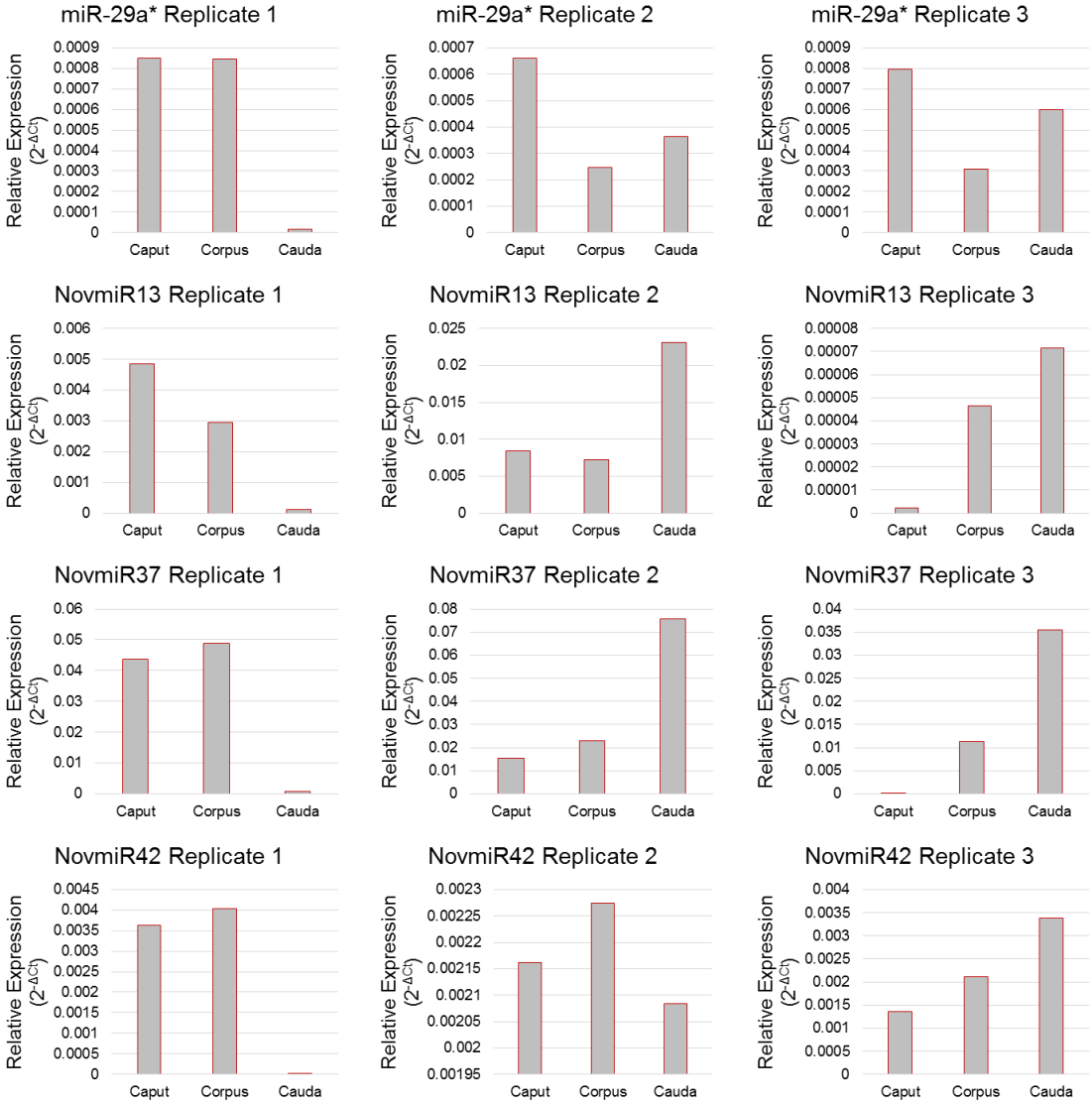

Appendix 50: TaqMan RT-qPCR validation of novel miRNAs in epididymal epithelial cells across each biological pool. Pooled biological samples differing to those employed in NGS analyses (n = 9-12 mice) were analysed in triplicate in order to verify the presence of novel miRNAs. All data were normalized against the U6 sRNA internal control.

PLOS | ONE

RESEARCH ARTICLE

Next Generation Sequencing Analysis Reveals Segmental Patterns of microRNA Expression in Mouse Epididymal Epithelial Cells

Brett Nixon[1]*, Simone J. Stanger[1], Bettina P. Mihalas[1], Jackson N. Reilly[1], Amanda L. Anderson[1], Matthew D. Dun[2], Sonika Tyagi[3], Janet E. Holt[2], Eileen A. McLaughlin[1]

1 Reproductive Science Group, School of Environmental and Life Sciences, Faculty of Science and IT, University of Newcastle, Callaghan, NSW, Australia, **2** School of Biomedical Sciences and Pharmacy, Faculty of Health and Medicine, University of Newcastle, Callaghan, NSW, Australia, **3** Australian Genome Research Facility Ltd, The Walter and Eliza Hall Institute, Parkville, VIC, Australia

* Brett.Nixon@newcastle.edu.au

Citation: Nixon B, Stanger SJ, Mihalas BP, Reilly JN, Anderson AL, Dun MD, et al. (2015) Next Generation Sequencing Analysis Reveals Segmental Patterns of microRNA Expression in Mouse Epididymal Epithelial Cells. PLoS ONE 10(8): e0135605. doi:10.1371/journal.pone.0135605

Editor: Suresh Yenugu, University of Hyderabad, INDIA

Received: May 7, 2015

Accepted: July 23, 2015

Published: August 13, 2015

Data Availability Statement: All relevant data are within the paper and its Supporting Information file. In addition, the data discussed in this publication have been deposited in NCBI's Gene Expression Omnibus and are accessible through GEO Series accession number GSE70197 (http://www.ncbi.nlm.nih.gov/geo/query/acc.cgi?acc=GSE70197).

Funding: This study was supported by a National Health and Medical Research Council of Australia (https://www.nhmrc.gov.au/) Project Grant (APP1062371) awarded to BN, EAM and JEH. The funders had no role in study design, data collection

Abstract

The functional maturation of mammalian spermatozoa is accomplished as the cells descend through the highly specialized microenvironment of the epididymis. This dynamic environment is, in turn, created by the combined secretory and absorptive activity of the surrounding epithelium and displays an extraordinary level of regionalization. Although the regulatory network responsible for spatial coordination of epididymal function remains unclear, recent evidence has highlighted a novel role for the RNA interference pathway. Indeed, as noncanonical regulators of gene expression, small noncoding RNAs have emerged as key elements of the circuitry involved in regulating epididymal function and hence sperm maturation. Herein we have employed next generation sequencing technology to profile the genome-wide miRNA signatures of mouse epididymal cells and characterize segmental patterns of expression. An impressive profile of some 370 miRNAs were detected in the mouse epididymis, with a subset of these specifically identified within the epithelial cells that line the tubule (218). A majority of the latter miRNAs (75%) were detected at equivalent levels along the entire length of the mouse epididymis. We did however identify a small cohort of miRNAs that displayed highly regionalized patterns of expression, including *miR-204-5p* and *miR-196b-5p*, which were down- and up-regulated by approximately 39- and 45-fold between the caput/caudal regions, respectively. In addition we identified 79 miRNAs (representing ~ 21% of all miRNAs) as displaying conserved expression within all regions of the mouse, rat and human epididymal tissue. These included 8/14 members of *let-7* family of miRNAs that have been widely implicated in the control of androgen signaling and the repression of cell proliferation and oncogenic pathways. Overall these data provide novel insights into the sophistication of the miRNA network that regulates the function of the male reproductive tract.

and analysis, decision to publish, or preparation of the manuscript.

Competing Interests: The authors have declared that no competing interests exist.

Introduction

Following their initial morphological differentiation, spermatozoa are released from the germinal epithelium of the testes in a functionally immature state, incapable of movement or any of the complex array of cellular interactions that are required for fertilization [1]. In all mammalian species studied to date, the acquisition of functional competence occurs progressively as the cells descend through the epididymis, a highly specialized region of the male reproductive tract linking the testis to the vas deferens. A hallmark of epididymal maturation is that the process is driven exclusively by extrinsic factors in the complete absence of nuclear gene transcription or *de novo* protein translation in the spermatozoa [2].

The first region of the epididymis that immature sperm encounter is that of the caput, wherein the cells are concentrated by a mechanism of resorption that rapidly removes almost all of the testicular fluid that enters the epididymis. As they leave this environment and enter the corpus epididymis, sperm begin to acquire the potential for both progressive motility and recognition of an ovum. These attributes continue to develop as the sperm move through the corpus, and reach an optimal level as they enter the cauda region where they are stored in quiescent state prior to ejaculation. Importantly, the epididymis is characterized by highly regionalized profiles of both gene and protein expression [3], that ultimately give rise to a dynamic intraluminal environment responsible for [4] promoting sperm maturation. While androgens and additional lumicrine factors synthesized in the testis have been implicated in coordinating the gene/protein expression along the length of the epididymis, the balance of evidence indicates that they alone cannot account for the complexity of the distinct intrasegmental microenvironments. Instead, elegant pioneering studies by the laboratories of Zhang [5–10] and Sullivan [11–13] have provided evidence that an additional tier of regulation involving specialized RNA molecules, termed microRNAs (miRNAs), may be active in the epididymal environment.

miRNAs are small single-stranded non-coding RNA molecules (~21–25 nucleotides) that form an integral part of a recently discovered RNA interference pathway. miRNAs are initially synthesized as primary transcripts (pri-miRNA) before being sequentially processed in the nucleus by the RNase DROSHA, and within the cytoplasm by the endoribonuclease DICER. This leads to the formation of a double-stranded mature miRNA, one strand of which is preferentially loaded into an effector miRNA-induced silencing complex (miRISC). In addition to the loaded miRNA, the miRISC complex comprises catalytic Argonaute (AGO) proteins that mediate the post-transcriptional regulation of target mRNAs. The fate of the targeted mRNA varies from increased degradation and hence translational repression, through to increased translation and protein synthesis, depending on both the complementarity of the miRNA—mRNA duplex and on the catalytic activity of the AGO proteins within the miRISC complex [14,15]. Recent advances in miRNA expression profiling have fuelled rapid growth in our appreciation of the tremendous number, diversity and importance of this mechanism of post-transcriptional gene regulation in development, disease and fertility [16].

Evidence secured by a number of independent groups indicates that miRNAs play an essential role in regulating the differentiation of spermatozoa in the testes, with inactivation of key genes such as *Dicer1* leading to a severe impact on the formation of mature germ cells [17–22]. However, an emerging body of evidence indicates that this role may also extend to the post-transcriptional regulation of gene expression within the epididymis. Indeed, complex profiles of several hundred miRNAs have been documented in the epididymis of species such as the human, rat, and bovine and several of these are significantly enriched and or unique to this tissue [8,12,23]. Furthermore, comparative profiling of epididymal miRNAs has revealed distinct temporal and spatial patterns of expression [9,12]. The notion that miRNAs may be critical in

establishing the unique epididymal environment and thus play a prominent role in promoting sperm maturation, is further supported by elegant global and targeted miRNA manipulation strategies. In the former studies, conditional knock-out of *Dicer1* in the proximal epididymis has been shown to elicit a rapid dedifferentiation of the epithelium, perturbation of steriod signaling, altered lipid homestatis, and a concomitant loss of fertility [24,25]. Similarly, defects in sperm fertility have also been documented following pertubation of gene expression via the injection of a single miRNA analog (agomir) directly into the epididymis of adult rats [10]. Notwithstanding these data, global patterns of differential miRNA expression have not been explored in the mouse epididymis. Therefore, the aim of the present investigation was to conduct a systematic analysis of the expression profile of miRNAs and key elements of their processing machinery within the adult mouse epididymis and in so doing provide novel insights into miRNA control of sperm fertilizing potential in this species.

Materials and Methods

Reagents

Unless specified, chemical reagents were obtained from Sigma (St. Louis, Mo, USA) or Life Technologies (Carlsbad, CA, USA) and were of research grade. The following primary antibodies were purchased to characterize proteins of interest: rabbit polyclonal anti-DICER1 antibody (Cat # ab13502; Abcam, Cambridge, United Kingdom), rabbit polyclonal anti-androgen receptor (Cat # SAB4501575, Sigma), rat monoclonal α-AGO2 (Cat # SAB4200085, Sigma), goat polyclonal anti-IZUMO1 (Cat # sc-79543, Santa Cruz Biotechnology, CA, USA), and rabbit polyclonal anti-cytokeratin 8 (Cat # ab59400, Abcam). Alexa Fluor 488-conjugated goat anti-rabbit (A11008), 594-conjugated goat anti-rat (A11007) and 594-conjugated goat anti-rabbit (A11012) antibodies were purchased from Life Technologies.

Ethics Statement

All experimental procedures were carried out with the approval of the University of Newcastle's Animal Care and Ethics Committee (ACEC) (approval number A-2013-322), in accordance with relevant national and international guidelines. Inbred Swiss mice were obtained from a breeding colony held at the institutes' Central Animal House and maintained according to the recommendations prescribed by the ACEC. Mice were housed under a controlled lighting regime (16L: 8D) at 21–22°C and supplied with food and water *ad libitum*. Prior to dissection, animals were euthanized via CO_2 inhalation.

Epididymal Epithelial Cell Isolation and Characterization

Immediately after adult male mice (8 weeks old) were euthanized, their vasculature was perfused with pre-warmed PBS to minimize the possibility of blood contamination. The epididymides were then removed, separated from fat and overlying connective tissue and carefully dissected into three anatomical regions corresponding to the caput, corpus and cauda. This material was then pooled and either subjected directly to RNA extraction and miRNA next-generation sequencing as described below to document the 'whole epididymal tissue' miRNA signature (three mice / replicate), or alternatively it was prepared for isolation of epididymal epithelial cells (nine—twelve mice / replicate). For the latter study, the bulk of the caudal spermatozoa were flushed from the lumen via retrograde perfusion with water-saturated paraffin oil. This was immediately followed by perfusion with modified Biggers, Whitten, and Whittingham media (BWW; [26]) composed of 91.5 mM NaCl, 4.6 mM KCl, 1.7 mM $CaCl_2 \bullet 2H_2O$, 1.2 mM KH_2PO_4, 1.2 mM $MgSO_4 \bullet 7H_2O$, 25 mM $NaHCO_3$, 5.6 mM D-glucose, 0.27 mM

sodium pyruvate, 44 mM sodium lactate, 5 U/ml penicillin, 5 μg/ml streptomycin, 20 mM Hepes buffer, and 3 mg/ml BSA, to remove any residual spermatozoa. Caput and corpus spermatozoa were removed by placing the tissue in a 500 μl droplet of BWW and making multiple incisions with a razor blade. Using a method adapted from Zuo *et al.* [27], the tissue was then washed free of spermatozoa by subjecting it to agitation, prior to being minced with forceps washed a further three times in sterile PBS and digested in 100 μg/ml trypsin (Promega, Madison, WI, USA) at 37°C for 30 minutes with vigorous shaking. Tissue clumps were collected by centrifugation (800 × g for 5 minutes) and digested in 1 mg/ml collagenase for 30 minutes with shaking at 37°C. The cells were subjected to a further centrifugation at 800 × g for 5 minutes and the supernatant was discarded. The cell pellet was then resuspended in Dulbecco's Modified Eagle Medium (DMEM) culture medium containing sodium pyruvate (1 mM), 10% FBS (v/v), penicillin (100 IU/ml), and streptomycin (100 μg/ml), before being filtered through a 70 μm cell strainer and incubated in 6-well plates at 32°C. After 4 hours of incubation, all non-epithelial cells (fibroblasts and muscle cells) were found attached to the base of the plate while the epithelial cells remained in suspension. These populations of isolated epithelial cells were washed in PBS and either fixed in 4% paraformaldehyde for immunocytochemical analysis or frozen at -80°C for downstream RNA isolation.

Enrichment of epididymal epithelial cells (>95%) was assessed by immunocytochemistry. For this purpose, isolated epithelial cells were fixed in paraformaldehyde (ProSciTech, Kirwan, QLD, Australia) and settled onto poly-l-lysine coated coverslips overnight at 4°C. All subsequent incubations were performed at 37°C in a humidified chamber, and all antibody dilutions and washes were conducted in PBS containing 0.1% Tween-20 (PBST). Fixed cells were permeabilized in 0.2% Triton X-100 / PBS for 10 minutes and blocked in 3% (w/v) bovine serum albumin (BSA) in PBST for 1 h. Slides were then sequentially probed with anti-androgen receptor and Alexa Fluor 594-conjugated secondary antibodies. After washing, the slides were dual labeled with FITC-conjugated peanut agglutinin (PNA, 5 μg/ml), a marker of the outer acrosomal membrane, and counterstained with 4',6-diamidino-2-phenylindole (DAPI) before being mounted with antifade medium (Mowiol 4–88). Labeled cells were viewed on an Axio Imager A1 microscope (Carl Zeiss MicroImaging, Inc., Thornwood, NY) equipped with epifluorescent optics and images captured with an Olympus DP70 microscope camera (Olympus America, Center Valley, PA). Upon confirmation of target cell enrichment, populations of isolated epididymal cells were then subjected to RNA extraction as described below.

Immunofluorescent Localization

In addition to isolated epithelial cells, whole mouse epididymal tissue was also paraformaldehyde fixed, embedded in paraffin and sectioned. Embedded tissue was dewaxed, rehydrated and subjected to antigen retrieval by boiling in 50 mM Tris-HCl (pH10) for 10 minutes. The tissue was then assessed for key components of the RNAi silencing machinery under similar conditions to those described for isolated cells. Briefly, tissue sections from three individual mice were labeled with anti-DICER and anti-AGO2 antibodies (diluted 1:150 in 1% BSA/PBS) overnight at 4°C. After incubation, the slides were washed three times, then sequentially incubated in goat anti-rabbit 488 Alexa Fluor and goat anti-rat 594 Alexa Flour (diluted 1:400 in 1% BSA/PBS) secondary antibodies for 1 h at 37°C. Sections were then washed and counterstained in DAPI before mounting in antifade reagent. Similarly, epididymal sections were labeled with anti-androgen receptor primary antibody (1:50) overnight at 4°C, followed by goat anti-rabbit 594 Alexa Fluor (1:400). Negative controls included slides in which the primary antibody / lectin was substituted with PBS. All sections were visualized as described for cells and, as anticipated, the negative controls showed no labeling.

RNA Extraction and miRNA Next-Generation Sequencing

Total RNA was extracted from whole epididymal tissue and purified epididymal epithelial cells (caput, corpus and cauda) using a Direct-zol RNA MiniPrep Kit (Zymo Research Corporation, Irvine, CA, USA) according to manufacturer's instructions before being incubated with 1% DNase (Promega) to eliminate genomic DNA contamination. Total RNA from each epididymal region was pooled from a minimum of three (whole tissue)—nine (isolated epithelial cells) animals to generate a single biological replicate. Two such replicates were subjected to Illumina TruSeq small RNA sample preparation protocol as per the manufacturers' instructions (Illumina Inc. San Diego, CA, USA) at the Australian Genome Research Facility (AGRF, Brisbane, QLD, Australia). The libraries so generated were analyzed in triplicate sequenced using an Illumina Hiseq-2000 RNA-seq platform as 50 bp single end chemistry at AGRF. Briefly, the sequence reads from all samples were analyzed for quality control, screened for the presence of any contaminants and trimmed based on their matches to: PhiX, Adaptors, ChrM or Mouse rRNA. Cleaned sequence reads were then aligned against two different databases: (i) Mus Musculus genome (Build version mm10), and (ii) microRNA database (miRBASE release21 at http://www.mirbase.org/). Alignment against the mature miRNA sequences for mouse miRNAs were summarized and counts were recorded for known miRNAs.

RNA quality was assessed at multiple points during our analysis. Firstly, the integrity of total RNA was evaluated immediately after isolation by resolution of an aliquot of the sample on a denaturing agarose gel and assessment of 28S and 18S rRNA bands. Additional quality control was conducted independently at the AGRF whereby after arrival, each sample was analyzed on an Agilent 2100 Bioanalyzer as per the manufacturers' instructions (Agilent Technologies, USA). Finally the samples were again analyzed after siRNA library construction to confirm the size of the products. Only samples that passed each quality control step were processed for next generation sequencing.

Differential miRNA expression analysis was undertaken using R script based on, limma and voom libraries (http://www.bioconductor.org/packages/release/bioc/vignettes/limma/inst/doc/usersguide.pdf). A count value of >10 was used as the cutoff for presence/absence and expression profiling comparisons were performed for mature miRNAs between the individual epididymal regions with a data filter set to $\geq$ 2 fold difference and false discovery rate (FDR) of 0.05. The data discussed in this publication have been deposited in NCBI's Gene Expression Omnibus [28] and are accessible through GEO Series accession number GSE70197 (http://www.ncbi.nlm.nih.gov/geo/query/acc.cgi?acc=GSE70197).

Real Time PCR Confirmation of Selected miRNAs

Validation of miRNA expression profiles was conducted using a quantitative real-time PCR (qRT-PCR) strategy with Taqman miRNA assay reagents according to the manufacturer's instructions (Life Technologies). The miRNAs selected for analysis were *let-7b-5p* (assay ID. 002619), *let-7c-5p* (assay ID. 000379), *miR-9-5p* (assay ID. 000583), *miR200c-3p* (assay ID. 002300), *miR-375-3p* (assay ID. 000564), *miR410-3p* (assay ID. 001274), *miR-470* (assay ID. 002588), *miR-467d-3p* (assay ID. 001826), and *miR486-5p* (assay ID. 001278). Real-time PCR was performed using a Light Cycler 96 SW 1.1 (Roche, Castle Hill, Australia). The U6 small nuclear RNA (snRNA) (assay ID. 001973) was employed as an endogenous control to normalize the expression levels of target genes, and relative expression levels were calculated using the $2^{-\Delta Ct}$ method [29]. All qRT-PCR assays were performed in triplicate using pooled biological samples (three mice / sample) differing from those employed for next generation sequence analyses.

In Silico Analysis of miRNAs and Target Prediction

The expression of miRNA displaying statistically significant patterns of expression was clustered (Cluster3, Stanford University, Palo Alto, CA, USA) and examined using heatmaps (Java Treeview, Stanford University) to visualize trends and consistency in miRNA expression in caput, corpus and caudal epididymal epithelial cells. To gain a better understanding of the function of the up and down-regulated miRNAs their mRNA targets were analyzed with Ingenuity Pathway Analysis (IPA) software (version 8.8, Ingenuity Systems, Redwood City, CA, USA) using the Core Analysis. Similarly we also interrogated IPA in order to identify the key effected pathways likely to be regulated by epithelial cell miRNAs using the microRNA filter and restricting our analysis to experimentally confirmed targets.

mECap transfection with miRNA Mimics

To confirm the functional significance of epididymal miRNAs, an immortalized mouse caput epididymal epithelial cell line (mECap) [30] was employed. This cell line was cultured in Dulbecco's modified Eagle's medium (DMEM; Life Technologies) supplemented with 0.45% glucose (w/v), 1% L-glutamine, 1% sodium pyruvate, 10% fetal bovine serum and 50 nM dihydrotestosterone (DHT). miRNA mimics of *miR-200c-3p*, *miR-486-5p* and a scrambled negative control (*mir*Vana) were transfected separately at a concentration 5 nM using lipofectamine 2000 along with a cherry red internal control (0.5 μg) in Opti-MEM (Life Technologies) as per manufacturer's instructions. At 24 h post-transfection, cells were harvested and the transfection efficiency was calculated. The relative mRNA levels of predicted miRNA targets (*Mapk14* and *Foxo1*) were then analysed by qRT-PCR. These experiments were performed in triplicate.

SDS-PAGE and Western Blotting

Proteins were extracted from epididymal tissue, isolated epididymal epithelial cells, and spermatozoa in a modified SDS-PAGE sample buffer (2% w/v SDS, 10% w/v sucrose in 0.1875 M Tris, pH 6.8) with protease inhibitor tablets by incubation at 100°C for 5 min. Insoluble matter was removed by centrifugation at 20000 × g for 10 min and protein estimations were performed using the DC Protein Assay kit (Bio-Rad, Hercules, CA). Proteins were boiled in SDS-PAGE sample buffer (2% v/v mercaptoethanol, 2% w/v SDS, and 10% w/v sucrose in 0.1875 M Tris, pH 6.8, with bromophenol blue) and resolved by SDS-PAGE on polyacrylamide gels followed by transfer onto nitrocellulose membranes. Membranes were blocked with 3% w/v BSA in Tris-buffered saline (TBS; pH 7.4) for 1 h before being probed with 1:1000 dilutions of primary antibody in TBS containing 1% w/v BSA and 0.1% v/v polyoxyethylenesorbitan monolaurate (Tween-20; TBS-T) for 2 h at room temperature. Blots were washed three times in TBS-T followed by incubation with 1:1000 horseradish peroxidase-conjugated secondary antibody in 1% w/v BSA/TBS-T for 1 h. Following three washes in TBS-T, proteins were detected using an enhanced chemiluminescence kit (GE Healthcare, Buckinghamshire, UK) and visualized on ImageQuant LAS 4000 (Fujifilm, Tempe, AZ, USA). All immunoblotting analyses were performed in triplicate and representative blots are presented.

Statistical Analysis

Statistical significance was determined using analysis of variance (ANOVA), Tukey-Kramer HSD and T-tests employing JMP software (version 9.0.0). $P < 0.05$ was considered significant. Experiments were performed in triplicate unless otherwise stated. All data are expressed as mean ± SEM.

Results

miRNA Processing Machinery Is Expressed throughout the Mouse Epididymis

To begin our analysis of the role of the RNA interference pathway in the regulation of mouse epididymal function we initially focused on determining the expression profile of two of the key elements involved in the generation of mature miRNAs, namely the endoribonuclease DICER1 and the catalytic component of the RNA-induced silencing complex (RISC), Argonaute 2 (AGO2). As shown in Fig 1, both proteins were clearly detected in the epithelium of all epididymal regions examined, suggesting the presence of an active RNA interference pathway throughout the tubule. Indeed, both DICER1 and AGO2 displayed strong co-localization within the peri-nuclear domain of the epididymal epithelium. An additional pool of labeling, albeit of lower intensity, was also detected throughout the cytoplasm of these cells. In addition, both DICER1 and AGO2 appeared to strongly label spermatozoa within the epididymal lumen.

The Mouse Epididymis Is Replete with miRNAs

Next generation sequence analysis was performed on whole mouse epididymal tissue to obtain an overview of segmentally regulated miRNA expression patterns within this tissue. This analysis revealed a profile of miRNAs of similar overall complexity to that described in other species [9,11,12] (S1 Table). In total, 370 unique miRNAs were identified, the greatest number of which were detected within the cauda epididymal tissue, followed by the caput and finally the corpus (Fig 2A). A majority of these miRNA species (75%) were conserved in all epididymal regions and displayed relative levels of expression that were indistinguishable along the entire length of the epididymis. Indeed, only 15% of miRNAs were uniquely expressed in any one epididymal region (Fig 2A), and less than 10% were characterized by significant variations in their relative expression levels (fold change of $\pm \geq 2$, FDR < 0.05) between the caput/corpus and corpus/cauda (Fig 2B).

The presence of so few intrasegmental changes in the miRNA profile detected in this, and previous analyses [12], stands in contrast to the pronounced spatial differences that have been documented in transcriptomic analyses of the epididymal tissue [3,31,32]. To investigate whether such differences reflect the potentially confounding influence of spermatozoa and/or fluid that convey miRNAs of testicular origin into the epididymal lumen, we refined our analysis to focus on miRNA signatures present exclusively in the epididymal epithelium. For this purpose, next generation sequencing was performed on highly enriched (>95%) populations of epididymal epithelial cells that were isolated as described in the Materials and Methods and initially validated through the use of light microscopy (Fig 3A) and immunocytochemistry with an anti-androgen receptor antibody (Fig 3B and 3C). As noted in Fig 3C, we did not detect any cells other than those expressing androgen receptor within this preparation. Indeed, the absence of sperm contamination was confirmed through counterstaining the slides with fluorescently conjugated PNA (marker of the sperm acrosome) (Fig 3C), and by immunoblotting of cell lysates with antibodies against the androgen receptor, cytokeratin 8, and IZUMO1 (an intrinsic sperm protein) (Fig 3D). As anticipated, no PNA labeling was observed within the epithelial cell preparations and similarly, no IZUMO1 protein could be detected in the epithelial cell lysates. In contrast, the epithelial cell lysates demonstrated strong labeling for both androgen receptor and cytokeratin 8.

Next generation sequencing of the isolated epithelial cell preparations led to the identification of a restricted subset of miRNAs (218), the majority of which (90%, 195) were also

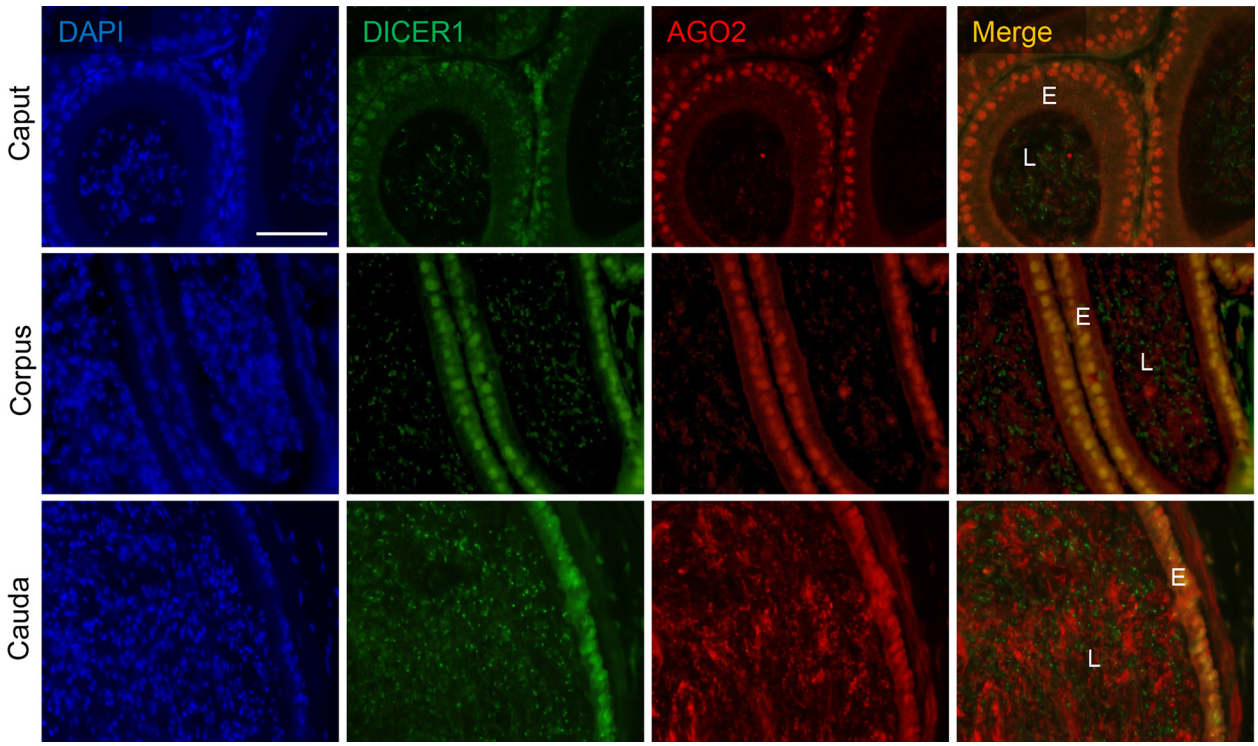

Fig 1. Assessment of key elements of the RNAi processing machinery in the mouse epididymis. Adult mouse epididymal sections were dual-labeled with anti-DICER1 and anti-AGO2 antibodies followed by either appropriate anti-rabbit 488 Alexa Fluor (green) or goat anti-rat 594 Alexa Flour-conjugated (red) secondary antibodies, respectively. The tissue sections were then counterstained with 4',6-diamidino-2-phenylindole (DAPI) and viewed using confocal microscopy. For clarity, DAPI labeling has been omitted from the merged images. E = epididymal epithelium, L = epididymal lumen. Scale bar = 20 μm. These experiments were replicated three times using independent samples from three mice and representative images are shown.

doi:10.1371/journal.pone.0135605.g001

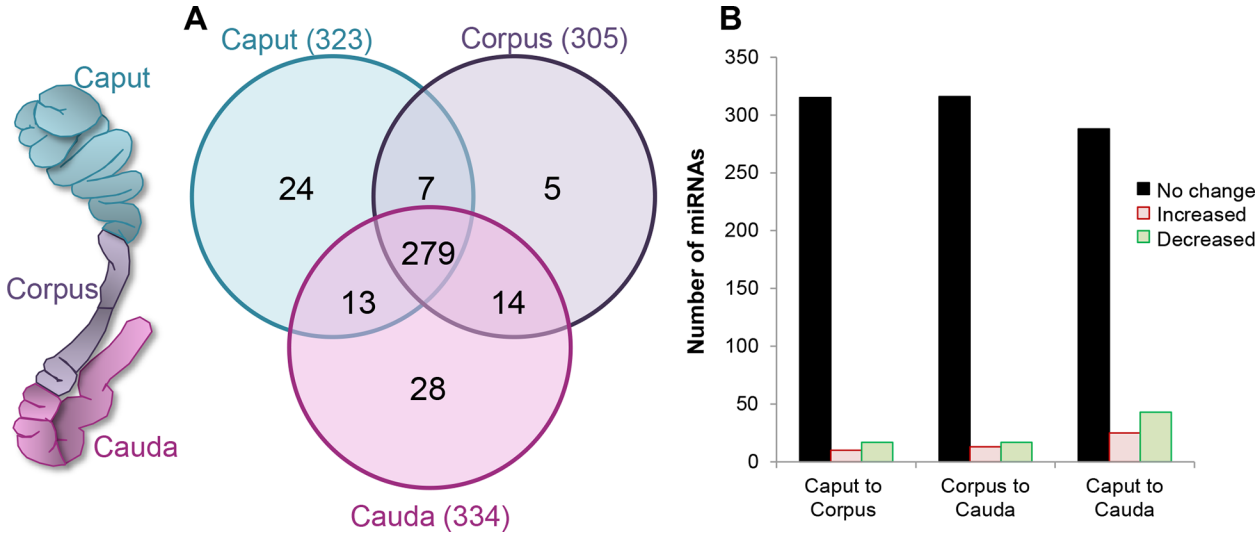

Fig 2. Determination of the miRNA signature present in whole mouse epididymal tissue. (A) Venn diagram depicting the number of miRNAs that were identified by next generation sequencing and their disruption within the caput, corpus and cauda regions of the adult mouse epididymis. (B) Graphical representation of miRNA distribution highlighting the number of significantly up- and down-regulated (threshold = ± ≥ 2 fold change and false discovery rate of < 0.05) miRNAs positively identified between each epididymal region. For the purpose of these analyses, an average count value of >10 across two biological replicates was used as the threshold for positive identification of each miRNA.

doi:10.1371/journal.pone.0135605.g002

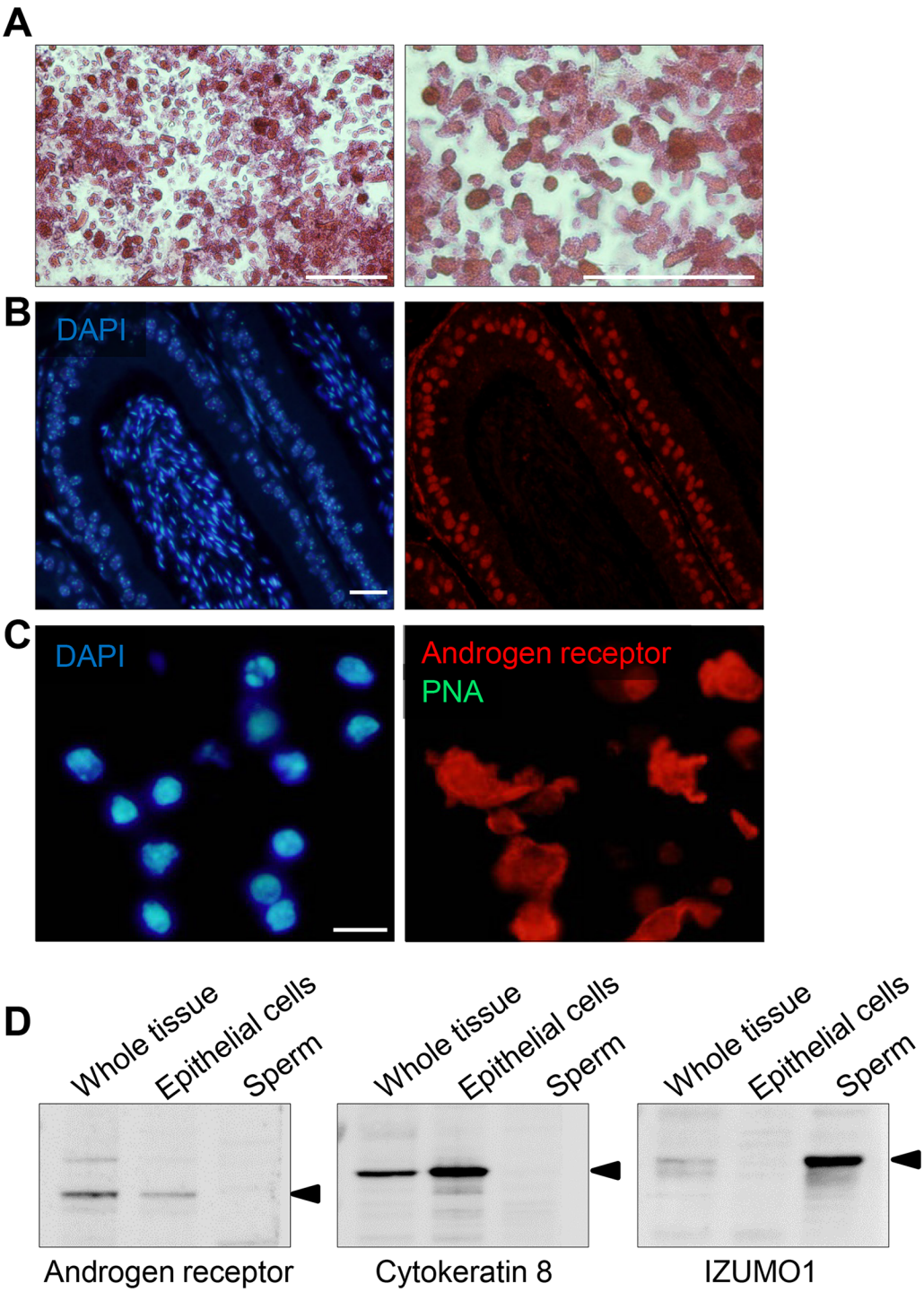

Fig 3. Isolation of highly enriched populations of epididymal epithelial cells. Epididymides were dissected from perfused adult mice and partitioned into the caput, corpus and cauda. The epithelial tissue was then cleared of spermatozoa, minced and sequentially digested in trypsin and collagenase. Epithelial cells were isolated by filtering through a 70 μm cell strainer and incubation in tissue culture plates prior to being fixed and assessed for overall purity by (A) staining with eosin and visualization by light microscopy (scale bar = 200 μm), (B,C) immunocytochemistry with anti-androgen receptor antibodies, and (D) immunoblotting with recognized epithelial / sperm cell markers. (B) The validity of androgen receptor antibodies for immunocytochemistry was initially assessed by labeling of mouse epididymal sections. These sections were then counterstained with DAPI and viewed using confocal microscopy (scale bar = 20 μm). (C) The identity of purified epithelial cells was confirmed by labeling with anti-androgen receptor and the possibility of sperm contamination assessed by co-staining with FITC conjugated PNA (a lectin that selectively labels the outer acrosomal membrane of spermatozoa). These preparations were then counterstained with DAPI (to detect all cells). This confirmed an absence of sperm contamination and epithelial cell enrichment of >95%. (D) As an

additional line of evidence, cell lysates prepared from whole epididymal tissue (sperm + epithelial cells), enriched epithelial cells, and spermatozoa were immunoblotted with antibodies against androgen receptor (110kDa), cytokeratin 8 (an epithelial cell marker, 54kDa), and the sperm protein IZUMO1 (60kDa). All experiments were replicated three times on independent samples and representative images are presented.

doi:10.1371/journal.pone.0135605.g003

represented in the former analysis (S1 Table). Of the novel miRNAs detected in this assay, several (23) were present in low abundance raising the possibility that their signal may have been masked during the analysis of whole tissue preparations. Within the epithelial cell miRNA profile, two thirds (144) were conserved across all epididymal regions, with only 16% being exclusively expressed in any one epididymal region (Fig 4A). These results compare favorably with the data obtained for whole epididymal tissue, with a noteworthy feature of both analyses being that few miRNAs were uniquely detected in the corpus (5/370 and 0/218, respectively) (Figs 2A and 4A). Similarly, only a relatively small subset of miRNAs displayed expression levels that differed significantly between the caput/corpus and corpus/cauda (15% and 12%, respectively) (Fig 4B and S2 Table). More prominent changes were observed when comparisons were conducted over the entire length of the tract with almost a quarter (24%) of all miRNAs being characterized by significant variations in expression between the caput/cauda epididymis (Fig 4B and S2 Table). Although these data suggest that the spatial patterns of miRNA expression are not clearly demarcated by the broad intrasegmental boundaries of the caput, corpus and cauda, quantitative analysis of differentially expressed miRNAs revealed that many underwent substantial fold changes between the caput/corpus and corpus/cauda (Fig 5). Among the clearest examples of these, *miR-196b-5p* experienced a 45-fold increase in expression between the caput and caudal regions, while conversely *miR-204-5p* was down-regulated by approximately 39-fold over the same regions (Fig 5C). Importantly, we recorded consistent results across each biological replicate both in terms of the overall number of miRNA reads (S2 Table) and the relative fold change between regions (Fig 6).

The deep sequencing strategy employed in the present study also afforded insight into the relative expression levels of the two mature products arising from each miRNA precursor within the epididymis (S1 Table). Where products arising from both the 5′ and 3′ arm of a precursor mir hairpin were detected, one form generally displayed dominant expression throughout each epididymal region (Fig 7). For instance, in the case of *miR-29a*, which has previously been implicated in androgen signaling within the mouse epididymis, the predominant product originated from the 3′ arm (*miR-29a-3p*) and was expressed at levels that were at least 30-fold higher than that of the alternative 5′ arm product (*miR-29a-5p*) (Fig 7A). These data accord with other tissues in which *miR-29a-3p* has also been shown to represent the predominant product generated from the *mir-29a* precursor (miRBASE).

Validation of Differentially Expressed miRNAs

In order to authenticate the next generation sequence data, nine differentially expressed miRNAs were selected for targeted validation using qRT-PCR. These candidate miRNAs included representatives that exhibited regulated patterns of expression from each of the two primary classes detected, namely: those with highest expression in the caput (*let-7c-5p*, *let-7b-5p*, *miR-375-3p*, *miR-9-5p*, *miR-467d-3p*, and *miR-200c-3p*), or highest expression in the cauda (*miR-410-3p*, *miR-486-5p*, and *miR470c-5p*) epididymis. All qRT-PCR experiments were performed in triplicate using pooled biological samples (n = 3 animals/sample) that differed from those employed for next generation sequence analyses. In each experiment, the U6 small nuclear RNA was employed as an endogenous control to normalize the expression levels of target miRNAs. This analysis confirmed that eight of the nine target miRNAs were indeed differentially expressed within the epididymis (Fig 8). Furthermore, each of these eight targets displayed an

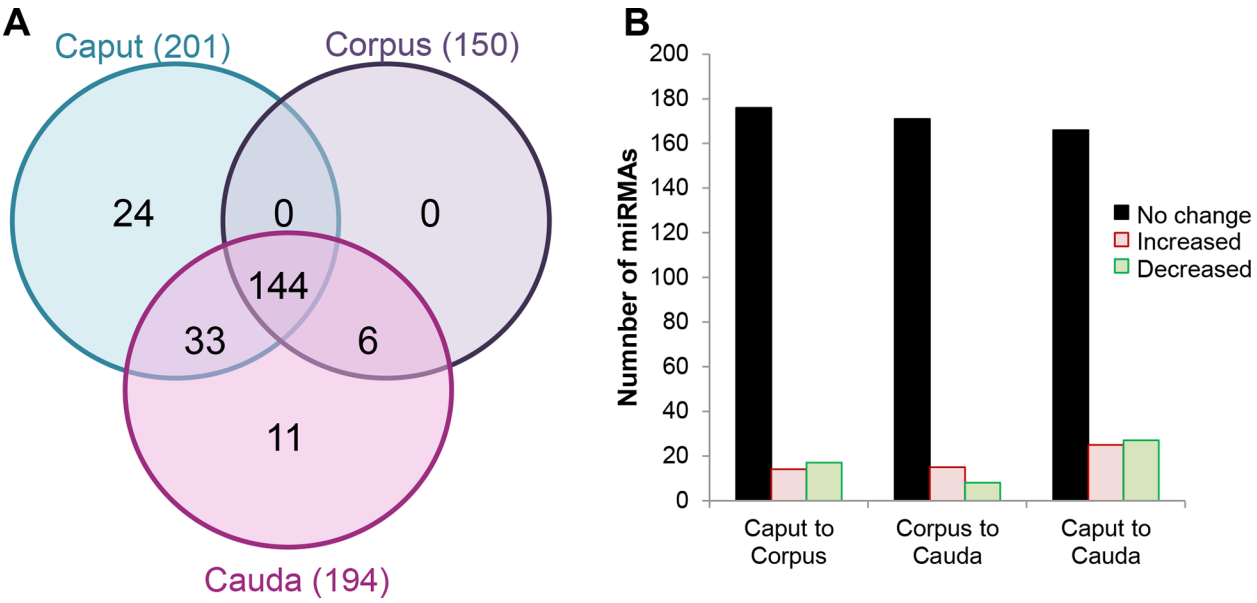

Fig 4. Determination of the miRNA signature present in enriched populations of epididymal epithelial cells. (A) Venn diagram depicting the number of miRNAs that were identified by next generation sequencing and their disruption within the epithelial cells of caput, corpus and caudal regions of the adult mouse epididymis. (B) Graphical representation of miRNA distribution highlighting the number of significantly up- and down-regulated (threshold = ± ≥ 2 fold change and false discovery rate of < 0.05) miRNAs positively identified in the epithelial cells of each epididymal region. For the purpose of these analyses, an average count value of >10 across two biological replicates was used as the threshold for positive identification of each miRNA.

doi:10.1371/journal.pone.0135605.g004

expression profile that closely mirrored the trends identified by next generation sequence analysis (Fig 8). In this context, qPCR confirmed highly significant down-regulation of *let-7c-5p*, *let-7b-5p*, *miR-375-3p*, *miR-467d-3p*, and *miR-200c-3p* between the proximal and distal epididymal segments. It also highlighted the caput-specific expression of *miR-9-5p*, and confirmed a significant up-regulation of *miR-486-5p* and *miR470c-5p* between the caput and corpus epididymis. Only *miR-410-3p* failed to present significant changes in expression, however this result may be attributed to the relatively low absolute expression of this miRNA (Fig 8). Taken together, these findings suggest that our data faithfully report the spatial patterns of mouse epididymal miRNA signatures.

Having identified significant changes in miRNA expression within the epididymal epithelium, we next examined their functional significance by using an *in silico* analysis of published transcriptomic databases [3,31,32] to correlate miRNA and validated mRNA target expression levels throughout the epididymis. This approach proved effective at identifying several mRNAs whose relative levels of expression were positively correlated with that of their targeting miRNA (s), a subset of which are represented in Fig 9. These studies were therefore extended by employing a knockdown strategy in which an immortalized mouse caput epididymal epithelial cell line (mECap) was co-transfected with a cherry red reporter and miRNA mimics of either *miR-200c*, *miR-486* (shown to be significantly up-regulated in the caput and caudal regions, respectively), or a scrambled negative control (*mir*Vana). At 24 h post-transfection, cells were harvested, the transfection efficiency was calculated (25–70%) and the relative levels of validated target mRNAs determined by qRT-PCR. As shown in Fig 10 this strategy proved effective in eliciting a significant reduction in the expression of both *Mapk14* (targeted by *miR-200c*) (Fig 10A) and *Foxo1* (targeted by *miR-486*) (Fig 10B) mRNA. The specificity of this post-transcriptional knockdown strategy was confirmed by the absence of a similar effect in mECap cells transfected with *mir*Vana scrambled controls.

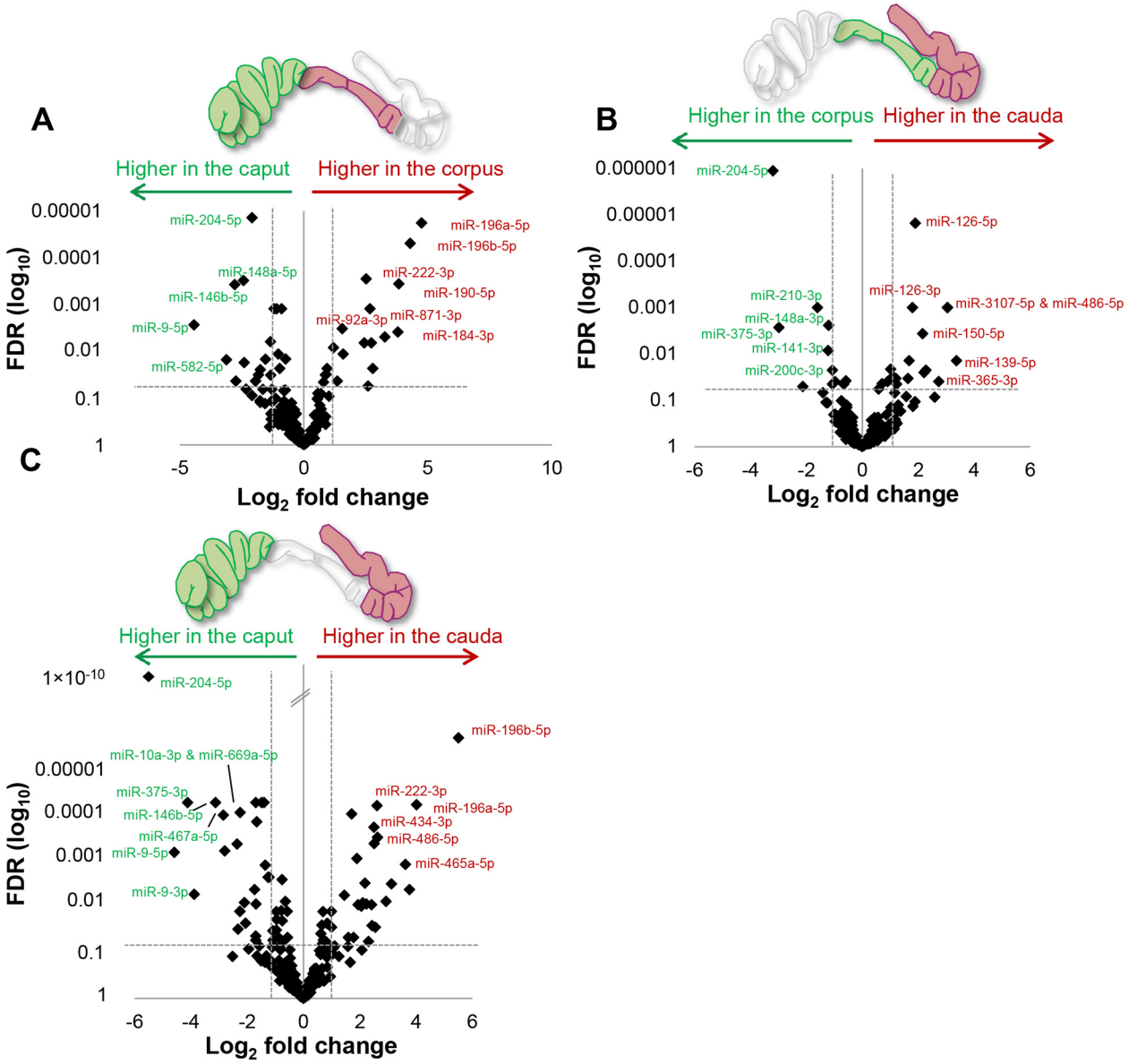

Fig 5. Volcano plots depicting the fold changes in miRNAs identified as being deferentially expressed within enriched populations of epididymal epithelial cells. Volcano plots highlighting the fold changes (x-axis) and false discovery rate (y-axis) of miRNAs that were identified as being differentially expressed in the epithelium between the (A) caput/corpus (B) corpus/cauda and (C) caput/cauda epididymis. Dotted lines depict thresholds values for significantly up- and down-regulated (± ≥ 2 fold change and false discovery rate of < 0.05) miRNAs identified between each epididymal region.

doi:10.1371/journal.pone.0135605.g005

The epididymal miRNA Signature Appears to be Poorly Conserved between Species

By exploiting the results of independent studies [7,12], we next sought to examine the level of conservation that exists between the miRNA signature of the mouse, rat and human epididymis. This survey focused on miRNAs identified in whole epididymal tissue (S1 Table) owing to the fact that previous global profiling studies have not been conducted on isolated epididymal cells. In addition, we were not able to distinguish between the two mature products arising from each miRNA precursor. Working within these limitations, and those associated with the alternative

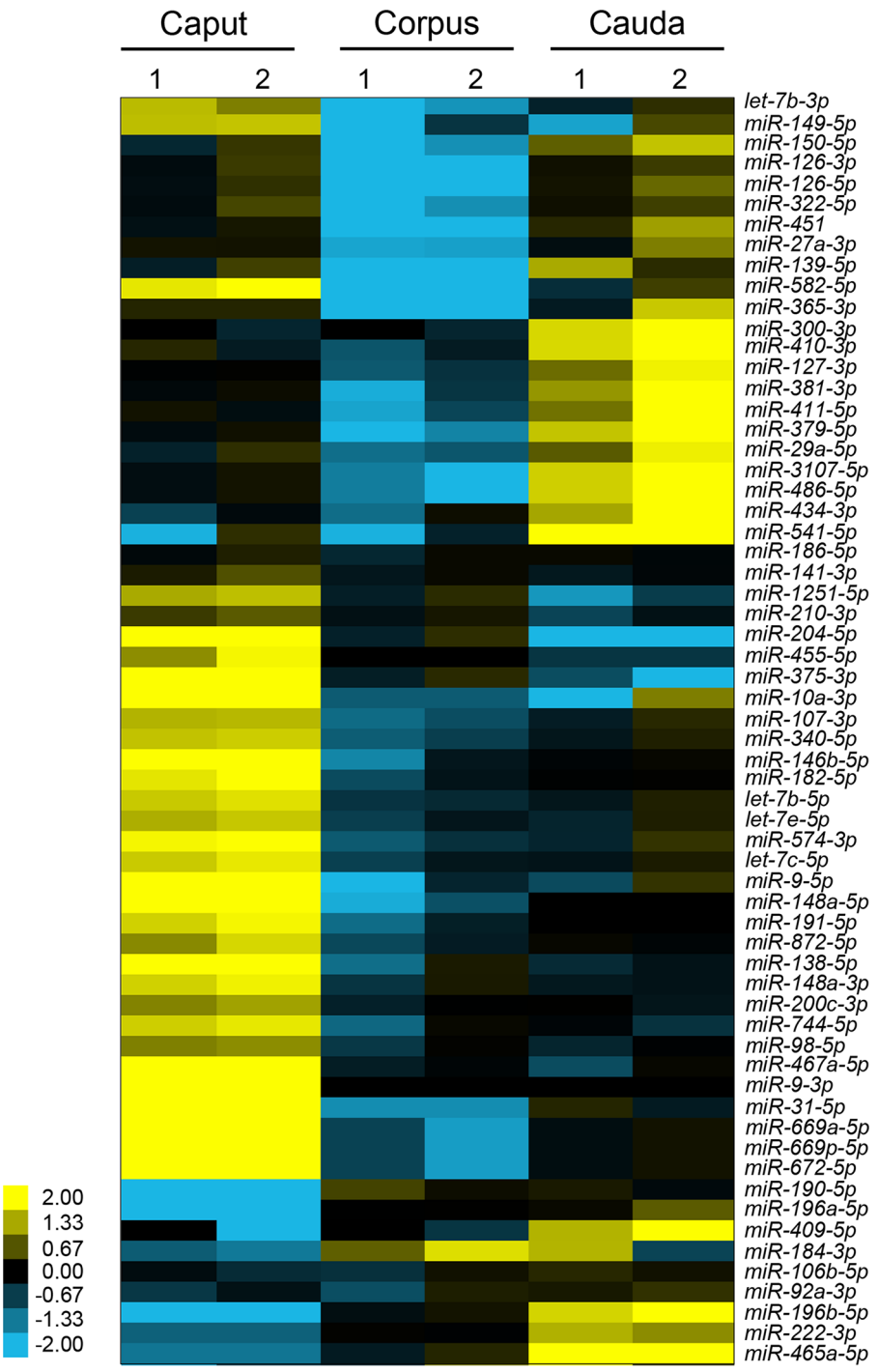

Fig 6. Analysis of the variability in miRNA expression between biological replicates. Hierarchical clustering of a subset of miRNAs that were identified as being differentially expressed between the epithelial cells from the caput/corpus, corpus/cauda, and caput/cauda was performed to assess overall variability between biological replicates. Cells within the matrix depict the relative expression level of a single miRNA within the 9 (caput/corpus)—12 (cauda) biological samples represented in each replicate. Yellow and blue shading represents the expression level (log_2 fold change) above and below the median for this miRNA in all epithelial samples (caput, corpus, and cauda) analyzed, respectively.

doi:10.1371/journal.pone.0135605.g006

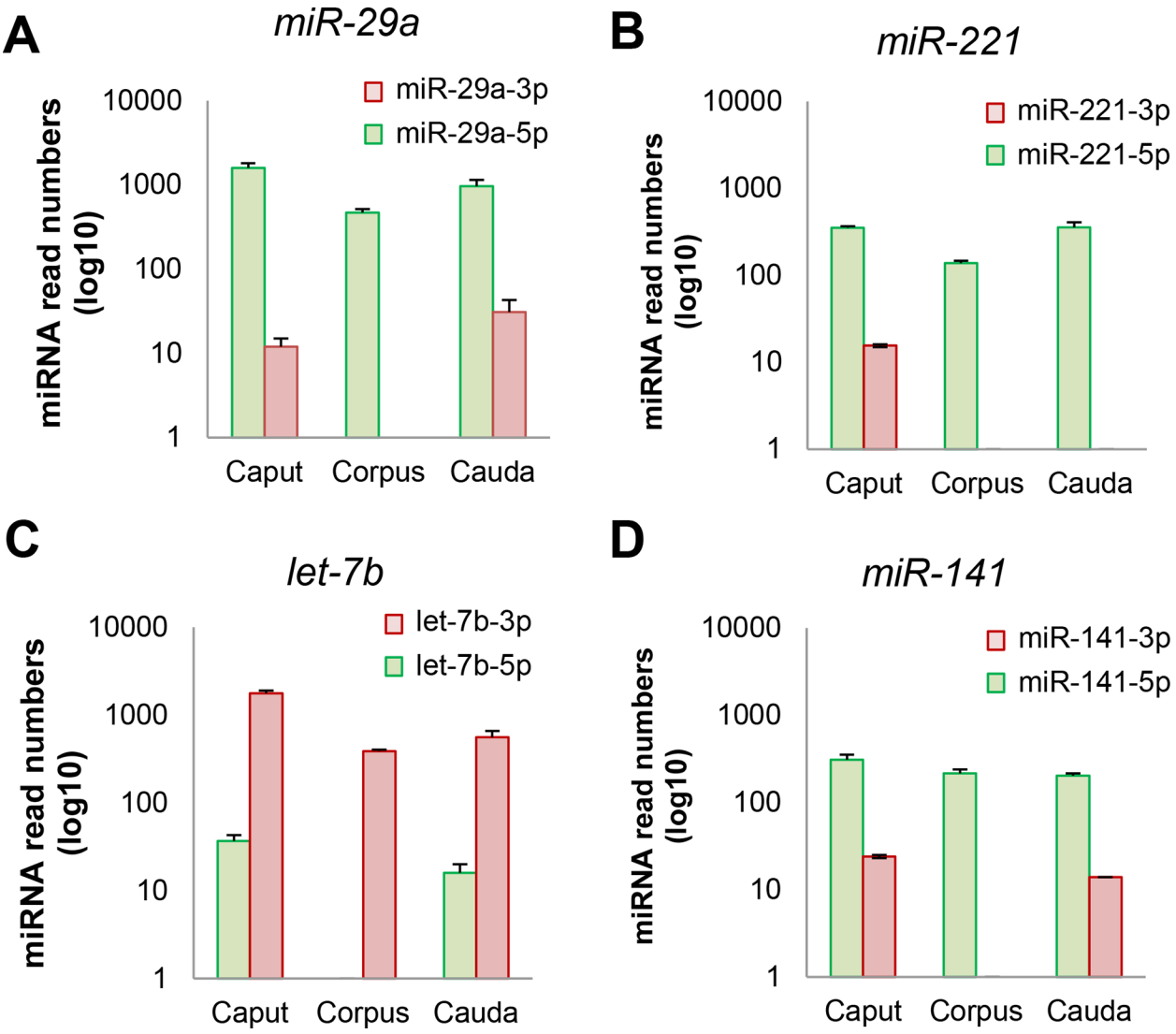

Fig 7. Determination of the relative expression levels of the mature products arising from representative miRNA precursors within the epididymis. Next generation sequencing revealed the relative expression levels of the two mature products arising from each miRNA precursor within the epididymis. Where products arising from both the 5′ and 3′ arm of a precursor mir hairpin were detected, one form generally dominated the expression profile throughout each epididymal region.

doi:10.1371/journal.pone.0135605.g007

sequencing strategies based on commercially available miRNA microarrays that were employed in preceding work, our interrogation of known epididymal miRNAs revealed that only 21% (97/463) were conserved across the mouse, rat, and human (S3 Table). Interestingly, most of these conserved miRNAs (81%) were found to be expressed in the all epididymal regions (caput, corpus and cauda) in all species suggesting that they play fundamental house-keeping roles in the regulation of this tissue (S4 Table). As might be expected, the greatest level of similarity was observed in comparisons between the mouse and rat with approximately 42% of epididymal miRNAs identified in both species (143/341). In contrast, 31% (131/417) of miRNAs were detected in both the mouse and human epididymis. Interestingly, among the conserved miRNAs found in all epididymal regions, we identified 8/14 and 4/7 members of the *let-7* family (*let-7a—let-7f*, *let-7i*) and *miR-30* (*miR-30a—miR-30d*) family, respectively. The former family is of particular interest owing to its established role as a tumor suppressor and its high level of sequence

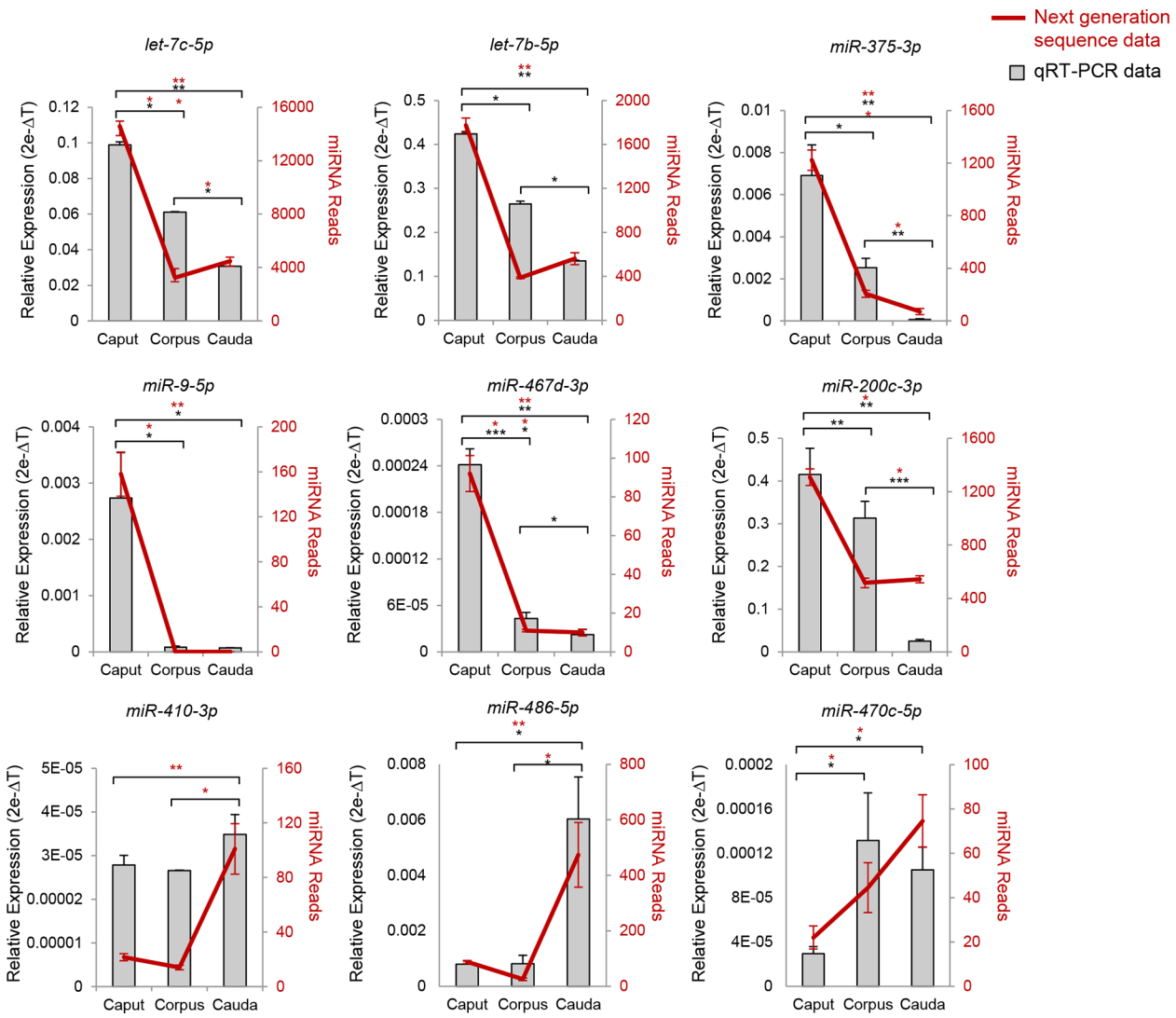

Fig 8. qRT-PCR validation of differentially expressed miRNAs within the mouse epididymis. In order to verify the next generation sequence data, nine differentially expressed miRNAs were selected for targeted validation using qRT-PCR, including representatives with highest expression in the proximal (caput: *let-7c-5p*, *let-7b-5p*, *miR-375-3p*, *miR-9-5p*, *miR-467d-3p*, and *miR-200c-3p*) and distal (cauda: *miR-410-3p*, *miR-486-5p*, and *miR470c-5p*) epididymis. qRT-PCR experiments were performed in triplicate using pooled biological samples (n = 3 mice / sample) differing from those employed for next generation sequence analyses. The U6 small nuclear RNA was employed as an endogenous control to normalize the expression levels of target miRNAs. * $P < 0.05$, ** $P < 0.01$, *** $P < 0.001$.

doi:10.1371/journal.pone.0135605.g008

and functional conservation across species [33]. Conversely, the 5 members of the *miR-888* cluster (*miR-890*, *miR-891a*, *miR-891b*, *miR-892a*, and *miR-892b*) that have been reported as being highly expressed in the corpus and caudal regions of the human epididymis [12] were not detected in our analysis of the mouse epididymis or in previous work on the rat epididymis [7].

This comparative analysis provided additional evidence for the differential expression of miRNAs in the epididymis of different species. For instance, *miR-32* and *miR-33* were found to be restricted to the caput epididymis of the mouse, while being absent in all regions of the rat epididymis, and present in the caput, corpus, and cauda of the human epididymis (S4 Table). Similarly, *miR-133b*, *miR-137*, *miR-155*, and *miR499* were exclusively expressed in the caudal region of the mouse epididymis but were widely distributed throughout the rat and/or human

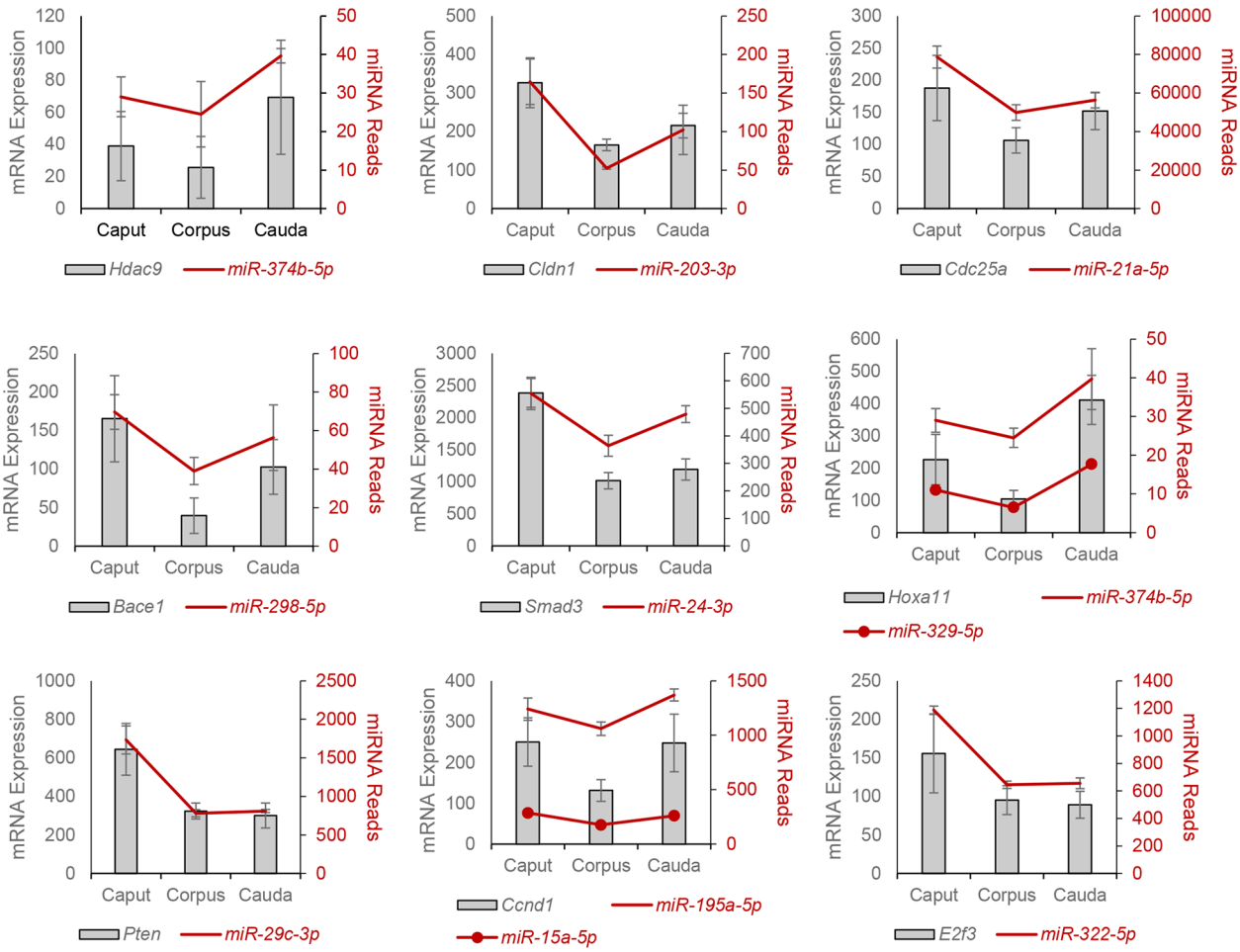

Fig 9. Correlation of miRNA expression profiles with that of their target mRNAs. An *in silico* analysis of published transcriptomic databases [3,31,32] was used to correlate miRNA and validated mRNA target (determined by IPA) expression levels throughout the epididymis. For the purpose of this comparison the mRNA expression levels reported in epididymal segments 2–5, 6–7, and 8–10 [3,31,32] were combined to represent overall expression in the caput, corpus, and cauda epididymis, respectively. A subset of 9 representative mRNA targets is depicted along with the relative levels of their targeting miRNA(s) as determined in the present study.

doi:10.1371/journal.pone.0135605.g009

epididymis (S4 Table). Among a myriad of alternative interesting expression profiles, *miR-329* and *miR-350* displayed a biphasic pattern of expression in the mouse epididymis (being present in the caput and cauda, but absent in the corpus), but were entirely absent in the rat epididymis and present in all regions of the human epididymis (S4 Table).

In Silico Analysis of miRNA Regulated Pathways in the Mouse Epididymal Epithelium

In order to gain an appreciation of the biological functions of miRNAs that are either uniformly or differentially expressed within the mouse epididymal epithelium, putative target genes were predicted through interrogation of Ingenuity Pathway Analysis (IPA) software using strict, experimentally validated filters. For both subsets of miRNAs, the putative target genes appeared to be involved in a range of biological processes with most of these mapping to the broad categories of regulating cellular, tissue, and organ development, cell-cell signaling and interaction, and cell death and survival (Fig 11A and 11B). Furthermore, within these

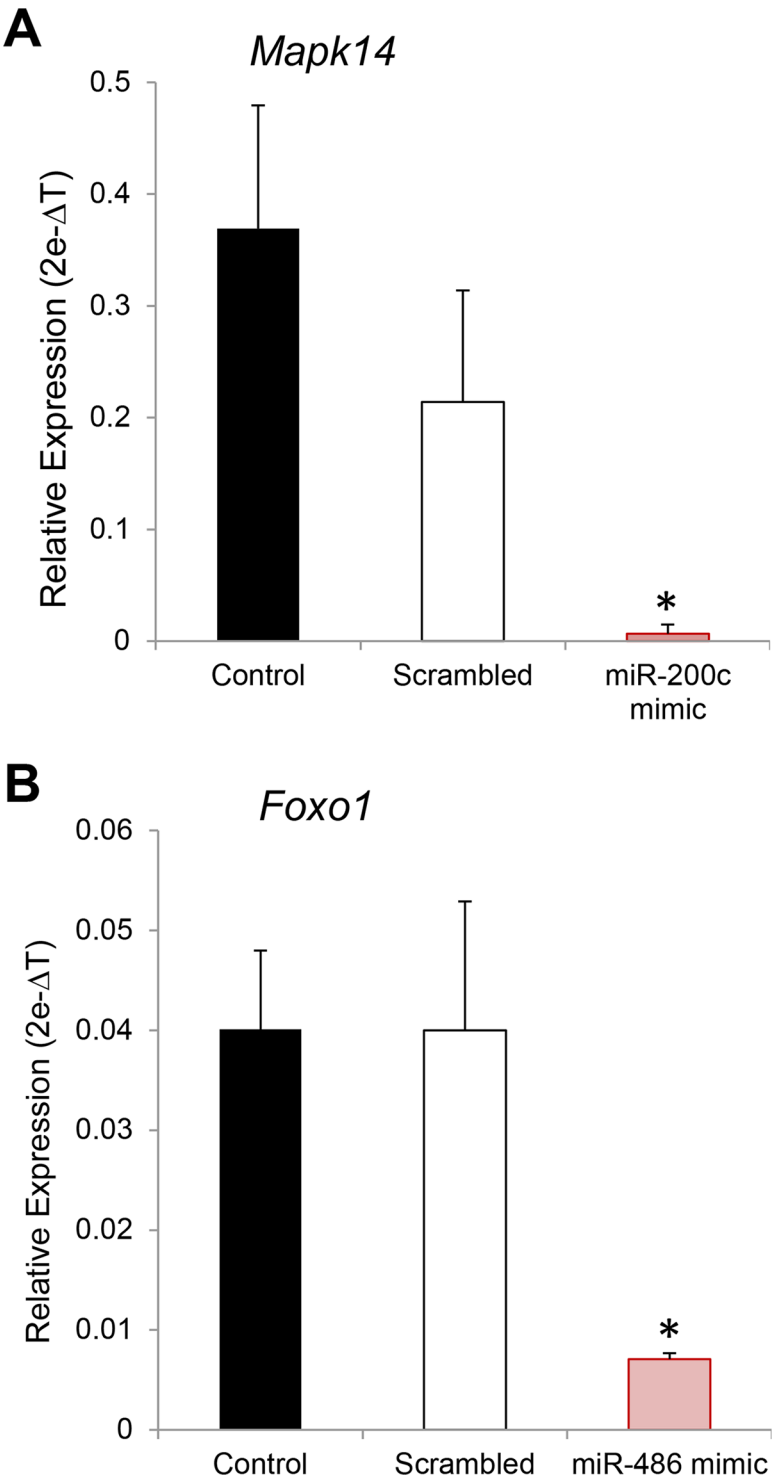

Fig 10. Examination of miRNA target gene knockdown. To confirm the functional significance of epididymal miRNAs, an immortalized mouse caput epididymal epithelial cell line (mECap) was co-transfected with a cherry red reporter and miRNA mimics of either (A) *miR-200c*, (B) *miR-486*, or a scrambled negative control (*mir*Vana). At 24 h post-transfection the relative levels of validated target mRNAs (*Mapk14* and *Foxo1*, respectively) were determined by qRT-PCR. These experiment were replicated three times and data are presented as mean ± SEM. * $P < 0.05$.

doi:10.1371/journal.pone.0135605.g010

categories we identified signaling cascades that are known to underpin key aspects of epididymal epithelium regulation and/or are implicated in sperm maturation/storage, suggesting that our analysis of miRNAs faithfully reported those of importance in epididymal function. For instance, among the 66 uniformly expressed miRNAs for which IPA assigned functions, we identified 12 candidates that have been implicated in androgen regulation, including: *let-7a-5p*, *miR-15a-5p*, *miR-17-5p*, *miR-19b-3p*, *miR-23a-3p*, *miR-24-3p*, *miR-27b-3p*, *miR-30a-5p*, *miR-34a-5p*, *miR-140-5p*, *miR-193a-3p*, *miR-205-5p* (S1 Fig). Similarly, within the differentially expressed pool of miRNAs, 10 were identified that are intimately involved in regulating intracellular trafficking pathways, including: *miR-7b-5p*, *miR-9-5p*, *miR-31-5p*, *miR-92a-3p*, *miR-106-5p*, *miR-126-3p*, *miR-150-5p*, *miR-204-5p*, *miR-222-3p*, *and miR-322-5p* (S2 Fig).

Discussion

In all mammalian species studied, spermatozoa acquire the ability to fertilize an ovum during their passage through the epididymis [34]. A defining feature of this post-testicular maturation is that it is driven exclusively by the complex external milieu in which spermatozoa are bathed during their descent through the luminal environment of the epididymal tubule. Similarly, the prolonged storage of viable spermatozoa in the distal regions of the tract is also reliant upon the creation and maintenance of a highly specialized microenvironment. While the molecular mechanisms responsible for the controlling these dynamic regionalized environments are largely unresolved, recent evidence has highlighted a novel and potentially extremely important role for the RNA interference pathway in species such as the rat, bovine and human [8,9,35]. Since this additional tier of regulation has yet to be investigated in the mouse, we have employed next generation sequencing technology to define the global miRNA signature, and their segmental patterns of expression, in the epididymis of this important model species.

In samples of whole epididymal tissue we were able to identify a total of 370 miRNAs, representing one of the most comprehensive global screens of miRNAs performed in this tissue to date. However, a limitation of this initial analysis was that it failed to distinguish between the populations of miRNAs uniquely synthesized in each epididymal region as opposed to those that originate upstream within the testes and/or proximal epididymis before being delivered to the luminal compartment of more distal regions. In this context, it is well known that both spermatozoa [36–39] and epididymal secretions [11] harbor a complex repertoire of RNA populations, including miRNAs, that could potentially serve to mask important intrasegmental changes in the epididymal epithelial miRNA profile. Accordingly, restriction of our analysis to focus on highly enriched populations of epithelial cells dramatically narrowed the scope of the epididymal miRNA signature. Of the 218 miRNAs identified in this latter screen, comparatively few (<15%) were found to be differentially expressed between the caput/corpus and corpus/cauda epididymis. An important caveat to this finding is that our studies did not discriminate miRNA expression between the initial segment and caput epididymidis, two key regions that are known to play unique roles in murine epididymal physiology.

While our miRNA expression data stand in marked contrast to the regionalized patterns of gene [3,21,22] and protein expression [4,40–42] that are hallmarks of epididymal function, they do accord with the miRNA profiles documented in other species [7,12] and may thus reflect the fact that even small changes in miRNA expression can have a significant impact on the mRNA/proteomic profile of these cells. In keeping with this notion, it is well established that a single miRNA can influence the stability of potentially hundreds of mRNA targets thus setting the scene for a highly complex network of miRNA/mRNA interactions within epididymal cells. Indeed, even under strict target prediction criteria, an impressive array of some 8493 genes were identified as being putatively regulated by the differentially expressed miRNAs

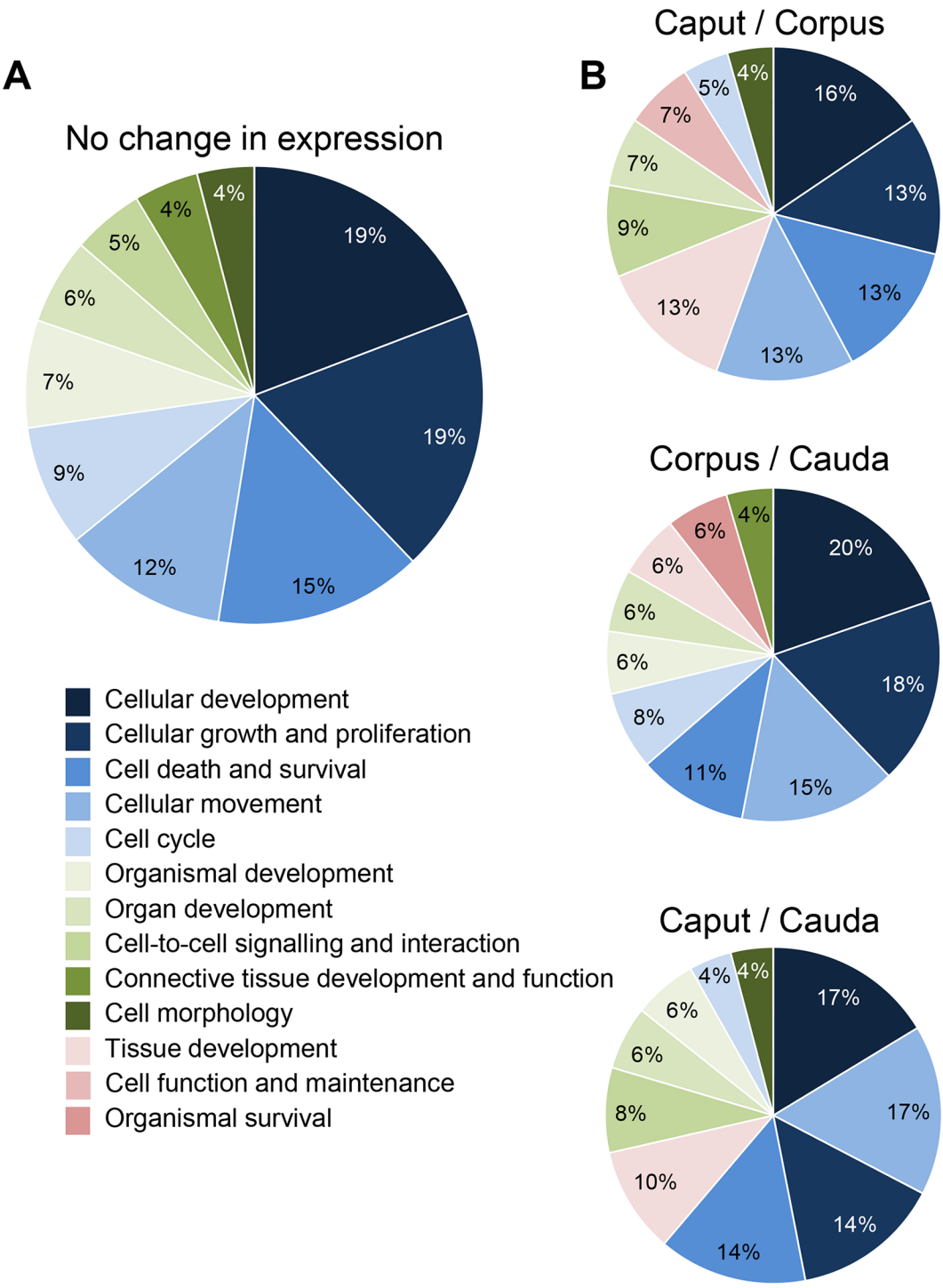

Fig 11. Key pathways regulated by epididymal miRNAs. Biological functions of miRNAs that were either (A) uniformly or (B) differentially expressed within the mouse epididymal epithelium were predicted through interrogation of Ingenuity Pathway Analysis (IPA) software. For both subsets of miRNAs, a majority of the experimentally validated target genes mapped to the broad categories of regulating cellular, tissue, and organ development, cell-cell signaling and interaction, and cell death and survival.

doi:10.1371/journal.pone.0135605.g011

identified in this study. Specific examples include *miR-204-5p*, which was down-regulated by approximately 39-fold between the caput/caudal regions, and has an estimated 530 predicted gene targets in the mouse [43]. Interestingly, one of the key validated targets for *miR-204-5p* is SPARC (secreted protein acidic and rich in cysteine), a matricellular protein that regulates cell adhesion, matrix assembly and remodeling [44], and one whose spatial pattern of mRNA expression closely resembles that of *miR-204-5p*. Similarly, *miR-196b-5p* which displayed a 45-fold up-regulation in expression over the same regions, has been predicted to be target some 160 genes [43]. Foremost amongst these are the genes for the Homeobox (Hox) transcription factors that confer anterior-posterior axial coordinates during vertebrate embryo development [45], and have been implicated in regulating segmental function of the adult mouse epididymis [46,47]. Interestingly, several members of the *Hox* gene family whose expression has been confirmed in the mouse epididymis [3,47] are represented among the known targets for numerous additional miRNAs identified in the present study. One such example is *Hoxa11*, a transcript that displays highest levels of expression in the cauda followed by the caput and finally the corpus [3,47]. This spatial pattern of expression closely mirrors that of *miR-23a*, *miR-143*, and *miR-150*, all of which putatively target the *Hoxa11* mRNA.

While these data support the importance of miRNAs in fine tuning the regulation of the epididymal environment responsible for sperm maturation, an unexpected finding was the relatively poor conservation of miRNA signatures recorded between species. Indeed, at the level of sensitivity afforded by these analyses only 21% of epididymal miRNAs were detected in the mouse, rat, and human. We concede that these values may represent an under-representation of the true level of conservation, since our studies are confounded by the technical issues arising from the use of alternative sequencing technologies (next generation sequencing in the present study vs miRNA microarrays in previous work [7,12]) and/or the confounding influence of miRNAs harbored by luminal spermatozoa. However, we cannot discount the possibility that they report genuine differences in epididymal physiology between species. Support for this assertion rests with the data emerging from global transcriptomic [3,31,32] and proteomic analyses [4,40,41] that have been applied to the study of epididymal function. These genome-wide approaches have highlighted that significant species-specific differences do indeed exist in the epididymal transcriptome/proteome, with each species appearing to have developed unique strategies for promoting sperm maturation and preservation within this organ [40]. Although, there is a clear need for additional comparative studies to resolve these issues, a noteworthy feature of the majority of the miRNAs that were found to be conserved in the epididymis of the mouse, rat and human was their ubiquitous expression along the entire length of the tubule.

This conservation suggests that this subset of miRNAs form an integral part of the cellular processes responsible for the maintenance of epididymal homeostasis, with putative functions extending from promoting the development of the male reproductive tract, the regulation of sperm maturation, the maintenance of epididymal tight junctions and possibly the restriction of cellular proliferation within the adult organ. The latter is a defining feature of the epididymis and one that has been implicated in conferring an extraordinary resistance to primary cancer development, metastasis and invasive growth within this organ (reviewed by [48]). Indeed, human epididymal cancers account for only 0.03% of male cancers, an incidence rate that is well below that of other male reproductive tract malignancies (e.g. testicular cancer, 1.5% and prostate cancer, 20%). It also contrasts the occurrence of renal cancers (3%) despite the fact that the kidney and epididymis share a common embryonic origin (reviewed by [48]). Such observations have led to the proposal that the epididymis may possess intrinsic inhibitory mechanism(s) that protect the organ against the development of cancers, with recent work implicating miRNAs as master regulators of this process [49]. This assertion is supported by the observation that the *let-7* family of miRNAs, which have well characterized roles in the

direct repression of cell proliferation and oncogenic pathways [33], featured prominently among the conserved epididymal miRNAs.

Let-7 (*lethal-7*) is a founding member of the miRNA family that was originally described in *Caenorhabditis elegans*, where it controls the timing of terminal differentiation, acting as a key regulator of multiple genes required for exit from the cell cycle (reviewed by [33]). The *let-7* miRNA family has since been shown to display a remarkable level of sequence and functional conservation across the animal kingdom, with 14 and 13 different family members represented in mouse and human, respectively [33]. Among these members, *let-7a/b/c/d/e/f*, and *let-7i* are ubiquitously expressed in the adult mouse, rat and human epididymis. Of these family members, previous work has shown that 5 (*let-7a/b/c/d* and *let-7f*) are widely expressed in newborn, young adult, and aged human epididymides [8]. This is consistent with current models of *let-7* function which indicate that the family members are barely detectable during embryonic development before being up-regulated in differentiated cells where they are likely to possess highly redundant roles through targeting of an overlapping set of mRNAs [33]. Of significance to epididymal function, such roles are known to extend from the regulation of cellular proliferation through to the control of androgen receptor expression. For instance, *let-7c* has been reported to negatively regulate androgen receptor by suppressing its transcriptional activator c-Myc [50]. Similarly, dysregulation of *let-7* leads to a less differentiated cellular state and the development of cell-based diseases such as cancer [51,52]. It remains to be determined whether the 8 *let-7* family members that are expressed in the epididymis have different activities or whether they collectively target a similar cohort of genes. Nevertheless, it is tempting to speculate that the redundancy in *let-7* expression may contribute to the stringent molecular mechanisms that help the epididymis evade tumorigenesis. The prospect that a similar function may extend to other miRNAs is suggested by the conservation of several miRNAs (e.g. *miR-25*, *miR-34a/b/c*, *miR-135a/b*, *miR-194*, and *miR-200a*) that are capable of directly targeting the Wnt/β-catenin, a signaling pathway that has been widely implicated in the control of oncogenic hallmarks such as cell proliferation, metastasis, angiogenesis, telomerase activity, and apoptosis (reviewed by [49]). Indeed, aberrant activation and/or dysregulation of Wnt/β-catenin signaling has been identified as key underlying lesion in a significant portion of all human cancers (reviewed by [53]).

In summary, the data obtained in the present study provides novel insights into the diversity of miRNAs that are expressed within the mouse epididymis. Our findings accord with previous work emphasizing the sophistication of the miRNA network that coordinates the microenvironment necessary for post-testicular sperm maturation and storage. Interestingly however, despite the marked division of labor that characterizes epididymal function, we found that segment-specific miRNA expression is not a prominent theme in the mouse epididymis, with relatively few of the detected miRNAs displaying a significant difference in expression level between the three segments examined. Our systematic profiling of whole tissue and enriched populations of epithelial cells also served to identify luminal spermatozoa and/or epididymal fluid as a major contributor to the overall epididymal miRNA signature. Accordingly, our future studies will focus on the characterization of miRNAs in the luminal environment in order to determine whether they too are integrated into the complex regulation of epididymal function. Ultimately this work promises to improve our understanding of male infertility and identify novel targets for male contraception.

Supporting Information

S1 ARRIVE Checklist. ARRIVE Guidelines Checklist. This file is the ARRIVE Guidelines Checklist.
(PDF)

S1 Fig. miRNA control of androgen regulation in the epididymis. Twelve of the miRNAs that were identified as being expressed at similar levels throughout all epididymal regions were mapped as putative regulators of the androgen signalling pathway (IPA: miRNA filter, experimentally observed).
(TIF)

S2 Fig. miRNA control of endocytotic pathways in the epididymis. Ten of the miRNAs that were identified as being differentially expressed within the mouse epididymis were mapped as putative regulators of the clathrin mediated endocytosis (IPA: miRNA filter, experimentally observed).
(TIF)

S1 Table. Comparison of miRNAs identified by deep sequencing within whole mouse epididymal tissue and highly enriched populations of epididymal epithelial cells.
(PDF)

S2 Table. Relative expression levels of miRNAs identified by deep sequencing within mouse epididymal epithelial cells.
(PDF)

S3 Table. Comparison of miRNAs identified within mouse, human and rat epididymal tissue.
(PDF)

S4 Table. Comparison of segmental expression of miRNAs identified within mouse, human and rat epididymal tissue.
(PDF)

Acknowledgments

The authors gratefully acknowledge funding from the National Health and Medical Research Council of Australia (APP1062371) to BN, EAM and JEH. The authors also acknowledge the Australian Genome Research Facility (Melbourne) for sequencing and initial bioinformatic analyses.

Author Contributions

Conceived and designed the experiments: BN JEH EAM. Performed the experiments: SJS BPM JNR ALA MDD. Analyzed the data: BN EAM JEH SJS BPM ST. Contributed reagents/materials/analysis tools: BN ST. Wrote the paper: BN SJS BPM JNR ALA MDD ST JEH EAM.

References

1. Hermo L, Pelletier RM, Cyr DG, Smith CE. Surfing the wave, cycle, life history, and genes/proteins expressed by testicular germ cells. Part 1: background to spermatogenesis, spermatogonia, and spermatocytes. Microsc Res Tech. 2010; 73: 241–278. doi: 10.1002/jemt.20783 PMID: 19941293
2. Aitken RJ, Nixon B, Lin M, Koppers AJ, Lee YH, Baker MA. Proteomic changes in mammalian spermatozoa during epididymal maturation. Asian J Androl. 2007; 9: 554–564. PMID: 17589795
3. Johnston DS, Jelinsky SA, Bang HJ, DiCandeloro P, Wilson E, Kopf GS, et al. The mouse epididymal transcriptome: transcriptional profiling of segmental gene expression in the epididymis. Biol Reprod. 2005; 73: 404–413. PMID: 15878890
4. Dacheux JL, Belleannee C, Jones R, Labas V, Belghazi M, Guyonnet B, et al. Mammalian epididymal proteome. Mol Cell Endocrinol. 2009; 306: 45–50. doi: 10.1016/j.mce.2009.03.007 PMID: 19464100

5. Li Y, Wang HY, Wan FC, Liu FJ, Liu J, Zhang N, et al. Deep sequencing analysis of small non-coding RNAs reveals the diversity of microRNAs and piRNAs in the human epididymis. Gene. 2012; 497: 330–335. doi: 10.1016/j.gene.2012.01.038 PMID: 22313525
6. Ma W, Hu S, Yao G, Xie S, Ni M, Liu Q, et al. An androgen receptor-microrna-29a regulatory circuitry in mouse epididymis. J Biol Chem. 2013; 288: 29369–29381. doi: 10.1074/jbc.M113.454066 PMID: 23960076
7. Ma W, Xie S, Ni M, Huang X, Hu S, Liu Q, et al. MicroRNA-29a inhibited epididymal epithelial cell proliferation by targeting nuclear autoantigenic sperm protein (NASP). J Biol Chem. 2012; 287: 10189–10199. doi: 10.1074/jbc.M111.303636 PMID: 22194605
8. Zhang J, Liu Q, Zhang W, Li J, Li Z, Tang Z, et al. Comparative profiling of genes and miRNAs expressed in the newborn, young adult, and aged human epididymides. Acta Biochim Biophys Sin (Shanghai). 2010; 42: 145–153.
9. Zhang YL, Zhang JS, Zhou YC, Zhao Y, Ni MJ. Identification of microRNAs and application of RNA interference for gene targeting in vivo in the rat epididymis. J Androl. 2011; 32: 587–591. doi: 10.2164/jandrol.111.013060 PMID: 21764899
10. Zhou Y, Zheng M, Shi Q, Zhang L, Zhen W, Chen W, et al. An epididymis-specific secretory protein HongrES1 critically regulates sperm capacitation and male fertility. PLoS One. 2008; 3: e4106. doi: 10.1371/journal.pone.0004106 PMID: 19116669
11. Belleannee C, Calvo E, Caballero J, Sullivan R. Epididymosomes convey different repertoires of microRNAs throughout the bovine epididymis. Biol Reprod. 2013; 89: 30. doi: 10.1095/biolreprod.113.110486 PMID: 23803555
12. Belleannee C, Calvo E, Thimon V, Cyr DG, Legare C, Garneau L, et al. Role of microRNAs in controlling gene expression in different segments of the human epididymis. PLoS One. 2012; 7: e34996. doi: 10.1371/journal.pone.0034996 PMID: 22511979
13. Belleannee C, Legare C, Calvo E, Thimon V, Sullivan R. microRNA signature is altered in both human epididymis and seminal microvesicles following vasectomy. Hum Reprod. 2013; 28: 1455–1467. doi: 10.1093/humrep/det088 PMID: 23539611
14. Truesdell SS, Mortensen RD, Seo M, Schroeder JC, Lee JH, LeTonqueze O, et al. MicroRNA-mediated mRNA translation activation in quiescent cells and oocytes involves recruitment of a nuclear microRNP. Sci Reports. 2012; 2: 842.
15. Ambros V. The functions of animal microRNAs. Nature. 2004; 431: 350–355. PMID: 15372042
16. Bartel DP. MicroRNAs: genomics, biogenesis, mechanism, and function. Cell. 2004; 116: 281–297. PMID: 14744438
17. Bouhallier F, Allioli N, Lavial F, Chalmel F, Perrard MH, Durand P, et al. Role of miR-34c microRNA in the late steps of spermatogenesis. RNA. 2010; 16: 720–731. doi: 10.1261/rna.1963810 PMID: 20150330
18. He Z, Kokkinaki M, Pant D, Gallicano GI, Dym M. Small RNA molecules in the regulation of spermatogenesis. Reproduction. 2009; 137: 901–911. doi: 10.1530/REP-08-0494 PMID: 19318589
19. Liu D, Li L, Fu H, Li S, Li J. Inactivation of Dicer1 has a severe cumulative impact on the formation of mature germ cells in mouse testes. Biochem Biophys Res Commun. 2012; 422: 114–120. doi: 10.1016/j.bbrc.2012.04.118 PMID: 22564735
20. McIver SC, Roman SD, Nixon B, McLaughlin EA. miRNA and mammalian male germ cells. Hum Reprod Update. 2012; 18: 44–59. doi: 10.1093/humupd/dmr041 PMID: 21989172
21. McIver SC, Stanger SJ, Santarelli DM, Roman SD, Nixon B, McLaughlin EA. A unique combination of male germ cell miRNAs coordinates gonocyte differentiation. PLoS One. 2012; 7: e35553. doi: 10.1371/journal.pone.0035553 PMID: 22536405
22. Nicholls PK, Harrison CA, Walton KL, McLachlan RI, O'Donnell L, Stanton PG. Hormonal regulation of sertoli cell micro-RNAs at spermiation. Endocrinology. 2011; 152: 1670–1683. doi: 10.1210/en.2010-1341 PMID: 21325043
23. Landgraf P, Rusu M, Sheridan R, Sewer A, Iovino N, Aravin A, et al. A mammalian microRNA expression atlas based on small RNA library sequencing. Cell. 2007; 129: 1401–1414. PMID: 17604727
24. Bjorkgren I, Gylling H, Turunen H, Huhtaniemi I, Strauss L, Poutanen M, et al. Imbalanced lipid homeostasis in the conditional Dicer1 knockout mouse epididymis causes instability of the sperm membrane. FASEB J. 2015; 29: 433–442. doi: 10.1096/fj.14-259382 PMID: 25366345
25. Bjorkgren I, Saastamoinen L, Krutskikh A, Huhtaniemi I, Poutanen M, Sipila P. Dicer1 ablation in the mouse epididymis causes dedifferentiation of the epithelium and imbalance in sex steroid signaling. PLoS One. 2012; 7: e38457. doi: 10.1371/journal.pone.0038457 PMID: 22701646
26. Dun MD, Anderson AL, Bromfield EG, Asquith KL, Emmett B, McLaughlin EA, et al. Investigation of the expression and functional significance of the novel mouse sperm protein, a disintegrin and

metalloprotease with thrombospondin type 1 motifs number 10 (ADAMTS10). Int J Androl. 2012; 35: 572–589. doi: 10.1111/j.1365-2605.2011.01235.x PMID: 22458710

27. Zuo WL, Li S, Huang JH, Yang DL, Zhang G, Chen SL, et al. Sodium coupled bicarbonate influx regulates intracellular and apical pH in cultured rat caput epididymal epithelium. PLoS One. 2011; 6: e22283. doi: 10.1371/journal.pone.0022283 PMID: 21887217
28. Edgar R, Domrachev M, Lash AE. Gene Expression Omnibus: NCBI gene expression and hybridization array data repository. Nucleic Acids Res. 2002; 30: 207–210. PMID: 11752295
29. Livak KJ, Schmittgen TD. Analysis of relative gene expression data using real-time quantitative PCR and the 2(-Delta Delta C(T)) Method. Methods. 2001; 25: 402–408. PMID: 11846609
30. Sipila P, Shariatmadari R, Huhtaniemi IT, Poutanen M. Immortalization of epididymal epithelium in transgenic mice expressing simian virus 40 T antigen: characterization of cell lines and regulation of the polyoma enhancer activator 3. Endocrinology. 2004; 145: 437–446. PMID: 14527890
31. Jelinsky SA, Turner TT, Bang HJ, Finger JN, Solarz MK, Wilson E, et al. The rat epididymal transcriptome: comparison of segmental gene expression in the rat and mouse epididymides. Biol Reprod. 2007; 76: 561–570. PMID: 17167166
32. Johnston DS, Turner TT, Finger JN, Owtscharuk TL, Kopf GS, Jelinsky SA. Identification of epididymis-specific transcripts in the mouse and rat by transcriptional profiling. Asian J Androl. 2007; 9: 522–527. PMID: 17589790
33. Roush S, Slack FJ. The let-7 family of microRNAs. Trends Cell Biol. 2008; 18: 505–516. doi: 10.1016/j.tcb.2008.07.007 PMID: 18774294
34. Cooper TG. The epididymis, sperm maturation and fertilisation. Berlin: Springer-Verlag; 1986.
35. Ni MJ, Hu ZH, Liu Q, Liu MF, Lu MH, Zhang JS, et al. Identification and characterization of a novel non-coding RNA involved in sperm maturation. PLoS One. 2011; 6: e26053. doi: 10.1371/journal.pone.0026053 PMID: 22022505
36. Krawetz SA, Kruger A, Lalancette C, Tagett R, Anton E, Draghici S, et al. A survey of small RNAs in human sperm. Hum Reprod. 2011; 26: 3401–3412. doi: 10.1093/humrep/der329 PMID: 21989093
37. Miller D, Briggs D, Snowden H, Hamlington J, Rollinson S, Lilford R, et al. A complex population of RNAs exists in human ejaculate spermatozoa: implications for understanding molecular aspects of spermiogenesis. Gene. 1999; 237: 385–392. PMID: 10521662
38. Miller D, Ostermeier GC. Spermatozoal RNA: Why is it there and what does it do? Gynecol Obstet Fertil. 2006; 34: 840–846. PMID: 16971154
39. Ostermeier GC, Goodrich RJ, Diamond MP, Dix DJ, Krawetz SA. Toward using stable spermatozoal RNAs for prognostic assessment of male factor fertility. Fertil Steril. 2005; 83: 1687–1694. PMID: 15950637
40. Guyonnet B, Dacheux F, Dacheux JL, Gatti JL. The epididymal transcriptome and proteome provide some insights into new epididymal regulations. J Androl. 2011; 32: 651–664. doi: 10.2164/jandrol.111.013086 PMID: 21764898
41. Dacheux JL, Belghazi M, Lanson Y, Dacheux F. Human epididymal secretome and proteome. Mol Cell Endocrinol. 2006; 250: 36–42. PMID: 16431015
42. Dacheux JL, Castella S, Gatti JL, Dacheux F. Epididymal cell secretory activities and the role of proteins in boar sperm maturation. Theriogenology. 2005; 63: 319–341. PMID: 15626402
43. Wong N, Wang X. miRDB: an online resource for microRNA target prediction and functional annotations. Nucleic Acids Res. 2015; 43: D146–152. doi: 10.1093/nar/gku1104 PMID: 25378301
44. Nagaraju GP, Dontula R, El-Rayes BF, Lakka SS. Molecular mechanisms underlying the divergent roles of SPARC in human carcinogenesis. Carcinogenesis. 2014; 35: 967–973. doi: 10.1093/carcin/bgu072 PMID: 24675529
45. Yekta S, Tabin CJ, Bartel DP. MicroRNAs in the Hox network: an apparent link to posterior prevalence. Nat Rev Genet. 2008; 9: 789–796. doi: 10.1038/nrg2400 PMID: 18781158
46. Bomgardner D, Hinton BT, Turner TT. Hox transcription factors may play a role in regulating segmental function of the adult epididymis. J Androl. 2001; 22: 527–531. PMID: 11451347
47. Bomgardner D, Hinton BT, Turner TT. 5' hox genes and meis 1, a hox-DNA binding cofactor, are expressed in the adult mouse epididymis. Biol Reprod. 2003; 68: 644–650. PMID: 12533430
48. Yeung CH, Wang K, Cooper TG. Why are epididymal tumours so rare? Asian J Androl. 2012; 14: 465–475. doi: 10.1038/aja.2012.20 PMID: 22522502
49. Wang K, Li N, Yeung CH, Li JY, Wang HY, Cooper TG. Oncogenic Wnt/beta-catenin signalling pathways in the cancer-resistant epididymis have implications for cancer research. Mol Hum Reprod. 2013; 19: 57–71. doi: 10.1093/molehr/gas051 PMID: 23155044

50. Nadiminty N, Tummala R, Lou W, Zhu Y, Zhang J, Chen X, et al. MicroRNA let-7c suppresses androgen receptor expression and activity via regulation of Myc expression in prostate cancer cells. J Biol Chem. 2012; 287: 1527–1537. doi: 10.1074/jbc.M111.278705 PMID: 22128178

51. Boyerinas B, Park SM, Hau A, Murmann AE, Peter ME. The role of let-7 in cell differentiation and cancer. Endocrine-Related Cancer. 2010; 17: F19–36. doi: 10.1677/ERC-09-0184 PMID: 19779035

52. Johnson CD, Esquela-Kerscher A, Stefani G, Byrom M, Kelnar K, Ovcharenko D, et al. The let-7 microRNA represses cell proliferation pathways in human cells. Cancer Res. 2007; 67: 7713–7722. PMID: 17699775

53. Kim W, Kim M, Jho EH. Wnt/beta-catenin signalling: from plasma membrane to nucleus. Biochem J. 2013; 450: 9–21. doi: 10.1042/BJ20121284 PMID: 23343194

BIOLOGY OF REPRODUCTION (2015) **93**(4):91, 1–20
Published online before print 2 September 2015.
DOI 10.1095/biolreprod.115.132209

The MicroRNA Signature of Mouse Spermatozoa Is Substantially Modified During Epididymal Maturation[1]

Brett Nixon,[2,3] Simone J. Stanger,[3] Bettina P. Mihalas,[3] Jackson N. Reilly,[3] Amanda L. Anderson,[3] Sonika Tyagi,[4] Janet E. Holt,[5] and Eileen A. McLaughlin[3]

[3]Reproductive Science Group, School of Environmental and Life Sciences, Faculty of Science and IT, University of Newcastle, Callaghan, New South Wales, Australia
[4]Australian Genome Research Facility Ltd, The Walter and Eliza Hall Institute, Parkville, Victoria, Australia
[5]School of Biomedical Sciences and Pharmacy, Faculty of Health and Medicine, University of Newcastle, Callaghan, New South Wales, Australia

ABSTRACT

In recent years considerable effort has been devoted to understanding the epigenetic control of sperm development, leading to an increased appreciation of the importance of RNA interference pathways, and in particular miRNAs, as key regulators of spermatogenesis and epididymal maturation. It has also been shown that sperm are endowed with an impressive array of miRNA that have been implicated in various aspects of fertilization and embryo development. However, to date there have been no reports on whether the sperm miRNA signature is static or whether it is influenced by their prolonged maturation within the male reproductive tract. To investigate this phenomenon, we employed next-generation sequencing to systematically profile the miRNA signature of maturing mouse spermatozoa. In so doing we have provided the first evidence for the posttesticular modification of the sperm miRNA profile under normal physiological conditions. Such modifications include the apparent loss and acquisition of an impressive cohort of some 113 and 115 miRNAs, respectively, between the proximal and distal epididymal segments. Interestingly, the majority of these changes occur late in maturation and include the uptake of novel miRNA species in addition to a significant increase in many miRNAs natively expressed in immature sperm. Because sperm are not capable of de novo transcription, these findings identify the epididymis as an important site in establishing the sperm epigenome with the potential to influence the peri-conceptual environment of the female reproductive tract, contribute to the inheritance of acquired characteristics, and/or alter the developmental trajectory of the resulting offspring.

AGO2, DICER1, epididymis, fertilization, male reproductive tract, microRNA, miRNA, next-generation sequencing, sperm, sperm maturation, spermatozoa

INTRODUCTION

In recent years it has become clear that the RNA interference (RNAi) pathway acts as a virtually ubiquitous tier of posttranscriptional gene regulation in a wide variety of eukaryotes, including animals [1, 2]. Critical elements of this pathway include a family of small single-stranded noncoding RNA molecules (~21–25 nucleotides) that are known as miRNA. The biogenesis of miRNAs originates from primary transcripts (pri-miRNA) that are sequentially processed in the nucleus by the RNase DROSHA, and within the cytoplasm by the endoribonuclease DICER. One strand of the resulting mature miRNA is preferentially loaded into an effector miRNA-induced silencing complex (miRISC), where it serves to guide the complex to target mRNA and facilitate the formation of a miRNA-mRNA duplex based on sequence complementarity. Once bound, the mRNA is usually targeted for increased degradation, and hence translational repression, via the catalytic activity of argonaute (AGO) proteins associated within the miRISC complex [1, 2]. With numbers of identified miRNAs now numbering in the thousands, they have been increasingly implicated in a broad range of developmental processes.

In terms of male reproduction, miRNAs and their associated processing machinery have been shown to play an essential role in regulating the differentiation of spermatozoa in the testes, with inactivation of genes such as dicer 1, ribonuclease type III (*Dicer1*) leading to a severe impact on the formation of mature germ cells [3–8]. However, an emerging body of evidence indicates that this role may also extend to the regulation of the posttesticular maturation and storage of spermatozoa within the male reproductive tract (epididymis) [9–12]. Indeed, a complex signature of several hundred miRNAs has been documented in the epididymis of species such as the mouse, human, rat, and bovine, and several of these are significantly enriched or uniquely expressed within this tissue [13–15]. In a majority of these global miRNA profiling studies, the authors have not distinguished between the precise contributions of the epididymal epithelium and those of the luminal contents. The latter comprises not only spermatozoa but also the highly specialized fluid environment responsible for promoting sperm maturation/storage. In our own systematic profiling of miRNAs present in whole epididymal tissue versus that of enriched populations of epithelial cells we have identified luminal spermatozoa and/or epididymal fluid as a major contributor to the overall epididymal miRNA signature [16].

These findings accord with established evidence that, despite their transcriptionally inert state, spermatozoa harbor

[1]Supported by the National Health and Medical Research Council of Australia (APP1062371).
[2]Correspondence: Brett Nixon, School of Environmental and Life Sciences, Discipline of Biological Sciences, University of Newcastle, University Drive, Callaghan, NSW 2308, Australia.
E-mail: Brett.Nixon@newcastle.edu.au

Received: 2 June 2015.
First decision: 30 June 2015.
Accepted: 24 August 2015.

eISSN: 1529-7268 http://www.biolreprod.org
ISSN: 0006-3363

diverse RNA populations including mRNAs and numerous small noncoding RNA species, including miRNAs, piRNAs, tRNA/rRNA-derived small RNAs, and snoRNAs [17–24]. These RNA species were originally thought to be remnants of untranslated mRNA stores generated during spermatogenesis and therefore to play a limited role in fertilization and early embryonic development. However, it is now apparent that paternal mRNAs and noncoding RNAs are delivered to the oocyte, along with the haploid genome, at the time of fertilization [25] and that the latter have the potential to modulate the stability and translational efficiency of maternal transcripts prior to activation of the zygotic genome [26–28]. Such findings are of significance because each of these contributions from the fertilizing spermatozoon represents a source of potential dysfunction. Indeed, aberrant embryo miRNA expression has been detected in human blastocysts derived from patients with male-factor infertility, suggestive of a contribution from subfertile sperm that adversely affected the phenotype of the resulting embryo [29]. Furthermore, different miRNA profiles have been identified in sperm samples exhibiting high levels of abnormal morphology and low motility compared to that of normal spermatozoa [17, 30–37]. It has therefore been proposed that the complement of sperm-borne miRNAs could hold considerable diagnostic value as noninvasive molecular markers of male infertility.

Despite the implications of this work, it has yet to be established whether such perturbations to the sperm miRNA content arise during testicular development, or alternatively whether they are influenced by altered profiles of miRNAs being conveyed to spermatozoa during their prolonged residence within the epididymis. We have therefore sought to determine whether the miRNA species present in mature spermatozoa cells are solely the remnants of the spermatogenic process, or whether they instead contain contributions of exogenous miRNAs that may be actively delivered to the sperm during their passage through the epididymis.

MATERIALS AND METHODS

Reagents

Unless specified, chemical reagents were obtained from Sigma or Life Technologies and were of research grade. The following primary antibodies were purchased to characterize proteins of interest: rabbit polyclonal anti-DICER1 antibody (ab13502; Abcam), rabbit polyclonal anti-androgen receptor (SAB4501575; Sigma), rat monoclonal anti-argonaute RISC catalytic subunit 2 (AGO2) (SAB4200085; Sigma), goat polyclonal anti-Izumo sperm-egg fusion 1 (IZUMO1) (sc-79543; Santa Cruz Biotechnology), and rabbit polyclonal anti-keratin 8 (ab59400; Abcam). Alexa Fluor 488-conjugated goat anti-rabbit (A11008), 594-conjugated goat anti-rat (A11007), and 594-conjugated goat anti-rabbit (A11012) antibodies were purchased from Life Technologies.

Ethics Statement

All experimental procedures were carried out with the approval of the University of Newcastle's Animal Care and Ethics Committee (ACEC) (approval number A-2013-322) in accordance with the specific guidelines and standards prescribed by the Society for the Study of Reproduction. Inbred Swiss mice were obtained from a breeding colony held at the institute's Central Animal House and maintained according to the recommendations prescribed by the ACEC. Mice were housed under a controlled lighting regime (16L:8D) at 21–22°C and supplied with food and water ad libitum. Prior to dissection, animals were euthanized via CO_2 inhalation.

Epididymal Sperm Isolation and Characterization

Immediately after adult male mice (8 wk old) were euthanized, their vasculature was perfused with prewarmed PBS to minimize the possibility of blood contamination. The epididymides were then removed, separated from fat and overlying connective tissue, and carefully dissected into three anatomical regions corresponding to the caput, corpus, and cauda. Caudal spermatozoa were collected from the lumen via retrograde perfusion with water-saturated paraffin oil as previously described [38]. In contrast, caput and corpus spermatozoa were recovered by placing the tissue in a 500-μl droplet of modified Biggers, Whitten, and Whittingham media (BWW; [39]) composed of 91.5 mM NaCl, 4.6 mM KCl, 1.7 mM $CaCl_2{\cdot}2H_2O$, 1.2 mM KH_2PO_4, 1.2 mM $MgSO_4{\cdot}7H_2O$, 25 mM $NaHCO_3$, 5.6 mM D-glucose, 0.27 mM sodium pyruvate, 44 mM sodium lactate, 5 U/ml penicillin, 5 μg/ml streptomycin, 20 mM Hepes buffer, and 3 mg/ml bovine serum albumin [BSA]) (pH 7.4; osmolarity 300 mOsm/kg). After multiple incisions were made with a razor blade, the spermatozoa were gently washed into the medium with mild agitation. All sperm preparations were then subjected to centrifugation ($400 \times g$ for 15 min) on a 27% Percoll density gradient. The pellet, consisting of an enriched population of >95% spermatozoa was resuspended in BWW and recentrifuged ($400 \times g$ for 2 min) to remove excess Percoll. A portion of the cells were then labeled with Diff-Quik in accordance with the manufacturer's protocols (Lab Aids Pty. Ltd.) [40]. The purity of this preparation was confirmed by microscopy (counting a minimum of 200 cells/sample) and immunoblotting with sperm- and tissue-specific markers (see below) (Fig. 1). Upon confirmation of sperm cell enrichment, samples were pooled and then subjected to RNA extraction as described below.

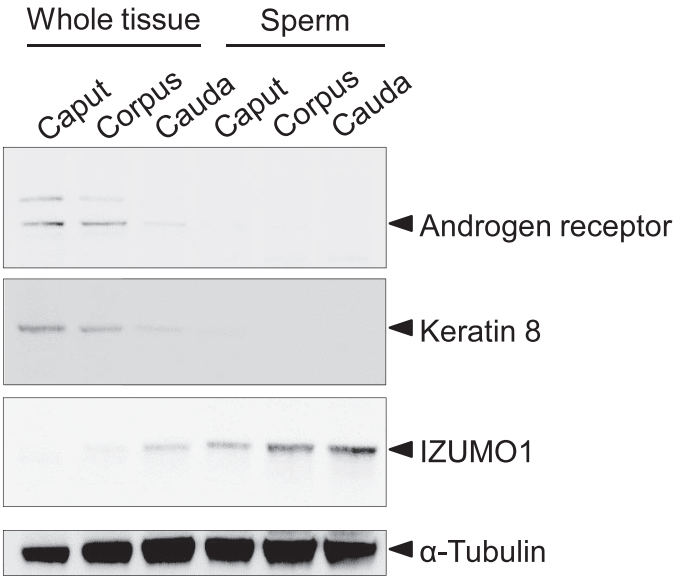

FIG. 1. Isolation and assessment of epididymal spermatozoa. The purity of sperm cell suspensions isolated from the caput, corpus, and cauda epididymis was assessed by immunoblotting with antibodies against tissue- (androgen receptor, 110 kDa; keratin 8, 54 kDa) and sperm- (IZUMO1, 60 kDa) specific markers. Anti-α-tubulin was included as a loading control. This analysis was repeated for each isolation and representative immunoblots are shown.

Immunofluorescent Localization

Testicular germ cells were isolated as previously described [41] and, together with purified epididymal spermatozoa, were assessed for key components of the miRNA biogenesis machinery. Briefly, germ cells and spermatozoa were settled onto poly-L-lysine-coated coverslips overnight at 4°C. All subsequent incubations were performed at 37°C in a humidified chamber, and all antibody dilutions and washes were conducted in PBS containing 0.1% Tween-20 (PBST). Fixed cells were permeabilized in 0.2% Triton X-100/PBS for 10 min and blocked in 3% (w/v) BSA in PBST for 1 h. Slides were then sequentially labeled with anti-DICER and anti-AGO2 antibodies (diluted 1:150) overnight at 4°C. After incubation, the slides were washed three times, then incubated in goat anti-rabbit 488 Alexa Fluor and goat anti-rat 594 Alexa Fluor (diluted 1:400) secondary antibodies for 1 h at 37°C. Cells were then washed and counterstained in 4′,6-diamidino-2-phenylindole (DAPI) before mounting in antifade reagent (Mowiol 4-88). Labeled cells were viewed on an Axio Imager A1 microscope (Carl Zeiss MicroImaging, Inc.) equipped with epifluorescent optics and images captured with an Olympus DP70 microscope camera (Olympus America).

RNA Extraction and miRNA Next-Generation Sequencing

Total RNA was extracted separately from purified populations of caput, corpus, and cauda epididymal spermatozoa ($\sim 25 \times 10^6$ sperm/sample) using a Direct-zol RNA MiniPrep Kit (Zymo Research Corporation) according to manufacturer's instructions before being incubated with 1% DNase (Promega) to eliminate genomic DNA contamination. This preparation of total RNA was pooled from a minimum of nine animals to generate a single biological replicate (comprising ~5 μg total RNA). One microgram from two such replicates was subjected to Illumina TruSeq small RNA sample preparation protocol as per the manufacturer's instructions (Illumina Inc.) at the Australian Genome Research Facility (AGRF; Brisbane, QLD, Australia). The libraries so generated were each analyzed in triplicate using an Illumina Hiseq-2000 RNA-seq platform as 50-bp single-end chemistry at AGRF. Briefly, the sequence reads from all samples were analyzed for quality control, screened for the presence of any contaminants, and trimmed based on their matches to PhiX, Adaptors, ChrM, or Mouse rRNA. Cleaned sequence reads were then aligned against two different databases: 1) *Mus musculus* genome (Build version mm10), and 2) miRNA database (miRBASE release20 at http://www.mirbase.org/). Alignment against the mature miRNA sequences for mouse miRNAs were summarized and counts were recorded for known miRNAs.

Differential miRNA expression analysis was undertaken using R script based on limma and voom libraries (http://www.bioconductor.org/packages/release/bioc/vignettes/limma/inst/doc/usersguide.pdf). A count value of >10 was used as the cutoff for presence/absence and expression-profiling comparisons were performed for mature miRNAs in the spermatozoa of individual epididymal regions with a data filter set to ≥2-fold difference and false discovery rate (FDR) of 0.05. The data discussed in this publication have been deposited in NCBI's Gene Expression Omnibus [42] and are accessible through GEO Series accession numbers GSE70197 (epididymal epithelial miRNAs) and GSE70198 (epididymal sperm miRNAs) (http://www.ncbi.nlm.nih.gov/geo/query/acc.cgi?acc=GSE70197; http://www.ncbi.nlm.nih.gov/geo/query/acc.cgi?acc=GSE70198).

Quantitative Real-Time PCR Confirmation of Selected miRNAs

Validation of miRNA expression profiles was conducted using a quantitative real-time PCR (qRT-PCR) strategy with Taqman miRNA assay reagents according to the manufacturer's instructions (Life Technologies). The miRNAs selected for analysis were *let-7b-5p* (assay ID 002619), *miR-465a-5p* (assay ID 001826), *miR-470-5p* (assay ID 002588), *miR-34b-5p* (assay ID 002617), *miR-34c-5p* (assay ID 000428), *miR-196b-5p* (assay ID 002215), *miR-145-5p* (assay ID 002278), *miR-181b-5p* (assay ID 001098) and *miR-127-3p* (assay ID 000452). Quantitative RT-PCR was performed on cDNA generated from 350 ng RNA using a Light Cycler 96 SW 1.1 (Roche). The U6 small nuclear RNA (assay ID 001973) was employed as an endogenous control to normalize the expression levels of target genes, and relative expression levels were calculated using the $2^{-\Delta Ct}$ method [43].

In Silico Analysis of miRNAs and Target Prediction

The miRNAs displaying statistically significant patterns of differential expression were clustered (Cluster3, Stanford University) and examined using heatmaps (Java Treeview, Stanford University) to visualize trends and consistency in miRNA expression in caput, corpus, and caudal epididymal spermatozoa. To gain a better understanding of the function of the miRNAs present within cauda epididymal spermatozoa, their mRNA targets were analyzed with Ingenuity Pathway Analysis (IPA) software (version 8.8, Ingenuity Systems) using the Core Analysis. Similarly, we also interrogated IPA in order to identify the key affected pathways likely to be regulated by caudal sperm miRNAs using the miRNA filter and restricting our analysis to experimentally confirmed targets.

SDS-PAGE and Western Blotting

Proteins were extracted in a modified SDS-PAGE sample buffer (2% w/v SDS, 10% w/v sucrose in 0.1875 M Tris, pH 6.8) with protease inhibitor tablets by incubation at 100°C for 5 min. Insoluble matter was removed by centrifugation at 20 000 × *g* for 10 min and protein estimations were performed using the DC Protein Assay kit (Bio-Rad). Proteins were boiled in SDS-PAGE sample buffer (2% v/v mercaptoethanol, 2% w/v SDS, and 10% w/v sucrose in 0.1875 M Tris, pH 6.8, with bromophenol blue) and resolved by SDS-PAGE on polyacrylamide gels followed by transfer onto nitrocellulose membranes. Membranes were blocked with 3% w/v BSA in Tris-buffered saline (TBS; pH 7.4) for 1 h before being probed with 1:1000 dilutions of primary antibody in TBS containing 1% w/v BSA and 0.1% v/v polyoxyethylenesorbitan monolaurate (Tween-20; TBS-T) for 2 h at room temperature. Blots were washed three times in TBS-T followed by incubation with 1:1000 horseradish peroxidase-conjugated secondary antibody in 1% w/v BSA/TBS-T for 1 h. Following three washes in TBS-T, proteins were detected using an enhanced chemiluminescence kit (Amersham) and visualized on ImageQuant LAS 4000 (Fujifilm).

Statistical Analysis

Statistical significance was determined using ANOVA, Tukey-Kramer HSD, and *t*-tests employing JMP software (version 9.0.0). $P < 0.05$ was considered significant. Experiments were performed in triplicate unless otherwise stated. Data are expressed as mean ± SEM.

RESULTS

The miRNA Signature of Mouse Spermatozoa Is Substantially Modified During Epididymal Maturation

Prior to undertaking a detailed analysis of sperm miRNA signatures, we first examined the level of enrichment achieved during the isolation of these cells. As shown in Supplemental Figure S1 (all supplemental data available online at www.biolreprod.org), highly purified populations of spermatozoa were recovered from the caput, corpus, and cauda epididymidis, with an estimation of <5% cellular contamination identified in each sample. This result was confirmed by immunoblotting of sperm lysates with established markers of epididymal epithelial cells, androgen receptor and keratin 8, neither of which were detected within this preparation (Fig. 1). Conversely, the intrinsic sperm protein, IZUMO1, was highly enriched in the isolated sperm samples (Fig. 1). Next-generation sequence analysis of these sperm preparations revealed that they harbor a complex array of some 262 mature miRNAs in the proximal segment (caput) of the epididymis (Fig. 2A and Table 1). Of these miRNAs, the highest signal intensities were associated with *miR-148a-3p, miR-10b-5p, miR-10a-5p, miR-22-3p*, and *let-7c-5p*, whereas conversely other members of these families (e.g., *miR-10a-3p*, *let-7f-1-3p*) were present at very low levels, thus establishing an impressive dynamic range of miRNA abundance of $>10^4$ orders of magnitude. Interestingly, however, this miRNA signature is modified by an apparent loss and gain of a substantial number of miRNAs as the spermatozoa progress through the corpus and cauda epididymal regions, such that the relative levels of only 44 of the total pool of miRNAs did not change significantly between all subpopulations of sperm examined (Fig. 2 and Table 1).

In the context of miRNA loss, this appeared to encompass the complete removal of 94 (~36%) of the caput sperm miRNAs such that they were below the level of detection in corpus spermatozoa (Fig. 2A and Table 1). These changes were accompanied by a significant reduction in the relative levels of expression (fold change of ≥ 2; FDR <0.05) of a further 7 (~3%) miRNAs (Fig. 2B and Table 1). In contrast, of the 169 miRNAs remaining in corpus spermatozoa, 41 (24%) of these were apparently lost as the cells transitioned into the cauda (Fig. 2A and Table 1), and almost half (81/169, 48%) experienced a significant reduction in their overall expression levels between these regions (Fig. 2B and Table 1). Although such pronounced changes may, in part, reflect the shedding of miRNAs along with the cytoplasmic droplet, a potentially more interesting finding was the acquisition of a relatively large cohort of miRNAs into the maturing sperm cells.

Indeed, accompanying sperm transport from the caput to the corpus, we observed a significant increase in the expression of 29 (17%) of the endogenous sperm miRNAs (Fig. 2B and

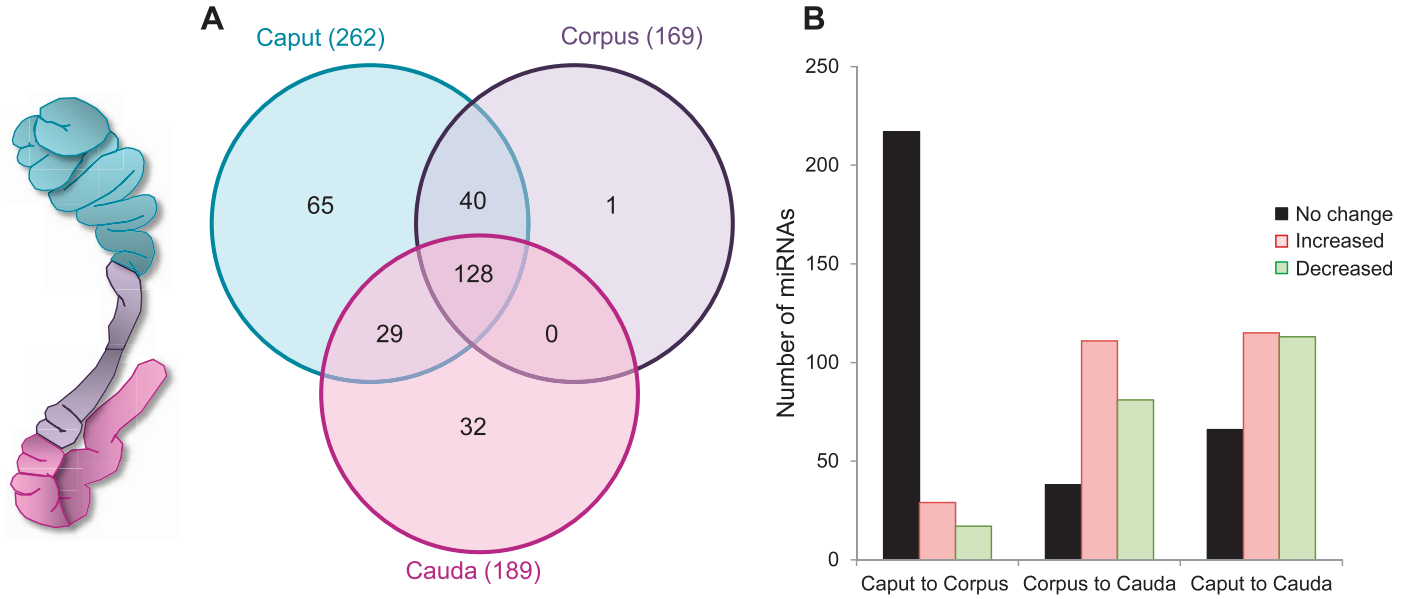

FIG. 2. Determination of the miRNA signature present in mouse epididymal spermatozoa. **A**) Venn diagram illustrating the number of miRNAs that were identified by next-generation sequencing and their disruption within spermatozoa sampled from the caput, corpus, and cauda regions of the adult mouse epididymis. **B**) Graphical representation of miRNA distribution highlighting the number of significantly up- and down-regulated (threshold = ± ≥2-fold change and FDR of <0.05) miRNAs positively identified in spermatozoa between each epididymal region. For the purpose of these analyses, an average count value of >10 across two biological replicates (with each replicate comprising pooled miRNA from a minimum of nine animals) was used as the threshold for positive identification of all miRNAs.

Table 1), in addition to the detection of a single novel miRNA within these cells (Fig. 2A and Table 1). By comparison, a total of 111 miRNAs, representing an impressive 59% of all caudal sperm miRNAs, experienced a significant increase in expression beyond the levels at which they were detected in corpus spermatozoa (Fig. 2B and Table 1). Between the same regions, 61 (32%) miRNAs were apparently acquired by the maturing spermatozoa, including the unexpected finding of 29 miRNAs that were originally detected in caput cells before being lost in those of the corpus (Fig. 2A and Table 1). At present we do not have a biological explanation for this intriguing observation.

Quantitative analysis of differentially expressed miRNAs revealed that many underwent substantial fold changes between the caput/corpus (Fig. 3A) and corpus/cauda epididymis (Fig. 3B). As anticipated, even more pronounced changes were apparent in comparisons of sperm from the caput and caudal segments of the organ (Fig. 3C). Among the numerous examples of these, miRNAs such as *miR-471-5p*, *miR-743a-5p*, *miR-871-5p*, *miR-880-3p*, *miR-465a-3p*, and *miR-470-5p* were characterized by increases in expression of >256-fold between the caput and caudal regions. Conversely, miRNAs *miR-181b-5p*, *miR127-3p*, *miR-150-5p*, and *let-7e-5p* were down-regulated by >32-fold over the same regions (Fig. 3C). Importantly, we recorded consistent results across each biological replicate in terms of both the overall number of miRNA reads (Table 1) and the relative fold change between regions (Fig. 4) that were detected by next-generation sequencing.

Validation of Differentially Expressed miRNAs

Given the novelty of our next-generation sequence data, nine differentially expressed miRNAs were selected for targeted validation via quantitative RT-PCR (qRT-PCR). These candidate miRNAs included representatives that exhibited gradients in expression ranging from highest expression in the caput (*let-7b-5p, miR-145-5p, miR-181b-5p, and miR-127-3p*) to highest expression in the cauda (*miR-465a-5p*, *miR-miR-470-5p, miR-34b-5p*, and *miR-34c-5p*) epididymis. All qRT-PCR experiments were performed in triplicate using three distinct pools of biological samples (n = 9 animals/sample) differing from those employed for next-generation sequence analyses. In each experiment, the U6 small nuclear RNA was employed as an endogenous control to normalize the expression levels of target miRNAs. This analysis confirmed the differential expression of each of the nine target miRNAs within epididymal spermatozoa (Fig. 5). Furthermore, each of these targets was shown to have an expression profile that closely mirrored the trends identified by next-generation sequence analysis (Fig. 5). In this context, qRT-PCR confirmed the peak of miR-196b-5p expression occurred within corpus spermatozoa, which contained significantly higher levels of this miRNA than either caput or caudal cells. In contrast, *miR-465a-5p*, *miR-470-5p*, *miR-34b-5p*, and *miR-34c-5p* each experienced a significant increase in expression in caudal spermatozoa compared to that of cells sampled from more proximal regions. Finally, *let-7b-5p*, *miR-145-5p*, *miR-181b-5p*, and *miR-127-3p* were each confirmed as being predominantly expressed in caput/corpus spermatozoa. Such findings attest to the accuracy of our data in reflecting the spatial patterns of mouse epididymal sperm miRNA signatures.

miRNAs Acquired by Spermatozoa Are Represented in Epididymal Epithelial Tissue

Having confirmed significant changes in the overall profile and relative levels of miRNAs present within maturing epididymal spermatozoa, we next sought to determine whether these changes may be attributed to miRNAs that are produced in the surrounding epithelial cells before being delivered to the luminal environment. For this purpose we compared the miRNA signature of epididymal spermatozoa with that of the surrounding epithelial cells determined in a previous study [16] (accession number GSE70197; Table 2). This analysis

TABLE 1. Relative expression levels of miRNAs identified by next-generation sequencing within mouse epididymal spermatozoa.

		miRNA reads[a]						False discovery rate (FDR)		
		Caput		Corpus		Cauda				
miRNA family	miRNA[b]	Replicate 1	Replicate 2	Replicate 1	Replicate 2	Replicate 1	Replicate 2	Caput to corpus	Corpus to cauda	Caput to cauda
miR-1	*miR-1a-3p*	14.001	24.001	5.001	3.001	0.001	0.001	0.593	0.000	0.001
let-7	*let-7a-1-3p*	71.501	71.501	6.501	3.001	14.501	24.501	0.085	0.029	0.647
	let-7a-5p	14 311.501	12 329.501	3013.501	1626.501	4195.501	2385.501	0.831	0.349	0.460
	let-7b-3p	98.001	88.001	5.001	5.001	3.001	2.001	0.027	0.104	0.000
	let-7b-5p	4725.001	3960.501	541.001	372.501	31.001	52.501	0.035	0.000	0.000
	let-7c-2-3p	71.501	71.501	6.501	3.001	14.501	24.501	0.085	0.029	0.647
	let-7c-5p	36 277.501	33 872.001	4673.501	2905.001	558.501	539.001	0.009	0.000	0.000
	let-7d-3p	278.001	227.001	32.001	23.001	109.001	126.001	0.193	0.001	0.005
	let-7d-5p	1117.001	1131.001	352.001	170.001	64.001	66.001	0.368	0.000	0.000
	let-7e-3p	10.001	17.001	1.001	0.001	0.001	0.001	0.144	0.252	0.004
	let-7e-5p	1201.001	1255.001	194.001	116.001	8.001	9.001	0.137	0.000	0.000
	let-7f-1-3p	16.001	15.001	0.001	2.001	0.001	0.001	0.180	0.161	0.003
	let-7f-5p	31 240.001	24 252.001	6293.001	3211.001	667.001	523.001	0.770	0.000	0.000
	let-7g-5p	9986.501	8215.001	2265.001	993.001	1493.501	945.501	0.860	0.028	0.009
	let-7i-5p	4828.501	4274.001	1784.001	876.001	613.501	443.501	0.032	0.000	0.001
	miR-7a-1-3p	16.001	15.001	1.001	3.001	16.001	8.001	0.764	0.010	0.006
miR-9	*miR-9-3p*	35.001	11.001	0.001	1.001	4.001	3.001	0.076	0.078	0.846
	miR-9-5p	925.001	434.001	21.001	72.001	161.001	87.001	0.032	0.032	0.679
miR-10	*miR-10a-3p*	22.001	24.001	3.001	3.001	0.001	2.001	0.836	0.058	0.016
	miR-10a-5p	47 525.001	46 473.001	7403.501	4490.501	2498.501	1343.501	0.032	0.000	0.000
	miR-10b-5p	55 694.001	52 687.001	9473.501	6702.501	2356.501	1294.501	0.264	0.000	0.000
miR-15	*miR-15a-5p*	197.001	141.001	20.001	20.001	91.001	86.001	0.313	0.000	0.001
	miR-15b-5p	479.001	364.001	95.001	41.001	1128.001	645.001	0.639	0.000	0.000
miR-16	*miR-16-2-3p*	1.001	3.001	1.001	0.001	12.001	13.001	0.318	0.000	0.000
	miR-16-5p	5240.001	4056.001	1281.001	1099.001	36 958.001	23 259.001	0.048	0.000	0.000
miR-17	*miR-17-3p*	10.001	6.001	1.001	0.001	18.001	13.001	0.441	0.000	0.000
	miR-17-5p	355.668	282.001	51.334	33.001	104.001	82.001	0.353	0.035	0.181
miR-18	*miR-18a-5p*	24.001	12.001	13.001	8.001	363.001	234.001	0.029	0.000	0.000
miR-19	*miR-19a-3p*	76.001	54.001	25.001	25.001	698.501	660.001	0.076	0.000	0.000
	miR-19b-3p	328.001	271.001	90.001	63.001	2127.501	1749.001	0.183	0.000	0.000
miR-20	*miR-20a-5p*	417.668	285.001	66.334	47.001	522.001	422.001	0.842	0.000	0.000
miR-21	*miR-21-3p*	57.001	42.001	14.001	6.001	1.001	1.001	0.836	0.004	0.003
	miR-21-5p	20 275.001	18 827.001	3490.001	2148.001	2871.001	2766.001	0.248	0.249	0.011
miR-22	*miR-22-3p*	47 505.001	38 984.001	6657.001	4319.001	94 291.001	53 998.001	0.038	0.000	0.000
	miR-22-5p	35.001	19.001	4.001	1.001	6.001	6.001	0.319	0.203	0.819
miR-23	*miR-23a-3p*	485.001	452.001	107.001	67.001	25.001	15.001	0.891	0.000	0.000
	miR-23b-3p	402.001	409.001	124.001	73.001	129.001	97.001	0.242	0.791	0.256
miR-24	*miR-24-2-5p*	49.001	72.001	21.001	9.001	13.001	6.001	0.420	0.122	0.399
	miR-24-3p	763.001	570.001	88.001	30.001	11.001	7.001	0.021	0.000	0.000
miR-25	*miR-25-3p*	1372.001	1008.001	434.001	388.001	17 920.001	8395.001	0.007	0.000	0.000
miR-26	*miR-26a-5p*	18 949.001	20 670.001	6011.001	3680.001	3801.001	2424.001	0.065	0.000	0.016
	miR-26b-5p	873.001	716.001	211.001	96.001	180.001	190.001	0.917	0.960	0.808
miR-27	*miR-27a-3p*	404.001	421.001	79.001	69.001	11.001	6.001	0.946	0.000	0.000
	miR-27a-5p	42.001	43.001	12.001	5.001	0.001	0.001	0.815	0.000	0.000
	miR-27b-3p	6512.001	6304.001	1264.001	767.001	1460.001	981.001	0.505	0.904	0.328
	miR-27b-5p	17.001	11.001	2.001	2.001	5.001	8.001	0.999	0.174	0.099
miR-28	*miR-28-3p*	64.001	43.001	8.001	9.001	39.001	15.001	0.922	0.027	0.010
	miR-28-5p	77.001	62.001	19.001	9.001	20.001	10.001	0.801	0.732	0.963
miR-29	*miR-29a-3p*	3575.001	2907.001	683.001	338.001	322.001	242.001	0.486	0.001	0.000
	miR-29a-5p	15.001	10.001	2.001	0.001	0.001	1.001	0.361	0.484	0.053
	miR-29b-3p	1187.001	761.001	208.001	84.001	21.001	18.001	0.472	0.000	0.000
	miR-29c-3p	527.001	420.001	64.001	36.001	9.001	14.001	0.085	0.000	0.000
miR-30	*miR-30a-3p*	723.001	623.501	113.001	71.001	336.001	173.501	0.319	0.002	0.011
	miR-30a-5p	1498.001	1207.001	550.001	355.001	1006.001	558.001	0.009	0.087	0.000
	miR-30b-5p	3004.001	2537.001	639.001	505.001	3611.001	2550.001	0.440	0.000	0.000
	miR-30c-2-3p	87.001	79.001	12.001	11.001	26.001	21.001	0.575	0.161	0.323
	miR-30c-5p	1507.001	1362.001	262.001	186.001	1760.001	994.001	0.610	0.000	0.000
	miR-30d-3p	64.001	68.001	17.001	5.001	36.001	32.001	0.807	0.015	0.007
	miR-30d-5p	1244.001	1105.001	374.001	287.001	2224.001	1218.001	0.043	0.000	0.000
	miR-30e-3p	426.001	361.501	75.001	32.001	454.001	236.501	0.323	0.000	0.000
	miR-30e-5p	201.001	165.001	61.001	39.001	188.001	137.001	0.160	0.001	0.000
miR-31	*miR-31-5p*	153.001	58.001	14.001	9.001	45.001	39.001	0.499	0.022	0.039
miR-34	*miR-34a-5p*	198.001	222.001	63.001	16.001	3.001	2.001	0.831	0.000	0.000
	miR-34b-3p	181.001	264.001	67.001	105.001	13 749.001	6723.001	0.071	0.000	0.000
	miR-34b-5p	427.001	562.001	74.001	73.001	2561.501	2159.001	0.689	0.000	0.000
	miR-34c-3p	64.001	91.001	19.001	33.001	2134.001	1281.001	0.137	0.000	0.000
	miR-34c-5p	5607.001	10 752.001	1106.001	1581.001	66 318.501	49 188.001	0.941	0.000	0.000
miR-92	*miR-92a-1-5p*	24.001	29.001	3.001	8.001	7.001	5.001	0.877	0.970	0.851
	miR-92a-3p	377.001	265.001	151.001	82.001	389.001	205.001	0.024	0.006	0.000
	miR-92b-3p	496.001	1181.001	19.001	39.001	12.001	6.001	0.006	0.036	0.000

TABLE 1. *Continued.*

		miRNA reads[a]						False discovery rate (FDR)		
		Caput		Corpus		Cauda				
miRNA family	miRNA[b]	Replicate 1	Replicate 2	Replicate 1	Replicate 2	Replicate 1	Replicate 2	Caput to corpus	Corpus to cauda	Caput to cauda
miR-93	*miR-93-5p*	645.001	447.001	132.001	113.001	5674.001	3430.001	0.316	0.000	0.000
miR-96	*miR-96-5p*	547.001	401.001	97.001	64.001	10.001	8.001	0.922	0.000	0.000
miR-98	*miR-98-5p*	1184.001	924.001	294.001	157.001	28.001	34.001	0.505	0.000	0.000
miR-99	*miR-99a-5p*	441.001	550.001	159.001	97.001	43.001	34.001	0.152	0.000	0.000
	miR-99b-3p	20.001	19.001	4.001	2.001	0.001	0.001	0.961	0.002	0.001
	miR-99b-5p	12 085.001	15 395.001	2200.001	1854.001	211.001	107.001	0.388	0.000	0.000
miR-100	*miR-100-5p*	2046.001	3338.001	471.001	502.001	24.001	21.001	0.870	0.000	0.000
miR-101	*miR-101a-3p*	388.001	362.001	162.001	66.001	5.001	15.001	0.160	0.000	0.000
	miR-101b-3p	39.001	40.001	20.001	12.001	27.001	22.001	0.032	0.522	0.001
miR-103	*miR-103-3p*	2483.001	2623.501	552.001	321.501	2849.501	1560.501	0.831	0.000	0.000
miR-106	*miR-106b-3p*	8.001	13.001	3.001	7.001	184.001	93.001	0.176	0.000	0.000
	miR-106b-5p	89.001	67.001	19.001	16.001	9.001	7.001	0.479	0.019	0.048
miR-107	*miR-107-3p*	108.001	125.501	7.001	6.501	12.501	10.501	0.019	0.484	0.014
miR-124	*miR-124-3p*	0.001	1.001	2.001	15.001	67.001	33.001	0.001	0.001	0.000
miR-125	*miR-125a-5p*	3483.001	3208.001	307.001	160.001	40.001	37.001	0.001	0.000	0.000
	miR-125b-1-3p	43.001	60.001	17.001	13.001	5.001	3.001	0.180	0.004	0.032
	miR-125b-2-3p	20.001	24.001	11.001	3.001	2.001	0.001	0.347	0.003	0.010
	miR-125b-5p	4811.001	5399.001	879.001	497.001	248.001	138.001	0.147	0.000	0.000
miR-126	*miR-126-3p*	1171.001	656.001	171.001	96.001	8.001	4.001	0.539	0.000	0.000
	miR-126-5p	7056.001	4889.001	1471.001	969.001	76.001	68.001	0.477	0.000	0.000
miR-127	*miR-127-3p*	1336.001	1332.001	613.001	456.001	7.001	6.001	0.002	0.000	0.000
miR-128	*miR-128-3p*	90.001	81.001	20.001	37.001	747.001	498.001	0.147	0.000	0.000
miR-130	*miR-130a-3p*	210.001	265.001	117.001	37.001	270.001	202.001	0.167	0.002	0.000
	miR-130b-3p	8.001	6.001	1.001	3.001	111.001	57.001	0.472	0.000	0.000
	miR-130b-5p	5.001	9.001	0.001	0.001	228.001	89.001	0.195	0.000	0.000
miR-132	*miR-132-3p*	19.001	30.001	4.001	8.001	14.001	8.001	0.532	0.402	0.065
miR-133	*miR-133a-3p*	62.001	133.001	49.501	16.501	0.001	1.501	0.187	0.000	0.000
miR-135	*miR-135a-2-3p*	17.001	22.001	3.001	0.001	0.001	0.001	0.153	0.073	0.001
	miR-135a-5p	1852.001	1615.001	115.001	55.001	40.001	18.001	0.000	0.000	0.000
	miR-135b-5p	7.001	14.001	2.001	4.001	2.001	1.001	0.505	0.388	0.851
miR-138	*miR-138-5p*	133.001	113.001	17.001	17.001	14.001	9.001	0.532	0.096	0.012
miR-140	*miR-140-3p*	9.001	5.001	2.001	3.001	71.001	33.001	0.162	0.000	0.000
	miR-140-5p	62.001	36.001	12.001	6.001	29.001	29.001	0.891	0.037	0.006
miR-141	*miR-141-3p*	481.501	552.501	157.501	99.501	22.501	21.501	0.176	0.000	0.000
	miR-141-5p	39.001	47.001	12.001	4.001	15.001	3.001	0.971	0.732	0.704
miR-142	*miR-142-3p*	54.001	24.001	6.001	16.001	16.001	22.001	0.467	0.404	0.050
	miR-142-5p	904.001	611.001	222.001	303.001	864.001	769.001	0.032	0.001	0.000
miR-143	*miR-143-3p*	23 654.001	40 144.001	12 206.001	5504.001	697.001	578.001	0.176	0.000	0.000
miR-144	*miR-144-3p*	30.001	12.001	9.001	12.001	0.001	2.001	0.076	0.002	0.042
	miR-144-5p	17.001	8.001	7.001	11.001	1.001	2.001	0.035	0.012	0.600
miR-145	*miR-145-3p*	38.001	60.001	12.001	5.001	0.001	0.001	0.983	0.000	0.000
	miR-145-5p	739.001	1206.001	330.001	118.001	5.001	5.001	0.790	0.001	0.001
miR-146	*miR-146a-5p*	988.001	433.501	205.501	226.001	15.001	9.501	0.055	0.000	0.000
	miR-146b-5p	357.001	308.501	16.501	27.001	13.001	8.501	0.016	0.045	0.000
miR-148	*miR-148a-3p*	85 808.001	58 126.001	12 570.001	6658.001	7955.001	5639.001	0.152	0.006	0.000
	miR-148a-5p	434.001	368.001	43.001	27.001	92.001	51.001	0.026	0.073	0.297
	miR-148b-3p	339.001	297.001	97.001	66.001	816.001	419.001	0.137	0.000	0.000
miR-148	*miR-148b-5p*	14.001	21.001	6.001	1.001	27.001	24.001	0.961	0.001	0.000
miR-149	*miR-149-5p*	93.001	80.001	3.001	3.001	0.001	2.001	0.048	0.087	0.000
miR-150	*miR-150-5p*	96.001	100.001	52.001	35.001	0.001	0.001	0.011	0.000	0.000
miR-151	*miR-151-3p*	959.001	898.001	158.001	107.001	491.001	280.001	0.355	0.000	0.001
	miR-151-5p	1044.001	1122.001	292.001	201.001	5333.001	2782.001	0.313	0.000	0.000
miR-152	*miR-152-3p*	188.001	135.001	43.001	37.001	10.001	1.001	0.319	0.000	0.000
	miR-152-5p	57.001	44.001	10.001	8.001	0.001	2.001	0.922	0.001	0.000
miR-153	*miR-153-3p*	20.001	23.001	8.001	11.001	11.001	16.001	0.135	0.868	0.035
miR-181	*miR-181a-1-3p*	51.001	62.001	15.001	6.001	0.001	0.001	0.944	0.000	0.000
	miR-181a-5p	9811.001	9398.001	1317.001	1111.001	97.001	59.001	0.085	0.000	0.000
	miR-181b-5p	347.501	264.001	53.001	55.001	3.001	0.001	0.971	0.000	0.000
	miR-181c-3p	254.001	347.001	42.001	30.001	17.001	15.001	0.235	0.005	0.000
	miR-181c-5p	6849.001	8008.001	1686.001	953.001	1876.001	904.001	0.946	0.313	0.221
	miR-181d-5p	865.501	809.001	159.001	105.001	64.001	29.001	0.608	0.000	0.000
miR-182	*miR-182-5p*	5726.001	3615.001	603.001	359.001	617.001	350.001	0.031	0.315	0.001
miR-183	*miR-183-5p*	1652.001	1495.001	223.001	161.001	450.001	253.001	0.085	0.057	0.991
miR-184	*miR-184-3p*	20.001	24.001	69.001	67.001	768.001	754.001	0.000	0.000	0.000
miR-185	*miR-185-5p*	20.001	12.001	6.001	5.001	0.001	0.001	0.135	0.000	0.001
miR-186	*miR-186-5p*	598.001	627.001	302.001	176.001	584.001	327.001	0.005	0.037	0.000
miR-187	*miR-187-3p*	109.001	94.001	26.001	16.001	2.001	3.001	0.631	0.000	0.000
miR-190	*miR-190-5p*	11.001	3.001	20.001	8.001	0.001	0.001	0.001	0.000	0.111
miR-191	*miR-191-5p*	31 793.001	23 996.001	3935.001	3149.001	37 377.001	19 958.001	0.094	0.000	0.000
miR-192	*miR-192-5p*	1682.001	4581.001	167.001	150.001	3210.001	2024.001	0.010	0.000	0.000

TABLE 1. *Continued.*

		miRNA reads[a]						False discovery rate (FDR)		
		Caput		Corpus		Cauda				
miRNA family	miRNA[b]	Replicate 1	Replicate 2	Replicate 1	Replicate 2	Replicate 1	Replicate 2	Caput to corpus	Corpus to cauda	Caput to cauda
miR-193	*miR-193-3p*	15.001	28.001	5.001	2.001	1.001	2.001	0.971	0.150	0.100
	miR-193b-3p	2.001	13.001	2.001	0.001	17.001	4.001	0.918	0.009	0.002
miR-194	*miR-194-5p*	94.001	286.001	13.001	6.001	176.001	91.001	0.068	0.000	0.001
miR-195	*miR-195-5p*	604.001	775.001	197.001	126.001	264.001	141.001	0.280	0.975	0.185
miR-196	*miR-196a-5p*	32.001	26.001	173.001	48.001	1.001	2.001	0.000	0.000	0.042
	miR-196b-5p	31.001	56.001	175.001	103.001	0.001	1.001	0.000	0.000	0.002
miR-199	*miR-199a-3p*	194.001	265.501	108.501	105.001	2.501	2.501	0.005	0.000	0.000
	miR-199a-5p	181.001	244.001	87.001	43.001	2.001	1.001	0.085	0.000	0.000
	miR-199b-3p	194.001	265.501	108.501	105.001	2.501	2.501	0.005	0.000	0.000
	miR-199b-5p	23.001	36.001	12.001	11.001	1.001	1.001	0.076	0.000	0.007
miR-200	*miR-200a-3p*	1820.501	1704.501	319.501	191.501	105.501	177.501	0.500	0.009	0.001
	miR-200a-5p	71.001	87.001	17.001	8.001	19.001	12.001	0.831	0.971	0.785
	miR-200b-3p	2113.001	1719.001	288.001	128.001	67.001	100.001	0.085	0.002	0.000
	miR-200b-5p	49.001	39.001	7.001	6.001	4.001	11.001	0.870	0.598	0.371
	miR-200c-3p	4121.001	3218.001	778.001	459.001	101.001	93.001	0.831	0.000	0.000
miR-203	*miR-203-3p*	192.001	111.001	19.001	8.001	9.001	3.001	0.109	0.037	0.000
miR-204	*miR-204-5p*	5699.001	4529.001	670.001	525.001	185.001	63.001	0.069	0.000	0.000
miR-205	*miR-205-5p*	3382.001	2904.001	934.001	289.001	25.001	23.001	0.922	0.000	0.000
miR-210	*miR-210-3p*	676.001	563.001	217.001	143.001	16.001	8.001	0.032	0.000	0.000
	miR-210-5p	35.001	40.001	7.001	2.001	8.001	1.001	0.529	0.569	0.145
miR-214	*miR-214-3p*	42.001	115.001	26.001	10.001	1.001	0.001	0.505	0.000	0.000
	miR-214-5p	21.001	14.001	11.001	5.001	0.001	0.001	0.058	0.000	0.001
miR-218	*miR-218-5p*	57.001	73.001	17.001	11.001	6.001	7.001	0.548	0.022	0.042
miR-221	*miR-221-3p*	645.001	594.001	101.001	51.001	14.001	7.001	0.133	0.000	0.000
	miR-221-5p	46.001	45.001	8.001	3.001	1.001	2.001	0.505	0.036	0.003
miR-222	*miR-222-3p*	83.001	77.001	83.001	59.001	18.001	11.001	0.000	0.000	0.586
miR-223	*miR-223-3p*	23.001	14.001	5.001	10.001	0.001	0.001	0.182	0.000	0.003
miR-295	*miR-295-3p*	0.001	0.001	0.001	0.001	8.001	14.001	0.035	0.000	0.000
miR-296	*miR-296-5p*	19.001	17.001	11.001	7.001	232.001	192.001	0.048	0.000	0.000
miR-301	*miR-301a-3p*	382.001	462.001	126.001	66.001	1359.501	867.001	0.392	0.000	0.000
	miR-301b-3p	4.001	0.001	0.001	1.001	47.501	15.001	0.212	0.000	0.000
miR-320	*miR-320-3p*	117.001	129.001	40.001	21.001	18.001	18.001	0.373	0.048	0.209
miR-322	*miR-322-5p*	254.001	233.001	36.001	20.001	10.001	7.001	0.176	0.001	0.000
miR-324	*miR-324-5p*	57.001	53.001	15.001	5.001	21.001	13.001	0.977	0.374	0.287
miR-326	*miR-326-3p*	24.001	14.001	4.001	8.001	2.001	0.001	0.329	0.007	0.032
miR-328	*miR-328-3p*	142.001	201.001	27.001	10.001	50.001	38.001	0.176	0.048	0.522
miR-331	*miR-331-3p*	7.001	4.001	4.001	3.001	14.001	7.001	0.043	0.118	0.000
miR-335	*miR-335-3p*	12.001	13.001	6.001	2.001	0.001	0.001	0.323	0.001	0.004
miR-338	*miR-338-3p*	23.001	10.001	3.001	6.001	1.001	0.001	0.416	0.008	0.025
miR-339	*miR-339-3p*	22.001	16.001	2.001	1.001	0.001	0.001	0.420	0.029	0.001
	miR-339-5p	20.001	28.001	2.001	0.001	1.001	3.001	0.071	0.512	0.117
miR-340	*miR-340-3p*	18.001	15.001	0.001	2.001	28.001	25.001	0.169	0.000	0.000
	miR-340-5p	2549.001	2324.001	345.001	306.001	3025.001	2709.001	0.231	0.000	0.000
miR-342	*miR-342-3p*	151.001	124.001	41.001	44.001	266.001	228.001	0.081	0.000	0.000
miR-350	*miR-350-3p*	7.001	6.001	5.001	7.001	134.001	112.001	0.009	0.000	0.000
miR-351	*miR-351-5p*	126.001	109.001	25.001	7.001	1.001	0.001	0.404	0.000	0.000
miR-361	*miR-361-5p*	104.001	121.001	15.001	12.001	25.001	10.001	0.408	0.962	0.258
miR-362	*miR-362-3p*	17.001	8.001	2.001	3.001	5.001	10.001	0.674	0.295	0.066
miR-365	*miR-365-3p*	29.001	55.001	11.001	10.001	9.001	6.001	0.402	0.280	0.808
miR-374	*miR-374-5p*	43.001	20.001	16.001	9.001	6.001	3.001	0.058	0.016	0.487
miR-375	*miR-375-3p*	7671.001	14150.001	433.001	325.001	7737.001	4045.001	0.001	0.000	0.001
miR-378	*miR-378-3p*	564.001	593.001	160.001	79.001	28.001	31.001	0.664	0.000	0.000
	miR-378-5p	14.001	15.001	2.001	0.001	1.001	0.001	0.176	0.440	0.015
	miR-378b	18.001	14.001	5.001	1.001	0.001	0.001	0.978	0.006	0.002
miR-379	*miR-379-5p*	45.001	27.001	11.001	7.001	0.001	0.001	0.344	0.000	0.000
miR-381	*miR-381-3p*	15.001	17.001	8.001	10.001	9.001	6.001	0.020	0.361	0.047
miR-410	*miR-410-3p*	18.001	20.001	9.001	17.001	16.001	11.001	0.017	0.784	0.007
miR-411	*miR-411-5p*	321.001	257.001	98.001	66.001	2.001	1.001	0.135	0.000	0.000
miR-421	*miR-421-3p*	47.001	53.001	16.001	15.001	8.001	6.001	0.131	0.017	0.260
miR-423	*miR-423-3p*	428.001	343.001	42.001	27.001	48.001	35.001	0.035	0.913	0.007
	miR-423-5p	40.001	56.001	12.001	10.001	32.001	18.001	0.456	0.118	0.007
miR-425	*miR-425-5p*	206.001	169.001	57.001	40.001	2995.001	1926.001	0.221	0.000	0.000
miR-429	*miR-429-3p*	1614.001	1565.001	172.001	115.001	78.001	166.001	0.061	0.153	0.001
miR-434	*miR-434-3p*	110.001	115.001	76.001	31.001	22.001	18.001	0.018	0.004	0.553
miR-449	*miR-449a-5p*	72.001	95.001	23.001	20.001	894.001	589.001	0.340	0.000	0.000
miR-450	*miR-450a-5p*	38.001	42.001	5.001	4.001	12.001	3.001	0.505	0.806	0.586
miR-451	*miR-451*	148.001	68.001	66.001	85.001	2.001	1.001	0.001	0.000	0.000
miR-455	*miR-455-5p*	33.001	18.001	7.001	4.001	0.001	0.001	0.560	0.000	0.000
miR-463	*miR-463-5p*	2.001	2.001	3.001	3.001	30.001	26.001	0.007	0.000	0.000
miR-465	*miR-465a-3p*	6.334	5.001	5.001	3.001	477.001	302.001	0.032	0.000	0.000

TABLE 1. *Continued.*

		miRNA reads[a]						False discovery rate (FDR)		
		Caput		Corpus		Cauda				
miRNA family	miRNA[b]	Replicate 1	Replicate 2	Replicate 1	Replicate 2	Replicate 1	Replicate 2	Caput to corpus	Corpus to cauda	Caput to cauda
	miR-465a-5p	20.001	32.001	11.001	17.001	1451.001	919.001	0.025	0.000	0.000
	miR-465b-3p	6.334	5.001	5.001	3.001	477.001	302.001	0.032	0.000	0.000
	miR-465b-5p	2.001	1.001	1.001	0.001	187.001	1.001	0.627	0.030	0.005
	miR-465c-3p	6.334	5.001	5.001	3.001	477.001	302.001	0.032	0.000	0.000
	miR-465c-5p	62.001	35.001	43.001	50.001	3486.001	1780.001	0.002	0.000	0.000
miR-466	*miR-466a-3p*	3.501	5.501	0.501	1.001	25.501	15.001	0.595	0.000	0.000
	miR-466b-3p	14.001	8.334	1.668	1.668	7.001	8.334	0.918	0.050	0.013
	miR-466c-3p	14.001	8.334	1.668	1.668	7.001	8.334	0.918	0.050	0.013
	miR-466e-3p	3.501	5.501	0.501	1.001	25.501	15.001	0.595	0.000	0.000
	miR-466p-3p	14.001	8.334	1.668	1.668	7.001	8.334	0.918	0.050	0.013
miR-467	*miR-467a-5p*	209.001	156.001	15.001	10.001	93.001	59.001	0.019	0.000	0.007
	miR-467b-5p	4.001	3.001	0.001	0.001	24.001	13.001	0.651	0.000	0.000
	miR-467c-5p	25.001	12.001	4.001	0.001	10.001	12.001	0.387	0.016	0.048
	miR-467d-3p	12.001	12.001	0.001	0.001	18.501	13.501	0.018	0.000	0.000
	miR-467d-5p	27.001	38.001	4.001	0.001	8.001	2.001	0.072	0.174	0.460
	miR-467e-5p	47.001	52.001	7.001	2.001	38.001	34.001	0.187	0.000	0.001
miR-470	*miR-470-3p*	1.001	2.001	1.001	1.001	29.001	28.001	0.080	0.000	0.000
	miR-470-5p	106.001	85.001	86.001	101.001	7779.001	4049.001	0.001	0.000	0.000
miR-471	*miR-471-3p*	3.001	1.001	0.001	3.001	66.001	45.001	0.242	0.000	0.000
	miR-471-5p	0.001	1.001	1.001	2.001	66.001	78.001	0.010	0.000	0.000
miR-484	*miR-484*	118.001	118.001	25.001	11.001	21.001	10.001	0.664	0.370	0.108
	miR-486-5p	373.001	188.001	124.001	185.001	25.501	11.001	0.008	0.000	0.011
miR-497	*miR-497-5p*	258.001	240.001	51.001	22.001	32.001	15.001	0.486	0.058	0.006
miR-499	*miR-499-5p*	4.001	1.001	1.001	0.001	14.001	19.001	0.453	0.000	0.000
miR-500	*miR-500-3p*	25.001	21.001	6.001	2.001	3.001	2.001	0.999	0.451	0.371
miR-501	*miR-501-3p*	146.001	149.001	31.001	30.001	202.001	118.001	0.575	0.000	0.000
miR-511	*miR-511-3p*	13.001	11.001	4.001	4.001	0.001	0.001	0.180	0.000	0.003
miR-532	*miR-532-3p*	26.001	12.001	3.001	0.001	10.001	1.001	0.355	0.280	0.924
	miR-532-5p	252.001	218.001	45.001	35.001	340.001	183.001	0.946	0.000	0.000
miR-541	*miR-541-5p*	29.001	10.001	4.001	6.001	1.001	0.001	0.394	0.005	0.016
miR-574	*miR-574-3p*	43.001	36.001	14.001	14.001	3.001	0.001	0.085	0.000	0.001
	miR-574-5p	18.001	15.001	5.001	3.001	0.001	0.001	0.519	0.001	0.002
miR-582	*miR-582-3p*	16.001	4.001	1.001	0.001	0.001	1.001	0.595	0.823	0.357
miR-598	*miR-598-3p*	6.001	18.001	3.001	1.001	2.001	2.001	0.836	0.852	0.941
miR-615	*miR-615-3p*	18.001	14.001	6.001	2.001	0.001	0.001	0.505	0.000	0.001
miR-652	*miR-652-3p*	46.001	73.001	20.001	16.001	2.001	4.001	0.172	0.001	0.007
miR-669	*miR-669a-3p*	11.001	12.001	2.001	3.001	21.001	15.501	0.560	0.002	0.000
	miR-669a-5p	28.834	18.168	1.001	1.001	23.834	16.168	0.076	0.000	0.000
	miR-669b-5p	9.001	11.001	0.001	1.001	0.001	2.001	0.368	0.990	0.260
	miR-669c-5p	25.001	36.001	4.001	2.001	18.001	9.001	0.387	0.014	0.038
	miR-669d-5p	12.001	15.001	1.001	1.001	15.001	11.001	0.488	0.002	0.002
	miR-669f-5p	26.334	16.668	1.001	0.001	4.334	2.668	0.026	0.031	0.696
	miR-669l-5p	14.001	8.001	1.001	1.001	5.001	13.001	0.803	0.060	0.058
	miR-669o-3p	11.001	12.001	2.001	3.001	21.001	15.501	0.560	0.002	0.000
	miR-669o-5p	17.001	5.001	1.001	0.001	13.001	11.001	0.486	0.005	0.008
	miR-669p-5p	28.834	18.168	1.001	1.001	23.834	16.168	0.076	0.000	0.000
miR-671	*miR-671-3p*	51.001	41.001	3.001	1.001	4.001	4.001	0.046	0.467	0.073
miR-672	*miR-672-5p*	523.001	295.001	59.001	46.001	176.001	126.001	0.391	0.005	0.018
miR-674	*miR-674-3p*	11.001	12.001	0.001	0.001	3.001	0.001	0.071	0.282	0.296
miR-676	*miR-676-3p*	29.001	32.001	11.001	6.001	105.001	58.001	0.262	0.000	0.000
	miR-676-5p	3.001	1.001	0.001	1.001	15.001	13.001	0.465	0.001	0.000
miR-720	*miR-720*	59.001	42.001	7.001	10.001	40.001	26.001	0.971	0.010	0.002
miR-741	*miR-741-3p*	57.001	47.001	62.001	43.001	1533.001	851.001	0.001	0.000	0.000
	miR-741-5p	3.001	0.001	0.001	1.001	35.001	43.001	0.167	0.000	0.000
miR-743	*miR-743a-3p*	10.001	14.001	2.001	11.001	714.001	427.001	0.201	0.000	0.000
	miR-743a-5p	0.001	1.001	1.001	1.001	70.001	54.001	0.007	0.000	0.000
	miR-743b-3p	71.001	63.001	45.001	55.001	3809.001	3078.001	0.014	0.000	0.000
	miR-743b-5p	3.001	1.001	1.001	0.001	34.001	22.001	0.319	0.000	0.000
miR-744	*miR-744-3p*	16.001	13.001	0.001	1.001	1.001	0.001	0.135	0.794	0.032
	miR-744-5p	370.001	304.001	64.001	37.001	15.001	17.001	0.608	0.001	0.000
miR-871	*miR-871-3p*	163.001	95.001	112.001	128.001	1327.001	723.001	0.000	0.000	0.000
	miR-871-5p	38.001	26.001	17.001	13.001	2766.001	1485.001	0.063	0.000	0.000
miR-872	*miR-872-3p*	67.001	98.001	14.001	4.001	90.001	57.001	0.242	0.000	0.000
	miR-872-5p	384.001	360.001	85.001	45.001	607.001	524.001	0.932	0.000	0.000
miR-874	*miR-874-3p*	15.001	18.001	3.001	5.001	2.001	0.001	0.573	0.031	0.058
miR-878	*miR-878-3p*	0.001	0.001	0.001	2.001	28.001	17.001	0.009	0.000	0.000
	miR-878-5p	6.001	19.001	3.001	12.001	360.001	272.001	0.118	0.000	0.000
miR-880	*miR-880-3p*	5.001	2.001	4.001	7.001	268.001	202.001	0.018	0.000	0.000
miR-881	*miR-881-3p*	140.001	138.001	77.001	114.001	4125.001	3886.001	0.007	0.000	0.000
miR-883	*miR-883a-3p*	7.001	5.001	4.001	1.001	201.001	160.001	0.180	0.000	0.000

TABLE 1. *Continued.*

		miRNA reads[a]						False discovery rate (FDR)		
		Caput		Corpus		Cauda				
miRNA family	miRNA[b]	Replicate 1	Replicate 2	Replicate 1	Replicate 2	Replicate 1	Replicate 2	Caput to corpus	Corpus to cauda	Caput to cauda
miR-883	*miR-883b-3p*	0.001	1.001	0.001	2.001	24.001	40.001	0.066	0.000	0.000
miR-1198	*miR-1198-5p*	44.001	48.001	14.001	8.001	4.001	0.001	0.505	0.001	0.002
miR-1249	*miR-1249-3p*	48.001	36.001	3.001	3.001	11.001	3.001	0.144	0.372	0.401
miR-1251	*miR-1251-5p*	18.001	22.001	2.001	0.001	1.001	0.001	0.069	0.440	0.004
miR-1839	*miR-1839-5p*	301.001	217.001	88.001	55.001	33.001	22.001	0.147	0.001	0.019
miR-1843	*miR-1843-3p*	9.001	15.001	0.001	0.001	1.001	0.001	0.032	0.574	0.037
	miR-1843-5p	115.001	91.001	17.001	15.001	19.001	17.001	0.831	0.752	0.470
	miR-1843b-5p	27.001	16.001	7.001	3.001	2.001	1.001	0.510	0.027	0.058
miR-3068	*miR-3068-3p*	17.001	6.001	6.001	2.001	3.001	0.001	0.264	0.059	0.392
	miR-3068-5p	12.001	11.001	1.001	0.001	0.001	0.001	0.180	0.243	0.006
miR-3096	*miR-3096-5p*	23.001	12.001	3.001	10.001	1.001	0.001	0.273	0.003	0.016
	miR-3096b-3p	14.001	12.001	0.001	1.001	7.001	5.001	0.144	0.006	0.097
miR-3107	*miR-3107-5p*	373.001	188.001	124.001	185.001	25.501	11.001	0.008	0.000	0.011
miR-3471	*miR-3471*	0.001	0.001	1.001	1.001	16.001	11.001	0.001	0.000	0.000
miR-3473	*miR-3473b*	22.001	10.001	15.001	11.001	1.001	1.001	0.005	0.000	0.118
Pre-miRNA family										
let-7	*let-7b*	8987.184	7465.068	904.868	682.201	90.168	84.168	0.000	0.000	0.000
	let-7c-1	10 697.684	8952.818	1458.034	816.951	185.501	153.751	0.001	0.000	0.000
	let-7c-2	11 682.684	9702.818	1436.534	826.951	201.251	173.251	0.001	0.000	0.000
mir-18	*mir-18a*	61.501	43.001	38.001	41.001	686.501	522.001	0.010	0.000	0.000
mir-20	*mir-20a*	235.001	164.001	35.001	14.001	296.001	197.001	0.048	0.000	0.000
mir-24	*mir-24-2*	2907.001	2775.001	443.001	297.001	47.001	32.001	0.008	0.000	0.000
mir-125	*mir-125a*	15 337.001	16 817.001	2238.001	1395.001	261.001	102.001	0.001	0.000	0.000
mir-190	*mir-190*	42.001	19.001	70.001	38.001	1.001	4.001	0.000	0.000	0.048
mir-192	*mir-192*	1080.001	2530.001	97.001	72.001	3087.001	1908.001	0.001	0.000	0.000
mir-194	*mir-194-2*	62.501	95.001	5.001	8.501	160.501	121.501	0.048	0.000	0.000
mir-196	*mir-196a-1*	23.001	29.001	65.001	30.501	1.001	3.001	0.000	0.000	0.033
	mir-196a-2	6.001	18.501	139.001	68.001	0.001	0.001	0.000	0.000	0.007
	mir-196b	35.001	55.501	178.001	92.501	2.001	3.001	0.000	0.000	0.007
mir-204	*mir-204*	3906.001	2341.001	449.501	292.001	45.001	26.001	0.008	0.000	0.000
mir-205	*mir-205*	6643.001	5648.001	1290.001	304.001	26.001	25.001	0.015	0.000	0.000
mir-451	*mir-451*	458.001	208.001	270.001	412.001	10.001	13.001	0.001	0.000	0.001
mir-463	*mir-463*	14.001	15.001	15.001	9.001	597.001	474.001	0.022	0.000	0.000
mir-465	*mir-465c-1*	119.951	107.251	75.001	80.251	6984.801	3938.901	0.007	0.000	0.000
	mir-465c-2	119.951	107.251	75.001	80.251	6984.801	3938.901	0.007	0.000	0.000
mir-467	*mir-467d*	141.001	135.001	9.001	4.001	202.001	110.001	0.002	0.000	0.000
mir-470	*mir-470*	38.001	46.001	47.001	70.001	4039.001	2091.001	0.001	0.000	0.000
mir-471	*mir-471*	6.001	9.001	7.001	12.001	240.001	286.001	0.016	0.000	0.000
mir-690	*mir-690*	1163.001	1030.001	1334.001	1757.001	87.001	71.001	0.000	0.000	0.000
mir-692	*mir-692-2*	88.501	104.501	73.001	165.501	1.001	1.001	0.003	0.000	0.000
mir-703	*mir-703*	96.001	126.001	147.001	165.001	1.001	3.001	0.000	0.000	0.000
mir-871	*mir-871*	112.501	85.001	104.001	115.001	3564.001	2122.501	0.000	0.000	0.000
mir-878	*mir-878*	16.001	36.001	24.001	30.001	1479.001	1081.001	0.008	0.000	0.000
mir-881	*mir-881*	91.001	90.001	75.001	66.001	3755.001	2970.001	0.003	0.000	0.000
mir-1306	*mir-1306*	12.001	7.001	7.001	17.001	210.001	133.001	0.022	0.000	0.000
mir-3084	*mir-3084*	95.001	39.001	84.001	63.001	3.001	2.001	0.001	0.000	0.002
mir-3096	*mir-3096b*	2636.501	2503.001	1284.001	2085.501	95.501	171.501	0.008	0.000	0.000
mir-5111	*mir-5111*	277.001	290.001	345.001	620.001	6006.001	3874.001	0.000	0.000	0.000

[a] Total RNA isolated from purified populations of spermatozoa was pooled from a minimum of nine animals to generate a single biological replicate. Two such replicates were analyzed in triplicate using an Illumina Hiseq-2000 RNA-seq platform. Each cell in the table represents the number of miRNA reads identified by this analysis. For the purpose of this study miRNAs/pre-miRNAs with an average of <10 reads between the two biological replicates were deemed below the threshold for positive identification.

[b] The 44 miRNAs whose relative levels did not change significantly between the different sperm populations are underlined.

confirmed that a majority of the miRNAs (213) we identified were common to both spermatozoa and epididymal epithelial cells. One key difference was that spermatozoa sampled from the proximal epididymis (caput) contained a substantial number of miRNAs (52) that were not represented in epithelial cells and were thus likely to have been incorporated into the cells prior to their entry into the epididymal lumen. A more surprising finding was that at least 30 of the miRNAs that were identified exclusively within populations of cauda spermatozoa were completely absent (or present at levels below that of the threshold set for positive identification) in epithelial cells from any of the epididymal segments examined. In a majority of cases, these miRNAs were present at only modest levels within the caudal spermatozoa. However, this subset also included miRNAs that were detected at relatively high levels within spermatozoa, including *miR-34c-3p*, *miR-880-3p*, *miR-883a-3p*, and several members of the *miR-465* family (*miR-465b-3p*, *miR-465b-5p*, and *miR-465c-3p*).

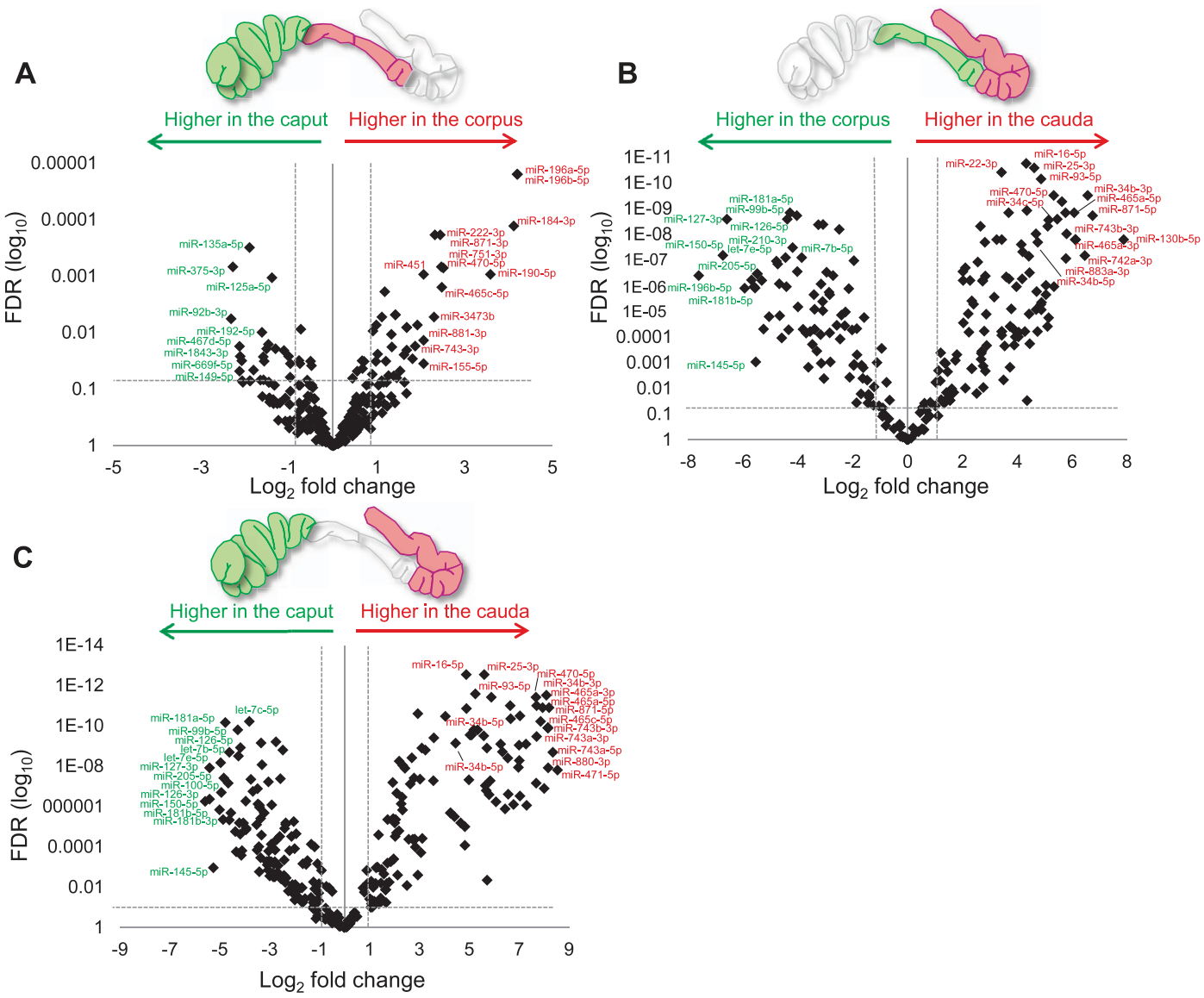

FIG. 3. Volcano plots depicting the fold changes in miRNAs identified as being differentially expressed within populations of epididymal spermatozoa. Volcano plots are presented that highlight the fold changes (x-axis) and FDR (y-axis) of miRNAs that were identified as being differentially expressed in spermatozoa between the (**A**) caput/corpus, (**B**) corpus/cauda, and (**C**) caput/cauda epididymis. Dotted lines depict thresholds values for significantly up- and down-regulated (± ≥2-fold change and FDR of <0.05) sperm miRNAs identified between each epididymal region.

Mouse Spermatozoa Possess Molecular Machinery Necessary for Processing miRNA

The deep sequencing strategy employed in the present study revealed that, in addition to an impressive cohort of mature miRNAs, epididymal spermatozoa also possessed several precursor miRNA species. Although these precursor miRNAs did not form a focus of the current study and we therefore did not pursue their complete characterization, we nevertheless noted that approximately half of these experienced a gradient of increasing expression as the sperm were conveyed distally through the epididymis (Supplemental Fig. S2). Similarly, mature miRNAs derived from this subset of precursors also appeared to mirror this trend of increasing expression (Supplemental Fig. S2). Although we cannot be certain such increases are attributed to the processing of the precursor miRNAs, we nevertheless began to investigate this prospect using immunocytochemistry to determine if essential elements of the miRNA processing machinery, namely DICER1 and AGO2, are present in isolated populations of testicular germ cells and epididymal spermatozoa. This analysis revealed intense DICER1 and AGO2 labeling in the peri-nuclear domain of spermatogonial stem cells (Spg), meiotic pachytene spermatocytes (PS), and postmeiotic round spermatids (RS) (Fig. 6). Furthermore, both of these proteins were retained in testicular spermatozoa, indicating that the cells are endowed with miRNA processing machinery as they leave the testicular environment. Interestingly, however, in these sperm cells, and those of their more mature counterparts sampled from the epididymis, DICER1 was not detected in the nuclear domain, being distributed instead in the anterior region of the sperm head and throughout the mid and principal pieces of the sperm flagellum (Fig. 6). AGO2 strongly colocalized with DICER1 within these domains, but an additional pool of the protein remained in the peri-nuclear domain (Fig. 6). It remains to be determined whether such enzymes are functional within the confines of maturing spermatozoa, a cell type that possesses minimal cytoplasm.

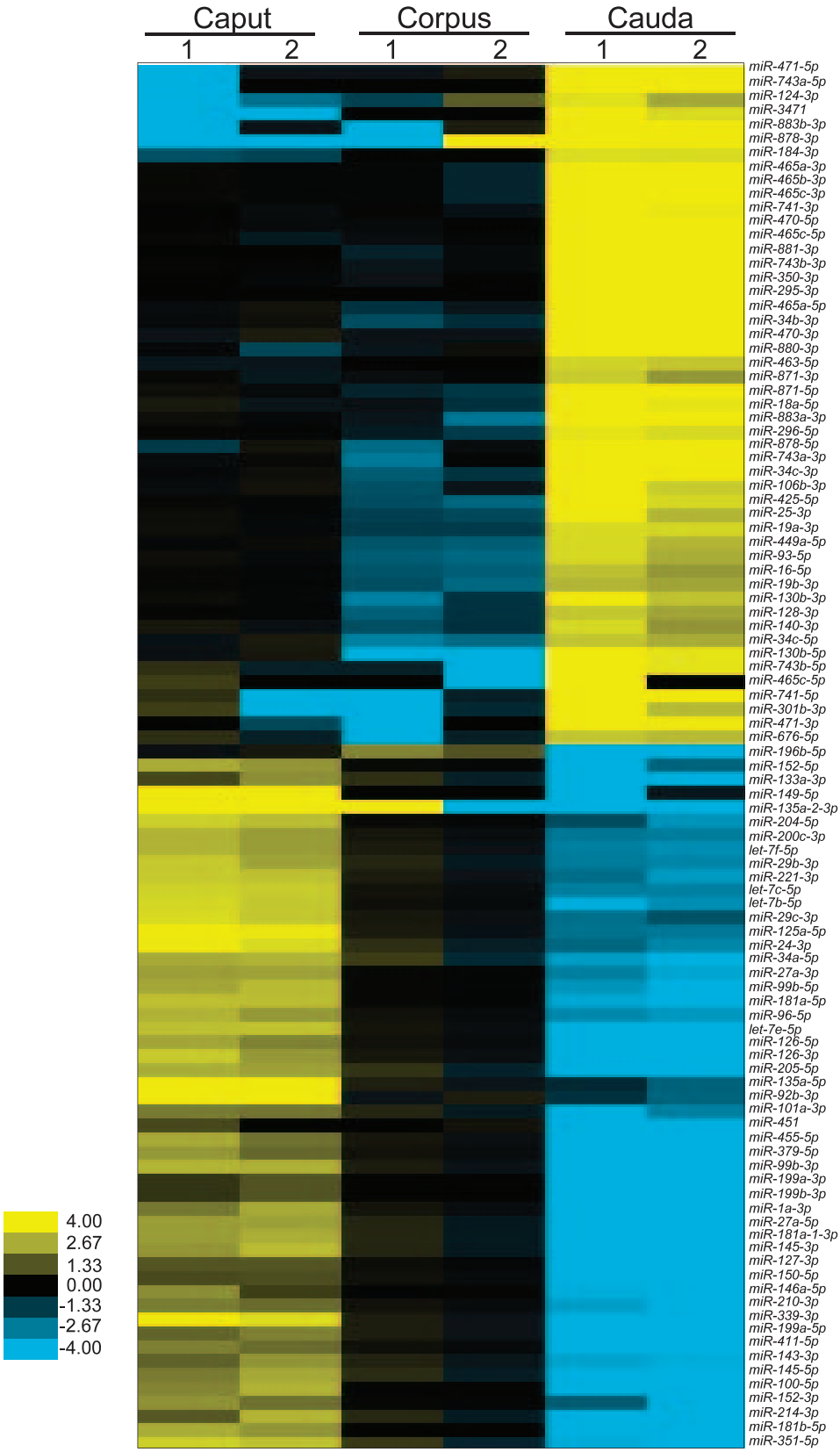

FIG. 4. Analysis of the consistency in miRNA expression between biological replicates. Heatmap of a subset of 100 miRNAs that were identified as displaying the greatest fold change in expression in spermatozoa sampled from the caput and caudal segments of the mouse epididymis. Cells within the matrix depict the relative expression level of a single miRNA within each biological replicate (representing pooled material from a minimum of nine animals). Yellow and blue shading represent the expression level ($\log_2$ fold change) above and below the median for this miRNA in all sperm samples (caput, corpus, and cauda) analyzed, respectively.

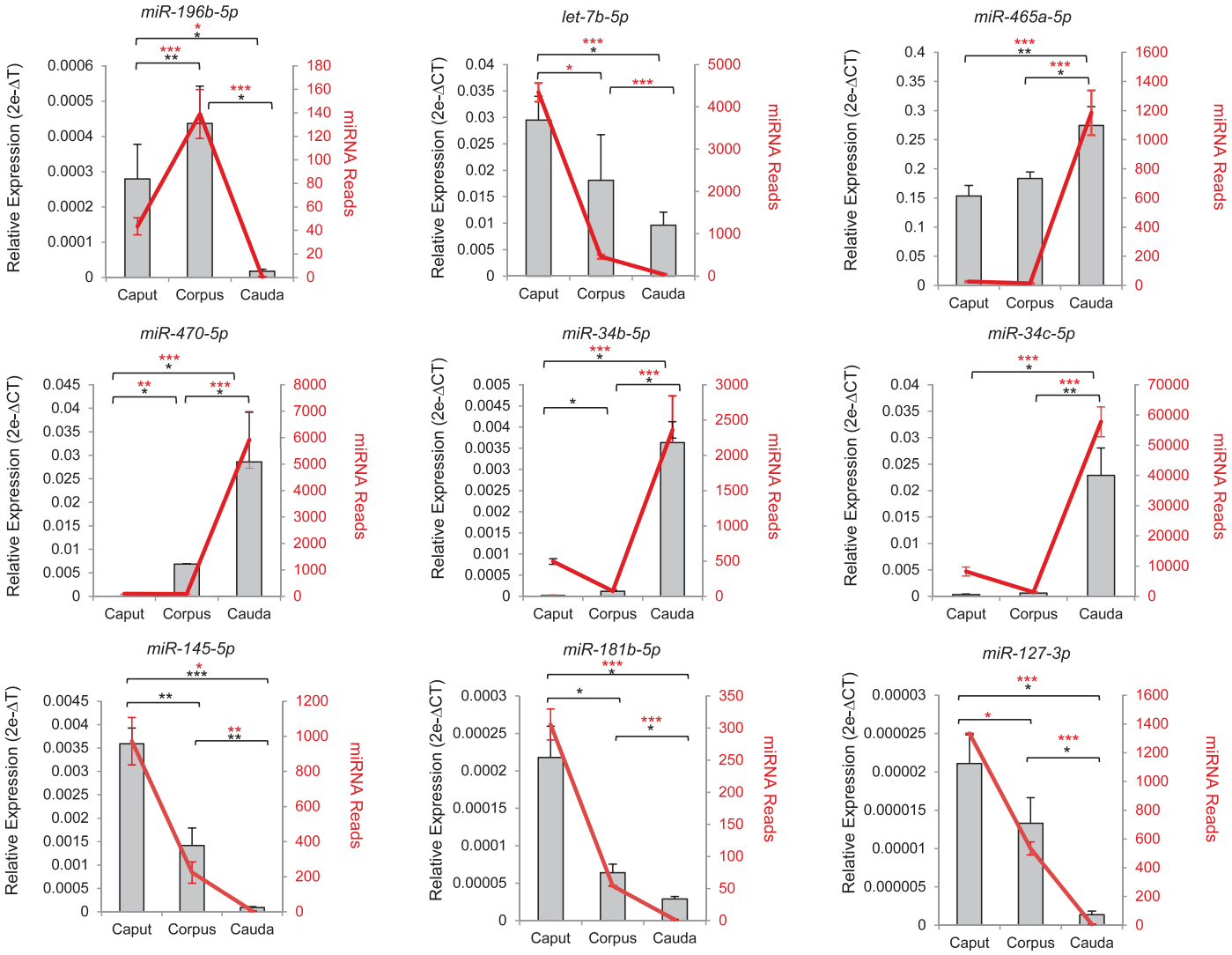

FIG. 5. The qRT-PCR validation of differentially expressed miRNAs within mouse epididymal spermatozoa. In order to verify the next-generation sequence data, nine miRNAs that displayed significantly different levels of expression were selected for targeted validation using qRT-PCR, including representatives with highest expression in spermatozoa from the proximal (caput: *let-7b-5p, miR-145-5p, miR-181b-5p,* and *miR-127-3p*; corpus: *miR-196b-5p*) and distal (cauda: *miR-465a-5p, miR-470-5p, miR-34b-5p,* and *miR34c-5p*) epididymis. The qRT-PCR experiments were performed in triplicate using three distinct pools of biological samples (n = 9 animals/sample) differing from those employed for next-generation sequence analyses. The U6 small nuclear RNA was employed as an endogenous control to normalize the expression levels of target miRNAs. Data are presented as mean ± SEM. $*P < 0.05$, $**P < 0.01$, $***P < 0.001$.

In Silico Analysis of Pathways Regulated by the miRNA Signature of Cauda Epididymal Spermatozoa

We next performed an in silico analysis of miRNA targets and their associated signaling pathways in order to gain insight into the functional role of sperm-borne miRNAs. For this analysis, we focused on the repertoire of miRNAs carried by caudal spermatozoa, as these are destined to be conveyed to the female reproductive tract and eventually the oocyte at the time of fertilization. Interrogation of IPA software using strict, experimentally validated filters revealed that caudal sperm miRNAs targeted genes that appeared to be involved in a range of biological processes, with over half (54%) mapping to the broad categories of regulating cellular development, cellular growth and proliferation, and cellular function and maintenance (Supplemental Fig. S3). Furthermore, within these categories we identified signaling cascades such as the transforming growth factor beta 1 (TGFB1) (Supplemental Fig. S4) and nuclear factor of kappa light polypeptide gene enhancer in B cells 1, p105 (NFKB1) (Supplemental Fig. S5) pathways as key targets of a multitude of the sperm-borne miRNAs. Indeed, at least 32 genes implicated in TGFB1 signaling cascades have been experimentally confirmed as targets for 28 of the caudal sperm miRNAs (Supplemental Fig. S4). Similarly, a further 28 of the caudal sperm miRNAs target 49 elements of NFKB1 (Supplemental Fig. S5). Such findings are of considerable significance in view of the well-documented role these pathways play in the immunological response of the female reproductive tract that is elicited upon introduction of seminal fluid and in embryonic development.

DISCUSSION

Our study reveals two key observations concerning mammalian sperm maturation. First, through the application of next-generation sequencing, we show that epididymal sperm harbor a complex repertoire of miRNAs. Second, this miRNA signature is modified as the cells descend through the

TABLE 2. Comparison of miRNAs identified by deep sequencing within mouse spermatozoa and highly enriched populations of epididymal epithelial cells.

miRNA family	miRNA	Spermatozoa (all epididymal regions)	Epithelial cells (all epididymal regions)	Spermatozoa			Epithelial cells[a]		
				Caput	Corpus	Cauda	Caput	Corpus	Cauda
miRNAs common to both spermatozoa and epithelial cells									
let-7	*let-7a-1-3p*	+	+	+	−	+	+	−	+
	let-7a-5p	+	+	+	+	+	+	+	+
	let-7b-3p	+	+	+	−	−	+	−	+
	let-7b-5p	+	+	+	+	+	+	+	+
	let-7c-2-3p	+	+	+	−	+	+	−	+
	let-7c-5p	+	+	+	+	+	+	+	+
	let-7d-3p	+	+	+	+	+	+	+	+
	let-7d-5p	+	+	+	+	+	+	+	+
	let-7e-5p	+	+	+	+	−	+	+	+
	let-7f-5p	+	+	+	+	+	+	+	+
	let-7g-5p	+	+	+	+	+	+	+	+
	let-7i-5p	+	+	+	+	+	+	+	+
miR-9	*miR-9-3p*	+	+	+	−	−	+	−	−
	miR-9-5p	+	+	+	+	+	+	−	−
miR-10	*miR-10a-3p*	+	+	+	−	−	+	−	−
	miR-10a-5p	+	+	+	+	+	+	+	+
	miR-10b-5p	+	+	+	+	+	+	+	+
miR-15	*miR-15a-5p*	+	+	+	+	+	+	+	+
	miR-15b-5p	+	+	+	+	+	+	+	+
miR-16	*miR-16-5p*	+	+	+	+	+	+	+	+
miR-17	*miR-17-5p*	+	+	+	+	+	+	+	+
miR-19	*miR-19a-3p*	+	+	+	+	+	+	−	+
	miR-19b-3p	+	+	+	+	+	+	+	+
miR-20	*miR-20a-5p*	+	+	+	+	+	+	+	+
miR-21	*miR-21-3p*	+	+	+	+	−	+	−	+
	miR-21-5p	+	+	+	+	+	+	+	+
miR-22	*miR-22-3p*	+	+	+	+	+	+	+	+
	miR-22-5p	+	+	+	−	−	+	−	+
miR-23	*miR-23a-3p*	+	+	+	+	+	+	+	+
	miR-23b-3p	+	+	+	+	+	+	+	+
miR-24	*miR-24-2-5p*	+	+	+	+	−	+	+	+
	miR-24-3p	+	+	+	+	−	+	+	+
miR-25	*miR-25-3p*	+	+	+	+	+	+	+	+
miR-26	*miR-26a-5p*	+	+	+	+	+	+	+	+
	miR-26b-5p	+	+	+	+	+	+	+	+
miR-27	*miR-27a-3p*	+	+	+	+	−	+	+	+
	miR-27b-3p	+	+	+	+	+	+	+	+
miR-28	*miR-28-3p*	+	+	+	−	+	+	+	+
	miR-28-5p	+	+	+	+	+	+	+	+
miR-29	*miR-29a-3p*	+	+	+	+	+	+	+	+
	miR-29a-5p	+	+	+	−	−	+	−	+
	miR-29b-3p	+	+	+	+	+	+	+	+
	miR-29c-3p	+	+	+	+	+	+	+	+
miR-30	*miR-30a-3p*	+	+	+	+	+	+	+	+
	miR-30a-5p	+	+	+	+	+	+	+	+
	miR-30b-5p	+	+	+	+	+	+	+	+
	miR-30c-2-3p	+	+	+	+	+	+	−	+
	miR-30c-5p	+	+	+	+	+	+	+	+
	miR-30d-3p	+	+	+	+	+	+	+	+
	miR-30d-5p	+	+	+	+	+	+	+	+
	miR-30e-3p	+	+	+	+	+	+	+	+
	miR-30e-5p	+	+	+	+	+	+	+	+
miR-31	*miR-31-5p*	+	+	+	+	+	+	−	+
miR-34	*miR-34a-5p*	+	+	+	+	−	+	+	+
	miR-34b-3p	+	+	+	+	+	+	−	+
	miR-34b-5p	+	+	+	+	+	+	+	+
	miR-34c-5p	+	+	+	+	+	+	+	+
miR-92	*miR-92a-3p*	+	+	+	+	+	+	+	+
	miR-92b-3p	+	+	+	+	−	+	−	+
miR-93	*miR-93-5p*	+	+	+	+	+	+	+	+
miR-96	*miR-96-5p*	+	+	+	+	−	+	+	+
miR-98	*miR-98-5p*	+	+	+	+	+	+	+	+
miR-99	*miR-99a-5p*	+	+	+	+	+	+	+	+
	miR-99b-3p	+	+	+	−	−	+	−	−
	miR-99b-5p	+	+	+	+	+	+	+	+

TABLE 2. *Continued.*

miRNA family	miRNA	Spermatozoa (all epididymal regions)	Epithelial cells (all epididymal regions)	Spermatozoa			Epithelial cells[a]		
				Caput	Corpus	Cauda	Caput	Corpus	Cauda
miR-100	*miR-100-5p*	+	+	+	+	+	+	+	+
miR-101	*miR-101a-3p*	+	+	+	+	+	+	+	+
	miR-101b-3p	+	+	+	+	+	+	+	+
miR-103	*miR-103-3p*	+	+	+	+	+	+	+	+
miR-106	*miR-106b-5p*	+	+	+	+	−	+	+	+
miR-107	*miR-107-3p*	+	+	+	−	+	+	−	+
miR-125	*miR-125a-5p*	+	+	+	+	+	+	+	+
	miR-125b-1-3p	+	+	+	+	−	+	−	−
	miR-125b-2-3p	+	+	+	−	−	+	−	+
	miR-125b-5p	+	+	+	+	+	+	+	+
miR-126	*miR-126-3p*	+	+	+	+	−	+	+	+
	miR-126-5p	+	+	+	+	+	+	+	+
miR-127	*miR-127-3p*	+	+	+	+	−	+	+	+
miR-128	*miR-128-3p*	+	+	+	+	+	+	−	+
miR-130	*miR-130a-3p*	+	+	+	+	+	+	+	+
miR-132	*miR-132-3p*	+	+	+	−	+	+	−	+
miR-133	*miR-133a-3p*	+	+	+	+	−	+	+	+
miR-135	*miR-135a-5p*	+	+	+	+	+	+	+	+
miR-138	*miR-138-5p*	+	+	+	+	+	+	−	−
miR-140	*miR-140-3p*	+	+	−	−	+	+	−	+
	miR-140-5p	+	+	+	−	+	+	+	+
miR-141	*miR-141-3p*	+	+	+	+	+	+	+	+
	miR-141-5p	+	+	+	−	+	+	−	+
miR-142	*miR-142-5p*	+	+	+	+	+	+	+	+
miR-143	*miR-143-3p*	+	+	+	+	+	+	+	+
miR-144	*miR-144-3p*	+	+	+	+	−	−	−	+
miR-145	*miR-145-3p*	+	+	+	−	−	+	+	+
	miR-145-5p	+	+	+	+	−	+	+	+
miR-146	*miR-146a-5p*	+	+	+	+	+	+	+	+
	miR-146b-5p	+	+	+	+	+	+	+	+
miR-148	*miR-148a-3p*	+	+	+	+	+	+	+	+
	miR-148a-5p	+	+	+	+	+	+	+	+
	miR-148b-3p	+	+	+	+	+	+	+	+
	miR-148b-5p	+	+	+	−	+	+	−	−
miR-149	*miR-149-5p*	+	+	+	−	−	+	−	+
miR-150	*miR-150-5p*	+	+	+	+	−	+	+	+
miR-151	*miR-151-3p*	+	+	+	+	+	+	+	+
	miR-151-5p	+	+	+	+	+	+	+	+
miR-152	*miR-152-3p*	+	+	+	+	−	+	+	+
	miR-152-5p	+	+	+	−	−	+	−	+
miR-153	*miR-153-3p*	+	+	+	−	+	+	−	−
miR-181	*miR-181a-1-3p*	+	+	+	+	−	+	−	+
	miR-181a-5p	+	+	+	+	+	+	+	+
	miR-181b-5p	+	+	+	+	−	+	+	+
	miR-181c-3p	+	+	+	+	+	+	+	+
	miR-181c-5p	+	+	+	+	+	+	+	+
	miR-181d-5p	+	+	+	+	+	+	+	+
miR-182	*miR-182-5p*	+	+	+	+	+	+	+	+
miR-183	*miR-183-5p*	+	+	+	+	+	+	+	+
miR-184	*miR-184-3p*	+	+	+	+	+	−	+	+
miR-186	*miR-186-5p*	+	+	+	+	+	+	+	+
miR-187	*miR-187-3p*	+	+	+	+	−	+	+	+
miR-190	*miR-190-5p*	+	+	−	+	−	−	+	+
miR-191	*miR-191-5p*	+	+	+	+	+	+	+	+
miR-192	*miR-192-5p*	+	+	+	+	+	+	+	+
miR-193	*miR-193-3p*	+	+	+	−	−	+	+	+
miR-194	*miR-194-5p*	+	+	+	−	+	+	−	+
miR-195	*miR-195-5p*	+	+	+	+	+	+	+	+
miR-196	*miR-196a-5p*	+	+	+	+	−	+	+	+
	miR-196b-5p	+	+	+	+	−	+	+	+
miR-199	*miR-199a-3p*	+	+	+	+	−	+	+	+
	miR-199a-5p	+	+	+	+	−	+	+	+
	miR-199b-3p	+	+	+	+	−	+	+	+
	miR-199b-5p	+	+	+	+	−	+	−	+
miR-200	*miR-200a-3p*	+	+	+	+	+	+	+	+
	miR-200a-5p	+	+	+	+	+	+	+	+
	miR-200b-3p	+	+	+	+	+	+	+	+
	miR-200b-5p	+	+	+	−	−	+	−	+
	miR-200c-3p	+	+	+	+	+	+	+	+
miR-203	*miR-203-3p*	+	+	+	+	−	+	+	+
miR-204	*miR-204-5p*	+	+	+	+	+	+	+	+

TABLE 2. *Continued.*

miRNA family	miRNA	Spermatozoa (all epididymal regions)	Epithelial cells (all epididymal regions)	Spermatozoa			Epithelial cells[a]		
				Caput	Corpus	Cauda	Caput	Corpus	Cauda
miR-205	*miR-205-5p*	+	+	+	+	+	+	+	+
miR-210	*miR-210-3p*	+	+	+	+	+	+	+	+
miR-214	*miR-214-3p*	+	+	+	+	−	+	+	+
miR-218	*miR-218-5p*	+	+	+	+	−	+	+	+
miR-221	*miR-221-3p*	+	+	+	+	+	+	+	+
	miR-221-5p	+	+	+	−	−	+	−	−
miR-222	*miR-222-3p*	+	+	+	+	+	+	+	+
	miR-301a-3p	+	+	+	+	+	+	+	+
miR-320	*miR-320-3p*	+	+	+	+	+	+	+	+
miR-322	*miR-322-5p*	+	+	+	+	−	+	+	+
miR-324	*miR-324-5p*	+	+	+	+	+	+	+	+
miR-326	*miR-326-3p*	+	+	+	−	−	+	−	+
	miR-328-3p	+	+	+	+	+	+	+	+
miR-338	*miR-338-3p*	+	+	+	−	−	+	−	+
miR-339	*miR-339-5p*	+	+	+	−	−	+	−	+
miR-340	*miR-340-5p*	+	+	+	+	+	+	+	+
miR-342	*miR-342-3p*	+	+	+	+	+	+	+	+
miR-350	*miR-350-3p*	+	+	−	−	+	+	−	−
miR-351	*miR-351-5p*	+	+	+	+	−	+	+	+
miR-361	*miR-361-5p*	+	+	+	+	+	+	+	+
miR-362	*miR-362-3p*	+	+	+	−	−	+	−	−
miR-365	*miR-365-3p*	+	+	+	+	−	−	−	+
miR-374	*miR-374-5p*	+	+	+	+	−	+	+	+
miR-375	*miR-375-3p*	+	+	+	+	+	+	+	+
miR-378	*miR-378-3p*	+	+	+	+	+	+	+	+
	miR-378-5p	+	+	+	−	−	+	−	−
miR-379	*miR-379-5p*	+	+	+	−	−	−	−	+
miR-381	*miR-381-3p*	+	+	+	−	−	−	−	+
miR-410	*miR-410-3p*	+	+	+	+	+	+	+	+
miR-411	*miR-411-5p*	+	+	+	+	−	+	+	+
miR-421	*miR-421-3p*	+	+	+	+	−	+	+	+
miR-423	*miR-423-3p*	+	+	+	+	+	+	+	+
	miR-423-5p	+	+	+	+	+	+	+	+
miR-425	*miR-425-5p*	+	+	+	+	+	+	+	+
miR-429	*miR-429-3p*	+	+	+	+	+	+	+	+
miR-434	*miR-434-3p*	+	+	+	+	+	+	+	+
miR-449	*miR-449a-5p*	+	+	+	+	+	+	−	+
miR-450	*miR-450a-5p*	+	+	+	−	−	+	−	+
miR-451	*miR-451*	+	+	+	+	−	+	−	+
miR-455	*miR-455-5p*	+	+	+	−	−	+	−	−
miR-465	*miR-465a-5p*	+	+	+	+	+	−	−	+
	miR-465c-5p	+	+	+	+	+	−	+	+
miR-467	*miR-467a-5p*	+	+	+	+	+	+	+	+
	miR-467d-5p	+	+	+	−	−	+	−	−
miR-470	*miR-470-5p*	+	+	+	+	+	+	+	+
miR-484	*miR-484*	+	+	+	+	+	+	+	+
miR-486	*miR-486-5p*	+	+	+	+	+	+	+	+
miR-497	*miR-497-5p*	+	+	+	+	+	+	+	+
miR-501	*miR-501-3p*	+	+	+	+	+	+	+	+
miR-532	*miR-532-5p*	+	+	+	+	+	+	+	+
miR-541	*miR-541-5p*	+	+	+	−	−	−	−	+
miR-574	*miR-574-3p*	+	+	+	+	−	+	−	+
miR-582	*miR-582-3p*	+	+	+	−	−	+	−	−
miR-652	*miR-652-3p*	+	+	+	+	−	+	+	+
miR-669	*miR-669a-5p*	+	+	+	−	+	+	−	−
	miR-669c-5p	+	+	+	−	+	+	−	−
	miR-669p-5p	+	+	+	−	+	+	−	−
miR-671	*miR-671-3p*	+	+	+	−	−	+	−	−
miR-672	*miR-672-5p*	+	+	+	+	+	+	+	+
miR-676	*miR-676-3p*	+	+	+	−	+	+	−	+
miR-720	*miR-720*	+	+	+	−	+	+	−	−
miR-741	*miR-741-3p*	+	+	+	+	+	−	+	+
miR-743	*miR-743b-3p*	+	+	+	+	+	−	+	+
miR-744	*miR-744-5p*	+	+	+	+	+	+	+	+
miR-871	*miR-871-3p*	+	+	+	+	+	+	+	+
	miR-871-5p	+	+	+	+	+	−	−	+
miR-872	*miR-872-3p*	+	+	+	−	+	+	+	+
	miR-872-5p	+	+	+	+	+	+	+	+
miR-881	*miR-881-3p*	+	+	+	+	+	−	+	+
miR-1198	*miR-1198-5p*	+	+	+	+	−	+	−	+
miR-1249	*miR-1249-3p*	+	+	+	−	−	+	−	−

TABLE 2. *Continued.*

miRNA family	miRNA	Spermatozoa (all epididymal regions)	Epithelial cells (all epididymal regions)	Spermatozoa			Epithelial cells[a]		
				Caput	Corpus	Cauda	Caput	Corpus	Cauda
miR-1251	*miR-1251-5p*	+	+	+	−	−	+	−	−
miR-1839	*miR-1839-5p*	+	+	+	+	+	+	+	+
miR-1843	*miR-1843-5p*	+	+	+	+	+	+	+	+
	miR-1843b-5p	+	+	+	−	−	+	−	−
miR-3096	*miR-3096-5p*	+	+	+	−	−	+	−	+
miR-3107	*miR-3107-5p*	+	+	+	+	+	+	+	+
miRNAs unique to spermatozoa									
miR-1	*miR-1a-3p*	+	−	+	−	−	−	−	−
let-7	*let-7e-3p*	+	−	+	−	−	−	−	−
	let-7f-1-3p	+	−	+	−	−	−	−	−
miR-7	*miR-7a-1-3p*	+	−	+	−	+	−	−	−
miR-16	*miR-16-2-3p*	+	−	−	−	+	−	−	−
miR-17	*miR-17-3p*	+	−	−	−	+	−	−	−
miR-18	*miR-18a-5p*	+	−	+	+	+	−	−	−
miR-27	*miR-27a-5p*	+	−	+	−	−	−	−	−
	miR-27b-5p	+	−	+	−	−	−	−	−
miR-34	*miR-34c-3p*	+	−	+	+	+	−	−	−
miR-92	*miR-92a-1-5p*	+	−	+	−	−	−	−	−
miR-106	*miR-106b-3p*	+	−	+	−	+	−	−	−
miR-124	*miR-124-3p*	+	−	−	−	+	−	−	−
miR-130	*miR-130b-3p*	+	−	−	−	+	−	−	−
	miR-130b-5p	+	−	−	−	+	−	−	−
miR-135	*miR-135a-2-3p*	+	−	+	−	−	−	−	−
	miR-135b-5p	+	−	+	−	−	−	−	−
miR-142	*miR-142-3p*	+	−	+	+	+	−	−	−
miR-144	*miR-144-5p*	+	−	+	−	−	−	−	−
miR-185	*miR-185-5p*	+	−	+	−	−	−	−	−
miR-193	*miR-193b-3p*	+	−	−	−	+	−	−	−
miR-210	*miR-210-5p*	+	−	+	−	−	−	−	−
miR-214	*miR-214-5p*	+	−	+	−	−	−	−	−
miR-223	*miR-223-3p*	+	−	+	−	−	−	−	−
miR-295	*miR-295-3p*	+	−	−	−	+	−	−	−
miR-296	*miR-296-5p*	+	−	+	−	+	−	−	−
miR-301	*miR-301b-3p*	+	−	−	−	+	−	−	−
miR-331	*miR-331-3p*	+	−	−	−	+	−	−	−
miR-335	*miR-335-3p*	+	−	+	−	−	−	−	−
miR-339	*miR-339-3p*	+	−	+	−	−	−	−	−
miR-340	*miR-340-3p*	+	−	+	−	+	−	−	−
miR-378	*miR-378b*	+	−	+	−	−	−	−	−
miR-463	*miR-463-5p*	+	−	−	−	+	−	−	−
miR-465	*miR-465a-3p*	+	−	−	−	+	−	−	−
	miR-465b-3p	+	−	−	−	+	−	−	−
	miR-465b-5p	+	−	−	−	+	−	−	−
	miR-465c-3p	+	−	−	−	+	−	−	−
miR-466	*miR-466a-3p*	+	−	−	−	+	−	−	−
	miR-466b-3p	+	−	+	−	−	−	−	−
	miR-466c-3p	+	−	+	−	−	−	−	−
	miR-466e-3p	+	−	−	−	+	−	−	−
	miR-466p-3p	+	−	+	−	−	−	−	−
miR-467	*miR-467b-5p*	+	−	−	−	+	−	−	−
	miR-467c-5p	+	−	+	−	+	−	−	−
	miR-467d-3p	+	−	+	−	+	−	−	−
	miR-467e-5p	+	−	+	−	+	−	−	−
miR-470	*miR-470-3p*	+	−	−	−	+	−	−	−
miR-471	*miR-471-3p*	+	−	−	−	+	−	−	−
	miR-471-5p	+	−	−	−	+	−	−	−
miR-499	*miR-499-5p*	+	−	−	−	+	−	−	−
miR-500	*miR-500-3p*	+	−	+	−	−	−	−	−
miR-511	*miR-511-3p*	+	−	+	−	−	−	−	−
miR-532	*miR-532-3p*	+	−	+	−	−	−	−	−
miR-574	*miR-574-5p*	+	−	+	−	−	−	−	−
miR-598	*miR-598-3p*	+	−	+	−	−	−	−	−
miR-615	*miR-615-3p*	+	−	+	−	−	−	−	−
miR-669	*miR-669a-3p*	+	−	+	−	+	−	−	−
	miR-669b-5p	+	−	+	−	−	−	−	−
	miR-669d-5p	+	−	+	−	+	−	−	−
	miR-669f-5p	+	−	+	−	−	−	−	−
	miR-669l-5p	+	−	+	−	−	−	−	−
	miR-669o-3p	+	−	+	−	+	−	−	−
	miR-669o-5p	+	−	+	−	+	−	−	−

TABLE 2. *Continued.*

miRNA family	miRNA	Spermatozoa (all epididymal regions)	Epithelial cells (all epididymal regions)	Spermatozoa			Epithelial cells[a]		
				Caput	Corpus	Cauda	Caput	Corpus	Cauda
miR-674	*miR-674-3p*	+	−	+	−	−	−	−	−
miR-676	*miR-676-5p*	+	−	−	−	+	−	−	−
miR-741	*miR-741-5p*	+	−	−	−	+	−	−	−
miR-743	*miR-743a-3p*	+	−	+	−	+	−	−	−
	miR-743a-5p	+	−	−	−	+	−	−	−
	miR-743b-5p	+	−	−	−	+	−	−	−
miR-744	*miR-744-3p*	+	−	+	−	−	−	−	−
miR-874	*miR-874-3p*	+	−	+	−	−	−	−	−
miR-878	*miR-878-3p*	+	−	−	−	+	−	−	−
	miR-878-5p	+	−	+	−	+	−	−	−
miR-880	*miR-880-3p*	+	−	−	−	+	−	−	−
miR-883	*miR-883a-3p*	+	−	−	−	+	−	−	−
	miR-883b-3p	+	−	−	−	+	−	−	−
miR-1843	*miR-1843-3p*	+	−	+	−	−	−	−	−
miR-3068	*miR-3068-3p*	+	−	+	−	−	−	−	−
	miR-3068-5p	+	−	+	−	−	−	−	−
miR-3096	*miR-3096b-3p*	+	−	+	−	−	−	−	−
miR-3471	*miR-3471*	+	−	−	−	+	−	−	−
miR-3473	*miR-3473b*	+	−	+	+	−	−	−	−
miRNAs unique to epithelial cells									
miR-129	*miR-129-2-3p*	−	+	−	−	−	−	−	+
miR-139	*miR-139-5p*	−	+	−	−	−	−	−	+
miR-300	*miR-300-3p*	−	+	−	−	−	−	−	+
miR-409	*miR-409-5p*	−	+	−	−	−	−	−	+
miR-582	*miR-582-5p*	−	+	−	−	−	+	−	−

[a] Data on epithelial cell miRNAs are from [16]. Please also see http://www.ncbi.nlm.nih.gov/geo/query/acc.cgi?acc=GSE70197.

epididymis. The extent of these changes rivals that of the more well-studied proteomic changes that have until now dominated our view of sperm maturation. Indeed, we found that such modification includes the apparent acquisition, late in maturation, of a cohort of novel miRNA species in addition to a significant increase in a substantial number of miRNA originally expressed in immature sperm. Because the balance of evidence indicates that sperm are transcriptionally quiescent cells that are incapable of gene transcription and hence the de novo miRNA biogenesis, this work provides the first evidence to support a novel contribution of the epididymal environment to the cellular acquisition of miRNAs.

Numerous studies have recently begun to document the presence of small noncoding RNAs in the epididymis with a majority focusing on the spatial and temporal expression profiles present in the whole organ. Such studies have revealed a rich and complex miRNA landscape that, in turn, has been implicated in regulating the androgen-dependent development and homeostasis of the organ [15, 44, 45]; indirectly contributing to the secretory and absorptive activities of the epithelium, and hence sperm maturation/storage, via the control of segmental patterns of gene expression [13, 46]; and contributing to reproductive pathologies such as age-dependent decline in male fertility [15]. However, through direct comparisons of epididymal somatic cells and whole epididymal tissue, our own work has identified luminal spermatozoa and/or the varied constituents of epididymal fluid as a major contributor to the overall epididymal miRNA signature [16]. Although this accords with the findings of the present study, we have yet to establish the mechanism(s) underpinning the apparent loss and gain of miRNAs. With regard to the loss of miRNAs, it is possible that at least a portion of these are packaged within the cytoplasmic droplet, a remnant of the extensive cytodifferentiation that occurs during spermiogenesis, that is progressively shed from the maturing spermatozoa [47].

In the context of miRNA acquisition, the pioneering studies of Sullivan and colleagues have established that this may involve bulk delivery via small exosome-like entities known as epididymosomes [48, 49]. Indeed, epididymosomes released from epididymal epithelial cells have been shown to carry a complex cargo of miRNAs that are available for transfer to the maturing sperm cell [50]. Furthermore, despite the limitations imposed by cross-species comparison and the application of alternative miRNA sequencing strategies, we have confirmed that 48/92 (52%) of the miRNAs that increased in expression between mouse caput and cauda spermatozoa have been detected in bovine epididymosomes (Supplemental Table S1). This model of transfer shares analogy with several other tissue systems in which there is now compelling evidence that miRNAs are actively secreted in membrane-enclosed exosomes and delivered into recipient cells where they function as endogenous miRNAs [51–53]. It is therefore conceivable that epididymosomes not only participate in a paracrine-like form of intercellular communication to coordinate the activity of the different epididymal segments [50], but may also convey miRNAs to the maturing sperm cells. At present it is not known how this mechanism could afford selective transfer, although distinct miRNA signatures have been recorded in epididymosomes originating from different epididymal regions, and similarly, these profiles also differ markedly from those of their parent epithelial cells [50].

Direct evidence that epididymosomes can act as vehicles for the trafficking of miRNAs to maturing spermatozoa is currently lacking; however, these entities are nevertheless able to form intimate associations with the sperm membrane that facilitate the transfer of protein cargo to the maturing cells [49, 54]. In addition, it has been known for some time that sperm can efficiently incorporate exogenous DNA and RNA via artificial

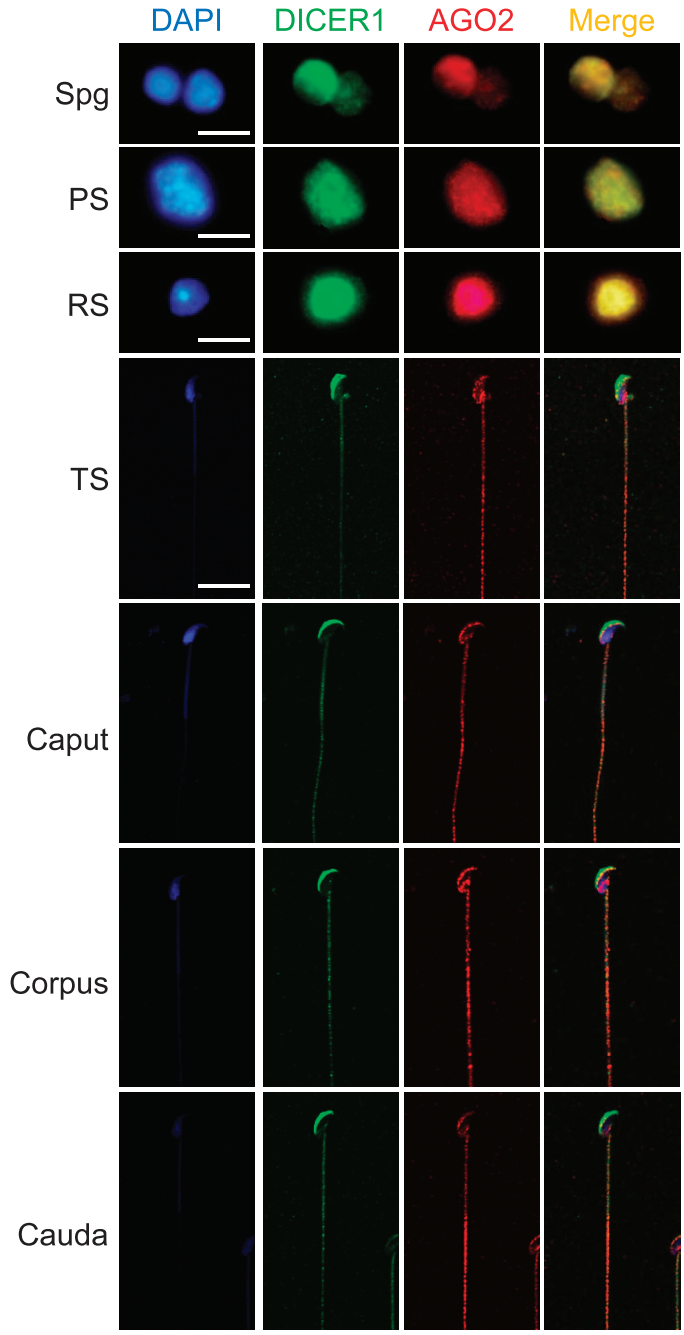

FIG. 6. Assessment of key elements of the miRNA biogenesis machinery in mouse spermatozoa. Mouse testicular germ cells (Spg; PS; RS; and TS, testicular sperm) and epididymal spermatozoa (caput, corpus, cauda) were dual labeled with anti-DICER1 and anti-AGO2 antibodies followed by either appropriate anti-rabbit 488 Alexa Fluor (green) or goat anti-rat 594 Alexa Fluor-conjugated (red) secondary antibodies, respectively. The cells were then counterstained with DAPI and viewed using confocal microscopy. Bar = 20 μm. These experiments were replicated three times using independent samples and representative images are shown.

liposomes [55]. Such findings take on added significance in view of recent evidence that exosomes secreted by somatic cells lying beyond the epididymal environment are able to facilitate the direct transmission of synthetic RNA to gametes within the organ [56]. This novel flow of information from somatic cells to gametes raises the intriguing possibility that epididymal-derived epididymosomes may not be the sole vector for exosome-mediated delivery of miRNAs to maturing spermatozoa. Although the concept that sperm can incorporate miRNA of nonepididymal origin requires considerable validation, it is interesting to note that a subset of the miRNA we identified as being acquired by spermatozoa did not appear to be represented in the epididymal epithelial miRNA signature (Table 2) [16].

Irrespective of the mechanism of delivery, our data suggest that the majority of the changes in the sperm miRNA are attributed to the caudal region. These data agree with our previous profiling of epididymal epithelial miRNA in which we identified the highest levels of miRNA synthetic activity in the cauda and far fewer changes associated with the corpus region [16]. However, they do stand in marked contrast to well-established paradigms of epididymal maturation that specify the majority of the changes in the functional profile of spermatozoa, along with that of their proteome, coincide with their passage through the distal caput/proximal corpus regions (reviewed by [57]). These data suggest that the modification of the sperm miRNA signature may not be intimately tied to the functional maturation of these cells. Support for this conclusion rests with data dating back to the early 1990s demonstrating that successful fertilization, and apparently normal embryo development, can be readily achieved with immature spermatozoa aspirated from the testes and proximal epididymal regions following intracytoplasmic sperm injection [58, 59]. Thus the epididymal miRNA acquired by spermatozoa during their prolonged storage in the cauda cannot be considered essential for zygote formation or embryo development. Rather, we speculate that these miRNAs may act as vectors for the transmission of transgenerational patterns of inheritance that alter the developmental trajectory of the offspring and/or have downstream roles in conditioning of the peri-conceptual environment in the female reproductive tract (reviewed by [60, 61]).

These possible effects accord with recent evidence implicating sperm-borne miRNA in mediating the memory of early life trauma [62] and with the predicted targets for many of the miRNAs carried by functionally competent spermatozoa. For instance, two of the most common intracellular pathways targeted by caudal sperm miRNAs are those centered on TGFB1 and NFKB1. These signaling cascades, in turn, regulate genes involved in early embryonic development and the resistance of embryos to embryopathic stresses [63, 64]. Interestingly, both pathways also have well-documented roles in modulating immunological responses in the female reproductive tract. For instance, the cytokine TGFB1 is one principal bioactive factor in mouse seminal plasma that is responsible for inducing the uterine leukocytic response following coitus [57, 58] and subsequently preparing the endometrial microenvironment to support embryo implantation [55, 59, 60]. TLR4 signaling, which acts via NFKB1, is now also implicated in seminal fluid signaling [65]. Understanding the mechanisms by which sperm miRNAs integrate into the regulation of these and potentially other physiological systems is clearly an exciting avenue for future research.

In conclusion, our results demonstrate for the first time that, far from being an intrinsic remnant of the events associated with spermatogenesis, sperm miRNA signatures are subject to modification during the posttesticular phase of their development. Such information is not only likely to find utility in the context of male infertility diagnosis and management, but may also be exploited to enhance our understanding of the transmission of epigenetic characteristics from fathers to offspring. Indeed, given this level of plasticity it will be of considerable interest to determine whether the profile of sperm-borne miRNA is vulnerable to perturbation following paternal

exposure to various forms of stress during their extended residence within the epididymal environment. In this context, conditions such as diet-induced paternal obesity have been shown to alter sperm miRNA content [66]. Similarly, exposure of male mice to chronic stress [28, 62], bulls to dietary toxins [67], and humans to cigarette smoke [68] have all been shown to be capable of significantly altering their sperm miRNA content. Moreover, such changes have been linked to pronounced heritable epigenetic alterations in the offspring, including impaired metabolic and reproductive health [66, 69] and adverse behavioral/neurological symptoms [28, 62]. Coupled with the demonstration that epididymosome miRNA cargo is also able to be selectively modified by various environmental/physiological insults [70], these data raise the intriguing possibility that the prolonged transit/storage within the epididymis may provide a previously unappreciated window of opportunity to alter the sperm-borne miRNA signature. Thus, further detailed analysis of the epididymal contribution to the sperm epigenome is warranted, particularly in the context of determining whether sperm with an ''immature'' miRNA profile can function normally.

ACKNOWLEDGMENT

The authors acknowledge the Australian Genome Research Facility (Melbourne) for sequencing and initial bioinformatic analyses.

REFERENCES

1. Ambros V. The functions of animal microRNAs. Nature 2004; 431: 350–355.
2. Baek D, Villen J, Shin C, Camargo FD, Gygi SP, Bartel DP. The impact of microRNAs on protein output. Nature 2008; 455:64–71.
3. Bouhallier F, Allioli N, Lavial F, Chalmel F, Perrard MH, Durand P, Samarut J, Pain B, Rouault JP. Role of miR-34c microRNA in the late steps of spermatogenesis. RNA 2010; 16:720–731.
4. He Z, Kokkinaki M, Pant D, Gallicano GI, Dym M. Small RNA molecules in the regulation of spermatogenesis. Reproduction 2009; 137:901–911.
5. Liu D, Li L, Fu H, Li S, Li J. Inactivation of Dicer1 has a severe cumulative impact on the formation of mature germ cells in mouse testes. Biochem Biophys Res Commun 2012; 422:114–120.
6. McIver SC, Roman SD, Nixon B, McLaughlin EA. miRNA and mammalian male germ cells.Hum Reprod Update 2012; 18:44–59.
7. McIver SC, Stanger SJ, Santarelli DM, Roman SD, Nixon B, McLaughlin EA. A unique combination of male germ cell miRNAs coordinates gonocyte differentiation. PLoS One 2012; 7:e35553.
8. Nicholls PK, Harrison CA, Walton KL, McLachlan RI, O'Donnell L, Stanton PG. Hormonal regulation of sertoli cell micro-RNAs at spermiation. Endocrinology 2011; 152:1670–1683.
9. Bjorkgren I, Gylling H, Turunen H, Huhtaniemi I, Strauss L, Poutanen M, Sipila P. Imbalanced lipid homeostasis in the conditional Dicer1 knockout mouse epididymis causes instability of the sperm membrane. FASEB J 2015; 29:433–442.
10. Bjorkgren I, Saastamoinen L, Krutskikh A, Huhtaniemi I, Poutanen M, Sipila P. Dicer1 ablation in the mouse epididymis causes dedifferentiation of the epithelium and imbalance in sex steroid signaling. PLoS One 2012; 7:e38457.
11. Bjorkgren I, Sipila P. The role of Dicer1 in the male reproductive tract. Asian J Androl 2015; 17:737–741.
12. Chu C, Zheng G, Hu S, Zhang J, Xie S, Ma W, Ni M, Tang C, Zhou L, Zhou Y, Liu M, Li Y, et al. Epididymal region-specific miRNA expression and DNA methylation and their roles in controlling gene expression in rats. PLoS One 2015; 10:e0124450.
13. Belleannee C, Calvo E, Thimon V, Cyr DG, Legare C, Garneau L, Sullivan R. Role of microRNAs in controlling gene expression in different segments of the human epididymis. PLoS One 2012; 7:e34996.
14. Landgraf P, Rusu M, Sheridan R, Sewer A, Iovino N, Aravin A, Pfeffer S, Rice A, Kamphorst AO, Landthaler M, Lin C, Socci ND, et al. A mammalian microRNA expression atlas based on small RNA library sequencing. Cell 2007; 129:1401–1414.
15. Zhang J, Liu Q, Zhang W, Li J, Li Z, Tang Z, Li Y, Han C, Hall SH, Zhang Y. Comparative profiling of genes and miRNAs expressed in the newborn, young adult, and aged human epididymides. Acta Biochim Biophys Sin (Shanghai) 2010; 42:145–153.
16. Nixon B, Stanger SJ, Mihalas BP, Reilly J, Anderson AL, Dun MD, Tyagi S, Holt JE, McLaughlin EA. Next generation sequencing analysis reveals segmental patterns of microRNA expression in mouse epididymal epithelial cells. PLoS One 2015; 10:e0135605.
17. Jodar M, Selvaraju S, Sendler E, Diamond MP, Krawetz SA, Reproductive Medicine Network. The presence, role and clinical use of spermatozoal RNAs. Hum Reprod Update 2013; 19:604–624.
18. Lalancette C, Miller D, Li Y, Krawetz SA. Paternal contributions: new functional insights for spermatozoal RNA. J Cell Biochem 2008; 104: 1570–1579.
19. Peng H, Shi J, Zhang Y, Zhang H, Liao S, Li W, Lei L, Han C, Ning L, Cao Y, Zhou Q, Chen Q, et al. A novel class of tRNA-derived small RNAs extremely enriched in mature mouse sperm. Cell Res 2012; 22: 1609–1612.
20. Sendler E, Johnson GD, Mao S, Goodrich RJ, Diamond MP, Hauser R, Krawetz SA. Stability, delivery and functions of human sperm RNAs at fertilization. Nucleic Acids Res 2013; 41:4104–4117.
21. Krawetz SA, Kruger A, Lalancette C, Tagett R, Anton E, Draghici S, Diamond MP. A survey of small RNAs in human sperm. Hum Reprod 2011; 26:3401–3412.
22. Miller D, Briggs D, Snowden H, Hamlington J, Rollinson S, Lilford R, Krawetz SA. A complex population of RNAs exists in human ejaculate spermatozoa: implications for understanding molecular aspects of spermiogenesis. Gene 1999; 237:385–392.
23. Miller D, Ostermeier GC. Spermatozoal RNA: why is it there and what does it do? Gynecol Obstet Fertil 2006; 34:840–846.
24. Ostermeier GC, Goodrich RJ, Moldenhauer JS, Diamond MP, Krawetz SA. A suite of novel human spermatozoal RNAs. J Androl 2005; 26: 70–74.
25. Dadoune JP. Spermatozoal RNAs: what about their functions? Microsc Res Tech 2009; 72:536–551.
26. Liu WM, Pang RT, Chiu PC, Wong BP, Lao K, Lee KF, Yeung WS. Sperm-borne microRNA-34c is required for the first cleavage division in mouse. Proc Natl Acad Sci U S A 2012; 109:490–494.
27. Ostermeier GC, Miller D, Huntriss JD, Diamond MP, Krawetz SA. Reproductive biology: delivering spermatozoan RNA to the oocyte. Nature 2004; 429:154.
28. Rodgers AB, Morgan CP, Bronson SL, Revello S, Bale TL. Paternal stress exposure alters sperm microRNA content and reprograms offspring HPA stress axis regulation. J Neurosci 2013; 33:9003–9012.
29. McCallie B, Schoolcraft WB, Katz-Jaffe MG. Aberration of blastocyst microRNA expression is associated with human infertility. Fertil Steril 2010; 93:2374–2382.
30. Curry E, Safranski TJ, Pratt SL. Differential expression of porcine sperm microRNAs and their association with sperm morphology and motility. Theriogenology 2011; 76:1532–1539.
31. Abu-Halima M, Hammadeh M, Backes C, Fischer U, Leidinger P, Lubbad AM, Keller A, Meese E. A panel of five microRNAs as potential biomarkers for the diagnosis and assessment of male infertility. Fertil Steril 2014; 102:989–997.
32. Tscherner A, Gilchrist G, Smith N, Blondin P, Gillis D, LaMarre J. MicroRNA-34 family expression in bovine gametes and preimplantation embryos. Reprod Biol Endocrinol 2014; 12:85.
33. Khazaie Y, Nasr Esfahani MH. MicroRNA and male infertility: a potential for diagnosis. Int J Fertil Steril 2014; 8:113–118.
34. Salas-Huetos A, Blanco J, Vidal F, Mercader JM, Garrido N, Anton E. New insights into the expression profile and function of micro-ribonucleic acid in human spermatozoa. Fertil Steril 2014; 102:213–222.e4.
35. Abu-Halima M, Hammadeh M, Schmitt J, Leidinger P, Keller A, Meese E, Backes C. Altered microRNA expression profiles of human spermatozoa in patients with different spermatogenic impairments. Fertil Steril 2013; 99:1249–1255. e16.
36. Hamatani T. Human spermatozoal RNAs. Fertil Steril 2012; 97:275–281.
37. Govindaraju A, Uzun A, Robertson L, Atli MO, Kaya A, Topper E, Crate EA, Padbury J, Perkins A, Memili E. Dynamics of microRNAs in bull spermatozoa. Reprod Biol Endocrinol 2012; 10:82.
38. Nixon B, MacIntyre DA, Mitchell LA, Gibbs GM, O'Bryan M, Aitken RJ. The identification of mouse sperm-surface-associated proteins and characterization of their ability to act as decapacitation factors. Biol Reprod 2006; 74:275–287.
39. Dun MD, Anderson AL, Bromfield EG, Asquith KL, Emmett B, McLaughlin EA, Aitken RJ, Nixon B. Investigation of the expression and functional significance of the novel mouse sperm protein, a disintegrin and metalloprotease with thrombospondin type 1 motifs number 10 (ADAMTS10). Int J Androl 2012; 35:572–589.

40. Kruger TF, Ackerman SB, Simmons KF, Swanson RJ, Brugo SS, Acosta AA. A quick, reliable staining technique for human sperm morphology. Arch Androl 1987; 18:275–277.
41. Baleato RM, Aitken RJ, Roman SD. Vitamin A regulation of BMP4 expression in the male germ line. Dev Biol 2005; 286:78–90.
42. Edgar R, Domrachev M, Lash AE. Gene Expression Omnibus: NCBI gene expression and hybridization array data repository. Nucleic Acids Res 2002; 30:207–210.
43. Livak KJ, Schmittgen TD. Analysis of relative gene expression data using real-time quantitative PCR and the 2(-Delta Delta C(T)) method. Methods 2001; 25:402–408.
44. Ma W, Hu S, Yao G, Xie S, Ni M, Liu Q, Gao X, Zhang J, Huang X, Zhang Y. An androgen receptor-microrna-29a regulatory circuitry in mouse epididymis. J Biol Chem 2013; 288:29369–29381.
45. Ma W, Xie S, Ni M, Huang X, Hu S, Liu Q, Liu A, Zhang J, Zhang Y. MicroRNA-29a inhibited epididymal epithelial cell proliferation by targeting nuclear autoantigenic sperm protein (NASP). J Biol Chem 2012; 287:10189–10199.
46. Li Y, Wang HY, Wan FC, Liu FJ, Liu J, Zhang N, Jin SH, Li JY. Deep sequencing analysis of small non-coding RNAs reveals the diversity of microRNAs and piRNAs in the human epididymis. Gene 2012; 497: 330–335.
47. Cortadellas N, Durfort M. Fate and composition of cytoplasmic droplet of hamster epididymal spermatozoa. J Morphol 1994; 221:199–210.
48. Sullivan R, Saez F, Girouard J, Frenette G. Role of exosomes in sperm maturation during the transit along the male reproductive tract. Blood Cells Mol Dis 2005; 35:1–10.
49. Sullivan R, Saez F. Epididymosomes, prostasomes, and liposomes: their roles in mammalian male reproductive physiology. Reproduction 2013; 146:R21–R35.
50. Belleannee C, Calvo E, Caballero J, Sullivan R. Epididymosomes convey different repertoires of microRNAs throughout the bovine epididymis. Biol Reprod 2013; 89:30.
51. Lotvall J, Valadi H. Cell to cell signalling via exosomes through esRNA. Cell Adh Migr 2007; 1:156–158.
52. Mittelbrunn M, Gutierrez-Vazquez C, Villarroya-Beltri C, Gonzalez S, Sanchez-Cabo F, Gonzalez MA, Bernad A, Sanchez-Madrid F. Unidirectional transfer of microRNA-loaded exosomes from T cells to antigen-presenting cells. Nat Commun 2011; 2:282.
53. Valadi H, Ekstrom K, Bossios A, Sjostrand M, Lee JJ, Lotvall JO. Exosome-mediated transfer of mRNAs and microRNAs is a novel mechanism of genetic exchange between cells. Nat Cell Biol 2007; 9: 654–659.
54. Sullivan R, Frenette G, Girouard J. Epididymosomes are involved in the acquisition of new sperm proteins during epididymal transit. Asian J Androl 2007; 9:483–491.
55. Bachiller D, Schellander K, Peli J, Ruther U. Liposome-mediated DNA uptake by sperm cells. Mol Reprod Dev 1991; 30:194–200.
56. Cossetti C, Lugini L, Astrologo L, Saggio I, Fais S, Spadafora C. Soma-to-germline transmission of RNA in mice xenografted with human tumour cells: possible transport by exosomes. PLoS One 2014; 9:e101629.
57. Aitken RJ, Nixon B, Lin M, Koppers AJ, Lee YH, Baker MA. Proteomic changes in mammalian spermatozoa during epididymal maturation. Asian J Androl 2007; 9:554–564.
58. Schoysman R, Vanderzwalmen P, Nijs M, Segal L, Segal-Bertin G, Geerts L, van Roosendaal E, Schoysman D. Pregnancy after fertilisation with human testicular spermatozoa. Lancet 1993; 342:1237.
59. Schoysman R, Segal L, Van Der Zwalmen P, Nijs M, Bertin G, Cittadini E, Cimino C, Ruvolo G, Cefalu E, Palermo R. Assisted fertilization with epididymal spermatozoa. Acta Eur Fertil 1993; 24:7–12.
60. Schjenken JE, Robertson SA. Seminal fluid and immune adaptation for pregnancy–comparative biology in mammalian species. Reprod Domest Anim 2014; 49(suppl 3):27–36.
61. Smythies J, Edelstein L, Ramachandran V. Molecular mechanisms for the inheritance of acquired characteristics-exosomes, microRNA shuttling, fear and stress: Lamarck resurrected? Front Genet 2014; 5:133.
62. Gapp K, Jawaid A, Sarkies P, Bohacek J, Pelczar P, Prados J, Farinelli L, Miska E, Mansuy IM. Implication of sperm RNAs in transgenerational inheritance of the effects of early trauma in mice. Nat Neurosci 2014; 17: 667–669.
63. Colas AR, McKeithan WL, Cunningham TJ, Bushway PJ, Garmire LX, Duester G, Subramaniam S, Mercola M. Whole-genome microRNA screening identifies let-7 and mir-18 as regulators of germ layer formation during early embryogenesis. Genes Dev 2012; 26:2567–2579.
64. Torchinsky A, Toder V. To die or not to die: the function of the transcription factor NF-kappaB in embryos exposed to stress. Am J Reprod Immunol 2004; 51:138–143.
65. Schjenken JE, Glynn DJ, Sharkey DJ, Robertson SA. TLR4 signaling is a major mediator of the female tract response to seminal fluid in mice. Biol Reprod 2015; 93:68.
66. Fullston T, Ohlsson Teague EM, Palmer NO, DeBlasio MJ, Mitchell M, Corbett M, Print CG, Owens JA, Lane M. Paternal obesity initiates metabolic disturbances in two generations of mice with incomplete penetrance to the F2 generation and alters the transcriptional profile of testis and sperm microRNA content. FASEB J 2013; 27:4226–4243.
67. Stowe HM, Calcatera SM, Dimmick MA, Andrae JG, Duckett SK, Pratt SL. The bull sperm microRNAome and the effect of fescue toxicosis on sperm microRNA expression. PLoS One 2014; 9:e113163.
68. Marczylo EL, Amoako AA, Konje JC, Gant TW, Marczylo TH. Smoking induces differential miRNA expression in human spermatozoa: a potential transgenerational epigenetic concern? Epigenetics 2012; 7:432–439.
69. Palmer NO, Bakos HW, Fullston T, Lane M. Impact of obesity on male fertility, sperm function and molecular composition. Spermatogenesis 2012; 2:253–263.
70. Belleannee C, Legare C, Calvo E, Thimon V, Sullivan R. microRNA signature is altered in both human epididymis and seminal microvesicles following vasectomy.Hum Reprod 2013; 28:1455–1467.

SCIENTIFIC REPORTS

OPEN

Received: 25 April 2016
Accepted: 26 July 2016
Published: 23 August 2016

Characterisation of mouse epididymosomes reveals a complex profile of microRNAs and a potential mechanism for modification of the sperm epigenome

Jackson N. Reilly[1], Eileen A. McLaughlin[1,2], Simone J. Stanger[1], Amanda L. Anderson[1], Kate Hutcheon[3], Kiralee Church[1], Bettina P. Mihalas[1], Sonika Tyagi[4], Janet E. Holt[5], Andrew L. Eamens[3] & Brett Nixon[1]

Recent evidence has shown that the sperm epigenome is vulnerable to dynamic modifications arising from a variety of paternal environment exposures and that this legacy can serve as an important determinant of intergenerational inheritance. It has been postulated that such exchange is communicated to maturing spermatozoa via the transfer of small non-protein-coding RNAs (sRNAs) in a mechanism mediated by epididymosomes; small membrane bound vesicles released by the soma of the male reproductive tract (epididymis). Here we confirm that mouse epididymosomes encapsulate an impressive cargo of >350 microRNAs (miRNAs), a developmentally important sRNA class, the majority (~60%) of which are also represented by the miRNA signature of spermatozoa. This includes >50 miRNAs that were found exclusively in epididymal sperm and epididymosomes, but not in the surrounding soma. We also documented substantial changes in the epididymosome miRNA cargo, including significant fold changes in almost half of the miRNAs along the length of the epididymis. Finally, we provide the first direct evidence for the transfer of several prominent miRNA species between mouse epididymosomes and spermatozoa to afford novel insight into a mechanism of intercellular communication by which the sRNA payload of sperm can be selectively modified during their post-testicular maturation.

Spermatozoa released from the germinal epithelium of the testes are functionally immature, lacking both motility and the potential to fertilise an ovum[1]. These attributes are progressively acquired as they traverse the several meters of the epididymal tubule, a highly specialised region of the extragonadal male reproductive tract[2]. Since spermatozoa are both transcriptionally and translationally quiescent, this functional transformation is driven exclusively by the luminal microenvironment that they encounter during their prolonged residence within this ductal system[3]. This environment is, in turn, created by the combined secretory and absorptive of the lining epithelium and characterised by considerable segment-segment variation[4]. A central component of epididymal soma-spermatozoa intercellular communication are epididymosomes, a heterogeneous population of small membrane bound vesicles that are released from the epididymal epithelium via an apocrine secretory mechanism[5–8].

[1]Priority Research Centre for Reproduction, School of Environmental and Life Sciences, Discipline of Biological Sciences, University of Newcastle, Callaghan, New South Wales 2308, Australia. [2]School of Biological Sciences, University of Auckland, Auckland 1142, New Zealand. [3]School of Environmental and Life Sciences, Discipline of Biological Sciences, University of Newcastle, Callaghan, New South Wales 2308, Australia. [4]Australian Genome Research Facility Ltd, The Walter and Eliza Hall Institute, Parkville, Victoria 3052, Australia. [5]School of Biomedical Sciences and Pharmacy, Faculty of Health and Medicine, University of Newcastle, Callaghan, New South Wales 2308, Australia. Correspondence and requests for materials should be addressed to B.N. (email: Brett.Nixon@newcastle.edu.au)

Similar to the exosome population documented in other somatic tissues and bodily fluids, epididymosomes are able to relay a complex macromolecular cargo to recipient cells[9–11]. As such, they have been implicated as holding major roles in the promotion of sperm maturation by virtue of their ability to exert paracrine control of the epididymal epithelium[11] and via the direct contact they have with the maturing sperm population[5–8]. Traditional paradigms have held that the key elements of this transfer are proteins that contribute to the acquisition of various functional attributes necessary to reach the site of fertilisation and engage in interactions with the oocyte[6,7]. However, recent evidence suggests that such exchange may extend to additional molecules such as small non-protein-coding RNAs (sRNAs)[12].

These data are of considerable interest in view of the potential role sRNAs play in altering the sperm epigenome, and further, manipulation of this specific cargo may mediate direct consequences in offspring if the paternal linage encounters environmental insult(s)[13,14]. In this context, a growing body of recent evidence has shown that the sperm epigenome is modified by exposure to a wide range of environmental stressors, including chronic stress[15,16], paternal diet[12,17,18] and cigarette smoke[19]. Since these epigenome perturbations are inheritable, they are capable of influencing the developmental trajectory and/or health of offspring. Such findings encourage detailed spatial and temporal documentation of these mechanism(s), to identify where and when such epigenetic information is relayed to developing gametes. In this regard, many studies have put forward the hypothesis that such alterations coincide with sperm passage through the epididymis[14,20], a time in which spermatozoa are known to be particularly vulnerable to a range of insults having left the relative protection afforded by the testicular germinal epithelium[21]. This agrees with our own evidence, that is; the sperm miRNA profile is dynamically modified as the cells migrate through the epididymis[22]. Furthermore, and in keeping with established paradigms of intercellular communication in other tissues[23,24], it has been repeatedly suggested that epididymosomes may serve as a vehicle to mediate soma-spermatozoa intercellular communication[14,20]. Notwithstanding the growing acceptance of this mechanism, and the elegant demonstration that bovine epididymosomes can deliver miRNA cargo to epididymal epithelial cells during *in vitro* co-culture[11], direct transfer of miRNAs from epididymosomes to spermatozoa has not yet been substantiated by conclusive experimental evidence.

While epididymosomes are beginning to emerge as attractive candidate vectors to facilitate the transfer of epigenetic information to spermatozoa, there remain fundamental challenges to this field of extracellular vesicle research. Not the least, is the development of robust and reproducible methods for epididymosome isolation and characterisation, particularly in the context of established laboratory models such as the rodents, where the scale of epididymal fluid recovery remains a particular challenge. Here, in an effort to address this limitation, we report the validation of a simple method of epididymosome isolation from differing segments of the mouse epididymis and the profiling of the miRNA content of these specialised extracellular vesicles. Additionally, we provide the first direct evidence for the selective transfer of miRNA cargo between epididymosomes and mouse spermatozoa.

Results

Isolation of epididymosomes from the mouse epididymis. Our initial studies focused on evaluating the suitability of a number of protocols for purification of epididymosomes, including: (i) ultracentrifugation, (ii) OptiPrep density-based separation, and (iii) a commercial total exosome isolation kit. Among these, the greatest consistency and highest recovery of enriched populations of epididymosomes was achieved using the OptiPrep density-based separation. This technique had the added advantage that it was scalable, thus enabling us to generate sufficient material for detailed endpoint analysis of epididymosome cargo. This technique was therefore used for all subsequent analyses to establish the miRNA cargo of epididymosomes derived from the different segments of the mouse epididymis.

A suite of confirmation assays were employed to assess the enrichment and purity of the epididymosome isolation via the OptiPrep protocol. The relatively low-density epididymosomes readily partitioned away from other contaminants in a translucent layer corresponding to fractions 9–11 of the OptiPrep density gradient. Quantitative analysis of these fractions confirmed they possessed the highest concentration of both total protein and RNA of each of the twelve fractions (Fig. 1a). Importantly, a consistent profile of protein and RNA enrichment (both peaking in fraction 10) was obtained irrespective of the epididymal segment from which the epididymosomes were isolated. Furthermore, we failed to observe any significant variation in the physical properties of the epididymosomes in fractions 9–11. In this context, sizing analysis confirmed the purity of these preparations revealing a heterogeneous population of particles of approximately 50 to 150 nm (Fig. 1b). Immunoblot assessment of the abundance of extracellular vesicle markers, FLOT1 and CD9, confirmed that both assessed markers partitioned almost exclusively into fractions 9 and 10 (Fig. 1c). Epididymosomes from these fractions also readily adhered to aldehyde/sulphate latex beads permitting their visualisation via labelling with both anti-FLOT1 and anti-CD9 antibodies (Fig. 1d). In contrast, no such labelling was detected in beads incubated with either anti-PLZF (an irrelevant protein control) or secondary antibody only negative controls (Supplementary Figure S1). Finally, ultrastructural analysis confirmed both the purity and sizing of the epididymosomes preparations (Fig. 1e). Taken together, these analyses confirm the successful isolation of epididymosomes from the intraluminal milieu of the mouse epididymis. Owing to the highest expression of extracellular vesicle markers (Fig. 1c) and the lowest size heterogeneity (Fig. 1b), fractions 9 and 10 were selected as the focus of our remaining studies. These fractions were pooled and, prior to next generation sequencing, each biological replicate was assessed via immunoblotting for a variety of markers to ensure: (i) minimal contamination with either blood (haemoglobin, HBB) and/or cytoplasmic droplets (arachidonate 15-lipoxygenase, ALOX15)[25], and (ii) enrichment of known epididymosome protein cargo (26S proteasome non-ATPase regulatory subunit 7, PSMD7; heat shock protein 90kDa beta member 1, HSP90B1; beta tubulin, TUBB)[10]. As shown in Fig. 1f, neither HBB nor ALOX15 were detected within the epididymosome preparations. In contrast, the epididymosome preparations did contain PSMD7, HSP90B1, and TUBB.

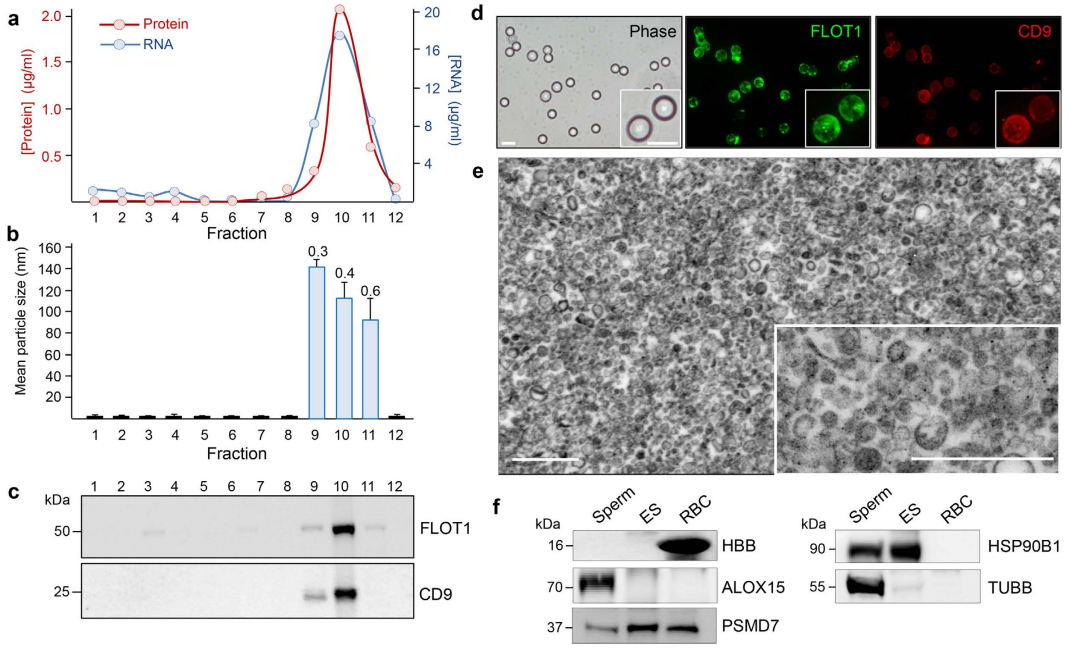

Figure 1. Assessment of epididymosome purity. A suite of assays were employed to assess the purity of epididymosomes isolated by OptiPrep density gradient fractionation. Briefly, twelve equal fractions were recovered after ultracentrifugation of the gradient and an aliquot of each prepared for (**a**) quantitative assessment of both protein and RNA content and (**b**) size heterogeneity. The latter was accomplished via measurement of mean particle size using dynamic light scattering. These data are reported as particle size (columns) and a polydispersity index value (numbers above columns), whereby the lower the value the more homogenous the preparation. (**c**) Immunoblot analyses were performed to determine distribution of the epididymosome markers flotillin 1 (FLOT1) and CD9 within each fraction. (**d**) The same markers were also used to dual-label epididymosomes bound to aldehyde/sulphate latex beads (FLOT1 green, CD9 red). Scale bar = 5 μm. (**e**) Epididymosome preparations were also assessed via transmission electron microscopy to confirm the size and heterogeneity of the isolated populations. Scale bar = 500 nm. (**f**) Epididymosome (ES) preparations (pooled fractions 9 and 10) were resolved by SDS-PAGE alongside cell lysates prepared from spermatozoa (sperm) and red blood cells (RBC) and immunoblotted with either anti-haemoglobin (HBB) or anti-arachidonate 15-lipoxygenase (ALOX15) antibodies to control for blood and/or cytoplasmic droplet contamination, respectively. Immunoblots were also probed with antibodies against known epididymosome protein cargo (26S proteasome non-ATPase regulatory subunit 7, PSMD7; heat shock protein 90kDa beta member 1, HSP90B1; beta tubulin, TUBB).

Characterisation of the miRNA signature of mouse epididymosomes. Next generation sequencing was employed to elucidate the miRNA cargo present in mouse epididymosomes. This approach identified a total of 358 miRNAs across the three epididymal segments surveyed (Supplementary Table S1). Among the 358 miRNAs detected, the highest read scores were returned for miRNAs: *miR-10b-5p*, *miR-10a-5p*, *miR-143-3p*, *miR-141-3p* and *miR-30a-5p*. Via normalisation based on total read counts for each library, a gradient of increasing miRNA profile complexity was noted between epididymosomes sampled from the proximal (caput) versus the distal (cauda) epididymal segments. Specifically, the overall number of epididymosome-borne miRNAs increased from 277 in the caput, to 322 in the cauda epididymis (Fig. 2a). Of these, a majority (~68%) were detected in each epididymosome fraction derived from the three epididymal segments examined. Further, profiling also revealed that only ~17% of detected miRNAs were unique to any one epididymal segment (Fig. 2a). Notwithstanding this striking conservation of epididymosome miRNA cargo, the profile for this sRNA species was far from static with substantial variations recorded in the relative abundance of numerous miRNAs between epididymal segments. For instance, of the 321 miRNAs present in both the caput and corpus epididymosomes, 28% exhibited significant differences in abundance (13% up- and 15% down-regulated) between the two segments (fold change of $\geq \pm 2$; FDR <0.05; Fig. 2b and Supplementary Table S2). A similar number of differentially accumulating miRNAs were identified among the 342 miRNAs detected in corpus and cauda epididymosome fractions (13% up- and 9% down-regulated; Fig. 2b and Supplementary Table S2). This trend was even more pronounced when considered across the entire length of the tract with almost half (~46%) of the 349 miRNAs identified in the caput and cauda segments showing significant fold changes (Fig. 2b and Supplementary Table S2).

Illustrative of the magnitude of these variations, several miRNAs were determined to have accumulation differences of greater than 64-fold between the different epididymal segments examined (Fig. 3 and Supplementary Table S2). Among the numerous examples of these, miRNAs *miR-208b-3p* and *miR-196b-5p* appeared to be selectively accumulating into cauda epididymosomes (compared to caput epididymosomes), such that these two

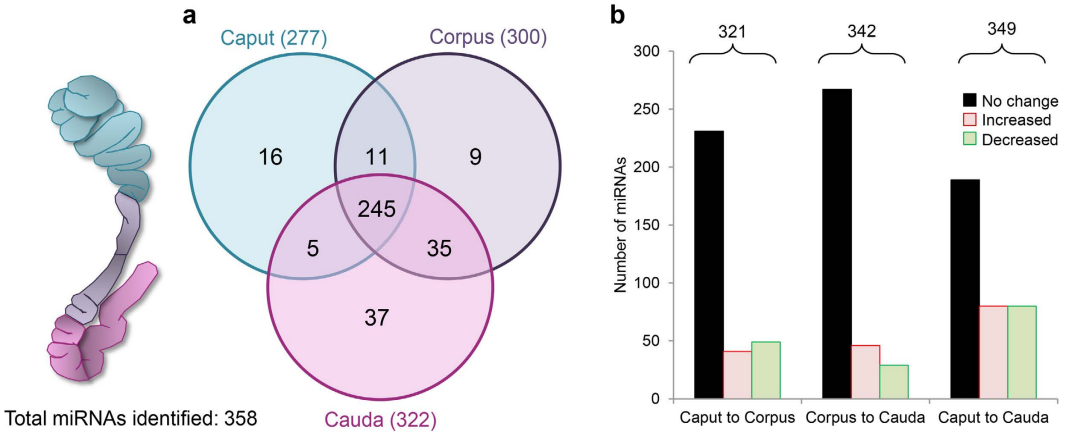

Figure 2. Evaluation of epididymosome miRNA signatures throughout the epididymis. (**a**) Venn diagram illustrating the total number of mature miRNAs identified in adult mouse epididymosomes by next generation sequencing and their distribution throughout the caput, corpus and caudal epididymal segments. (**b**) Graphical representation of the proportion of miRNAs identifying those that were either present at equivalent levels (unchanged) or alternatively, were significantly up- or down-regulated (increased or decreased, respectively) (threshold = ±≥2-fold change and false discovery rate of <0.05) across different epididymal segments. Post normalisation average counts of ≥10 reads / million across each of three biological replicates (n = 9–12 mice/ replicate) were used as a detection sensitivity threshold for the positive identification of epididymosome miRNAs reported in this study.

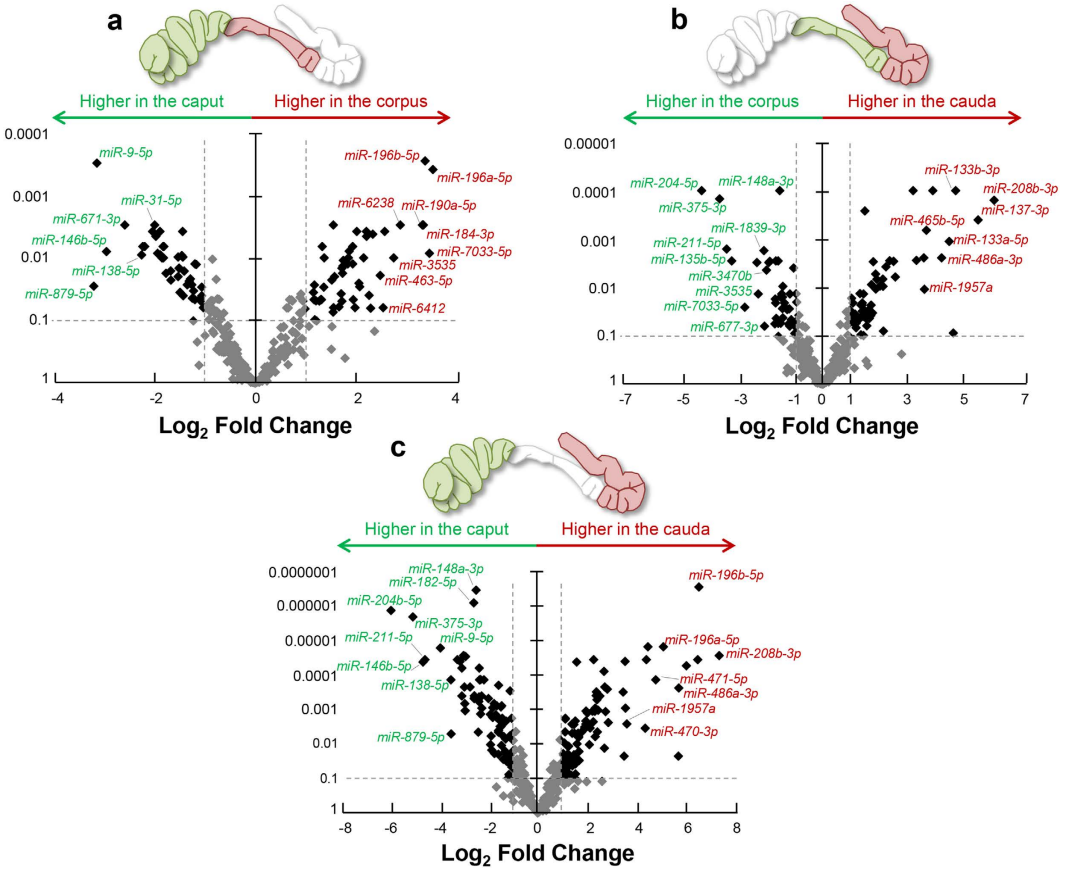

Figure 3. Volcano plots depicting fold changes associated with differentially accumulated epididymosome miRNAs. Volcano plots were constructed to demonstrate the fold change (x-axis) and false discovery rate (y-axis) of miRNAs that were determined to be differentially accumulated in epididymosomes isolated from the (**a**) caput/corpus, (**b**) corpus/cauda, and (**c**) caput/cauda epididymis. Thresholds denoting significant increases or decreases in miRNA accumulation are depicted by dotted lines (threshold = ±≥2 fold change and false discovery rate of <0.05).

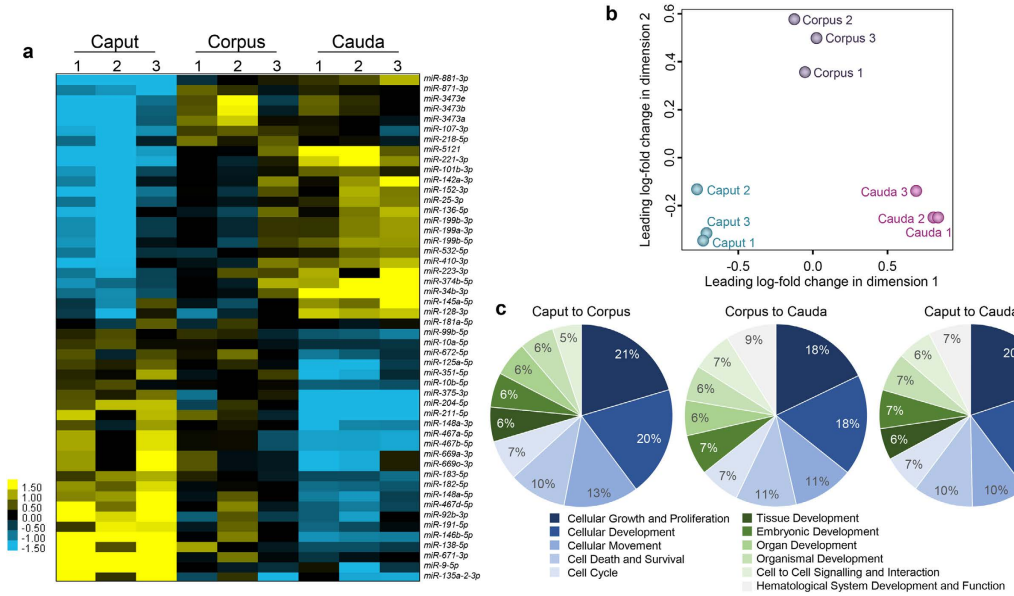

Figure 4. Profiling of variability in epididymosome miRNA abundance across biological replicates and determination of the putative biological functions regulated by differentially accumulating miRNAs. (**a**) Hierarchical clustering of the 50 miRNAs that exhibited the highest fold changes between epididymal segments was performed to assess consistency among the three biological replicates subjected to next generation sequencing. Cells within the matrix depict the relative abundance of a single miRNA, with yellow and blue colouring representing the accumulation (log_2 fold change), above and below the median accumulation of this miRNA, in all biological replicates respectively. (**b**) Multi-dimension scaling analysis of normalised miRNA data based on leading log fold changes of the miRNAs showing the relationship between biological replicates. Three distinct populations are shown, corresponding to epididymosomes sampled from each epididymal segment. (**c**) Biological functions of differentially accumulating epididymosome miRNAs were predicted through interrogation of Ingenuity Pathway Analysis software. A majority of the experimentally validated target genes mapped to the broad categories of regulating cellular growth and proliferation, cell development, and cell death and survival.

miRNAs were 147 and 84 fold more abundant, respectively (Fig. 3c). Conversely, miRNAs *miR-204b-5p* and *miR-375-3p* returned an opposing accumulation profile for epididymosomes sampled from the same two epididymal segments (i.e. caput and cauda) with their respective levels reduced ~55 and 32 fold, respectively (Fig. 3c).

Notably, we recorded consistent results across all biological replicates, both in terms of the overall number of miRNA reads that were detected by next generation sequencing (Supplementary Table S1) and the relative fold change between segments as reported by hierarchal clustering analysis (Fig. 4a), and multi-dimensional scaling (MDS; Fig. 4b). MDS clearly illustrated tight clustering of the biological replicates representing epididymosomes sampled from the three epididymis segments analysed, thus enabling clear differentiation of each population of epididymosomes on the basis of their epididymal segment of origin (Fig. 4b). Despite this clustering, an *in silico* analysis of the key biological pathways potentially targeted by differentially accumulating miRNAs revealed considerable conservation, with a majority centred on regulation of the broad categories of cellular growth and proliferation, cellular development, and cell death and survival (Fig. 4c). Such categories accord with those previously documented for the miRNA cargo identified in mouse epididymal spermatozoa[22]. In this context, it was also notable that 6–7% of all differentially accumulated epididymosome miRNAs mapped to the category of embryonic development (Fig. 4c).

Validation of epididymosome miRNA abundance. To confirm the next generation sequencing data, the levels of eight miRNAs were quantified by RT-qPCR. The selected miRNAs fall into one of two groupings: i) high accumulation in the caput (*miR-375*, *miR -467a*, *miR-467d* and *miR-467e*), or ii) high accumulation in the cauda epididymis (*miR-34b*, *miR-34c*, *miR-139* and *miR-196b*). These analyses confirmed the sequencing data with each of the eight assessed miRNAs returning differential accumulation profiles across the three analysed segments of the epididymis from which epididymosomes were harvested (Fig. 5). Both assessment strategies were also highly suggestive that miRNA incorporation into epididymosomes is selective. For instance, *miR-34c* and *miR-467e* were found to be predominantly accumulated into epididymosomes in the cauda and caput epididymis, respectively. In contrast, the expression of *miR-34c* was some 2-fold higher in the epithelium of the caput epididymis versus that of the cauda, and in the case of *miR-467e*, we failed to detect this miRNA in the epithelium of any segment of the epididymis (Supplementary Table S3)[26]. We did however note close similarities in the trends of miRNA abundance within both epididymosomes and spermatozoa

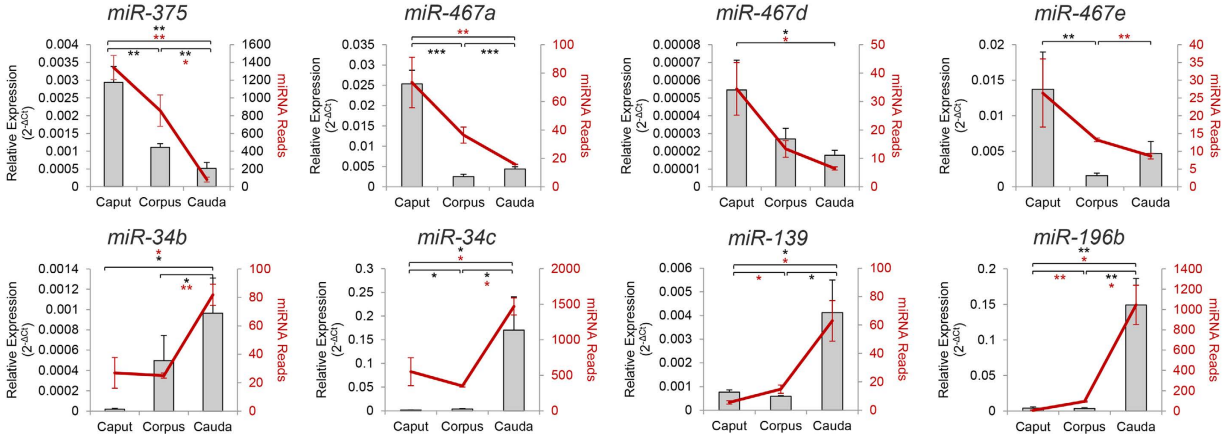

Figure 5. RT-qPCR validation of the abundance of differentially accumulating epididymosome miRNAs. Next generation sequence data were validated via the targeted RT-qPCR amplification of differentially accumulating miRNAs. Candidate miRNAs included representatives with the highest abundance (according to sequencing data) in epididymosomes from the proximal (caput: *miR-375*, *miR-467a*, *miR-467d* and *miR-467e*) or distal epididymis (cauda: *miR-34b*, *miR-34c*, *miR-139* and *miR-196b*). cDNA generation and RT-qPCR validations were performed in triplicate using three pools of biological samples (n = 6–9 mice per sample) differing from those used for next generation sequence analyses. Expression levels of target miRNAs were normalised against the U6 small nuclear RNA control (determined to uniformly accumulate across samples by sequencing). Values are shown as an average ± SEM. *P < 0.05, **P < 0.01, ***P < 0.001. NGS reads are represented as dark red line graphs while the relative abundance ($2^{-\Delta Ct}$) of each miRNA assessed by RT-qPCR is represented by the grey columns.

sampled from equivalent segments (Supplementary Table S3)[22]. In this context, *miR34c* and *miR-467e* were again most abundant in cauda and caput spermatozoa, respectively[22].

Comparison of the miRNA profile of epididymal epithelial cells, spermatozoa and epididymosomes. To build on these observations, we profiled two previously generated sequencing datasets[22,26] to compare the miRNA signatures of mouse epididymal epithelial cells (accession number GSE70197), spermatozoa (accession number GSE70198), and epididymosomes (this study). This analysis revealed a number of striking results, including; only ~46% (190) of the 412 miRNAs identified across the three individual experiments performed were represented in each dataset (Supplementary Table S3). Further, 164 of the total number of miRNAs detected in epididymosomes (n = 358) were either absent, or below the established detection sensitivity, in the epididymal soma. These included several highly abundant epididymosome miRNAs, namely *miR-21a-5p* (20,283 reads) and *miR-6240* (2,427 reads; Supplementary Table S1). Such data accord with independent evidence that a portion of miRNAs are selectively packaged into epididymosomes thus precluding their accumulation in the parent epithelial cells from which they originate[11]. In contrast to the epithelial cell-epididymosome comparison, this approach also revealed substantial overlap in the miRNA profiles of spermatozoa and epididymosomes (Supplementary Table S3). More specifically, spermatozoa share 242 (82%) of their total pool (n = 295) of miRNAs with that of epididymosomes. In addition, 52 miRNAs detected in both our spermatozoa/epididymosome datasets were further determined to be absent in our epididymal epithelial cell miRNA profiles.

Linear regression analysis was also undertaken to gauge similarities in the relative abundance of miRNAs that were detected in mouse epididymal epithelial cell, spermatozoa and epididymosome datasets (Fig. 6). A strongest positive correlation was detected in comparisons of the abundance of miRNAs in caput-corpus epithelial cells and spermatozoa ($R^2 = 0.792$ and 0.812, respectively). Similar positive correlations were also observed when comparing miRNA abundance between sperm-epididymosomes and between epithelial cells-epididymosomes however, the correlation coefficient was lower among these datasets. A notable exception to this trend was that the miRNA profile of cauda sperm was markedly different to that of cauda epithelial cells and epididymosomes ($R^2 = 0.042$ and 0.002, respectively), while comparison of miRNA abundance between cauda epithelial cells-epididymosomes revealed a strong positive correlation ($R^2 = 0.768$). These observations parallel our previous analyses, which demonstrated that the miRNA signature of cauda spermatozoa is highly dissimilar to that of caput and corpus spermatozoa[22]. Further, comparison of miRNA abundance between epithelial cells-epididymosomes revealed that epididymosomes are substantially enriched in multiple miRNAs, particularly in the corpus and cauda epididymal segments. The observed miRNA enrichment within epididymosomes relative to parent epididymal cells provides ancillary evidence for the highly selective compartmentalisation and export of epithelium-generated miRNAs.

miRNAs are directly transferred from epididymosomes to mouse spermatozoa. We next sought to investigate the potential for epididymosome-mediated transfer of miRNAs to spermatozoa. Although such a mode of intercellular trafficking has been confirmed for protein cargo[27], it remains to be proven as a mechanism for transfer of miRNAs to maturing mouse spermatozoa. For the purpose of this study, we employed a co-incubation strategy originally developed for investigating of the delivery of epididymosome protein cargo to

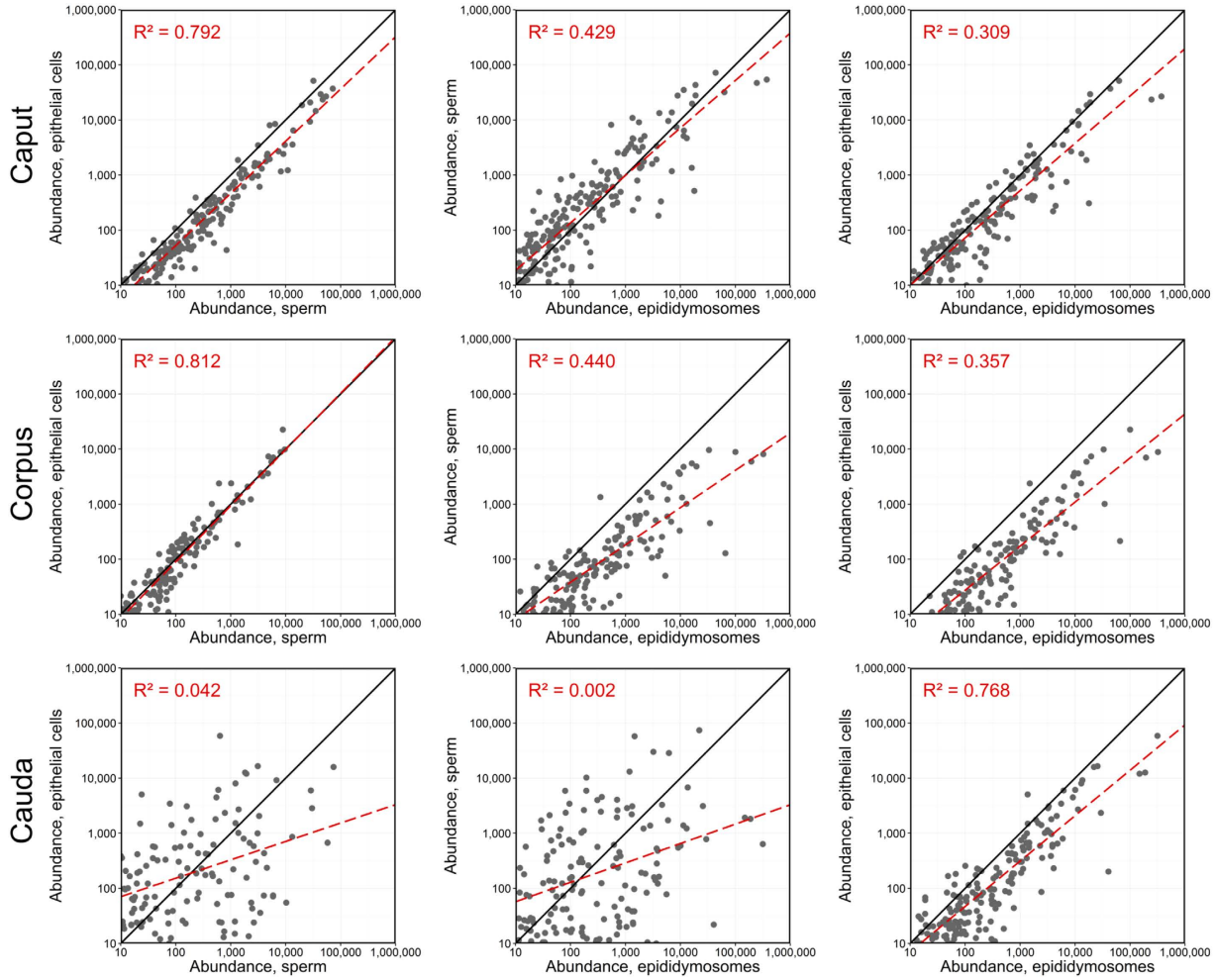

Figure 6. Linear regression modelling of miRNA accumulation in sperm, epithelial cell and epididymosome populations. Scatterplots of genome-wide miRNA accumulation between epididymal sperm, epithelial cell and epididymosome datasets revealed substantial correlation in the miRNA signature between cell types. Linear regression modelling (red dashed line) and calculation of R^2 values was performed in R.

spermatozoa in the bovine model[27]. The utility of this protocol was initially assessed by labelling of epididymosomes with carboxyfluorescein diacetate succinimidyl ester (CFSE). As anticipated based on an absence of esterase activity, the labelled epididymosomes did not yield any fluorescent signal following adherence to aldehyde/sulphate latex beads (Fig. 7a). In contrast, approximately 30% of the live sperm population were strongly labelled following co-incubation with CFSE loaded epididymosomes (Fig. 7b). Notably, this labelling appeared highly selective such that it was exclusively detected in the head and mid-piece of the flagellum and further appeared restricted to live spermatozoa, with no staining observed in any of the dead cells. To control for the possibility of non-specific labelling due to the presence of unbound CFSE, spermatozoa were also directly labelled with CFSE, revealing a distinct pattern of labelling that was present in all cells. Specifically, the dye readily labelled the entire sperm cell, including both the head and mid/principal piece of the flagellum (Fig. 7c). In contrast to epididymosome-mediated labelling, direct labelling of the sperm population also yielded CFSE fluorescence, albeit less intense, in dead cells (Fig. 7c). The selectivity of CFSE internalisation was further evidenced via the use of a competition assay whereby spermatozoa were incubated with varying proportions of CFSE labelled (0%, 25%, 50%, 100%) versus non-labelled (100%, 75%, 50%, 0%) epididymosomes (Fig. 7d). As shown, this experiment established a strong dose-response relationship, whereby the more CFSE labelled epididymosomes present in the co-incubation suspension, the greater the percentage of spermatozoa that stained with CFSE.

Having established the suitability of a co-incubation protocol to track spermatozoa-epididymosome interactions, we next investigated whether such interactions facilitated the transfer of miRNA cargo to spermatozoa. Five miRNAs (*miR-191*, *miR-375*, *miR-467a*, *miR-467d*, *miR-467e*) were selected for inclusion in this analysis based on their high abundance in caput epididymosomes. As illustrated in Fig. 8, this strategy proved effective in demonstrating significant accumulation of each of the five target miRNAs into spermatozoa. Since, only ~30% of the live sperm population were able to consistently internalise the CSFE dye during epididymosome co-incubation (Fig. 7d), it is considered likely that miRNA transfer efficacy would be considerably higher if this analysis was

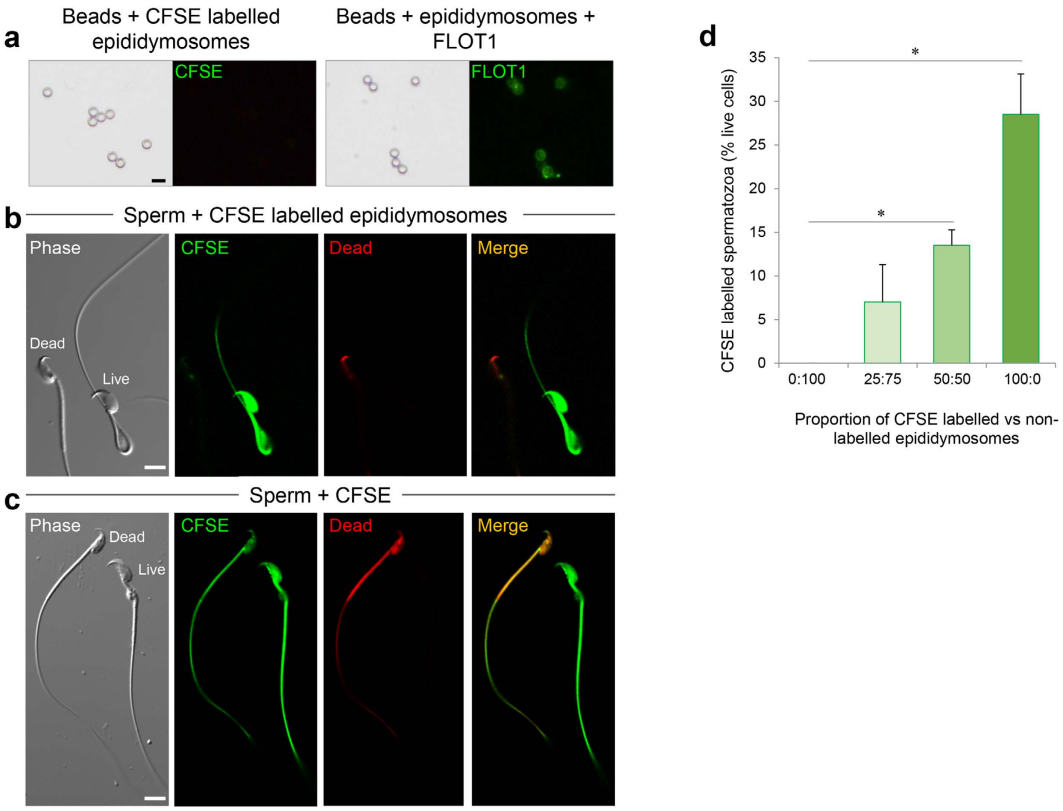

Figure 7. Assessment of sperm-epididymosome interaction. The ability of epididymosomes to interact and deliver encapsulated cargo to spermatozoa was investigated after co-incubation. Prior to analysis, preparations of caput and corpus epididymosomes were pooled and labelled with carboxyfluorescein diacetate succinimidyl ester (CFSE). (**a**) CFSE labelled epididymosomes were concentrated by binding to sulphate/aldehyde latex beads and examined by fluorescence microscopy, revealing no labelling. The efficacy of epididymosome bead binding was assessed by subsequent labelling with FLOT1. (**b**) CFSE labelled epididymosomes were washed prior to co-incubation with caput spermatozoa. After washing, spermatozoa were subsequently counterstained with live/dead stain (red = dead cells) and assessed via confocal microscopy. (**c**) Controls included caput sperm incubated directly with CFSE, caput sperm co-incubated with unlabelled epididymosomes and caput sperm incubated in media alone. The latter two treatments yielded no fluorescence labelling and consequently are not shown. Scale bars = 5 μm. (**d**) An additional competition assay was also performed as outlined for (**b**) with the exception that spermatozoa were co-incubated with varying proportions of non-labelled versus CFSE labelled epididymosomes. The efficacy of CFSE dye internalisation was subsequently recorded and are plotted as a percentage of live CFSE labelled spermatozoa.

restricted to the live cell only population. Nevertheless, the data presented in Fig. 8 provide the first evidence that identifies mouse spermatozoa as recipients of epididymosome-mediated transfer of miRNA cargo.

Discussion

This study extends on the previous work that has identified the miRNA class of sRNA as an additional and potentially developmentally important tier of regulation in the male reproductive tract[11,22,26,28–30]. Through development of a tractable protocol for the isolation of mouse epididymosomes, here we provide novel insight into the complexity of the segment specific miRNA profiles of these extracellular vesicles as well as exploring their capacity to deliver this important regulatory cargo to maturing spermatozoa. Our data indicate that, in addition to the more widely reported role as transporters of protein[7,31,32] and lipid cargo[9], epididymosomes are also carriers of miRNA, a developmentally important class of regulatory RNA. Further, many of the profiled miRNA were determined to be at considerably enriched levels compared to parent cells (the epididymal epithelial cells). Indeed, almost a third of the miRNAs detected in the epididymosome fraction were not present in our equivalent profiling of epididymal epithelial cell miRNAs[26]. While we cannot entirely discount the possibility that such differences may, in part, reflect either: (i) greater depth of sequence coverage achieved in our current analysis, (ii) profiling of a subset of epididymosomes originating from a non-surveyed epithelial cell population upstream of the caput epididymis, or (iii) contamination of our samples with vesicles released from ruptured cytoplasmic droplets; the data presented here does nevertheless accord with independent evidence that the epididymosome miRNA signature diverges from that of the epithelial cells from which they originate[11]. Taken together, the observations made to date present strong evidence that the packaging of the molecular cargo into epididymosomes is a highly selective, rather than stochastic process. Such a model draws support from a wealth of extracellular vesicle based

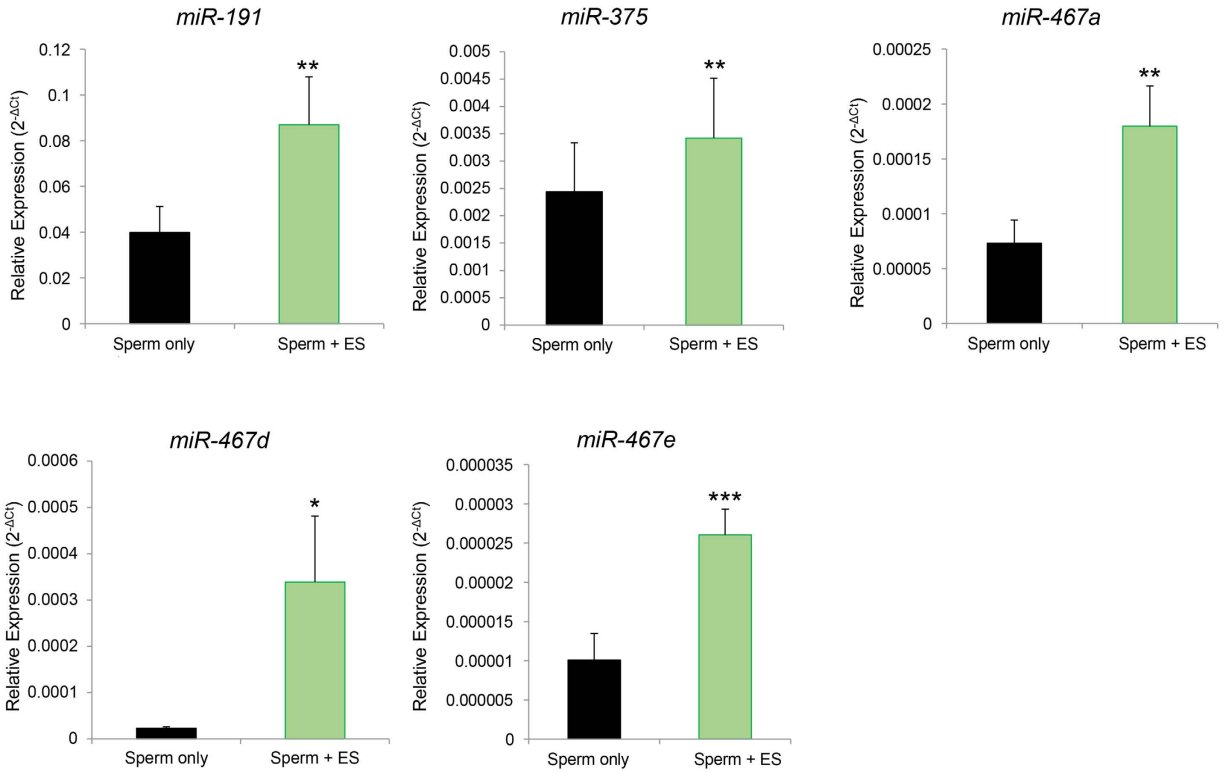

Figure 8. Examination of miRNA transfer to sperm after co-incubation with epididymosomes. The ability of sperm-epididymosome interaction to facilitate transfer of miRNA cargo to sperm was directly assessed by RT-qPCR amplification of candidate miRNAs (*miR-191*, *miR-375*, *miR-467a*, *miR-467d*, and *miR-467e*) from sperm that were incubated in either media alone (sperm only) or epididymosomes (sperm + ES). Analyses were performed in triplicate using three biological samples (n = 3 mice/sample). Values are shown as average abundance ± SEM. $*P < 0.05$, $**P < 0.01$, $***P < 0.001$.

studies[33–35], which have shown that abundant RNA species in extracellular vesicles can remain virtually undetectable in the parent cell[36]. However, the precise sorting mechanism responsible for discriminating the molecular payload of these vesicles from that of their parent cells remains poorly understood. While the presence of consensus exomotifs (e.g. GGAG and CCCU)[37] have been reported within the 3′ half of the mature sRNA sequence of miRNAs selectively incorporated into some exosome populations, similar motifs were only detected in the 3′ half of a small portion (25/358; ~7%) of the epididymosome-borne miRNAs identified here (Supplementary Figure S2). Such findings do not preclude the possibility that alternative exomotifs may be present among these miRNAs or that non canonical pathways[38] may be adopted for the extracellular export of miRNA in the epididymis.

The epididymis may represent an interesting model to address the question of selective vesicle packaging considering the substantive segment-segment variation in epididymosome miRNA profiles reported here. Indeed, we identified marked changes in epididymosome miRNA profiles between epididymal segments, including an apparent gradient of increasing profile complexity between the proximal and distal epididymal segments. This finding mirrors that of the sperm miRNA profile, that is; progressive modification of the miRNA profile as the sperm descend through the proximal epididymal segments (caput and corpus) before undergoing extensive changes coincident with their prolonged residence in the distal (cauda) epididymis[22]. These miRNA profiles do however, contrast with well established paradigms of epididymal sperm maturation that attribute the majority of functional changes to the proximal segments (distal caput/proximal corpus)[39]. From these data we infer that the modification of the sperm miRNA profile is not strictly tied to the functional maturation of these cells. Irrespective, they identify the epididymis as an important site in establishment of the sperm epigenome, and since these cells are incapable of *de novo* transcription, they also firmly implicate epididymosomes as a conduit for the transfer of such developmentally important regulatory information. Consistent with this hypothesis, we identified substantial overlap in the miRNA signature of both spermatozoa and epididymosomes with as many as 82% of sperm-borne miRNAs also being detected in epididymosomes. Prominent among these were members of the *let7, miR-30, miR-465, miR-466, miR-467*, and *miR-669* clusters.

We further exploited a co-incubation strategy originally developed in the bovine model[27] to provide proof-of-concept that mouse epididymosomes can directly interact with homologous spermatozoa. Moreover, we demonstrate that this is a productive interaction leading to an apparent uptake, and significant accumulation, of several prominent epididymosome miRNAs. While we have yet to explore the full extent of miRNA transfer facilitated during this interaction, we did make the striking observation that it was highly selective. In this context, an encapsulated tracer dye (CFSE) was exclusively delivered from epididymosomes to the sperm head and mid-piece of the flagellum. Given the transcriptionally inert state of the mature spermatozoon, it is considered unlikely the

uptake of miRNA into these intracellular domains would have any direct impact on the functional profile of these cells. Such restricted deposition would however, ideally position the miRNAs for entry into the oocyte cytosol at the time of fertilisation, thus enhancing the prospect that these miRNAs could serve as mediators of the epigenetic regulation of the resultant embryo. However, proof of an epigenetic regulatory role for epididymosome delivered miRNAs requires further evidence demonstrating that sperm-borne miRNAs control transcription homeostasis in fertilised oocytes, zygotes and two-cell embryos[40]. It is also notable that the sperm domains labelled with CFSE here perfectly align with the distribution of proteins trafficked to bovine spermatozoa via epididymosomes, which are also found to preferentially localise to the acrosomal and mid-piece domains[27]. The mechanism(s) by which such selective recognition and uptake of epididymosome cargo may be conferred have yet to be fully elucidated, but could conceivably involve complementary ligands/receptors furnished on the surface of the epididymosomes and the recipient spermatozoa[41]. In this context, previous work has shown that epididymosomes contain a variety of candidate adhesion molecules, including tetraspanins (CD9), integrins, and milk fat globule-epidermal growth factor 8 protein[42]. A similar repertoire of ligands have been documented on a variety of extracellular vesicles suggesting that they may be a universal feature to help target these entities and ensure selectivity in their uptake among the hundreds of cell types that they may encounter[35].

As an additional tier of specificity, it was also noted that epididymosomes appeared to exclusively interact with live cells; we consistently failed to detect any fluorescent dye labelling of dead or moribund cells. Importantly, such selectivity was not artefactual as illustrated by the strong fluorescent signal generated throughout the entire spermatozoon (both live and dead cells) upon direct incubation with free CSFC. An important precedent for these findings has been provided by the work of Sullivan and colleagues who have shown that epididymosomes constitute a heterogeneous pool that can be subdivided into at least two populations on the basis of size and the presence/absence of CD9[32,43]. The smaller of these (~10 to 100 nm) bear the CD9 antigen and bind preferentially to live spermatozoa, whereas the larger CD9 negative sub-population possess higher affinity for dead cells[6]. While the scale of epididymosome recovery from mice precluded the possibility of exploring such heterogeneity, the characteristics of the epididymosomes isolated here (i.e. CD9 positive, diameter of 50 to 150 nm) suggest that our isolation protocol may have been biased toward the former population. In any case, the ability of epididymosomes to actively bind live cells supports the concept that this interaction is tightly regulated and raises the intriguing possibility that the epididymis is able to discriminate cell quality and restrict its investment to the processing of viable cells[6].

Taken together, this work substantiates the growing consensus that the epididymis serves as a key staging point for establishment of the sperm epigenome[14]. Importantly, this epigenome may be altered by a range of environmental insults[44]. The relatively high degree of overlap documented among reported epididymosome miRNA profiles (Supplementary Tables S4 and S5)[11,45] strongly suggests that this mode of intercellular communication may be highly conserved across mammalian species. Indeed, notwithstanding limitations imposed by the use of different methodology for miRNA identification (next generation sequencing versus microarray approaches), our mouse epididymosome dataset comprised as many as 88% of the miRNAs that have previously been documented in bovine epididymosomes[11] (Supplementary Table S5). Further, and while beyond the scope of the present study, it is likely that epididymosome function may also extend to the horizontal transfer of additional species of regulatory non-protein-coding RNA, including (but not limited to) transfer RNA fragments (tRFs), piwi-interacting RNAs (piRNAs), and other subclasses of small-interfering RNA (siRNA), thus potentially contributing to pronounced epigenetic alterations (such as metabolic/reproductive disruption and adverse behavioural symptoms) on subsequent generations[15,16,46]. Indeed, the recent studies of Rando and colleagues (2016) present compelling evidence that dietary perturbations can alter the profile of tRFs delivered to sperm via epididymosomes[12]. Further exploration of this pathway for information transfer is thus likely to prove a productive avenue for future research, particularly in the context of addressing pertinent questions, such as: how do epididymal soma respond to environmental cues to alter the molecular cargo of epididymosomes[14]? This is particularly perplexing in view of the fact that many of the stressors linked to changes in the sperm epigenome[15,17,19] occur at sites distal from the male reproductive tract and that this tissue apparently lacks the innervation[3] required for conveying extrinsic stress-induced neuronal factors directly to the sperm. This has encouraged speculation that the heterogeneous population of epididymosomes that sperm encounter may include contributions, albeit minor, from somatic cells that lay beyond that of the male reproductive tract[13]. While the validity of such a model awaits further scrutiny, it is notable that genetic markers originating from distal somatic cells have been detected in epididymal mouse spermatozoa and crude preparations of plasma extracellular vesicles[47].

Notably, although a focus for our work has been epididymosome-sperm interactions, this does not discount the possibility that these extracellular vesicles hold a fundamental role in relaying regulatory information to enforce the strict control of epididymal epithelial cell function. Certainly, extracellular vesicles are replete in most biological fluids and have been conclusively shown to convey miRNA cargo to recipient cells where they act to initiate RNA regulatory pathways[48]. Further support for this form of paracrine regulation has been afforded by the elegant study of Sullivan and colleagues who have shown that epididymosomes can bind, and subsequently transfer miRNAs, directly to cultured epididymal epithelial cells[11]. Such a mechanism could underpin the control of at least a portion of the >17,000 genes that are known to be expressed in the mouse epididymis[49] and conceivably account (at least partially) for the segment-specific patterns of gene expression and/or protein abundance that characterise this ductal system[3]. Indeed, comprehensive transcriptomic analyses have led to the demarcation of 6 unique transcriptional units within the mouse epididymis[49]. Thus, in dividing the epididymis into three broad anatomical segments, we may have inadvertently overlooked some of the subtlety associated with epididymosome miRNA profiles. Despite this, an analysis of the key biological pathways potentially targeted by differentially accumulating miRNAs revealed a majority centred on regulation of cellular growth and proliferation, cellular development, and cell death and survival, as might be expected of molecules involved in the maintenance of epididymal homeostasis. Given that epididymosomes also feature among the constituents of seminal fluid that

are delivered to the female tract at the time of ejaculation, it must also be considered that they could exert similar regulatory control within the female reproductive with potential implications for conditioning of the periconceptual environment[50,51].

In summary, this study reports the comprehensive mapping of the miRNA profile of mouse epididymosomes under normal physiological conditions. In so doing, we have revealed a complex profile that is discrete from that of their parent cells. These data support the selective processing and packaging of the macromolecular cargo of epididymosomes, and demonstrate that this selective packaging further extends to their downstream interactions with spermatozoa. The significance of such findings lie in their validation of a widely promulgated model of intercellular communication between the epididymal soma and maturing germ cells. In addition to potential implications for epigenetic mechanisms of inheritance, these data identify epididymosomes as a potential conduit for modulating the environments of both the male and female reproductive tracts through the delivery of RNA silencing substrates. Further research is now warranted to explore the extent of the role epididymosomes play in such phenomena.

Methods

Reagents. All reagents used were of research grade and, unless specified, were obtained from Sigma Aldrich (St. Louis, Mo, USA) or ThermoFisher Scientific (Waltham, MA, USA).

Ethics statement. All experimental procedures were carried out with the approval of the University of Newcastle's Animal Care and Ethics Committee (approval number A-2013-322), in accordance with relevant national and international guidelines. Inbred Swiss mice were housed under a controlled lighting regime (16L: 8D) at 21–22 °C and supplied with food and water *ad libitum*. Prior to dissection, animals were euthanized via CO_2 inhalation.

Epididymosome isolation. Immediately after adult male mice (8 weeks old) were euthanised, their vasculature was perfused with pre-warmed PBS to minimise the possibility of blood contamination. The epididymides were then removed, carefully separated from fat and overlying connective tissue and dissected into three anatomical segments corresponding to the caput, corpus and cauda. Luminal fluid was aspirated from each segment by placing the tissue in a 500 μl droplet of modified Biggers, Whitten, and Whittingham media (BWW; pH 7.4, osmolarity 300 mOsm/kg[52,53]) and making multiple incisions with a razor blade. The tissue was then subjected to mild agitation and the medium subsequently filtered through 70 μm membranes. This suspension was then divided into three equal aliquots and prepared for epididymosome isolation using either differential centrifugation[54], a commercial exosome isolation protocol (Total Exosome Isolation kit, Invitrogen) or OptiPrep (Sigma-Aldrich) density gradients[55]. Of these, the OptiPrep density gradients proved most suitable and were therefore adopted for use in all subsequent experiments. This protocol involved sequential centrifugation of the epididymal fluid suspensions with increasing velocity (500 × g, 2,000 × g, 4,000 × g, 8,000 × g, 17,000 × g) to eliminate all cellular debris before layering the supernatant onto a discontinuous OptiPrep gradient (40%, 20%, 10%, and 5%), created by diluting 60% OptiPrep with a solution of 0.25 M sucrose, 10 mM Tris. The gradient was ultracentrifuged (100,000 × g, 18 h, 4 °C), after which twelve equivalent fractions were collected, diluted in PBS and subjected to a final ultracentrifugation spin (100,000 × g, 3 h, 4 °C). Notably, approximately 30–40% of the sperm cells recovered during the initial centrifugation step (500 × g), had shed their cytoplasmic droplet. While, it is considered unlikely that these relatively large entities (0.5 to 2.0 μm in diameter) would be co-purified with epididymosomes (~50 to 150 nm in diameter), it is acknowledged that they contain spherical vesicles (~60 to 100 nm in diameter)[56] that could be released if cytoplasmic droplets were ruptured. Thus, to control for this possibility, all isolated epididymosome preparations were immunoblotted with the antibodies against the cytoplasmic droplet marker, ALOX15[25].

Epididymosome characterisation. Isolated epididymosome fractions were characterised on the basis of their purity, particle size and overall homogeneity. Each sample was initially analysed on a Zetasizer Nano ZS (Malvern Instruments, Malvern, United Kingdom) to determine mean particle size in addition to the amount of variation within a sample. The latter is reported in the form of a polydispersity index (PDI), whereby low PDI values reflect highly monodisperse preparations, and values >1 indicate that the sample returned a varied size distribution. Each sample was analysed a minimum of 10 times, with 10 cycles per analysis. Epididymosome size and purity was further assessed via conventional transmission electron microscopy, whereby pelleted epididymosomes were sequentially fixed in 2.5% glutaraldehyde and 2% osmium tetroxide before being embedded in Spurr's resin as previously described[57]. Embedded resin blocks were sectioned with a diamond knife and micrographs were captured on a transmission electron microscope at 80 kV. Epididymosomes were further visualised via binding to 4 μm aldehyde/sulphate latex beads (ThermoFisher Scientific) and fluorescent labelling of recognised extracellular vesicle surface markers, including CD9 and flotillin 1 (FLOT1)[58] using established protocols for extracellular vesicle analysis[59]. As a final complementary validation strategy, isolated populations of epididymosomes were prepared for immunoblotting with a suite of antibodies recommended for experimental validation of extracellular vesicles, including anti-CD9, anti-FLOT1, anti-PSMD7, anti-HSP90B1, and anti-TUBB antibodies.

RNA extraction and next-generation sequencing of the small RNA fraction. Total RNA was extracted from purified epididymosomes using a Direct-zol RNA MiniPrep Kit (Zymo Research Corporation, Irvine, CA, USA) according to manufacturers' instructions before being incubated with 1% DNase (Promega) to eliminate genomic DNA contamination[53]. Total RNA from each epididymal segment (caput, corpus, cauda) was pooled from a minimum of nine animals to generate a single biological replicate. Three such biological replicates were subjected to Illumina TruSeq small RNA sample preparation protocol as per the manufacturers' instructions (Illumina Inc. San Diego, CA, USA) at the Australian Genome Research Facility (AGRF, Melbourne, VIC,

Australia). The miRNA libraries generated from the three biological replicates were analysed in triplicate and sequenced using an Illumina Hiseq-2000 RNA-seq platform as 50 base-pair (bp) single end chemistry at AGRF as previously described[22,26,53]. Briefly, the sequence reads from all samples were analysed for quality control on an Agilent 2100 Bioanalyser (Agilent Technologies, Santa Clara, CA, USA) and screened for the presence of contaminants by matching against the contaminant database (containing PhiX, ChrM, rDNA and Illumina small RNA adaptor sequences) using cutadapt[60] and bowtie aligner. The cleaned sequence reads were then processed through the quantification modules miRDEEP2 ver2.0.0.7 pipeline for known miRNA expression profiling[61].

miRNA read counts were normalised as per library size, and a normalised count value of >10 counts per million (CPM) was used as the detection threshold for miRNA presence per library. The edgeR[62] and limma Bioconductor package were used to perform sample diagnostics and differential expression analysis with a data filter set to $\geq$2-fold difference and false discovery rate (FDR) of 0.05. A multi dimension scaling (MDS) plot[63] was generated to visualise the relationship between the set of samples in each biological replicate. For this purpose, the leading log-fold change was plotted for dimensions 1 and 2 using all miRNA counts, with samples displaying similar expression profiles clustering together. All data discussed in this publication have been deposited in NCBI's Gene Expression Omnibus and are accessible through GEO accession number GSE79500 (http://www.ncbi.nlm.nih.gov/geo/query/acc.cgi?acc=GSE79500).

Real time PCR validation of miRNA read data. Validation of the next generation sequencing generated miRNA profiles was conducted using quantitative real-time PCR (RT-qPCR) with (non-locked nucleic acid modified) TaqMan miRNA assay reagents to detect and amplify only mature forms of each miRNA under analysis in accordance with the manufacturer's instructions (ThermoFisher Scientific). The miRNAs selected for analysis were *miR-375* (assay ID 000564), *miR-139-5p* (assay ID 002689), *miR-191-5p* (assay ID 002299), *miR-196b-5p* (assay ID 002215), *miR-151* (assay ID 001190), *miR-34b-5p* (assay ID 002617), *miR-34c-5p* (assay ID 000428), *miR-467a-5p* (assay ID 001826), *miR467d* (assay ID 002518) and *miR-467e* (assay ID 002568). RT-qPCR was performed using a Light Cycler 96 SW 1.1 (Roche, Castle Hill, Australia). RT-qPCR data was normalised against the U6 small nuclear RNA (snRNA; assay ID 001973) as this endogenous snRNA was identified as evenly abundant across each epididymis segment, and relative abundance was calculated using the $2^{-\Delta Ct}$ method[64]. All sRNA RT-qPCR analyses were performed in triplicate using pooled biological samples (6–9 mice/sample). However, due to limitations in generating the volume of epididymosome material required for total RNA extraction for sRNA sequencing, the cDNA used for these RT-qPCR analyses was synthesised from a separate pool of animals to that used for sequencing.

Transfer of epididymosome miRNA cargo to spermatozoa. Epididymal spermatozoa were isolated as previously described[22] prior to co-incubation with purified epididymosomes using methodology optimised for the *in vitro* transfer of proteins between bovine epididymosomes and spermatozoa[27]. The suitability of this protocol was initially assessed by preloading epididymosomes with carboxyfluorescein diacetate succinimidyl ester (CFSE), a non-fluorescent membrane permeant dye. Upon entry into a cell, the acetate groups of CFSE are rapidly removed by intracellular esterases yielding a highly fluorescent, non-membrane permeant carboxyfluorescein label that is capable of forming stable conjugates with primary amines. For this study, freshly isolated epididymosomes were pooled from the caput epididymal segment of six animals and resuspended in modified BWW (pH 6.5) supplemented with 1 mM $ZnCl_2$ (Zn-BWW)[27] before being split into two equal samples. The samples were either labelled with CFSE (1 μM) for 30 min at 37 °C, or treated with an equivalent volume of DMSO prior to being washed in PBS and subjected to ultracentrifugation (100,000 × g, 3 h, 4 °C). The resultant epididymosome pellets were resuspended in Zn-BWW and co-incubated with caput spermatozoa (2×10^6) for 3 h at 37 °C in 5% CO_2 with gentle agitation[27]. Following incubation, spermatozoa were pelleted by centrifugation (400 × g, 3 min), resuspended in Zn-BWW, and their viability assessed by co-labelling with Live/Dead fixable far red dead cell stain (ThermoFisher Scientific) for 15 min at 37 °C. The sperm suspensions were then washed three times by centrifugation (400 × g, 3 min) in Zn-BWW before mounting and visualisation by confocal microscopy. Additional controls for this experiment included incubation of labelled epididymosomes with aldehyde/sulphate beads and direct CFSE (1 μM) labelling of populations of caput spermatozoa (2×10^6) for 3 h at 37 °C in 5% CO_2. In addition, a competition experiment was performed whereby spermatozoa were incubated with varying proportions of non-labelled versus CFSE labelled epididymosomes in order to assess the dye internalisation efficacy achieved in this assay.

To assess epididymosome-mediated transfer of miRNAs to spermatozoa, freshly purified caput and corpus epididymosomes were pooled from three animals and resuspended with 2×10^6 caput spermatozoa in 250 μl of Zn-BWW or an equivalent volume of Zn-BWW medium only (control). Epididymosomes and spermatozoa were then co-incubated as described above before the spermatozoa were pelleted by centrifugation (400 × g, 3 min). The cells were then resuspended in pre-warmed PBS and washed three times to remove any unbound or peripherally adherent epididymosomes, before being processed for total RNA extraction. The relative level of candidate miRNAs was subsequently quantified by RT-qPCR to determine the efficacy of miRNA transfer.

***In silico* analysis of identified miRNAs and target prediction.** *In silico* analysis of miRNA profiles was undertaken using a suite of techniques[53]. Briefly, miRNAs were log transformed, subject to hierarchical median gene clustering (Cluster3, Stanford University, Palo Alto, CA, USA) and examined using heatmaps (Java Treeview, Stanford University) to ensure consistency among biological replicates, and via volcano plots to visualise trends associated with differentially accumulating miRNA in the epididymosomes of each epididymal segment. Ingenuity Pathway Analysis (IPA) software (v8.8, Ingenuity Systems, Redwood City, CA, USA) was utilised to further investigate miRNAs determined to have significant fold changes in accumulation between epididymal

segments. To identify biological pathways that may be influenced by differentially accumulating miRNAs, gene targets of these miRNAs were predicted using experimentally validated filters.

Statistical analysis. JMP Software (v12.2.0) was used to perform multivariate correlation analyses and Student T-tests to determine statistical significance with a significance threshold of $P < 0.05$. Linear regression modelling was performed in R. All experiments were performed in triplicate and all data are expressed as mean ± SEM.

References

1. Hermo, L., Pelletier, R. M., Cyr, D. G. & Smith, C. E. Surfing the wave, cycle, life history, and genes/proteins expressed by testicular germ cells. Part 1: Background to spermatogenesis, spermatogonia, and spermatocytes. *Microsc Res Tech* **73,** 241–278, doi: 10.1002/jemt.20783 (2010).
2. Cornwall, G. A. New insights into epididymal biology and function. *Hum Reprod Update* **15,** 213–227, doi: 10.1093/humupd/dmn055 (2009).
3. Robaire, B., Hinton, B. T. & Orgebin-Crist, M. C. In *Knobil and Neill's Physiology of Reproduction, 3rd Edition* (ed. J. D. Neill) Ch. 22, 1071–1148 (Elsevier, 2006).
4. Dacheux, J. L., Dacheux, F. & Druart, X. Epididymal protein markers and fertility. *Anim Reprod Sci*, doi: 10.1016/j.anireprosci.2016.02.034 (2016).
5. Sullivan, R. & Saez, F. Epididymosomes, prostasomes, and liposomes: their roles in mammalian male reproductive physiology. *Reproduction* **146,** R21–R35, doi: 10.1530/rep-13-0058 (2013).
6. Sullivan, R. Epididymosomes: a heterogeneous population of microvesicles with multiple functions in sperm maturation and storage. *Asian J Androl* **17,** 726–729, doi: 10.4103/1008-682X.155255 (2015).
7. Martin-DeLeon, P. A. Epididymosomes: transfer of fertility-modulating proteins to the sperm surface. *Asian J Androl* **17,** 720–725, doi: 10.4103/1008-682x.155538 (2015).
8. Martin-DeLeon, P. A. Epididymal SPAM1 and its impact on sperm function. *Mol Cell Endocrinol* **250,** 114–121, doi: 10.1016/j.mce.2005.12.033 (2006).
9. Rejraji, H. *et al.* Lipid remodeling of murine epididymosomes and spermatozoa during epididymal maturation. *Biol Reprod* **74,** 1104–1113, doi: 10.1095/biolreprod.105.049304 (2006).
10. Girouard, J., Frenette, G. & Sullivan, R. Comparative proteome and lipid profiles of bovine epididymosomes collected in the intraluminal compartment of the caput and cauda epididymidis. *Int J Androl* **34,** e475–e486, doi: 10.1111/j.1365-2605.2011.01203.x (2011).
11. Belleannee, C., Calvo, E., Caballero, J. & Sullivan, R. Epididymosomes convey different repertoires of microRNAs throughout the bovine epididymis. *Biol Reprod* **89,** 30, doi: 10.1095/biolreprod.113.110486 (2013).
12. Sharma, U. *et al.* Biogenesis and function of tRNA fragments during sperm maturation and fertilization in mammals. *Science* **351,** 391–396, doi: 10.1126/science.aad6780 (2016).
13. Smythies, J., Edelstein, L. & Ramachandran, V. Molecular mechanisms for the inheritance of acquired characteristics-exosomes, microRNA shuttling, fear and stress: Lamarck resurrected? *Front Genet* **5,** 133, doi: 10.3389/fgene.2014.00133 (2014).
14. Eaton, S. A. *et al.* Roll over Weismann: extracellular vesicles in the transgenerational transmission of environmental effects. *Epigenomics* **7,** 1165–1171, doi: 10.2217/epi.15.58 (2015).
15. Rodgers, A. B., Morgan, C. P., Bronson, S. L., Revello, S. & Bale, T. L. Paternal stress exposure alters sperm microRNA content and reprograms offspring HPA stress axis regulation. *J Neurosci* **33,** 9003–9012, doi: 10.1523/jneurosci.0914-13.2013 (2013).
16. Rodgers, A. B., Morgan, C. P., Leu, N. A. & Bale, T. L. Transgenerational epigenetic programming via sperm microRNA recapitulates effects of paternal stress. *Proc Natl Acad Sci USA* **112,** 13699–13704, doi: 10.1073/pnas.1508347112 (2015).
17. Fullston, T. *et al.* Paternal obesity initiates metabolic disturbances in two generations of mice with incomplete penetrance to the F2 generation and alters the transcriptional profile of testis and sperm microRNA content. *FASEB J* **27,** 4226–4243, doi: 10.1096/fj.12-224048 (2013).
18. Chen, Q. *et al.* Sperm tsRNAs contribute to intergenerational inheritance of an acquired metabolic disorder. *Science* **351,** 397–400, doi: 10.1126/science.aad7977 (2016).
19. Marczylo, E. L., Amoako, A. A., Konje, J. C., Gant, T. W. & Marczylo, T. H. Smoking induces differential miRNA expression in human spermatozoa: a potential transgenerational epigenetic concern? *Epigenetics* **7,** 432–439, doi: 10.4161/epi.19794 (2012).
20. Bale, T. L. Epigenetic and transgenerational reprogramming of brain development. *Nat Rev Neurosci* **16,** 332–344, doi: 10.1038/nrn3818 (2015).
21. Hermo, L., Pelletier, R. M., Cyr, D. G. & Smith, C. E. Surfing the wave, cycle, life history, and genes/proteins expressed by testicular germ cells. Part 1: background to spermatogenesis, spermatogonia, and spermatocytes. *Microsc Res Tech* **73,** 241–278, doi: 10.1002/jemt.20783 (2010).
22. Nixon, B. *et al.* The microRNA signature of mouse spermatozoa is substantially modified during epididymal maturation. *Biol Reprod*, doi: 10.1095/biolreprod.115.132209 (2015).
23. Colombo, M., Raposo, G. & Thery, C. Biogenesis, secretion, and intercellular interactions of exosomes and other extracellular vesicles. *Annu Rev Cell Dev Biol* **30,** 255–289, doi: 10.1146/annurev-cellbio-101512-122326 (2014).
24. Raposo, G. & Stoorvogel, W. Extracellular vesicles: exosomes, microvesicles, and friends. *J Cell Biol* **200,** 373–383, doi: 10.1083/jcb.201211138 (2013).
25. Fischer, K. A. *et al.* 15-Lipoxygenase is a component of the mammalian sperm cytoplasmic droplet. *Reproduction* **130,** 213–222, doi: 10.1530/rep.1.00646 (2005).
26. Nixon, B. *et al.* Next generation sequencing analysis reveals segmental patterns of microRNA expression in mouse epididymal epithelial cells. *PLoS One* **10,** e0135605, doi: 10.1371/journal.pone.0135605 (2015)
27. Frenette, G., Lessard, C. & Sullivan, R. Selected proteins of "prostasome-like particles" from epididymal cauda fluid are transferred to epididymal caput spermatozoa in bull. *Biol Reprod* **67,** 308–313, 10.1095/biolreprod67.1.308 (2002).
28. Bjorkgren, I. *et al.* Dicer1 ablation in the mouse epididymis causes dedifferentiation of the epithelium and imbalance in sex steroid signaling. *PLoS One* **7,** e38457, doi: 10.1371/journal.pone.0038457 (2012).
29. Bjorkgren, I. *et al.* Imbalanced lipid homeostasis in the conditional Dicer1 knockout mouse epididymis causes instability of the sperm membrane. *FASEB J* **29,** 433–442, doi: 10.1096/fj.14-259382 (2015).
30. Belleannee, C. *et al.* Role of microRNAs in controlling gene expression in different segments of the human epididymis. *PLoS One* **7,** e34996, doi: 10.1371/journal.pone.0034996 (2012).
31. Frenette, G., Girouard, J. & Sullivan, R. Comparison between epididymosomes collected in the intraluminal compartment of the bovine caput and cauda epididymidis. *Biol Reprod* **75,** 885–890, doi: 10.1095/biolreprod.106.054692 (2006).
32. Frenette, G. *et al.* Characterization of two distinct populations of epididymosomes collected in the intraluminal compartment of the bovine cauda epididymis. *Biol Reprod* **83,** 473–480, doi: 10.1095/biolreprod.109.082438 (2010).
33. Valadi, H. *et al.* Exosome-mediated transfer of mRNAs and microRNAs is a novel mechanism of genetic exchange between cells. *Nat Cell Biol* **9,** 654–659, doi: 10.1038/ncb1596 (2007).

34. Thery, C. Exosomes: secreted vesicles and intercellular communications. *F1000 Biol Rep* **3,** 15, doi: 10.3410/B3-15 (2011).
35. Lee, Y., El Andaloussi, S. & Wood, M. J. Exosomes and microvesicles: extracellular vesicles for genetic information transfer and gene therapy. *Hum Mol Genet* **21,** R125–R134, doi: 10.1093/hmg/dds317 (2012).
36. Li, C. C. *et al.* Glioma microvesicles carry selectively packaged coding and non-coding RNAs which alter gene expression in recipient cells. *RNA Biol* **10,** 1333–1344, doi: 10.4161/rna.25281 (2013).
37. Villarroya-Beltri, C. *et al.* Sumoylated hnRNPA2B1 controls the sorting of miRNAs into exosomes through binding to specific motifs. *Nat Commun* **4,** 2980, doi: 10.1038/ncomms3980 (2013).
38. Guduric-Fuchs, J. *et al.* Selective extracellular vesicle-mediated export of an overlapping set of microRNAs from multiple cell types. *BMC Genomics* **13,** 357, doi: 10.1186/1471-2164-13-357 (2012).
39. Aitken, R. J. *et al.* Proteomic changes in mammalian spermatozoa during epididymal maturation. *Asian J Androl* **9,** 554–564, doi: 10.1111/j.1745-7262.2007.00280.x (2007).
40. Yuan, S. *et al.* Sperm-borne miRNAs and endo-siRNAs are important for fertilization and preimplantation embryonic development. *Development* **143,** 635–647, doi: 10.1242/dev.131755 (2016).
41. Al-Dossary, A. A., Bathala, P., Caplan, J. L. & Martin-DeLeon, P. A. Oviductosome-Sperm Membrane interaction in cargo delivery: Detection of fusion and underlying molecular players using three-dimensional super-resolution structured illumination microscopy (SR-SIM). *J Biol Chem* **290,** 17710–17723, doi: 10.1074/jbc.M114.633156 (2015).
42. Machtinger, R., Laurent, L. C. & Baccarelli, A. A. Extracellular vesicles: roles in gamete maturation, fertilization and embryo implantation. *Hum Reprod Update* **22,** 182–193, doi: 10.1093/humupd/dmv055 (2016).
43. D'Amours, O. *et al.* Epididymosomes transfer epididymal sperm binding protein 1 (ELSPBP1) to dead spermatozoa during epididymal transit in bovine. *Biol Reprod* **87,** 94, doi: 10.1095/biolreprod.112.100990 (2012).
44. Lane, M., Robker, R. L. & Robertson, S. A. Parenting from before conception. *Science* **345,** 756–760, doi: 10.1126/science.1254400 (2014).
45. Belleannee, C., Legare, C., Calvo, E., Thimon, V. & Sullivan, R. microRNA signature is altered in both human epididymis and seminal microvesicles following vasectomy. *Hum Reprod* **28,** 1455–1467, doi: 10.1093/humrep/det088 (2013).
46. Palmer, N. O., Bakos, H. W., Fullston, T. & Lane, M. Impact of obesity on male fertility, sperm function and molecular composition. *Spermatogenesis* **2,** 253–263, doi: 10.4161/spmg.21362 (2012).
47. Cossetti, C. *et al.* Soma-to-germline transmission of RNA in mice xenografted with human tumour cells: possible transport by exosomes. *PLoS One* **9,** e101629, doi: 10.1371/journal.pone.0101629 (2014).
48. Thery, C., Zitvogel, L. & Amigorena, S. Exosomes: composition, biogenesis and function. *Nat Rev Immunol* **2,** 569–579, doi: 10.1038/nri855 (2002).
49. Johnston, D. S. *et al.* The mouse epididymal transcriptome: transcriptional profiling of segmental gene expression in the epididymis. *Biol Reprod* **73,** 404–413, doi: 10.1095/biolreprod.105.039719 (2005).
50. Sharkey, D. J., Schjenken, J. E., Mottershead, D. G. & Robertson, S. A. Seminal fluid factors regulate activin A and follistatin synthesis in female cervical epithelial cells. *Mol Cell Endocrinol* **417,** 178–190, doi: 10.1016/j.mce.2015.09.022 (2015).
51. Schjenken, J. E. & Robertson, S. A. Seminal Fluid Signalling in the Female Reproductive Tract: Implications for Reproductive Success and Offspring Health. *Adv Exp Med Biol* **868,** 127–158, doi: 10.1007/978-3-319-18881-2_6 (2015).
52. Biggers, J. D., Whitten, W. K. & Whittingham, D. G. In *Methods in Mammalian Embryology* (ed. J. C. Daniel) 86–116 (Freeman Press, 1971).
53. Anderson, A. L. *et al.* Assessment of microRNA expression in mouse epididymal epithelial cells and spermatozoa by next generation sequencing. *Genom Data* **6,** 208–211, doi: 10.1016/j.gdata.2015.09.012 (2015).
54. Thery, C., Amigorena, S., Raposo, G. & Clayton, A. Isolation and characterization of exosomes from cell culture supernatants and biological fluids. *Curr Protoc Cell Biol* Chapter 3, Unit 3 22, doi: 10.1002/0471143030.cb0322s30 (2006).
55. Tauro, B. J. *et al.* Comparison of ultracentrifugation, density gradient separation, and immunoaffinity capture methods for isolating human colon cancer cell line LIM1863-derived exosomes. *Methods* **56,** 293–304, doi: 10.1016/j.ymeth.2012.01.002 (2012).
56. Hermo, L., Dworkin, J. & Oko, R. Role of epithelial clear cells of the rat epididymis in the disposal of the contents of cytoplasmic droplets detached from spermatozoa. *Am J Anat* **183,** 107–124, doi: 10.1002/aja.1001830202 (1988).
57. Reid, A. T. *et al.* Glycogen synthase kinase 3 regulates acrosomal exocytosis in mouse spermatozoa via dynamin phosphorylation. *FASEB J* **29,** 2872–2882, doi: 10.1096/fj.14-265553 (2015).
58. Principe, S. *et al.* In-depth proteomic analyses of exosomes isolated from expressed prostatic secretions in urine. *Proteomics* **13,** 1667–1671, doi: 10.1002/pmic.201200561 (2013).
59. Ng, Y. H. *et al.* Endometrial exosomes/microvesicles in the uterine microenvironment: a new paradigm for embryo-endometrial cross talk at implantation. *PLoS One* **8,** e58502, doi: 10.1371/journal.pone.0058502 (2013).
60. Martin, M. Cutadapt removes adapter sequences from high-throughput sequencing reads. *EMBnet.journal* **17,** 10–12, doi: 10.14806/ej.17.1.200 (2011).
61. Friedlander, M. R. *et al.* Discovering microRNAs from deep sequencing data using miRDeep. *Nat Biotechnol* **26,** 407–415, doi: 10.1038/nbt1394 (2008).
62. McCarthy, D. J., Chen, Y. & Smyth, G. K. Differential expression analysis of multifactor RNA-Seq experiments with respect to biological variation. *Nucleic Acids Res* **40,** 4288–4297, doi: 10.1093/nar/gks042 (2012).
63. Ritchie, M. E. *et al.* limma powers differential expression analyses for RNA-sequencing and microarray studies. *Nucleic Acids Res* **43,** e47, doi: 10.1093/nar/gkv007 (2015).
64. Schmittgen, T. D. & Livak, K. J. Analyzing real-time PCR data by the comparative C(T) method. *Nat Protoc* **3,** 1101–1108, doi: 10.1038/nprot.2008.73 (2008).

Acknowledgements

The authors acknowledge Dr Roger Liang for his assistance with the sizing of isolated epididymosome fractions. Financial support for this project was provided by the National Health and Medical Research Council of Australia (Project Grant APP1062371 to B.N., E.A.M. and J.H.). JNR is the recipient of a University of Newcastle PhD scholarship.

Author Contributions

J.N.R., S.J.S., A.L.A., K.H., K.C. and B.P.M. carried out the laboratory work and participated in data analysis and drafting of the manuscript; S.T. performed next generation sequence analyses and bioinformatics. E.A.M., J.E.H. and A.L.E. participated in the design of the study, data analysis, and drafting of the manuscript; B.N. conceived of the study, designed the study, coordinated the study and helped draft the manuscript. All authors gave final approval for publication.

Additional Information

Accession codes: All data discussed in this publication have been deposited in NCBI's Gene Expression Omnibus and are accessible through GEO accession number GSE79500 (http://www.ncbi.nlm.nih.gov/geo/query/acc.cgi?acc=GSE79500).

Supplementary information accompanies this paper at http://www.nature.com/srep

Competing financial interests: The authors declare no competing financial interests.

How to cite this article: Reilly, J. N. *et al.* Characterisation of mouse epididymosomes reveals a complex profile of microRNAs and a potential mechanism for modification of the sperm epigenome. *Sci. Rep.* **6**, 31794; doi: 10.1038/srep31794 (2016).